JAERI 1314

One-, Two- and Three-Dimensional Transport Codes Using Multi-Group Double-Differential Form Cross Sections

November 1988

日 本 原 子 力 研 究 所

Japan Atomic Energy Research Institute

日本原子力研究所研究成果編集委員会

委員長　更田　豊治郎（理事）

委　　員

井川　勝市（燃料・材料工学部）
石黒　幸雄（原子炉工学部）
岩田　忠夫（物理部）
江連　秀夫（動力試験炉部）
海老沼幸夫（技術情報部）
金子　義彦（原子炉工学部）
工藤　博司（アイソトープ部）
近藤　育郎（JT-60試験部）
斉藤　伸三（高温工学試験研究炉設計室）
白井　英次（研究炉管理部）
竹田　辰興（核融合研究部）
立川　圓造（化学部）
飛岡　利明（原子炉安全工学部）
中井　洋太（物理部）
備後　一義（保健物理部）
藤城　俊夫（燃料安全工学部）
藤野　威男（化学部）
船橋　昭昌（臨界プラズマ研究部）
幕内　恵三（開発部）
宮田定次郎（研究部）
宮本　喜晟（高温工学部）
森内　　茂（環境安全研究部）
安川　　茂（動力炉開発・安全性研究管理部）
八巻　治恵（原子力船技術部）
山本　　章（材料試験炉部）
横村　武宣（原子力船研究開発室）
吉田　弘幸（企画室）

Japan Atomic Energy Research Institute

Board of Editors

Toyojiro Fuketa (Chief Editor)

Kazuyoshi Bingo
Takeo Fujino
Katsuichi Ikawa
Yoshihiko Kaneko
Keizo Makuuchi
Shigeru Moriuchi
Eiji Shirai
Toshiaki Tobioka
Shigeru Yasukawa
Yukio Ebinuma
Toshio Fujishiro
Yukio Ishiguro
Ikuro Kondo
Yoshiaki Miyamoto
Yohta Nakai
Enzo Tachikawa
Jikei Yamaki
Takeyoshi Yokomura
Hideo Ezure
Akimasa Funahashi
Tadao Iwata
Hiroshi Kudo
Teijiro Miyata
Shinzo Saito
Tatsuoki Takeda
Akira Yamamoto
Hiroyuki Yoshida

JAERIレポートは，日本原子力研究所が研究成果編集委員会の審査を経て不定期に公刊している研究報告書です。

入手の問合わせは，日本原子力研究所技術情報部情報資料課（〒319-11茨城県那珂郡東海村）あて，お申しこしください。なお，このほかに財団法人原子力弘済会資料センター（〒319-11 茨城県那珂郡東海村日本原子力研究所内）で複写による実費頒布をおこなっております。

JAERI reports are reviewed by the Board of Editors and issued irregularly.

Inquiries about availability of the reports should be addressed to Information Division Department of Technical Information, Japan Atomic Energy Research Institute, Tokai-mura, Naka-gun, Ibaraki-ken 319-11, Japan.

©Japan Atomic Energy Research Institute, 1988

編集兼発行　日本原子力研究所
印　　刷　いばらき印刷㈱

One-, Two- and Three-Dimensional Transport Codes Using Multi-Group Double-Differential Form Cross Sections

Takamasa MORI, Masayuki NAKAGAWA and Makoto SASAKI*

Department of Reactor Engineering
Tokai Research Establishment,
Japan Atomic Energy Research Institute
Tokai-mura, Naka-gun, Ibaraki-ken, Japan

(Received June 16, 1988)

Abstract

We have developed a group of computer codes to realize the accurate transport calculation by using the multi-group double-differential form cross section. This type of cross section can correctly take account of the energy-angle correlated reaction kinematics. Accordingly, the transport phenomena in materials with highly anisotropic scattering are accurately calculated by using this cross section. They include the following four codes or code systems:

PROF-DD : a code system to generate the multi-group double-differential form cross section library by processing basic nuclear data file compiled in the ENDF/B-IV or -V format,

ANISN-DD : a one-dimensional transport code based on the discrete ordinate method,

DOT-DD : a two-dimensional transport code based on the discrete ordinate method,

MORSE-DD : a three-dimensional transport code based on the Monte Carlo method.

In addition to these codes, several auxiliary codes have been developed to process calculated results. This report describes the calculation algorithm employed in these codes and how to use them.

Keywords: Transport Calculation, Multi-Group, Double-Differential Form Cross Section, 1-D S_n, 2-D S_n, 3-D Monte Carlo, User Manual

* Visiting researcher from Japan Information Service Co., Ltd.

多群二重微分型断面積を用いる一，二，三次元輸送計算コード

日本原子力研究所東海研究所原子炉工学部

森　貴正・中川正幸・佐々木誠*

1988年6月16日受理

要　　旨

輸送計算を正確に行うために，多群二重微分型断面積を使用する一連の輸送計算コードを開発した。多群二重微分型断面積は散乱後のエネルギーと散乱角の相関関係を正確に取り扱うことができる。従って，この断面積を使用することにより非等方性の強い散乱を有する物質中の輸送現象を正しく計算することができる。開発したコードおよびコードシステムは以下の通りである：

PROF-DD　：ENDF/B-IVまたは-V形式の核データファイルを処理して，多群二重微分型断面積ライブラリを作成するコードシステム，

ANISN-DD　：ディスクリートオーディネート法による一次元輸送計算コード，

DOT-DD　：ディスクリートオーディネート法による二次元輸送計算コード，

MORSE-DD　：モンテカルロ法による三次元輸送計算コード。

これらのコードの他に，計算結果を処理するためにいくつかの補助コードを開発した。本報告には，これらのコードに使用されている計算アルゴリズムおよび各コードの使用法が記載されている。

* 日本情報サービス㈱

Contents

1. Introduction 1
2. Multi-Group Double-Differential Form Cross Section Library 3
   2.1 Definition of Double-Differential Form Cross Section 3
   2.2 Caluculation of Multi-Group Double-Differential Form Cross Section 4
   2.3 Formulation of Collision Source with Use of DDX Library 6
   2.4 Available DDX Library 7
3. PROF-DD: Multi-Group DDX Library Generation Code System 9
   3.1 General Feature of PROF-DD 9
   3.2 MCFILEF 10
      3.2.1 Input Instruction 11
      3.2.2 Sample Input, JCL and I/O Files 12
   3.3 RESENDD 13
      3.3.1 Input Instruction for the PROF-DD System 13
      3.3.2 Sample Input, JCL and I/O Files 14
   3.4 SPINPTF 14
      3.4.1 Input Instruction 14
      3.4.2 Sample Input, JCL and I/O Files 16
   3.5 PROF-DDX 17
      3.5.1 Outline of PROF-DDX 17
      3.5.2 Input Instruction 21
      3.5.3 Sample Input, JCL and I/O Files 21
   3.6 DDXLIBMK 22
      3.6.1 Input Instruction 22
      3.6.2 Sample Input, JCL and I/O Files 23
      3.6.3 Structure of DDX Library 23
4. ANISN-DD: One-Dimensional S_n Transport Code 25
   4.1 New Features of ANISN-DD 25
      4.1.1 Cross Section 25
      4.1.2 Solution Algorithm and Angular Transfer Probability 27
   4.2 Input Instruction 29
      4.2.1 Input Data for Additional Options of ANISN-DD 29
      4.2.2 ANISN-DD Input Data with FIDO Format 33
   4.3 Job Control Instruction 38
      4.3.1 Job Control Statements 38
      4.3.2 I/O File Requirement 38
      4.3.3 Memory Requirement 43
   4.4 Sample Problem and Input Data 44
5. DOT-DD: Two-Dimensional S_n Transport Code 47
   5.1 New Features of DOT-DD 47
      5.1.1 Cross Section 47
      5.1.2 Solution Algorithm and Angular Transfer Probability 48
      5.1.3 First Collision Source 48
      5.1.4 Speed-Up of Calculation 53
      5.1.5 Restart Function of DOT-DD 54
   5.2 Input Instruction 54

5.2.1 DOT-DD 54
5.2.2 UNCL-DD 64
5.3 Job Control Instruction 68
5.3.1 Job Control Statements 68
5.3.2 I/O File Requirements 68
5.3.3 Memory Requirements 76
5.4 Sample Problem 76
5.4.1 Specification of Sample Problem 76
5.4.2 Sample Input 79
5.4.3 Comparison of Computer Resources Required 81
6. MORSE-DD: Three-Dimensional Monte Carlo Code 82
6.1 New Features of MORSE-DD 82
6.1.1 Cross Section 82
6.1.2 Geometry 83
6.1.3 External Source 84
6.1.4 Variance Reduction Techniques 89
6.1.5 Tallies 91
6.1.6 Super-Group Treatment of Random Walk Process 93
6.2 Input Instruction 94
6.2.1 MORSE-DD 94
6.2.2 Additional Input for MORSE-DSG 110
6.3 Job Control Instruction 110
6.3.1 Job Control Statements 110
6.3.2 I/O File Requirements 113
6.3.3 Memory Requirements 116
6.4 Sample Problem and Input Data 116
6.5 Auxiliary Codes and Supplementary Subroutines 119
6.5.1 Supplementary Subroutines 119
6.5.2 ZRECNO 119
7. Auxiliary Codes 122
7.1 REACT 122
7.2 MONTA 127
8. Comparison of Sample Problem Results Using DDX and P_ℓ Cross Sections 130
9. Summary 136
Acknowledgment 136
References 137
Appendices 139
1. FIDO Format 139
2. LINEAR, RECENT and SIGMA1 Codes 142
3. Angular Transfer Probability for S_n Calculation 147

目　　次

1. 序 …… 1
2. 多群二重微分型断面積ライブラリー …… 3
2.1 二重微分型断面積の定義 …… 3
2.2 多群二重微分型断面積の計算 …… 4
2.3 DDX ライブラリーによる散乱源の定式化 …… 6
2.4 使用できる DDX ライブラリー …… 7
3. PROF-DD: 多群 DDX ライブラリー作成コードシステム …… 9
3.1 PROF-DD の概要 …… 9
3.2 MCFILEF …… 10
3.2.1 入力形式 …… 11
3.2.1 入力データ，JCL の例と I/O ファイル …… 12
3.3 RESENDD …… 13
3.3.1 PROF-DD システムにおける入力形式 …… 13
3.3.2 入力データ，JCL の例と I/O ファイル …… 14
3.4 SPINPTF …… 14
3.4.1 入力形式 …… 14
3.4.2 入力データ，JCL の例と I/O ファイル …… 16
3.5 PROF-DDX …… 17
3.5.1 PROF-DDX の概要 …… 17
3.5.2 入力形式 …… 21
3.5.3 入力データ，JCL の例と I/O ファイル …… 21
3.6 DDXLIBMK …… 22
3.6.1 入力形式 …… 22
3.6.2 入力データ，JCL の例と I/O ファイル …… 23
3.6.3 DDX ライブラリーの構成 …… 23
4. ANISN-DD: 一次元 S_n 法輸送計算コード …… 25
4.1 ANISN-DD の修正 …… 25
4.1.1 断面積 …… 25
4.1.2 解法と角度遷移確率 …… 27
4.2 入力形式 …… 29
4.2.1 ANISN-DD の追加オプションに対する入力データ …… 29
4.2.2 FIDO フォーマットによる ANISN-DD の入力データ …… 33
4.3 ジョブ制御 …… 38
4.3.1 ジョブ制御文 …… 38
4.3.2 必要な入出力ファイル …… 38
4.3.3 必要な記憶容量 …… 43
4.4 例題と入力データ …… 44
5. DOT-DD: 二次元 S_n 法輸送計算コード …… 47
5.1 DOT-DD の修正 …… 47
5.1.1 断面積 …… 47
5.1.2 解法と角度遷移確率 …… 48
5.1.3 第一衝突散乱源 …… 48
5.1.4 計算の高速化 …… 53
5.1.5 DOT-DD のリスタート機能 …… 54
5.2 入力形式 …… 54

5.2.1 DOT-DD …… 54
5.2.2 ÚNCL-DD …… 64
5.3 ジョブ制御 …… 68
5.3.1 ジョブ制御文 …… 68
5.3.2 必要な入出力ファイル …… 68
5.3.3 必要な記憶容量 …… 76
5.4 例題 …… 76
5.4.1 例題の詳細 …… 76
5.4.2 入力データ …… 79
5.4.3 必要な計算機資源の比較 …… 81
6. MORSE-DD: 三次元モンテカルロコード …… 82
6.1 MORSE-DD の修正 …… 82
6.1.1 断面積 …… 82
6.1.2 幾何形状 …… 83
6.1.3 外部線源 …… 84
6.1.4 分散低減法 …… 89
6.1.5 タリー …… 91
6.1.6 ランダムウォーク過程のスーパーグループによる取り扱い …… 93
6.2 入力形式 …… 94
6.2.1 MORSE-DD …… 94
6.2.2 MORSE-DSG …… 110
6.3 ジョブ制御 …… 110
6.3.1 ジョブ制御文 …… 110
6.3.2 必要な入出力ファイル …… 113
6.3.3 必要な記憶容量 …… 116
6.4 例題と入力データ …… 116
6.5 補助コードとサブルーチン …… 119
6.5.1 補助サブルーチン …… 119
6.5.2 ZRECNO …… 119
7. 補助コード …… 122
7.1 REACT …… 122
7.2 MONTA …… 127
8. DDX と P_ℓ 展開型断面積による例題計算結果の比較 …… 130
9. まとめ …… 136
謝辞 …… 136
参考文献 …… 137
付録 …… 139
1. FIDO フォーマット …… 139
2. LINEAR, RECENT と SIGMA 1 コード …… 142
3. S_n 計算のための角度遷移確率 …… 147

List of Tables

Table 2.1 Structure of 125-group double-differential form cross section library
Table 2.2 Indentification number of nuclides prepared in 125-group DDL/B4 and /J3P1 libraries
Table 3.1 PROF-DDX file requirement
Table 4.1 ANISN-DD file requirement
Table 5.1 DOT-DD file requirement
Table 5.2 UNCL-DD file requirement
Table 5.3 Material composition for sample problems
Table 5.4 Computer resources required by sample problems
Table 6.1 Body data required by each body type
Table 6.2 Geometry input for source
Table 6.3 MORSE-DD file requirement
Table 6.4 MORSE-DSG file requirement
Table 7.1 Identification of reaction cross sections in 125-group library for response calculation
Table 7.2 MONTA file requirement
Table 8.1 Outgoing neutron energy from elastic scattering with an incident energy 15 MeV
Table 8.2 Comparison of calculated tritium production rates
Table A2.1 LINEAR file requirement
Table A2.2 RECENT file requirement
Table A2.3 SIGMA1 file requirement
Table A2.4 Input instruction for LINEAR
Table A2.5 Input instruction for RECENT
Table A2.6 Input instruction for SIGMA1
Table A3.1 File name of angular transfer probability
Table A3.2 Quadrature set of S_8
Table A3.3 Quadrature set of S_{16}

List of Figures

Fig.2.1 Diagram for illustrating the scattering kinematics in the(E,E')plane and the integration limits in the calculation of multi-group DDX
Fig.3.1 Flow chart of the PROF-DD system
Fig.3.2 I/O files for MCFILEF
Fig.3.3 Sample JCL and input data for MCFILEF
Fig.3.4 Sample JCL and input data for RESENDD, SPINPTF and PROF-DDX
Fig.3.5 I/O files for RESENDD
Fig.3.6 I/O files for SPINPTF
Fig.3.7 Flow chart of PROF-DDX
Fig.3.8 Lethargy width of scattered neutron vs. $A\beta$
Fig.3.9 Fine energy meshes for numerical integration with respect to E and E' in the subroutines TRANSM and TRANS2
Fig.3.10 Sample JCL and input data for DDXLIBMK(compilation of DDX library)
Fig.3.11 I/O files for DDXLIBMK
Fig.4.1 Job control statements for ANISN-DD
Fig.4.2 Schematic diagram of ANISN-DD sample problem
Fig.4.3 Sample input for ANISN-DD
Fig.5.1 Example of regions W_m and D_k on a unit sphere
Fig.5.2 Diagram for illustrating the calculation algorithm of $S(C_k \cap W_m)$
Fig.5.3 Diagram for illustrating the calculation algorithm of $S(T_l)$
Fig.5.4 Sub-regions on a unit sphere defined to calculate angular transfer probabilities ("Igloo" type)
Fig.5.5 Sub-regions on a unit spere defined to calculate angular transfer probabilities ("Honeycomb" type)
Fig.5.6 Job control statements for successive execution of UNCL-DD and DOT-DD
Fig.5.7 Calculation model of angle-dependent leakage spectra from Li_2O slab (DOT-DD sample problem 1)
Fig.5.8 Schematic diagram for DOT-DD sample problem 2
Fig.5.9 Sample input for UNCL-DD
Fig.5.10 Sample input for DOT-DD
Fig.6.1 Unit body of elliptical torus, ELT
Fig.6.2 Rotation of flight direction and spatial coordinates
Fig.6.3 Job control statements for MORSE-DD
Fig.6.4 Job control statements for MORSE-DSG
Fig.6.5 Sample input for MORSE-DD
Fig.7.1 Sample JCL and input data for REACT
Fig.7.2 Ordering of quadrature directions in S_6 approximation
Fig.7.3 Sample JCL and input data for MONTA
Fig.8.1 Leakage neutron spectra from a 20 cm thick lithium slab calculated by ANISN-DD (ANISN-DD sample problem)
Fig.8.2 Leakage neutron spectra from a Li_2O cylinder of 31.4 cm radius and 5.06 cm thickness calculated by DOT-DD (DOT-DD sample problem 1)
Fig.8.3 Tritium production rates calculated by DOT-DD (DOT-DD sample problem 2)
Fig.8.4 Leakage neutron spectra from a Li_2O cylinder of 30 cm radius and 60 cm thickness calculated by DOT-DD (DOT-DD sample problem 2)
Fig.A2.1 Sample JCL and input data for LINEAR, RECENT and SIGMA1

1. Introduction

Anisotropy of neutron scattering plays an important role in the energy and spatial distributions of neutrons at the high energy region as encountered in fusion reactor shielding and blanket neutronics calculations. The conventional multi-group method using the P_l expansion for anisotropic scattering sometimes significantly mispredicts the neutron transport phenomena in the materials with highly anisotropic scattering cross sections[1),2)]. The use of the lower order P_l expansion of the angular distribution leads to negative elements of energy transfer matrices, hence sometimes to negative flux. Moreover, the conventional multi-group method cannot accurately take account of the energy-angle correlated kinematics for neutron scattering. In order to overcome such problems, the use of the double-differential form scattering cross section (DDX) was proposed for the accurate treatment of the energy-angle correlated kinematics by Takahashi et al. [1)]. The transport codes using this type of cross section can treat accurately the highly anisotropic scattering.

The DDX method has been improved in JAERI to be directly used in the existing codes based on the multi-group scheme[3),4),5),6)], and a group of computer codes have been developed to realize the accurate transport calculation for fusion neutronics by using the multi-group DDX. They include the following codes;

PROF-DD	:	a code system to generate the multi-group DDX library by processing basic nuclear data file compiled in the ENDF/B-IV or -V format,
ANISN-DD	:	a one-dimensional transport code based on the discrete ordinate method,
DOT-DD	:	a two-dimensional transport code based on the discrete ordinate method,
MORSE-DD	:	a three-dimensional transport code based on the Monte Carlo method.

These transport codes are modified versions of widely-used and well-established codes, ANISN[7),8)], DOT 3.5[9)] and MORSE-CG[10)], respectively. The developed codes can use not only the DDX but also the conventional P_l expansion type cross sections. These transport codes can be applied to neutron and/or gamma-ray transport problems. The PROF-DD code system, however, can generate a DDX library only for neutron transport calculation. Accordingly, only the conventional P_l cross section can be used for a gamma-ray transport calculation at the present stage. In addition to these codes, the following auxiliary codes have been also developed to extend the applicability:

DDXPLOT	:	to plot the multi-group DDX calculated by the PROF-DD code system,
MONTA	:	to calculate the angular transfer probability for one- and two- dimensional S_n transport calculation by the Monte Carlo method,
UNCL-DD	:	to calculate the first collision source for two-dimensional DOT-DD calculation,
REACT	:	to calculated reaction rate by using calculated fluxes by these transport codes,
PLTJOINT	:	to plot the results by the transport codes.

Some of these codes have been already published and released for user's applications[3),4),5),11)], and the validation tests of the produced DDX library have been extensively carried out by the MORSE-DD code and reported elsewhere[6)]. After the first versions were released, several improvements for these codes have also been made. This report includes a reference manual of these codes for users. In Chapter 2, the definition of multi-group DDX and the transport calculation using them are given. The PROF-DD code system is described in Chapter 3. In Chapters 4 to 6, the one-dimensional code ANISN-DD, the two-dimensional code DOT-DD together with UNCL-DD and the three-dimensional code MORSE-DD are presented. Auxiliary codes, MONTA and REACT are described in Chapter 7. In each chapter, we give

new features of each code and how to use it. No description of DDXPLOT and PLTJOINT is given in this report. For these tow codes, a user should refer the reports 4 and 11. The results of sample problems for each code are presented in Chapter 8, and they are compared with those by the conventional P_l method.

2. Multi-Group Double-Differential Form Cross Section Library

2.1 Definition of Double-Differential Form Cross Section

The collision source term in the transport equation is written as

$$q(r,\Omega,E)=\int dE'\int d\Omega'\Psi(r,\Omega',E')\sum_j N_j\ \{\sigma_{el}^j(\Omega'\to\Omega,E'\to E)+\sum_i\sigma_{in,i}^j(\Omega'\to\Omega,E'\to E)+\sum_m m\sigma_{n,mn}^j(\Omega'\to\Omega,E'\to E)+\sum_X\sigma_{n,n'X}^j(\Omega'\to\Omega,E'\to E)\}\ , \tag{2-1}$$

where σ^j denotes the microscopic differential cross section of nuclide j, and the subscript el stands for elastic scattering, (in,i) discrete and continuum level inelastic scattering, (n,mn) neutron multiplying reaction emitting m neutrons, $(n,n'X)$ neutron and charged particle emission. If we define the production cross section by

$$\sigma_{pr}(E)=\sigma_{el}(E)+\sum_i\sigma_{in,i}(E)+\sum_m m\sigma_{n,mn}(E)+\sum_X\sigma_{n,n'X}(E). \tag{2-2}$$

Equation (2-1) can be written as

$$q(r,\Omega,E)=\int dE'\int d\Omega'\Psi(r,\Omega',E')\times\sum_j N_j\ \{\sigma_{pr}^j(E')\sum_x R_x^j(E')P_x^j(\mu;E'\to E)\}\ , \tag{2-3}$$

where

$$\mu=\Omega\cdot\Omega' \text{ and } R_x(E')=m_x\,\sigma_x(E')/\sigma_{pr}(E').$$

$P_x(\mu;E'\to E)$ is the energy-angle distribution of neutrons emitted from the reaction x. Summation over all reaction types is reduced to the double-differential form cross section:

$$\sigma_x(\mu;E'\to E)=\sigma_{pr}(E')\sum_x R_x(E')P_x(\mu;E'\to E)=\sigma_{pr}(E')I(\mu;E'\to E), \tag{2-4}$$

where

$$I(\mu;E'\to E)=\sum_x R_x(E')P_x(\mu;E'\to E)\cdot \tag{2-5}$$

The energy-angle distribution function $P_x(\mu;E'\to E)$ can be written as

$$P_x(\mu;E'\to E)=g_x(E;E')h_x(\mu;E',E), \tag{2-6}$$

where $g_x(E;E')$ is an energy distribution of secondary neutron and $h_x(\mu;E'\to E)$ an angular distribution of this neutron. These functions can be calculated based on the kinematics, if it is known, as follows:

$$g_x(E;E')=\frac{f_x(\mu_c;E')}{2\pi}\left|\frac{d\mu_c}{dE}\right|=\frac{f_x(\mu_c;E')}{2\pi}\frac{2}{(1-\alpha)E'\beta_x(E')}, \tag{2-7}$$

$$h_x(\mu;E',E)=\delta(\mu-\mu_x^*) \tag{2-8}$$

where f_x is an angular distribution in the center of mass (CM) system, and

$$\alpha=\left(\frac{A-1}{A+1}\right)^2, \tag{2-9}$$

$$\mu_c=\left\{\frac{(A+1)^2}{2A}\frac{E}{E'}-\frac{A}{2}\beta(E')^2-\frac{1}{2A}\right\}\frac{1}{\beta_x(E')}\ , \tag{2-10}$$

$$\mu_x^* = \frac{A+1}{2}\sqrt{\frac{E}{E'}} - \frac{A-1}{2}\sqrt{\frac{E'}{E}} - \frac{AQ_x}{2\sqrt{EE'}}, \tag{2-11}$$

$$\beta_x(E') = \sqrt{1+\frac{A+1}{A}\frac{Q_x}{E'}}. \tag{2-12}$$

In these equations, A and Q_x are the ratio of the mass of the target atom to that of neutron and the Q-value of reaction x, respectively. When the kinematics are not known, functions g_x and h_x are given in Files 4 and 5 of evaluated data file with ENDF/B format, respectively, or $P_x(\mu;E'\to E)$ is given explicitly in File 6.

2.2 Calculation of Multi-Group Double-Differential Form Cross Section

The multi-group form of energy-angle distribution of secondary neutrons from the reaction x within the g-th energy group in the k-th angular interval $P_x(k;g'\to g)$ is obtained by

$$P_x(k;g'\to g) = \frac{\int_{\Delta_{g'}} dE' \int_{\Delta_g} dE \int_{\Delta\mu_k} 2\pi d\mu \sigma_x(E') P_x(\mu;E'\to E)\Psi_w(E')}{\int_{\Delta E_{g'}} dE'\sigma_x(E')\Psi_w(E')}, \tag{2-13}$$

where $\Psi_w(E)$ is a weighting function. When the kinematics for reaction x are known, Eq. (2-13) can be calculated as follows:

$$\begin{aligned} P_x(k;g'\to g) &= \frac{1}{\sigma_{xg'}\Psi_{wg'}} \int_{E_{g'+1}}^{E_{g'}} dE' \int_{E_{g+1}}^{E_g} dE \int_{\mu_{k+1}}^{\mu_k} 2\pi d\mu\ \sigma_x(E') \frac{f_x(\mu_c;E')}{2\pi} \\ &\times \frac{2}{(1-\alpha)E'\beta(E')}\ \delta(\mu-\mu_x^*)\Psi_w(E') \\ &= \frac{1}{\sigma_{xg'}\Psi_{wg'}} \int_{E_{g'+1}}^{E_{g'}} dE' \int_{E_{g+1}}^{E_g} dE\ \sigma_x(E') f_x(\mu_c;E')\Psi_w(E') \\ &\times \frac{2}{(1-\alpha)E'\beta_x(E')} \\ &\times \left[H(\mu_k-\mu_x^*(E',E)) - H(\mu_{k+1}-\mu_x^*(E',E))\right], \end{aligned} \tag{2-14}$$

where H is the Heaviside step function defined by

$$H(x) = \begin{cases} 1, & \text{if } x \geqq 0 \\ 0, & \text{if } x < 0. \end{cases}$$

In the PROF-DD system, it is assumed that

$$f_x(\mu_c;E') = f_{xg'}(\mu_c) \text{ (=constant within the g'-th group).}$$

This assumption seems reasonable since no large variation is found in the angular distribution of secondary neutrons within an energy group. When $\mu-\mu_x^*(E',E)=0$,

$$E' = \frac{E}{(A-1)^2}\left\{\mu - \sqrt{A^2-1-A(A-1)\frac{Q_x}{E}+\mu^2}\right\}. \tag{2-15}$$

This relation is plotted in **Fig. 2.1** for some values of μ. The integrand in Eq. (2-14) has non-zero values in the region between the two curves assigned by $\mu=\mu_k$ and $\mu=\mu_{k+1}$. Therefore the integration with respect to E' and E is carried out in the hatched region in this figure, for instance.

As for the reactions such as continuum inelastic scattering, the integration with respect to E and μ can be carried out separately as follows:

$$P_x(k;g'\to g) = P_1(k;g')\cdot P_2(g;g'), \tag{2-16}$$

where

$$P_1(k;g') = \int_{\Delta E_{g'}} dE' \int_{\Delta\mu_k} d\mu\ h_x(\mu;E')\sigma_x(E')\Psi_w(E')/\sigma_{xg'}\Psi_{wg'}, \tag{2-17}$$

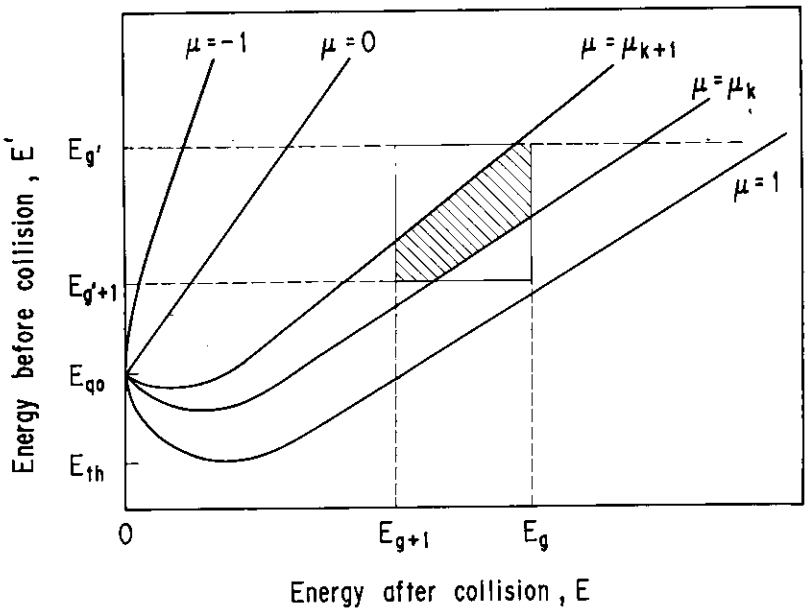

$$E_{qo} = \frac{A}{A-1} Q$$

$$E_{th} = \frac{A+1}{A} Q$$

Fig. 2.1 Diagram for illustrating the scattering kinematics in the (E, E') plane and the integration limits in the calculation of multi-group DDX.

$$P_l(g;g') = \int_{\Delta E_{g'}} dE' \int_{\Delta E_g} dE\ g_x(E;E')\sigma_x(E')\Psi_w(E')/\sigma_{xg'}\Psi_{wg'}. \tag{2-18}$$

The factor $\sigma_x(E')\Psi_w(E')$ in these two equations is assumed to be constant. Instead of Eq. (2-16), if required, we can adopt the following probability calculated with additional assumption that no neutron emerges in the direction k from the scattering reaction with higher energy than E^*_{max}, which is determined on the basis of the two-body reaction kinematics. With this assumption, the probability of Eq. (2-16) is modified as follows:

$$P_x(k;g' \to g) = 0.0 \quad \text{for all } g \text{ such that } E_{g-1} \geqq E^*_{max}, \tag{2-19}$$

and they are renormalized as

$$\sum_g P_x(k;g' \to g) = P_l(k;g'). \tag{2-20}$$

If $P_x(\mu;E' \to E)$ is explicitly given in the evaluated data file (File 6), this probability can be processed as follows: At first,

$$P_x(\mu;g' \to g) = \int_{\Delta E_{g'}} dE' \int_{\Delta E_g} dE\ P_x(\mu;E' \to E)\sigma_x(E')\Psi_w(E')/\sigma_{xg'}\Psi_{wg'}, \tag{2-21}$$

then

$$P_x(k;g \to g') = \int_{\Delta\mu_k} d\mu\ P_x(\mu;g' \to g). \tag{2-22}$$

In the PROF-DD system, the lowest energy group is assigned to the thermal neutron group. The energy-angle distribution of neutrons scattered into this group is automatically calculated, though several optional procedures are prepared for the calculation of the self-group scattering cross section as mentioned in Chapter 3.

By using $P_x(k;g' \to g')$, the multi-group DDX is written as

$$\sigma_s(k;g' \to g) = \sigma_{pr,g'} I(k;g' \to g), \tag{2-23}$$

where I is the energy-angle distribution calculated by

$$I(k;g'\to g)=\sum_x R_x(g')P_x(k;g'\to g). \tag{2-24}$$

2.3 Formulation of Collision Source with Use of DDX Library

In the transport calculation, only the collision source term differs from the conventional one when the DDX is used. The collision term of Eq. (2-1) is rewritten by using the DDX as

$$q_g(r,\Omega)=\sum_{g'}\int d\Omega'\psi_{g'}(r,\Omega')\frac{\Sigma_S^J(k;g'\to g)}{2\pi\Delta\mu_k}, \tag{2-25}$$

where k indicates an angle bin such that $\mu_{k+1}<\Omega\cdot\Omega'<\mu_k$ and $\Delta\mu_k=\mu_k-\mu_{k+1}$, and $\Sigma_S^J(k;g'\to g)$ is the macroscopic DDX of material J calculated by

$$\Sigma_S^J(k;g'\to g)=\sum_j N\sigma_s^j(k;g'\to g),$$

$$=\sum_j N\sigma_{pr,g'}^j F^j(k;g'\to g). \tag{2-26}$$

In the S_n transport code, Eq. (2-25) is calculated as follows:

$$q_{g,m}=\sum_{g'}\sum_{m'}\psi_{g',m'}\cdot w_{m'}\cdot\sum_k\frac{\Sigma_s^J(k;g'\to g)}{2\pi\Delta\mu_k}$$

$$\times\frac{1}{4\pi w_{m'}\cdot w_m}\int_{\Delta\Omega_{m'}}d\Omega'\int_{\Delta\Omega_m}d\Omega\delta_{\mu^*,k}, \tag{2-27}$$

where

$$\delta_{\mu^*,k}=\begin{cases}1 & \text{for } \mu_{k-1}\leqq\mu^*=\Omega\cdot\Omega'\leqq\mu_k\\ 0 & \text{otherwise,}\end{cases}$$

and m and w_m denote the quadrature direction and its weight, respectively. $\Delta\Omega_m$ is a solid angle corresponding to the direction m and given by $\Delta\Omega_m=4\pi w_m$. Note that $q_{g,m}$ and $\phi_{g',m'}$ in Eq. (2-27) are the scattering source and angular flux per unit weight, respectively. Equation (2-27) is rewritten as

$$q_{g,m}=\sum_{g'}\sum_{m'}\phi_{g',m'}\cdot w_{m'}\cdot\sum_k\Sigma_S^J(k;g'\to g)\times P(k,m',m)$$

$$=\sum_{g'}\sum_{m'}\phi_{g',m'}\cdot w_{m'}\cdot\Sigma^J(g'\to g,m'\to m), \tag{2-28}$$

where $P(k,m',m)$ is the angular transfer probability defined by

$$P(k,m',m)=\frac{1}{2\pi\Delta\mu_k}\frac{4\pi}{\Delta\Omega_{m'}\cdot\Delta\Omega_m}\int_{\Delta\Omega_{m'}}d\Omega'\int_{\Delta\Omega_m}d\Omega\,\delta_{\mu^*,k}, \tag{2-29}$$

and $\Sigma^J(g'\to g,m'\to m)$ is the scattering kernel matrix defined by

$$\Sigma^J(g'\to g,m'\to m)=\sum_k\Sigma_S^J(k;g'\to g)\times P(k,m',m). \tag{2-30}$$

The angular transfer probability P is symmetric for the indeces m and m', and it satisfies the following relations.

$$\sum_k\frac{\Delta\mu_k}{2}P(k,m',m)=1 \qquad \text{for all } m' \text{ and } m, \tag{2-31}$$

$$\sum_m w_m P(k,m',m)=1 \qquad \text{for all } m' \text{ and } k, \tag{2-32}$$

$$\sum_{m'}\sum_{m} w_{m'} w_m P(k,m',m) = 1 \qquad \text{for all } k. \tag{2-33}$$

In the Monte Garlo calculation, the scattering angle and secondary energy group are directly determined from the energy-angle distribution $I(k;g' \rightarrow g)$, as described in Chapter 6.

2.4 Available DDX Library

The multi-group DDX libraries DDL/B4 and DDL/J3P1 have been produced from ENDF/B-IV[12] and JENDL-3PR1[13] by using the PROF-DD code system. The JENDL-3PR1 nuclear data have been evaluated and released for fusion neutronics applications as a preliminary version of JENDL-3. The number of energy group is 125, and 20 equi-cosine bins are employed as the angular mesh. In the production of the library, a 1/E spectrum above 0.32 eV and the Maxwellian below this energy are used as a weighting function. The details have been described in Reference 4, where this library is named as DDXLIB3. Note that the last group is assigned to a thermal group and the cross sections of this group can be replaced with those given by a user in a transport calculation. The energy group structure and the identification number for each nuclide are shown in **Tables 2.1** and **2.2**, respectively. This library contains production, fission, capture, $\nu *$ fission, total cross sections and the energy-angle distributions of secondary neutrons for each nuclide. The format of the library is described in Section 3.6.3.

Table 2.1 Structure of 125-group double-differential form cross section library

Group	Energy range	Lethargy width	Group	Energy range	Lethargy width
1	1.6487E+07 – 1.6231E+07	0.015625	32	1.0157E+07 – 9.9999E+06	0.015625
2	1.6231E+07 – 1.5980E+07	0.015625	33	9.9999E+06 – 9.3940E+06	0.06250
3	1.5980E+07 – 1.5732E+07	0.015625	34	9.3940E+06 – 8.8249E+06	0.06250
4	1.5732E+07 – 1.5488E+07	0.015625	35	8.8249E+06 – 8.2902E+06	0.06250
5	1.5488E+07 – 1.5248E+07	0.015625	36	8.2902E+06 – 7.7879E+06	0.06250
6	1.5248E+07 – 1.5012E+07	0.015625	37	7.7879E+06 – 7.3161E+06	0.06250
7	1.5012E+07 – 1.4779E+07	0.015625	38	7.3161E+06 – 6.8728E+06	0.06250
8	1.4779E+07 – 1.4550E+07	0.015625	39	6.8728E+06 – 6.4564E+06	0.06250
9	1.4550E+07 – 1.4324E+07	0.015625	40	6.4564E+06 – 6.0652E+06	0.06250
10	1.4324E+07 – 1.4102E+07	0.015625	41	6.0652E+06 – 5.6978E+06	0.06250
11	1.4102E+07 – 1.3883E+07	0.015625	42	5.6978E+06 – 5.3525E+06	0.06250
12	1.3883E+07 – 1.3668E+07	0.015625	43	5.3525E+06 – 5.0282E+06	0.06250
13	1.3668E+07 – 1.3456E+07	0.015625	44	5.0282E+06 – 4.7236E+06	0.06250
14	1.3456E+07 – 1.3248E+07	0.015625	45	4.7236E+06 – 4.4374E+06	0.06250
15	1.3248E+07 – 1.3042E+07	0.015625	46	4.4374E+06 – 4.1686E+06	0.06250
16	1.3042E+07 – 1.2840E+07	0.015625	47	4.1686E+06 – 3.9160E+06	0.06250
17	1.2840E+07 – 1.2641E+07	0.015625	48	3.9160E+06 – 3.6787E+06	0.06250
18	1.2641E+07 – 1.2445E+07	0.015625	49	3.6787E+06 – 3.4559E+06	0.06250
19	1.2445E+07 – 1.2252E+07	0.015625	50	3.4559E+06 – 3.2465E+06	0.06250
20	1.2252E+07 – 1.2062E+07	0.015625	51	3.2465E+06 – 3.0498E+06	0.06250
21	1.2062E+07 – 1.1875E+07	0.015625	52	3.0498E+06 – 2.8650E+06	0.06250
22	1.1875E+07 – 1.1691E+07	0.015625	53	2.8650E+06 – 2.6914E+06	0.06250
23	1.1691E+07 – 1.1510E+07	0.015625	54	2.6914E+06 – 2.5284E+06	0.06250
24	1.1510E+07 – 1.1331E+07	0.015625	55	2.5284E+06 – 2.3752E+06	0.06250
25	1.1331E+07 – 1.1156E+07	0.015625	56	2.3752E+06 – 2.2313E+06	0.06250
26	1.1156E+07 – 1.0983E+07	0.015625	57	2.2313E+06 – 2.0961E+06	0.06250
27	1.0983E+07 – 1.0812E+07	0.015625	58	2.0961E+06 – 1.9691E+06	0.06250
28	1.0812E+07 – 1.0645E+07	0.015625	59	1.9691E+06 – 1.8498E+06	0.06250
29	1.0645E+07 – 1.0480E+07	0.015625	60	1.8498E+06 – 1.7377E+06	0.06250
30	1.0480E+07 – 1.0317E+07	0.015625	61	1.7377E+06 – 1.5335E+06	0.12500
31	1.0317E+07 – 1.0157E+07	0.015625	62	1.5335E+06 – 1.3533E+06	0.12500

Table 2.1 (Continued)

Group	Energy range	Lethargy width	Group	Energy range	Lethargy width
63	1.3533E+06 – 1.1943E+06	0.12500	95	2.4787E+04 – 2.1874E+04	0.12500
64	1.1943E+06 – 1.0540E+06	0.12500	96	2.1874E+04 – 1.9304E+04	0.12500
65	1.0540E+06 – 9.3013E+05	0.12500	97	1.9304E+04 – 1.5034E+04	0.25000
66	9.3013E+05 – 8.2083E+05	0.12500	98	1.5034E+04 – 1.1709E+04	0.25000
67	8.2083E+05 – 7.2438E+05	0.12500	99	1.1709E+04 – 9.1186E+03	0.25000
68	7.2438E+05 – 6.3927E+05	0.12500	100	9.1186E+03 – 7.1016E+03	0.25000
69	6.3927E+05 – 5.6415E+05	0.12500	101	7.1016E+03 – 5.5307E+03	0.25000
70	5.6415E+05 – 4.9786E+05	0.12500	102	5.5307E+03 – 4.3073E+03	0.25000
71	4.9786E+05 – 4.3936E+05	0.12500	103	4.3073E+03 – 3.3546E+03	0.25000
72	4.3936E+05 – 3.8774E+05	0.12500	104	3.3546E+03 – 2.6125E+03	0.25000
73	3.8774E+05 – 3.4218E+05	0.12500	105	2.6125E+03 – 2.0346E+03	0.25000
74	3.4218E+05 – 3.0197E+05	0.12500	106	2.0346E+03 – 1.5846E+03	0.25000
75	3.0197E+05 – 2.6649E+05	0.12500	107	1.5846E+03 – 1.2341E+02	0.25000
76	2.6649E+05 – 2.3517E+05	0.12500	108	1.2341E+03 – 9.6109E+02	0.25000
77	2.3517E+05 – 2.0754E+05	0.12500	109	9.6109E+02 – 5.8293E+02	0.50000
78	2.0754E+05 – 1.8315E+05	0.12500	110	5.8293E+02 – 3.5357E+02	0.50000
79	1.8315E+05 – 1.6163E+05	0.12500	111	3.5357E+02 – 2.1445E+02	0.50000
80	1.6163E+05 – 1.4264E+05	0.12500	112	2.1445E+02 – 1.3007E+02	0.50000
81	1.4264E+05 – 1.2588E+05	0.12500	113	1.3007E+02 – 7.8891E+01	0.50000
82	1.2588E+05 – 1.1109E+05	0.12500	114	7.8891E+01 – 4.7850E+01	0.50000
83	1.1109E+05 – 9.8035E+04	0.12500	115	4.7850E+01 – 2.9023E+01	0.50000
84	9.8035E+04 – 8.6515E+04	0.12500	116	2.9023E+01 – 1.7603E+01	0.50000
85	8.6515E+04 – 7.6349E+04	0.12500	117	1.7603E+01 – 1.0677E+01	0.50000
86	7.6349E+04 – 6.7378E+04	0.12500	118	1.0677E+01 – 6.4758E+00	0.50000
87	6.7378E+04 – 5.9461E+04	0.12500	119	6.4758E+00 – 3.9278E+00	0.50000
88	5.9461E+04 – 5.2474E+04	0.12500	120	3.9278E+00 – 2.3823E+00	0.50000
89	5.2474E+04 – 4.6308E+04	0.12500	121	2.3823E+00 – 1.4449E+00	0.50000
90	4.6308E+04 – 4.0867E+04	0.12500	122	1.4449E+00 – 8.7640E−01	0.50000
91	4.0867E+04 – 3.6065E+04	0.12500	123	8.7640E−01 – 5.3157E−01	0.50000
92	3.6065E+04 – 3.1827E+04	0.12500	124	5.3157E−01 – 3.2241E−01	0.50000
93	3.1827E+04 – 2.8087E+04	0.12500	125	3.2241E−01 – 1.0010E−05	10.38000
94	2.8087E+04 – 2.4787E+04	0.12500			

Table 2.2 Identification number of nuclides prepared in 125-group DDL/B4 and /J3P1 libraries*

Element	ID number		Element	ID number	
	ENDF/B4	JENDL-3PR1		ENDF/B4	JENDL-3PR1
H	1269		Si	1194	
^{6}Li	1271	306	K	1150	
^{7}Li	1272	307	Ca	1195	
^{12}C	1274	612	Cr	1191	2400
^{9}Be	1289	409	Fe	1192	2600
^{14}N	1275		Ni	1190	2800
^{16}O	1276	816	^{55}Mn	1197	
^{23}Na	1156		Cu	1295	
Mg	1280		Mo	1287	
^{27}Al	1193		Pb	1288	

* This library is called as DDXLIB3 in Reference 4.
Weighting spectrum : Maxwellian <0.32 eV,
1/E >0.32 eV.

3. PROF–DD : Multi–Group DDX Library Generation Code System

3.1 General Feature of PROF–DD

A flow chart of the PROF–DD system is shown in **Fig. 3.1**. This system consists of five steps corresponding to five independent codes. In this chapter, the descriptions are given for each step in the order of calculation flow. The outline of each step is as follows:

MCFILEF : A control file for the PROF–DDX code, which contains energy group and angle bin structures of produced DDX, is generated by the MCFILEF code. A user should run this code prior to executing the following job.

RESENDD : Doppler broadened pointwise cross sections of one nuclide specified by an input data is prepared as a PROF–DDX input file. The RESENDD code which is a modified version of RESEND is used in this step. This code can be replaced by another one which has a similar function, for example, a set of the modified LINEAR, RECENT and SIGMA1 codes[15),16)].

SPINPTF : The SPINPTF code prepares an input data file for the PROF–DDX code by combining the control file and other input data. Some parameters assigned by the MCFILEF code can be changed in this step. A weighting function is produced from the data in the control file or read from an input file.

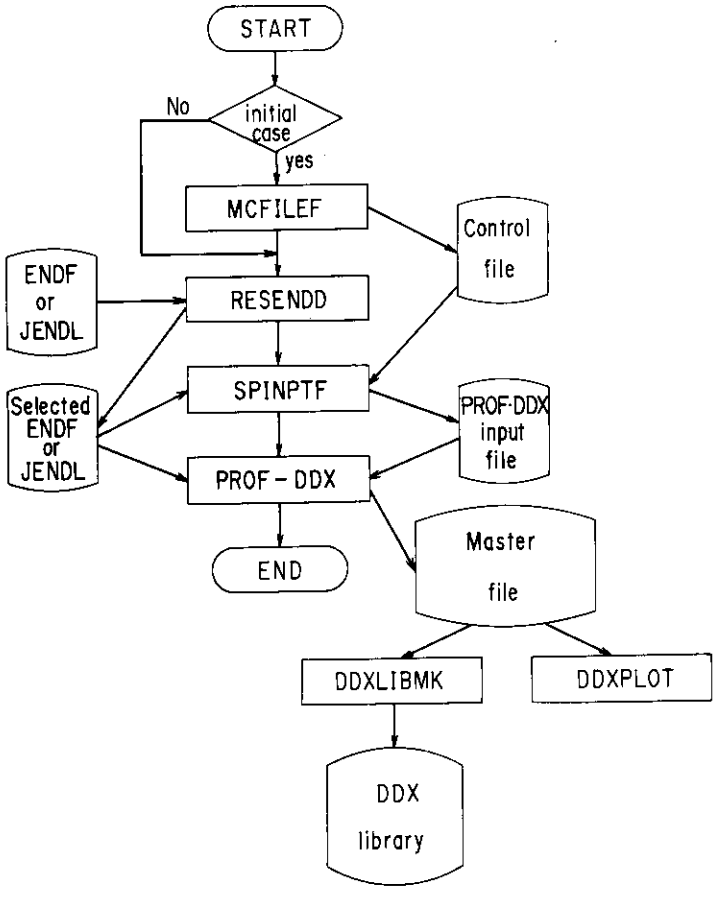

Fig. 3.1 Flow chart of the PROF–DD system.

PROF-DDX : The PROF-DDX code is a main code in this system. This code calculates multigroup cross sections and energy-angle distributions (DDX). The calculated DDX are saved on a master PDS (Partitioned Data Set with undefined record format) file with a member name assigned by the code.

DDXLIBMK : The DDXLIBMK code reads the DDX in a master file and edits a DDX library in a specified format for a transport code such as the MORSE-DD code. This code can also print out the DDX data in the master file.

This system has the following functions:

(1) Production of multi-group DDX library

Type of processed reactions

(i) File 4 + kinematics

elastic scattering	(MT=2)
(n,2n) first emitted neutron	(MT=6-9)
discrete level inelastic scattering	(MT=51-90)

(Two optional procedures are available. See 3.2.1)

(ii) File 4 + File 5*

(n,2n) direct	(MT=16)
(n,3n)	(MT=17)
(n,n'α)	(MT=22)
(n,n'3α)	(MT=23)
(n,2nα)	(MT=24)
(n,3nα)	(MT=25)
(n,n'p)	(MT=28)
(n,2n) 2nd neutron	(MT=46-49)
continuum level inelastic scattering	(MT=91)

*File 6 can be processed if it is available.

(Four optional procedures are available. See 3.2.1)

(iii) Absorption reaction

MT=102-109, 111-114

(iv) Fission reaction

MT=18

Weighting function

(i) Maxwellian + $1/E^{\alpha}$ + fission spectrum

(ii) Maxwellian + $1/E^{\alpha}$ + Gaussian

(iii) Arbitrary spectrum

(2) Production of cross section library for reaction rate calculation

Type of reaction ; any reaction specified by a user

Weighting function ; the same as in (1)

3.2 MCFILEF

The MCFILEF code prepares a control file for the PROF-DDX code. This file contains some parameters such as energy group and angle bin structures of produced DDX, which are commonly used in calculating DDX for each nuclide. Some parameters to determine a weighting function are set by the MCFILEF code. The following process is carried out:

(1) Parameters which define a produced DDX library are read from card-image input and written on a control file.

(2) Consistency among input data is checked.

(3) Energy group and angle bin structures are stored in a master PDS file with member names fixed by the code as follows:

BPDSHD01 : number of energy groups,

BPDSHD02 : energy group boundaries,

BPDSHD03 : number of angle bins,

BPDSHD04 : angle bin boundaries.

3.2.1 Input Instruction

The following FORTRAN77 free-formatted data are read from card-image input on the I/O unit 5.

CARD A (*)

1) NGRMX number of energy groups ($1 \leqq NGRMX \leqq 150$)

2) MAXMU number of angle bins ($1 \leqq MAXMU \leqq 40$)

3) IEOPT input option for energy group structure

$\leqq 0$, energy boundaries are given from high to low energy in eV unit.

$\geqq 1$, maximum energy and lethargy widths are given.

4) ISW option for defining angle bin boundaries

$=-1$, arbitrary angle bin boundaries are read from card-image input.

$=0$, angle bins with equal width of $\cos\theta$ ($\Delta\mu_k = 2/MAXMU$) are defined by the code.

$=1$, angle bins with equal width of θ ($\Delta\theta_k = \pi/MAXMU$) are defined by the code.

5) NO40 option for treatment of the NGRMX-th group (thermal energy group)

$=-2$, NGRMX-group DDX library is produced with reaction cross sections of the NGRMX-th group which are read from card-image input on the I/O unit 5. Isotropic scattering is assumed in this group.

$=-1$, NGRMX-group DDX library is produced with reaction cross sections of the NGRMX-th group which are calculated by the PROF-DDX code. Isotropic scattering is assumed in this group.

$=0$, (NGRMX-1)-group DDX library is produced with slowing down cross sections to the NGRMX-th group, i.e. (NGRMX-1) reaction cross sections and (MGRMX-1) * NGRMX * MAXMU/2 self- and down-scattering probabilities are calculated.

$=1$, (NGRMX-1)-group DDX library is produced. The slowing down cross sections to the NGRMX-th group is added to the self-group scattering of the (NGRMX-1)-th group.

6) IUP2 option for calculation of energy-angle distribution based on kinematics

$=1$, collision density within a group is assumed to be constant in lethargy.

$=2$, collision density is calculated by $\sigma_x(E')\Psi_w(E')$.

7) IF45 option for calculation of energy-angle distribution from File 4 and 5 or File 6

$=1$, isotropic scattering in the laboratory system is assumed.

$=2$, angular distribution is taken from File 4.

$=3$, angular distribution is taken from File 4 and scattering probability is set to be 0.0 for neutron emitted with higher energy than that determined by the two-body reaction kinematics in each direction.

$=4$, energy-angle distribution is obtained by integrating the energy-angle distribution data in File 6 if they are given. When they are not given, IF45 is set to be 2 by the PROF-DDX code.

(*) means FORTRAN77 free-formatted input.

8) IPDS option for output on a master PDS file
=0, no effect
=1, numbers of energy groups and angle bins, energy group and angle bin structures are stored with the member names fixed by the MCFILEF code.

CARD B (*) (Enter if IEOPT≦0)
(EN(i), i=1, NGRMX+1) energy boundaries from high to low (eV)

CARD C (*) (Enter if IEOPT≧1)
1) EMAX upper energy boundary of 1st group (eV)
2) (Du(i), i=1, MGRMX) lethargy width of group i
It is required that Du(i)=2^n * Du(1), where n is an integer except for i= MGRMX.

CARD D (*) (Enter if ISW=−1)
(TABMU(i), i=1, MAXMU+1) angle meshes from +1 to −1

CARD E (*)
$E_1, E_2, T, \alpha, A_1, A_2$ parameters to define a weighting function
The SPINPTF code generates a weighting function $\Psi_w(E)$ as follows:

$\Psi_w(E) = C_1 E \exp(-E/kT)$ $(E \leqq E_1)$
$\Psi_w(E) = 1/E^{\alpha}$ $(E_1 \leqq E \leqq E_2)$
$\Psi_w(E) = C_2 \exp(-E/A_1)\sinh\sqrt{A_2 E}$ $(E \geqq E_2$ and $A_2 > 0)$
$\Psi_w(E) = C_2 \exp\left[-\{(E-A_1)/(0.426609A_2)\}^2/2\right]$ $(E \geqq E_2$ and $A_2 < 0)$

where C_1 and C_2 are determined from the continuous condition. If E_1=0.0, then the following values are adopted:
$E_1 = 10^{-5}$, $E_2 = 2\times10^{+7}$, T=300, α=1.0, $A_1 = 10^{+6}$, $A_2 = 2\times10^{-6}$.
If an arbitrary spectrum is used as a weighting function, this is read in by the SPINPTF code instead of using Ψ_w shown above.

CARD F (*)
EPSPR error criterion
If $R_{xg'} <$ EPSPR, $R_{xg'}$ is set 0.0. If $I(k;g' \to g) <$ EPSPB(=EPSPR^2), I is set 0.0. After checking, these values are recalculated.

3.2.2 Sample Input, JCL and I/O Files

The I/O files used in the MCFILEF code are shown in **Fig. 3.2**. A list of sample input and Job Control Language (JCL) to produce the DDL/B4 and J3P1 libraries is given in **Fig. 3.3**.

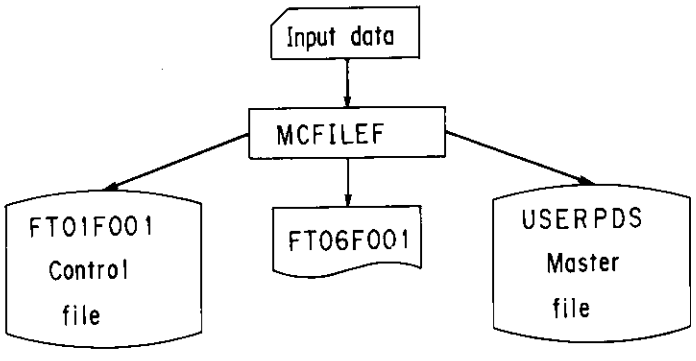

Fig. 3.2 I/O files for MCFILEF.

```
//JCLG  JOB
// EXEC JCLG
//SYSIN DD DATA,DLM='++'
// JUSER XXXXXXXX,TA.MORI,0431.110
 T.1 C.0 W.0 I.3
 OPTP MSGCLASS=R,PASSWORD=XX
//************ 'J3803.DDX.CNTL(MCFILEF)' ********************************
//*                                                                      *
//*          ****************************                                *
//*          *       M C F I L E F      *                                *
//*          ****************************                                *
//*                                                                      *
//MCFILEF  EXEC LMGO,LM='J3803.PROFDD',PNM=MCFILEF
//*-------  USERPDS  : MASTER FILE  -----------------------------------
//USERPDS DD DSN=J3803.DDXLIB3.PDS125G.DATA,DISP=MOD
//*
//*-------  FT01F001 : CONTROL FILE -----------------------------------
//FT01F001 DD DSN=J3803.DDXLIB3.CNTL.DATA,DISP=OLD
//*
//SYSIN DD *
  125 20 1 0 -1 2 2 1  / #A
 1.6487E+07  32(0.015625) 28(0.0625) 36(0.125) 12(0.25) 16(0.5) 10.38/#C
 3.2241E-1  2.E+7   300.   1.   1.E+06   2.E-6 / #E WEIGHTING FUNCTION
  1.E-10 / #F
++
//
```

Fig. 3.3 Sample JCL and input data for MCFILEF.

3.3 RESENDD

The RESENDD code selects one nuclide from the ENDF/B formatted data file and performs resonance cross section and Doppler broadening calculations to produce temperature dependent pointwise cross section data file. This code has been developed by Nakagawa[14] . The details of this code is given in Reference 14. Some parameters which should be specified to run the PROF-DD system are described briefly in this section together with input instructions and sample JCL. The RESENDD code can be replaced by computer codes which have similar functions, for example, the LINEAR, RECENT and SIGMA1 codes[15),16)], of which the description is given in Appendix 2. We recommend to use the latter set of codes in processing the data of some nuclides like hydrogen for which the evaluated cross sections are given at sparse energy points in the lower energy region ($<$ 100 keV). The RESENDD code might give unreasonable Doppler broadened cross sections for such nuclides since this code adds no new energy points in the Doppler broadening calculation whether they are necessary or not to keep the accuracy.

3.3.1 Input Instruction for the PROF-DD System

The parameters which should be specified are as follows.

1) Job-condition data

Job-condition inputs for RESENDD should be entered in a form of "Parameter name = value". The parameters which should be specified are as follows:

MAT ; MAT number to be selected
TEMP ; temperature in Kelvin
ERR ; accuracy of calculation
LSIG(=1E-10); option on negative cross sections
OUTF (=2) ; data set reference number of an output file
FORM ; format of an input file
4 : ENDF/B-IV Format
5 : ENDF/B-V Format

OFORM (=4) ; format of an output file
OPT (=2) ; output option

Values in parentheses are standard values for this system. It should be noted that the present version of PROF-DDX can process the data for a number of energy points less than 100,000. A user has to set ERR by which RESENDD produces energypoints less than 100,000. If more points than 100,000 are generated, the job is terminated by printing error messages at the following step (SPINPTF).

2) LABEL statement
3) Title (66A1)
4) GO statement
5) EOF statement
6) STOP statement

3.3.2 Sample Input, JCL and I/O Files

The following is a sample input for the RESENDD code used in the system.

```
//SYSIN DD *
MAT=1272, TEMP=300.0, ERR=0.01, LSIG=1.E-10, OPT=2, FORM=4, OFORM=4,
OUTF=2
LABEL
  7-LI ENDF/B-IV
GO
EOF
STOP
/*
```

Figure 3.4 shows a sample JCL for a continuous run of the RESENDD, SPINPTF and PROF-DDX codes. The I/O files used in the RESENDD code are shown in **Fig. 3.5**.

3.4 SPINPTF

The SPINPTF code produces an input data file for the PROF-DDX code from the control file generated by the MCFILEF code. The following process is carried out:

(1) The SPINPTF code sets up input parameters for the PROF-DDX code based on the control file and other data read from card-image input.
(2) A weighting function is calculated or read from a file.
(3) An input file for the PROF-DDX code is prepared.

3.4.1 Input Instruction

One line is read from card-image input on the I/O unit 5 by the SPINPTF code with the FORTRAN77 free format.

CARD A (*)

1) IPRINT output option
   = 0, brief print
   = 1, detailed print (a lot of outputs)
2) IFLXW option on a weighting function
   = 0, a weighting function is calculated with parameters in the control file as described in Section 3.1.
   = N, a weighting function is read from a file (I/O unit N).
3) IUP2 option for calculation of DDX based on kinematics

```
//JCLG  JOB
// EXEC JCLG
//SYSIN DD DATA,DLM='++'
// JUSER  XXXXXXXX,T.MORI,0431.110
   T.5 C.5 W.2 P.0 I.4
 OPTP  MSGCLASS=R,PASSWORD=XX
//******      'J3803.DDX.CNTL(PROFUP)'     ***********
//*PROC=J2608.PROCLIB.CNTL
//*
//*  ***********************************************
//*  ****                                       ****
//*  ****            R E S E N D D              ****
//*  ****                                       ****
//*  ***********************************************
//*
//RESENDD  EXEC RESENDD
//*---------  FT01F001 : ENDF/B      ---------------------------------
//FT01F001 DD DSN=J3770.J3PR1.DATA(LI6),LABEL=(,,,IN),DISP=SHR
//*
//*---------  FT02F001 : SELECTED ENDF/B POINTWISE DATA  --------------
//FT02F001 DD DSN=&&BTOB,SPACE=(TRK,(100,10)),DISP=(NEW,PASS),
//   DCB=(RECFM=FB,LRECL=80,BLKSIZE=3200,BUFL=3200,DSORG=PS),UNIT=WK10
//*
//SYSIN DD *
 MAT= 306,TEMP=300.0,ERR=0.01,LSIG=1.E-10,OUTF=2,OPT=2,FORM=4,OFORM=4
LABEL
LI-6J3
GO
EOF
STOP
/*
//*
//*  ***********************************************
//*  ****                                       ****
//*  ****            S P I N P T F              ****
//*  ****                                       ****
//*  ***********************************************
//*
//SPINPTM  EXEC LMGO,LM='J3803.PROFDD',PNM=SPINPTFL
//*---------  FT01F001 : CONTROL FILE FROM MCFILEF  -------------------
//FT01F001 DD DSN=J3803.DDXLIB3.CNTL.DATA,DISP=SHR,LABEL=(,,,IN)
//*
//*---------  FT02F001 : SELECTED ENDF/B POINTWISE DATA FROM RESENDD --
//FT02F001 DD DSN=&&BTOB,DISP=(OLD,PASS)
//*
//*---------  FT08F001 : INPUT DATA FILE FOR PROFDDX  -----------------
//FT08F001 DD DSN=&&DATA,SPACE=(TRK,(100,10)),DISP=(NEW,PASS),
//   DCB=(RECFM=FB,LRECL=80,BLKSIZE=3200,BUFL=3200,DSORG=PS),UNIT=WK10
//*
//SYSIN  DD  *
  0 0 0 0  0.0              / IPRNT IFLXW IUP2 IF45 EPSPR
/*
//*
//*  ***********************************************
//*  ****                                       ****
//*  ****           P R O F - D D X             ****
//*  ****                                       ****
//*  ***********************************************
//*
// EXEC ANY
//PROFDDX  EXEC LMGO,LM='J3803.PROFDD',PNM=PROFDDXL,OBSIZE=137
//*---------  FT05F001 : INPUT DATA FILE FROM SPINPTF  ----------------
//FT05F001 DD DSN=&&DATA,DISP=(OLD,DELETE)
//*
//*---------  PDSOUT1  : MASTER PDS FILE ( DDX )  ---------------------
//*          PDSOUT2  : PDS FILE ( REACTION CX DATA )
//PDSOUT1  DD DSN=J3803.DDXLIB3.PDS125G.DATA,DISP=SHR
//PDSOUT2  DD DSN=J3803.PDSTEMP.DATA,DISP=SHR
//*
//*---------  FT01 --> FT75 : WORK FILE -------------------------------
//FT01F001 DD DSN=&&WK01,UNIT=WK10,SPACE=(TRK,(200,50))
//FT02F001 DD DSN=&&WK02,UNIT=WK10,SPACE=(TRK,(200,50))
//FT03F001 DD DSN=&&WK03,UNIT=WK10,SPACE=(TRK,(200,50))
//FT04F001 DD DSN=&&WK04,UNIT=WK10,SPACE=(TRK,(200,50))
//FT08F001 DD DSN=&&BTOB,DISP=(OLD,DELETE)
//FT51F001 DD DSN=&&WK51,UNIT=WK10,SPACE=(TRK,(200,50))
//FT53F001 DD DSN=&&WK53,UNIT=WK10,SPACE=(TRK,(200,50))
//FT54F001 DD DSN=&&WK54,UNIT=WK10,SPACE=(TRK,(200,50))
//FT55F001 DD DSN=&&WK55,UNIT=WK10,SPACE=(TRK,(200,50))
//FT74F001 DD DSN=&&WK74,UNIT=WK10,SPACE=(TRK,(200,50))
//FT75F001 DD DSN=&&WK75,UNIT=WK10,SPACE=(TRK,(200,50))
//*
//*---------  FT72F001 : TEMPORARY OUTPUT OF DDX DATA  ----------------
//FT72F001 DD DSN=&&WK72,UNIT=WK10,SPACE=(TRK,(50,10))
//*
//*---------  FT90F001 : CHECK WRITE ( FB FILE ) ----------------------
//FT90F001 DD DUMMY
//*T90F001 DD SYSOUT=*
//*
//*---------  FT80F001 : CARD-IMAGE INPUT FILE   ----------------------
//FT80F001 DD *
     0     0
LI6D
++
//
```

Fig. 3.4 Sample JCL and input data for RESENDD, SPINPTF and PROF-DDX.

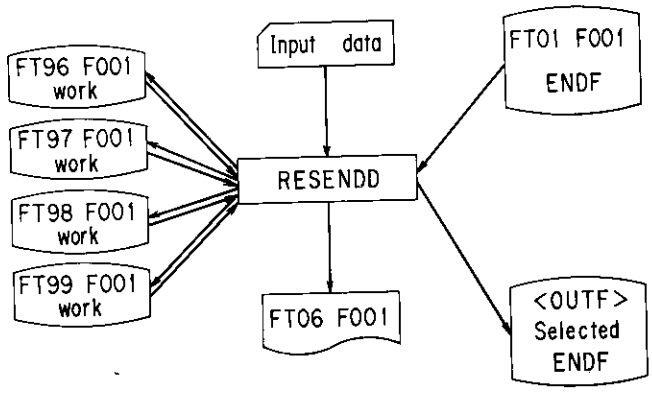

Fig. 3.5 I/O files for RESENDD.

See input instruction for the MCFILEF code. If IUP2=0, the data in a control file is adopted.

4) IF45 option for calculation of DDX from Files 4 and 5
See input instruction for the MCFILEF code. If IF45=0, the data in a control file is adopted.

5) EPSPR error criterion
See input instruction for the MCFILEF code. If EPSPR=0.0, the data in a control file is adopted. If EPSPR=0.0, an error check is not performed (i.e. EPSPR=0.0).

3.4.2 Sample Input, JCL and I/O Files

A list of sample input and JCL is shown in **Fig. 3.4**. The I/O files used in the SPINPTF code is shown in **Fig. 3.6**. A weighting function in the I/O unit IFLXW should be given in the following form when IFLUX=0.

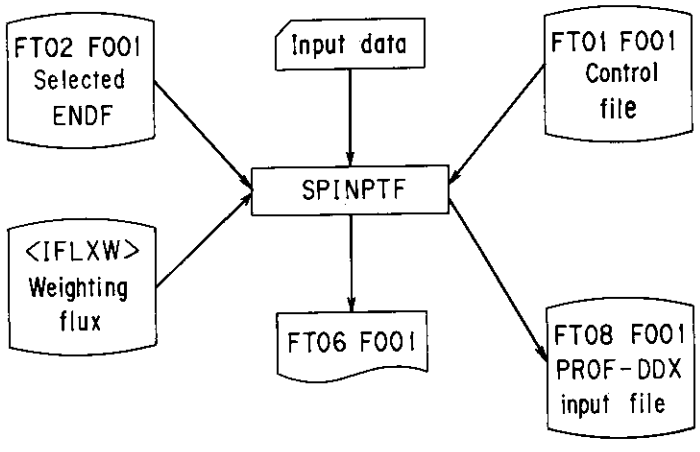

Fig. 3.6 I/O files for SPINPTF.

DATA 1 (2I6)

N1, N2 : numbers of interpolation ranges and energy points.

DATA 2 (12I6)

(NBT(i), JNT(i), i=1, N1)

NBT(i) : point number of the end point in the i-th interpolation range.
Note that NBT(N1)=N2.

JNT(i) : interpolation scheme for the i-th interpolation ragne. Parameter values of 1～5 have the same meaning as used in ENDF/B files.

DATA 3 (6E12.5)

(E(i), F(i), i=1, N2)

E(i) : energy in eV of the i-th point.
The relation E(i)<E(i +1) should be satisfied.

F(i) : weight of the i-th point.

3.5 PROF-DDX

3.5.1 Outline of PROF-DDX

The PROF-DDX code is a main code in the system, which calculates

(1) multi-group reaction cross section weighted with the input function for neutron transport calculation,

(2) multi-group energy-angle distribution,

(3) multi-group reaction cross section for reaction rate calculation, and

(4) stores these cross sections into the master PDS files labeled with member names.

The flow chart of the PROF-DDX code is shown in **Fig. 3.7**. The functions of important subroutines are briefly described below.

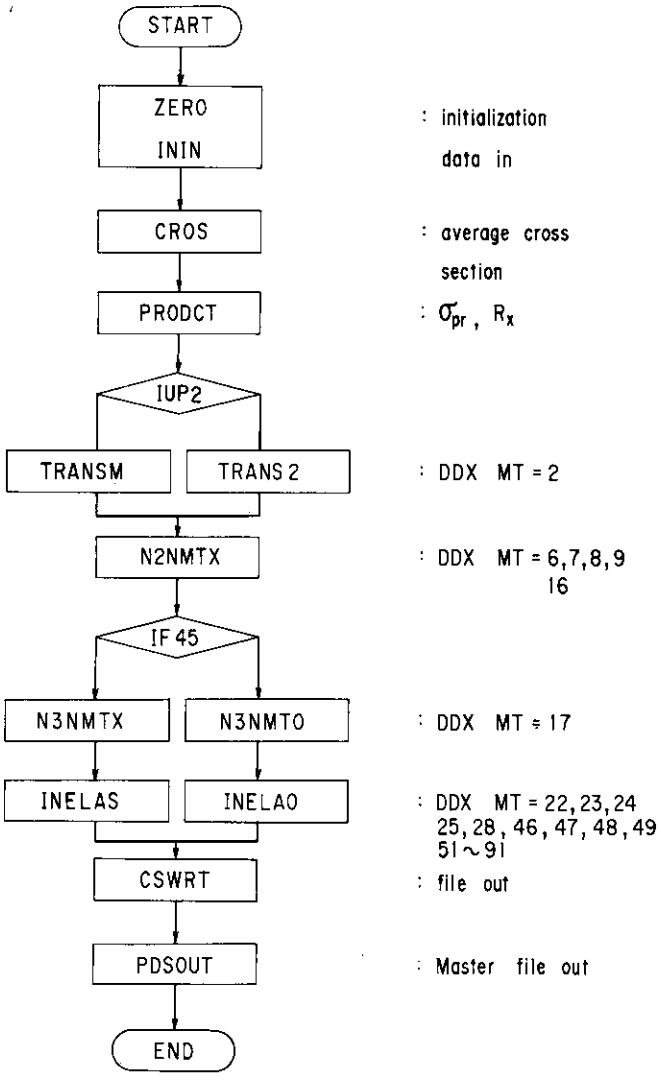

Fig. 3.7 Flow chart of PROF-DDX.

CROS

This subroutine calculates averaged cross sections for each group and each reaction, and stores them in a PDS file (PDSOUT2) with a member name assigned by a user if it is required.

PRODCT

Production cross section $\sigma_{pr\cdot g'}$ and the ratio $R_{xg'}=\sigma_{xg'}/\sigma_{pr\cdot g'}$ are calculated in this subroutine. The following check is carried out. If $R_{xg'}$ is less than EPSPR, then $R_{xg'}$ and $\sigma_{xg'}$ are set to be 0.0, where EPSPR is an input value. After this check, $\sigma_{pr\cdot g'}$ and $R_{xg'}$ are recalculated.

TRANSM, TRANS2

These subroutines calculate energy-angle distributions by Eq. (2-14) on the basis of the reaction kinematics. The processed reactions are elastic scattering(MT=2), discrete level inelastic scattering (MT =51~90) and sequential (n,2n) reactions (MT=6~9). In TRANSM, a collision density within a group is assumed to be constant in lethargy. In TRANS2, this assumption is not used. The calculation procedure in TRANS2 is as follows:

(1) Fine energy meshes used for the integration in Eq. (2-14) are determined by the following method. Incident neutron energy group, g', is divided into $IND_{g'}$ fine energy intervals of equal lethargy width $\Delta U_{fg'}$. $IND_{g'}$ is determined such that

$$IND_{g'}=\Delta U_{g'}/\Delta U_f,$$

where

$$\Delta U_f=\frac{\Delta U_1}{INK}\leqq\frac{\xi}{50}=-\frac{\ln\{(A-1)/(A+1)\}^2}{50}$$

with a minimum integer INK, where $\Delta U_{g'}$ and A are lethargy width of the g'-th group and mass of target atom, respectively.

Then, $IND_{g'}$ is modified as follows:

$IND_{g'}=8$, if $IND_{g'}<8$.

$IND_{g'}=32$ if $E_{th}\in g'$-th group and if $IND_{g'}\leqq 32$.

Then $\Delta U_{fg'}=\Delta U_{g'}/IND_{g'}$. The slowing-down energy range for each incident energy E' is divided into $INDO$ energy intervals of equal lethargy width. The following value is adopted for $INDO$.

$$INDO=\begin{cases}\text{MAXMU}*IND_0/2 & \text{for MT}=2,\\ N1*N2 & \text{for MT}\neq 2,\end{cases}$$

where $IND_0=\xi/\Delta U_f$,

$$N0=\begin{cases}1.5 & \text{if } INK\geqq 2,\\ 3 & \text{if } INK=1,\end{cases}$$

$$N1=\text{MAX}\left[IND_0*N0,\ 3*\text{MAXMU}\right],$$

$$N2=\begin{cases}1 & \text{for } \beta>\beta_{1U},\\ 2 & \text{for } \beta_{2U}<\beta<\beta_{1U} \text{ or } \beta_{1L}<\beta<\beta_{2L},\\ 4 & \text{for } \beta_{2L}<\beta<\beta_{2U},\end{cases}$$

where β_{1X} and β_{2X} are β values of Eq. (2-12) at which the lethargy width of slowing-down energy range is two or four times larger than that by elastic scattering, respectively, as shown in **Fig. 3.8** for A=7.

(2) The values $\sigma_x\Psi_w$' cross sections multiplied by a weighting function are calculated at each fine energy point.

(3) The P_l expansion coefficients for scattering anisotropy are calculated for each energy group as follows:

$$f^l_{xg'}=\frac{\int_{\Delta E_{g'}} f^l_x(E)\sigma_x(E)\Psi_w(E)dE}{\int_{\Delta E_{g'}}\sigma_x(E)\Psi_w(E)dE}.$$

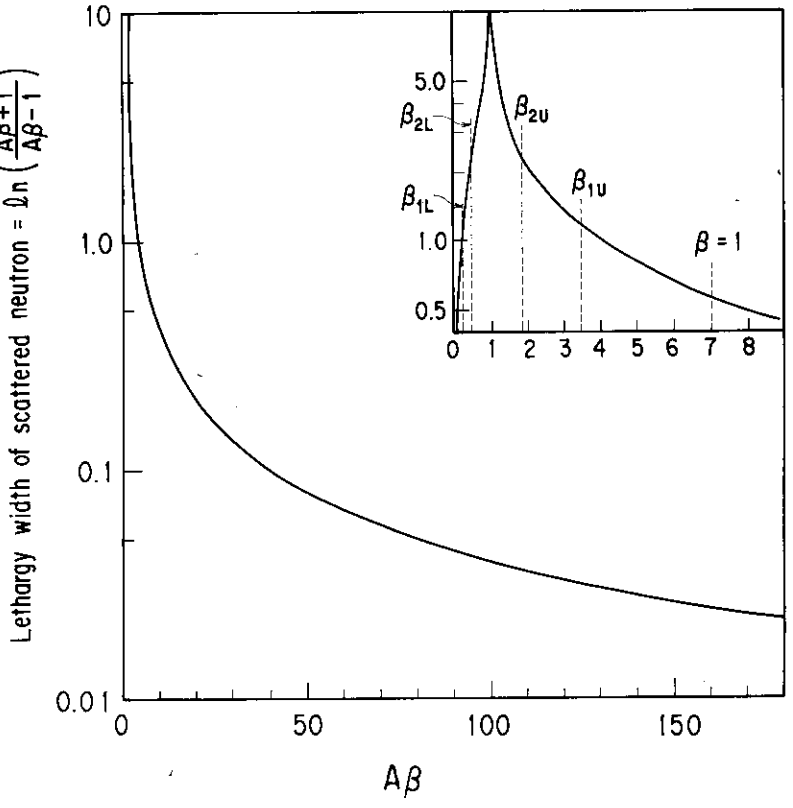

Fig. 3.8 Lethargy width of scattered neutron vs. $A\beta$.

If the angular distributions are given in the form of table, the coefficients $f_x(E)$ are calculated by using the data in the table prior to calculating $f_{xg'}(E)$ shown above.

(4) The numerical integration with respect to E and E' is carried out based on the fine energy meshes shown in **Fig. 3.9**. The following algorithm is applied for each incident neutron energy group g' and each reaction x.

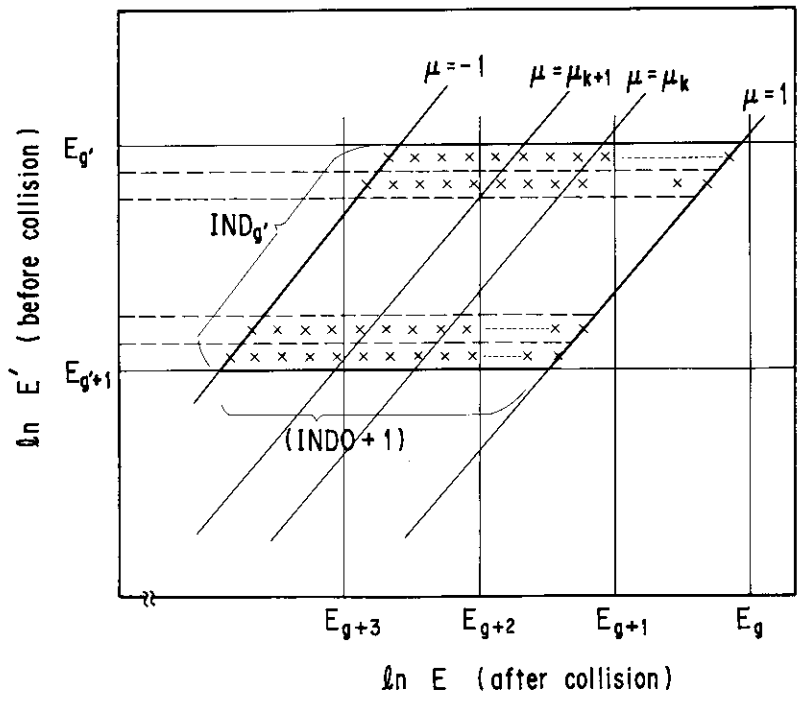

Fig. 3.9 Fine energy meshes for numerical integration with respect to E and E' in the subroutines TRANSM and TRANS2.

For each fine energy interval i ($i=1$, $IND_{g'}$),

$ii = IND_{g'} + 1 - i$,

$\Delta U^{ii} = \Delta U_{g'} * (ii-1) + \Delta U_{g'}/2$,

$E' = E_{g'} * \exp(-\Delta U^{ii})$,

$$\beta = \sqrt{1 + \frac{A+1}{A}\frac{Q_x}{E'}},$$

$$\alpha_{high} = \left(\frac{A\beta+1}{A+1}\right)^2,$$

$$\alpha_{low} = \left(\frac{A\beta-1}{A+1}\right)^2,$$

$$\xi_x = \ln\frac{\alpha_{high}}{\alpha_{low}},$$

$\Delta U_x = \xi_x / INDO$.

For each outgoing energy mesh boundary j ($j=1$, $INDO+1$),

$U_m = \Delta U_x * (j-1) \longrightarrow E_m = E' \exp(-U_m)$,

$U_h = U_m - \Delta U_x/2 \longrightarrow E_h = E' \exp(-U_h) \quad (j \neq 1)$,

$U_l = U_m + \Delta U_m/2 \longrightarrow E_l = E' \exp(-U_l) \quad (j \neq INDO+1)$,

$\Delta E = E_h - E_l$,

$$\mu_c = \left\{\frac{(A+1)^2}{2A}\frac{E}{E'} - \frac{A}{2}\beta(E')^2 - \frac{1}{2A}\right\}\frac{1}{\beta_x(E')},$$

$$f_{g'}(\mu_c) = \sum_{l=0}^{L}\frac{(2l+1)}{2} f_{g'}^l P_l(\mu_c),$$

$$\mu = \frac{A+1}{2}\sqrt{\frac{E}{E'}} - \frac{A-1}{2}\sqrt{\frac{E'}{E}} - \frac{AQ_x}{2\sqrt{EE'}},$$

$$P_x(k;g\rightarrow g) = P_x(k;g\rightarrow g) + \frac{2\sigma_x(E')\Psi_w(E')f_{g'}(\mu_c)\Delta E}{(1-\alpha)\beta E'}$$

for $E_{g-1} < E_m < E_g$ and $\mu_{k-1} < \mu < \mu_k$.

After the calculation is performed for all i and j, the normalization is performed as

$$\sum_{g,k} P_x(k;g'\rightarrow g) = R_{xg'}.$$

IMAT, IMATLI

These subroutines calculate Eq. (2-16) for reactions such as continuum inelastic scattering, for which reaction kinematics are not known. Hence, energy-angle distributions are obtained by calculating energy distribution and angle distribution separately from the data in Files 4 and 5. In IMAT calculations, however, scattering is assumed to be isotropic in the laboratory system (IF45=1). The subroutine IMATLI can process both files (IF45=2 or 3). A user should specify the parameter IF45. As an optional calculation (IF45=3), IMATLI can calculate the energy-angle distribution by setting $P_x(k,g'\rightarrow g)=0$ for $g < g^k_{max}$, where the g^k_{max}-th group includes the energy E^*_{max} which is the maximum energy of scattered neutron in the k-th direction predicted by the two-body reaction kinematics. The data in File 4 are processed by the subroutine LIF4. The summation of the calculated distribution for reaction x is normalized to be $R_{xg'}$.

DDXF6

This subroutine calculates the energy-angle distribution from the data in File 6 (IF45=4). The summation of the calculated distribution for reaction x is normalized to be $R_{xg'}$.

CSWRT

The subroutine CSWRT is called after all the probabilities are calculated. This subroutine sets $I(k; g' \rightarrow g) = 0.0$ if it is less than EPSPB given by a user, and renormalize $\sum_{g,k} I(k;g' \rightarrow g)$ to be unity. Then the result is written on a file (I/O unit 72).

PDSOUT

The subroutine PDSOUT reads the data from the I/O unit 72 and stores them on a master PDS file (PDSOUT1) with the following member names:

B4aaaaCT ; MATNO, MAXMU, MAXI, MGRMX, IDMAX, ISMAX and (MAXSD(i), i=1, MAXI),

B4aaaaAT ; ZA and AWR,

B4aaaaTA ; production, fission, absorption, $\nu *$ fission and total cross sections,

B4aaaaTB ; double-differential scattering probabilities $I(k;g' \rightarrow g)$,

where aaaa is the NAME with 4 letters given by a user (see 3.5.2).

3.5.2 Input Instructions

The following free-formatted data are read from the I/O unit 80.

CARD A (*)

1) IOPT option of PROF-DDX calculation
   = 0, calculation of multi-group DDX
   = 1, calculations of multi-group DDX and response cross section
   = 2, calculation of response cross section
2) IREACT number of reactions to be processed (no meaning if IOPT=0)
   These are usually used as detector responses.

CARD B (*) (Enter if IOPT≧1)

(IMT(i), i=1, IREACT) MT number of the i-th reaction being stored in a PDS file (PDSOUT 2) for the reaction rate calculation

CARD C (2A4) (Enter if IOPT≧1)

TITLE(i) ID name assigned to the i-th reaction in a PDS file (PDSOUT2)
IREACT lines are necessary for CARD C.

CARD D (A4) (Enter if IOPT≦1)

NAME ID name assigned to the calculated DDX in a master PDS file (PDSOUT1)
If NAME=' ', the calculated DDX are not stored.

CARD E (*) (Enter if NO40=-2 (see MCFILEF))

XT, XPR, XC, XF, XNF total, production, absorption excluding fission, fission and $\nu *$ fission cross sections of the MGRMX-th group

3.5.3 Sample Input, JCL and I/O Files

Sample input for a simultaneous calculation of DDX and three responses is as follows:

```
//FT80F001 DD *
    1   3
    18  102  107
AAAAAAAA
```

```
BBBBBBBB
CCCCCCCC
XXXX
/*
```

If only the DDX calculation is required, then

```
//FT80F001 DD *
    0     0
XXXX
/*
```

A sample JCL is shown in **Fig. 3.4** together with those for the RESENDD and SPINPTF codes. The I/O files used in the PROF–DD code are summarized in **Table 3.1**.

Table 3.1 PROF–DDX file requirement

I/O unit	Contents	Remarks	I/O[a]
PDSOUT1	DDX data	Master PDS[b] file	O
PDSOUT2	Response	PDS[b] file	O
5	Card-image input	Output of SPINPTF ⟨FT08F001⟩	I
6	Printout		O
8	ENDF/B file (pointwise data)	Output of RESENDD ⟨OUTF⟩	I
72	Scratch	Temporary output of DDX	I/O
80	Card-image input	Option for fileout etc.	I
90	Scratch	Check write	O
1 – 4 51 53 54 55 74 75	Scratch	Temporary storage for nuclear data (MF = 3, 4 and 5)	I/O

[a] I and O mean read-only and write-only files, respectively.
[b] A PDS file is a partitioned data set with undefined record format, whose DCB (Data Control Block) parameters are normally RECFM = U and BLKSIZE = 900.

3.6 DDXLIBMK

The DDXLIBMK code accesses the master PDS files and performs the following functions:

(1) to edit a DDX library from the master files for a transport code such as MORSE–DD,
(2) to print out the DDX data in the master file,
(3) to retreave energy and angle boundaries from a control file into the master file, and
(4) to retreave the binary data produced by the PROF–DDX code (I/O unit 72) into the master file.

3.6.1 Input Instruction

CARD A (*)

1) ISW function selector
   = 1, compilation of a DDX library for a transport code such as the MORSE–DD code
   = 2, print out of the DDX data in a master file
   = 3, retreaval of energy and angle boundaries from a control file into a master file

= 4, retreaval of the binary data from the PROF-DDX code (I/O unit 72) into a master file

CARD B (*) (Enter if ISW=1)

1) NMAT number of elements to be compiled in a DDX library
2) NOPT output format
   ≠ 2, binary for MORSE-DD etc.
   = 2, formatted

CARD C (A4) (Enter is ISW=1)

NAME(i) ID name for the i-th element in a master file assigned by a user as an input data for the PROF-DDX code

NMAT lines should be repeated for CARD C.

CARD D (A4) (Enter if ISW=2)

NAME ID name of an element to be printed out

CARD E (*) (Enter if ISW=2)

NINT number of incident groups to be printed out

CARD F (*) (Enter if ISW=2)

(IGINT(i), i=1, NINT) incident energy group to be printed out

CARD G (A4) (Enter if ISW=4)

NAME ID name assigned to the present DDX data

3.6.2 Sample Input, JCL and I/O Files

A list of sample input and JCL for compiling the DDX library is shown in **Fig. 3.10**. The I/O files required are shown in **Fig. 3.11**.

3.6.3 Structure of DDX Library

The DDX library is edited by the DDXLIBMK code in the following form.

m=1, NMAT
1) MAXI, IDUMMY, IDUMMY, MATNO, (Title(i), i=1, 12)
2) (MAXSD(i), i=1, MAXI)
3) (σ_{prg},σ_{fg},$\nu\sigma_{fg}$,σ_{tg}, i=1, MAXI)
   n=1, MAXI
4) (($I(k;g'\rightarrow g)$, k=1, MAXMU), g=1, MAXSD(g'))

When this library is used in a transport calculation, cross section data for each element can be identified by MATNO which is a Material Number (MAT) given for each element in the evaluated nuclear data library.

When NOPT on CARD B is equal to 2, the library with the following format is generated.

m=1, NMAT	
1) MAXI, IDUMMY, IDUMMY, MATNO, (Title(i), i=1, 12)	(4I6, 12A4)
2) (MAXSD(i), i=1, MAXI)	(12I6)
3) (σ_{prg},σ_{fg},σ_{ag},$\nu\sigma_{fg}$,σ_{tg}, i=1, MAXI)	(10E12.5)
n=1, MAXI	
4) (($I(k;g'\rightarrow g)$, k=1, MAXMU), g=1, MAXSD(g'))	(10E12.5)

```
//JCLG  JOB
// EXEC JCLG
//SYSIN DD DATA,DLM='++'
// JUSER  XXXXXXXX,TA.MORI,0431.110
  T.3 C.3 W.0 P.0 I.5
 OPTP  MSGCLASS=R,PASSWORD=XX
//**********   J3803.DDX.CNTL(DDXLIBMK)   *************
//*            PRODUCTION OF DDX LIBRARY
//*
//*     ****************************************
//*     *          D D X L I B M K             *
//*     ****************************************
//*
//DDXLIBMK  EXEC LMGO,LM=J3803.PROFDD,PNM=DDXLIBMK
//*
//*---------  FT08F001 : DDX LIBRARY      ----------------------------
//FT08F001 DD DSN=J3803.DDXLIB3.DATA,DISP=OLD,
// DCB=(RECFM=VBS,LRECL=X,BLKSIZE=23476)
//*
//*---------  USERPDS  : MASTER FILE      ----------------------------
//USERPDS  DD DSN=J3803.DDXLIB3.PDS125G.DATA,DISP=SHR,LABEL=(,,,IN)
//*
//SYSIN DD *
   1
  29 1
1269
1271
1272
1274
1289
1275
1276
1156
1280
1193
1194
1150
1195
1191
1192
1190
1197
1295
1287
1288
0306
0307
0409
0612
0816
2400
2600
2800
1277
/*
++
//
```

Fig. 3.10 Sample JCL and input data for DDXLIBMK (compilation of DDX library).

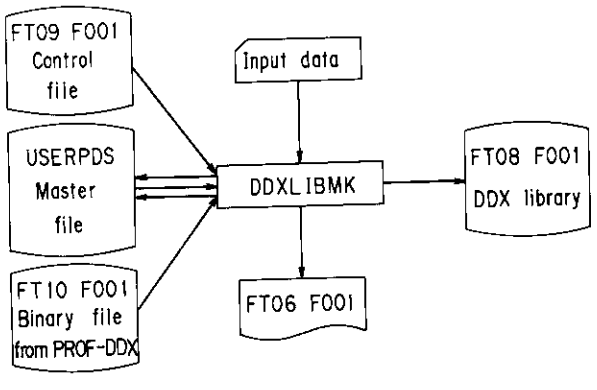

Fig. 3.11 I/O files for DDXLIBMK.

4. ANISN-DD: One-Dimensional S_n Transport Code

4.1 New Features of ANISN-DD

Since a one-dimensional S_n transport code is widely used for parameter survey calculations and for benchmark calculations to check cross section data, it is meaningful to develop a new version using the DDX library and hence to improve its accuracy. The widely used one-dimensional S_n code ANISN[7] was modified in JAERI to ANISN-JR[8] in order to extend the applicability by adding some optional functions concerning input, output and so on. At the present work, the ANISN-JR code has been modified to use the DDX library. The newly developed code named as ANISN-DD has the following functions in addition to those of the original code:

(1) forward transport calculation in one-dimensional slab, sphere and cylinder geometry with external volume and/or shell sources by using the DDX library.
(2) collapsing macroscopic or microscopic DDXs into those with fewer energy groups and fewer angle bins,
(3) adjoint transport calculation by using the DDX library,
(4) solving several types of eigenvalue problems by using the DDX library.

4.1.1 Cross Section

The ANISN-DD code can use both the DDX library and the conventional P_l cross section library. The format of cross section library is given in Section 4.3.2. The mixing and collapsing procedures of P_l cross sections are similar to those in the original code. Those of the DDX are described in this section.

(1) Preparation of Macroscopic Cross Section – Cross Section Mixing

In ANISN-DD, a user can directly use a processed macroscopic cross section library and bypass the cross section mixing process by setting the input value IANISN=3. When the cross section mixing is required (IANISN=2 or 4), a user must specify the input parameters MTP and MT of 15$ data. The parameters MTP and MT are the sum of numbers of constituent nuclides for each material and the number of materials for which the macroscopic cross sections are prepared, respectively. The following additional data are also required for the cross section mixing: the numbers of constituent nuclides for MT materials MB(j) (10$ data in Data Block 4), and three arrays of MTP length, MC(i), XMD(i) and MTT(i) (11$, 12* data in Data Block 4 and 13$ data in Data Block 2), which are the identification number, atomic number density and I/O unit number from which the microscopic cross sections are read, respectively. Accordingly, MTP is determined by

$$\mathrm{MTP}=\sum_{\mathrm{j}=1}^{\mathrm{MT}}\mathrm{MB(j)}. \tag{4-1}$$

By using these data, the macroscopic cross sections for the J-th material are produced as follows:

$$IS=\sum_{\mathrm{j}=1}^{J-1}\mathrm{MB(j)}+1, \tag{4-2}$$

$$IE=\sum_{\mathrm{j}=1}^{J}\mathrm{MB(j)}, \tag{4-3}$$

$$\Sigma_{a,g}^{J}=\sum_{\mathrm{i}=IS}^{IE}\mathrm{XMD(i)}\times\left\{\sigma_{c,g}^{\mathrm{MC(i)}}+\sigma_{f,g}^{\mathrm{MC(i)}}\right\}, \tag{4-4}$$

$$\nu\Sigma^J_{f,g}=\sum_{i=IS}^{IE}\mathrm{XMD(i)}\times\nu\sigma^{\mathrm{MC(i)}}_{f,g}, \tag{4-5}$$

$$\Sigma^J_{t,g}=\sum_{i=IS}^{IE}\mathrm{XMD(i)}\times\sigma^{\mathrm{MC(i)}}_{t,g}, \tag{4-6}$$

$$\Sigma^J_s(k;\ g\rightarrow g')=\sum_{i=IS}^{IE}\mathrm{XMD(i)}\times\sigma^{\mathrm{MC(i)}}_{pr,g}\times f^{\mathrm{MC(i)}}(k;\ g\rightarrow g'), \tag{4-7}$$

where $X^{MC(i)}$ is a cross section or a scattering probability for the nuclide with the identification number MC(i), which is read from the I/O unit MTT(i). This mixing process is carried out by using the direct access file. After the process for all materials is completed, the elements of scattering matrices are rearranged into the group-independent form library, which is suitable for an ANISN-DD calculation. The rearrangement of cross sections for the adjoint calculation is also performed through this process, if necessary. The thermal cross sections in the DDX library can be replaced with those given by a user if necessary.

The format of group-independent form library is described in Section 4.3.2. In the case of IANISN=3, this group-independent form library should be provided by a user.

(2) Collapsing of DDX

In ANISN-DD, the macroscopic or microscopic cross sections can be collapsed into those with fewer energy groups and fewer angle bins by using a zonal neutron flux as a weighting function. See the descriptions for IFG in 15$ array, 19$, 27$, 28$ and 29$ arrays in Data Block 4. It is assumed that the same flux can be used as a weighting function in collapsing of energy-angle distribution. A user can obtain three types of collapsed cross sections described below. The collapsing is performed by using the following formulae :

Microscopic cross section for a component i in a zone r

$$\tilde{\sigma}^{i,r}_{\chi,G}=\sum_{g\in G}\phi^r_g\sigma^i_{\chi,g}/\sum_{g\in G}\phi^r_g, \tag{4-8}$$

$$\tilde{f}^{i,r}(K;\ G'\rightarrow G)=\sum_{g'\in G'}\sum_{g\in G}\sum_{k\in K}\phi^r_g\sigma^i_{pr,g'}f^i(k;\ g'\rightarrow g)/\sum_{g'\in G'}\phi^r_g\sigma^i_{pr,g'}. \tag{4-9}$$

Macroscopic cross section for a material m in a zone r

$$\tilde{\Sigma}^m_{\chi,G}=\sum_{g\in G}\phi^r_g\Sigma^m_{\chi,g}/\sum_{g\in G}\phi^r_g, \tag{4-10}$$

$$\tilde{\Sigma}^m_s(K;\ G'\rightarrow G)=\sum_{g'\in G'}\sum_{g\in G}\sum_{k\in K}\phi^r_g\Sigma^m_s(k;\ g'\rightarrow g)/\sum_{g'\in G'}\phi^r_{g'}, \tag{4-11}$$

$$\tilde{\Sigma}^m_{pr,G'}=\sum_G\sum_K\tilde{\Sigma}^m_s(K;\ G'\rightarrow G), \tag{4-12}$$

$$\tilde{f}^m(K;\ G'\rightarrow G)=\tilde{\Sigma}^m_s(K;\ G'\rightarrow G)/\tilde{\Sigma}^m_{pr,G'}. \tag{4-13}$$

Macroscopic cross section for a cell R (cell averaging)

$$\tilde{\Sigma}^R_{\chi,G}=\sum_{r\in R}\phi^r_G V^r\Sigma^r_{\chi,G}/\sum_{r\in R}\phi^r_G V^r, \tag{4-14}$$

$$\tilde{\Sigma}^R_s(K;\ G'\rightarrow G)=\sum_{r\in R}\phi^r_{G'}V^r\Sigma^r_s(K;\ G'\rightarrow G)/\sum_{r\in R}\phi^r_{G'}V^r, \tag{4-15}$$

$$\tilde{\Sigma}^R_{pr,G'}=\sum_G\sum_K\tilde{\Sigma}^R_s(K;\ G'\rightarrow G), \tag{4-16}$$

$$\tilde{f}_R(K;\ G'\rightarrow G)=\tilde{\Sigma}^R_s(K;\ G'\rightarrow G)/\tilde{\Sigma}^R_{pr,G'}. \tag{4-17}$$

The output format of collapsed cross sections, as described in Section 4.3.2, is similar to that of the

original DDX library in the case of microscopic cross sections and that of either the original one or the group-independent form library in the case of macroscopic cross sections.

4.1.2 Solution Algorithm and Angular Transfer Probability

The solution algorithm is similar to that used in ANISN-JR or ANISN[7] except for the calculation of scattering source. In the S_n method using the DDX library, the scattering source expressed as Eq. (2-25) is not calculated with P_l moments of flux but with angular fluxes by Eq. (2-28) with the angular transfer probabilities. ANISN-DD calculates the angular transfer probabilities by the following method or reads them from an input file and calculates the scattering kernel matrix defined by Eq. (2-30). Then the code writes those in a scratch file after multipling by the quadrature weight.

(1) Angular Transfer Probability for Slab and Sphere Geometry

In the case of slab or sphere geometry, Eq. (2-29) is explicitly written as

$$P(k,m',m)=\frac{1}{2\pi\Delta\mu_k}\frac{1}{4\pi w_m w_m}\int_{\mu m-1/2}^{\mu m-1/2}2\pi d\mu\int_{\mu m'-1/2}^{\mu m'+1/2}d\mu'\int_0^{2\pi}d\varphi'\delta_{\mu^*,k}, \tag{4-18}$$

where

$$\mu^*=\mu\mu'+\sqrt{1-\mu^2}\sqrt{1-\mu'^2}\cos\varphi', \tag{4-19}$$

and $\mu_{m\pm1/2}$ are the boundaries of the m-th quadrature direction which are defined recurrently by

$$\mu_{1/2}=-1,\quad \mu_{m+1/2}=\mu_{m-1/2}+2w_m. \tag{4-20}$$

We introduce the function $p(k,\mu',\mu)$ representing the last factor of Eq. (4-18):

$$\begin{aligned}p(k'\mu,'\mu)&=\int_0^{2\pi}d\varphi'\delta_{\mu^*,k}\\&=2\int_{\beta_1}^{\beta_2}d\lambda\ \left|\frac{d\varphi'}{d\lambda}\right|\delta_{\mu^*,k},\end{aligned} \tag{4-21}$$

where

$$\lambda=\mu\mu'+\sqrt{1-\mu^2}\sqrt{1-\mu'^2}\cos\varphi', \tag{4-22}$$

$$\beta_1=\mu\mu'-\sqrt{1-\mu^2}\sqrt{1-\mu'^2}, \tag{4-23}$$

$$\beta_2=\mu\mu'+\sqrt{1-\mu^2}\sqrt{1-\mu'^2}. \tag{4-24}$$

Carrying out the integration in Eq. (4-21), we obtain the following formulae.

When $|\mu|\neq1$ and $|\mu'|\neq1$,

$$p(k,\mu',\mu)=2\left[\sin^{-1}\frac{\beta_2-\mu\mu'}{\sqrt{1-\mu^2}\sqrt{1-\mu'^2}}-\sin^{-1}\frac{\mu_{k-1}-\mu\mu'}{\sqrt{1-\mu^2}\sqrt{1-\mu'^2}}\right],$$

$$\text{for } \beta_1<\mu_{k-1}<\beta_2<\mu_k, \tag{4-25}$$

$$p(k,\mu',\mu)=2\left[\sin^{-1}\frac{\mu_k-\mu\mu'}{\sqrt{1-\mu^2}\sqrt{1-\mu'^2}}-\sin^{-1}\frac{\mu_{k+1}-\mu\mu'}{\sqrt{1-\mu^2}\sqrt{1-\mu'^2}}\right],$$

$$\text{for } \beta_1\leq\mu_{k+1} \text{ and } \mu_k\leq\beta_2, \tag{4-26}$$

$$p(k,\mu',\mu)=2\left[\sin^{-1}\frac{\mu_k-\mu\mu'}{\sqrt{1-\mu^2}\sqrt{1-\mu'^2}}-\sin^{-1}\frac{\beta_1-\mu\mu'}{\sqrt{1-\mu^2}\sqrt{1-\mu'^2}}\right],$$

$$\text{for } \mu_{k+1}<\beta_1<\mu_k<\beta_2, \tag{4-27}$$

and

$$p(k,\mu',\mu)=0,$$

$$\text{for otherwise.} \tag{4-28}$$

When $|\mu|=1$ or $|\mu'|=1$,

$$p(k, \mu', \mu)=2\pi, \quad \text{for } \mu_{k+1}<\mu\mu'<\mu_k, \tag{4-29}$$

and

$$p(k, \mu', \mu)=0, \quad \text{for otherwise.} \tag{4-30}$$

The integration in Eq. (4-18) over μ and μ' is performed numerically as follows :

$$\mu_{min}^{DDX}=\min_k \Delta\mu_k, \tag{4-31}$$

$$\mu_{max}^{Sn}=\max_m |\mu_m-\mu_{m-1}|. \tag{4-32}$$

Each interval $2w_m$ corresponding to the m-th quadrature direction is divided into n sub-intervals with a width Δ_m :

$$\Delta_m=\frac{2w_m}{n}, \tag{4-33}$$

where

$$n=4\times\frac{\mu_{max}^{Sn}}{\mu_{min}^{DDX}}. \tag{4-34}$$

Then, the angular transfer probability is

$$P(k'm,'m)=\frac{1}{\pi\Delta\mu_k n^2}\sum_{l=1}^{n}\sum_{l'=1}^{n}p(k,\mu_{m'-1/2}+\frac{2l'-1}{2}\Delta_{m'},\mu_{m-1/2}+\frac{2l-1}{2}\Delta_m),$$

$$\text{for } |\mu_m|\neq 1 \text{ and } |\mu_{m'}|\neq 1, \tag{4-35}$$

and

$$P(k, m', m)=\frac{1}{\pi\Delta\mu_k \cdot n}\sum_{l=1}^{n}p(k, \mu_{m'}, \mu_{m-1/2}+\frac{2l-1}{2}\Delta_m),$$

$$\text{for } |\mu_{m'}|=1. \tag{4-36}$$

Similarly, $P(k, m', m)$ is calculated for $|\mu_m|=1$.

The probability P is normalized as follows :

$$\sum_m w_m P(k, m', m)=1 \qquad \text{for all } k \text{ and } m'. \tag{4-37}$$

If $\sum_m P(k, m', m)=0$ for some k, then, larger n is selected again, and w_m is divided into finer sub-intervals. The procedure mentioned above is repeated until Eq. (4-37) is satisfied.

As a result of the renormalization, the following relation is always conserved :

$$\sum_m w_m \cdot \Sigma(g'\to g, m'\to m)=\sum_k \Sigma_s(k; g'\to g). \tag{4-38}$$

(2) Angular Transfer Probability for Infinite Cylinder Geometry

In this case, the angular flux depends on the angle φ. Therefore, the angular transfer probability cannot be obtained in the same manner as mentioned above. On the other hand, it can be calculated on the basis of the assumption that each quadrature weight w_m is sufficiently small compared with the angle bin width $\Delta\mu_k$.

Let $\Omega_{m'_1}=(\mu', \eta', \xi')$ and $\Omega_m=(\mu, \eta, \xi)$ be incident and outgoing directions of a scattered particle, respectively. In an infinite cylinder geometry, angular fluxes are the same for the following four directions :

$$\Omega_{m'_1}=(\mu', \eta', \xi'), \ \Omega_{m'_2}=(\mu', -\eta', \xi'), \ \Omega_{m'_3}=(\mu', \eta', -\xi'),$$

$$\text{and } \Omega_{m'_4}=(\mu', -\eta', -\xi').$$

For each direction, cosine of scattering angle is defined by

$$\lambda_1=(\Omega_{m'_1},\Omega_m)=\mu'\mu+\eta'\eta+\xi'\xi, \tag{4-39}$$

$$\lambda_2=(\Omega_{m'_2},\Omega_m)=\mu'\mu-\eta'\eta+\xi'\xi, \tag{4-40}$$

$$\lambda_3=(\Omega_{m'_3},\Omega_m)=\mu'\mu+\eta'\eta-\xi'\xi, \tag{4-41}$$

$$\lambda_4=(\Omega_{m'_4},\Omega_m)=\mu'\mu-\eta'\eta-\xi'\xi. \tag{4-42}$$

Then we can write

$$P(k,\ m',\ m)=\frac{2}{\Delta\mu_k}\times(\text{Number of }\lambda_i\text{ such that }\mu_{k+1}<\lambda_i<\mu_k). \tag{4-43}$$

When the present assumption is not satisfied, $P(k,\ m',\ m)$ should be calculated by a more sophisticated method. The MONTA code, which performs the integration in Eq.(2-29) by the Monte Carlo method, has been prepared for this purpose. A description of the MONTA code is given in Section 7.2.

4.2 Input Instruction

The input data for ANISN-DD consist of two parts: input data required in the original ANISN with use of the FIDO format and additional input data for new options in ANISN-DD with use of the FORTRAN77 free format, which are the same as those used in ANISN-JR. At first, the data for the additional options (Section A to G) are read with the FORTRAN77 free format. Then, the ANISN input data[7] are read with the FIDO format. Finally, the optional data for reaction rate calculations (Section H) are read with a specified format. At the end of the input data, a "STOP" line is required, which contains four letters "STOP" at column 1-4 on a line. In order to print out the input data, it is required to enter "LIST" at column 1-4 on the first line. The FIDO format is described in Appendix 1. Note that "$" in the FIDO format can be replaced by "¥".

4.2.1 Input Data for Additional Options of ANISN-DD

The ANISN-DD code reads the following data with the FORTRAN77 free format except for those in Section H.

(1) Section A

1) IANISN cross section type and execution mode

P_l mode;

=0, original format

=1, format of the cross section generated by RADHEAT-V3[17]

DDX mode;

=2, mixing of DDX type cross section only

=3, flux calculation by using DDX type cross section already mixed

=4, both of 2 and 3

2) ITMAX maximum execution time in minutes

If ITMAX=0, this option is ignored. The ANISN-DD code checks ITMAX at the end of each outer iteration, and if it has been exceeded, the problem is terminated with full output.

3) IENRGY input option for 17* (distributed volume source) or 18* (shell source)

=0, normal

=1, enter 17* or 18* data for each group with "T"

4) IINPT option for source input

=0, from card-image input on I/O unit 5
=1, from I/O unit 25

(2) Section B

1) IIBOUD output option for total flux
=0, print total fluxes at the midpoint of each mesh interval
=1, print total fluxes at the boundary of each mesh interval

2) IISPTM output option for neutron spectrum (total flux)
=0, no effect
=1, calculate and print neutron spectrum $\phi_g/\Delta E_g$
=2, calculate and print neutron spectrum $\phi_g/\Delta U_g$
If IISPTM=1 or 2, energy group boundaries should be specified by Section D.

3) IIANLL output option for angular flux
=0, print angular fluxes at all spatial meshes
=1, print angular fluxes only at required meshes
=2, print angular fluxes only at required meshes and write boundary angular fluxes of mesh NOANLL(1) on I/O unit 16 for use as a shell source in the next run
=3, print angular fluxes at the midpoint of required mesh intervals (effective only in DDX mode)
The required meshes or mesh intervals are given by Section E and Section F. If the print out of angular fluxes is required, ID1=1 or 3 must be entered in 15$ array.

4) IGMNEWnumber of total energy groups
The absolute value of IGMNEW must equal IGM in 15$ array. In *DDX* mode, a negative value means that the cross sections of group | IGMNEW | are given in Section X, and the mixed DDX has | IGMNEW | energy groups.

5) IGMNEU number of neutron groups
The first IGMNEU groups are assigned to neutrons, and the remainder to gamma-rays. If only neutron is considered, IGMNEU = | IGMNEW | .

6) NACTPR print option for activities
=0, no effect
=1, print activities for each group and zone
If the activity calculation is required, ID3>0 must be entered in 15$ array. Activation cross sections must be included in a cross section library.

7) NREACT option for arbitrary reaction rate calculation
=0, no effect
=1, calculate reaction rates for neutron and gamma-ray
=2, calculate reaction rates and also collapse response functions of detectors
=3, also write the collapsed response functions of detectors on card- image file (I/O unit 7)
The response functions for neutron and gamma-ray are given in Section H. To collapse the response functions, IFG=1 in 15$ array, and arrays 27$ and 28$ must be entered.

8) NASYMMoption for quadrature set
=0, no effect
=1, use asymmetric quadrature set (only in P_l mode)
The reflective condition for left boundary can not be used.

9) NRESAT option for restart
=0, no effect

=1, write/read final fluxes on a file for use as an initial flux guess in the next run
Final fluxes are written on the I/O unit 15 and read from 14. For the first run, NRESAT=1, IFN=1 or 2 (in 15$ array) must be specified, and for the following run, NRESAT=1 and IFN=3.

10) NXSOUT option for collapsing of cross sections

P_l mode;

=0, no effect

=1, obtain a few group cross sections for DOT, TWOTRAN or MORSE, and write them on I/O unit 40 (IFG=1 in 15$, and 27$ 28$ 29$ arrays)
In this case, input data on Section G are necessary.

DDX mode;

=0, write collapsed cross sections on I/O unit 11 in the form of group- independent library (ICON=2, 3 in 27$)
This library can be used without mixing process by ANISN-DD and DOT-DD.

=1, write collapsed macroscopic or microscopic cross sections on I/O unit 11 in the form of original DDX library

If collapsed cross sections are required, IFG=1 in 15$ array and 19$ 27$ 28$ 29$ arrays must be entered.

11) NPLOT output option for I/O unit 30

=0, no effect

=1, obtain the file for plotting on I/O unit 30

If angular fluxes are required, ID1=1 or 3 must be entered in 15$ array.

12) NAOUT option for card-image output of angular flux

=0, no effect

=N, write angular flux at the N-th spatial mesh on I/O unit 7

13) LENGPL P_l; maximum P_l order of collapsed cross sections (effective only if NXSOUT=1)
DDX; unumber of DDX angle bins
This parameter must equal to ISCT in 15$ array.

(3) Section C (IISPTM=1)

1) NOYGRE number of energies to be specified in Section D
NOYGRE = 1GM+1 for neutron or gamma-ray problem
NOYGRE = 1GM+2 for coupled neutron and gamma-ray problem

(4) Section D (IISPTM=1)

(YGRENE(I), I=1, NOYGRE) energy group boundaries given in descending order of energy in eV

(5) Section E (IIANLL≧1)

1) NOANNO number of mesh boundaries or midpoints to print angular fluxes (≦10)

(6) Section F (IIANLL≧1)

(NOANLL(I), I=1, NOANNO) mesh numbers to print angular fluxes

(7) Section G (NXSOUT=1 and IANISN≦1)

1) NACT number of detectors for which response functions are added at the top of cross section table
2) IDOT output format for collapsed cross section
   =0, TWOTRAN format
   =1, DOT format
3) NPU output of collapsed cross section
   =0, print only
   =1, write on card-image file (I/O unit 7)
   =2, write on file (I/O unit 40)
   =3, add cross sections to the file produced in the previous case (I/O unit 40)
4) IGNT number of groups of (n,2n) down scattering
   Normally, total number of neutron groups is entered. When IDOT=1, IGNT is put to be zero.
5) IGMN number of energy groups of collapsed cross sections
   Cross sections of the first IGMN groups are output. Note that IGMN must be less than or equal to the number of collapsed groups determined from input data in 28$ array.
6) ITL2 length of output cross section table
   Specify ITL2=NACT+IGMN+3 for DOT and ITL2=NACT+IGMN+5 for TWOTRAN.

(8) Section M (IANISN≧2)

(XMU(M), M=1, LENGPL+1) angular mesh boundaries of DDX from 1.0 to −1.0
The input values are replaced with those read in from the I/O unit 24 (group-independent library) if IANISN=3.

(9) Section X (IANISN≧2 and IGMNEW<0)

Enter the following thermal group cross sections for required nuclide:

nuclide ID, $\sigma_{production}$, $\sigma_{fission}$, $\sigma_{capture}$, $\nu\sigma_{fission}$, σ_{total}.

Data input for Section X is terminated by an arbitrary negative integer and /. If no data is given for some nuclides in this section, thermal cross sections of those nuclides are set to be 0.0.

(10) Section H (NREACT≠0)

Section H must be placed after the data for the first case of ANISN-DD run. Section H gives the names of detectors and their response functions. When the neutron and gamma-ray responses are calculated, Section H for neutron and gamma-ray must be given, that is, at first the neutron's data and the gamma-ray's data.

CARD H-1 format (I5)

1) NELM number of detectors for which the response functions for neutrons or gamma-rays are stored

CARD H-2 format (I5, 4A4) (NELM>0)

1) NAME identification number for the detector
2) DXCM title of the detector

CARDS H-3 format (6E12.5) (NELM>0)

1) (OSIG(I), I=1, NG) response function of the detector in descending order of energy
The parameter NG is the number of neutron groups or gamma-ray groups.

The CARD H-2 and CARD H-3 data are repeated by NELM times.

4.2.2 ANISN-DD Input Data with FIDO Format

<Data Block 0>

Problem title (A48)

* Control Data

<Data Block 1>

/15$/ Integer data

1) ID problem ID number
2) ITH problem type
   =0, forward calculation
   =1, adjoint calculation
3) ISCT P_l; maximum order of Legendre expansion of scattering
   DDX; number of DDX angle bins
4) ISN order of angular quadrature
5) IGE geometry type
   =1, slab; =2, cylinder;
   =3, sphere
6) IBL left boundary condition
   =0, vacuum (no incoming flux)
   =1, reflective
   =2, periodic
   =3, white/albedo
7) IBR right boundary condition with the same options as IBL
8) IZM number of zones
9) IM number of mesh intervals
10) IEVT eigenvalue type
   =0, fixed source
   =1, k calculation
   =2, a calculation
   =3, concentration search
   =4, zone width search
   =5, outer radius search
   =6, buckling search
11) IGM number of energy groups (equal to | IGMNEW)
12) IHT position of σ_t in cross section table (=3 in DDX mode, automatically set)
13) IHS P_l ; position of $\sigma_{g\cdot g}$ in cross section table
   DDX; position of the beginning of $\sigma_{g\cdot g}$ (=4, automatically set)

14) IHM cross section table length
(automatically set in DDX mode)

15) MS P_l ; mixing table length
DDX; no effect

16) MCR number of cross section sets to be read from card-image input on I/O unit 5
(automatically set to be 0 in DDX mode)

17) MTP P_l ; number of cross section sets from file
DDX; sum of the numbers of nuclides used in each material

18) MT P_l ; total number of cross section sets
DDX; number of mixtures to be prepared by mixing process (IANISN=2, 4), or number of mixtures in group-independent library (IANISN=3)

19) IDFM density factors (21 *)
=0, not used
=1, used

20) IPVT type of parametric eigenvalue search
=0, no effect
=1, search for specified k_{eff}
=2, search for specified α
The k_{eff} or α value is entered as PV in 16 * array.

21) IQM distributed-volume source (17 *)
=0, no effect
=1, enter distributed source

22) IPM shell source (18 *)
=0, no effect
=1, enter shell source by group and angle
=IM, enter shell source by interval, group and angle

23) IPP interval number containingshell source (IPM=1)
If IPM≠1, IPP=0 must be entered.

24) IIM maximum number of inner iterations

25) ID1 output option
=0, no effect
=1, print angular flux
=2, write scalar flux on card-image file (I/O unit 7)
=3, both 1 and 2

26) ID2 cross section type and fixed source (P_l mode only)
=0, no effect
=1, use specially prepared group-independent cross section file containing MTP materials
=2, use cross sections and fixed source from previous problem

27) ID3 number of activities calculated by zone (22$ and 23$)
If ID3=0, no activity calculation is performed. Activation cross sections must be contained in a cross section library.

28) ID4 interval-wise activities
=0, no effect
=1, calculate ID3 (not ID4) activities by interval

29) ICM maximum number of outer iterations

30) IDAT1 storage mode
=0, all data stored in core if possible

=1, cross sections and fixed source stored on disk
=2, fluxes and currents (angular flux) on disk also
=3, scattering kernel matrices multiplied by the quadrature weight are stored by incident group for one outgoing group on I/O unit 60; if IDAT1 < 3, all matrices for one outgoing group are written in one record. (effective only in DDX mode)

31) IDAT2 calculation selector
=0, no effect
=1, execute diffusion solution for specified groups (24$)

32) IFG cross section collapsing
=0, no collapsing
=1, flux weighted cross section (27$ and 28$)

33) IFLU flux calculation model
=0, mixed linear-step mode
The step model is used when a linear extrapolation yields negative flux.
=1, linear model only
=2, step model only

34) IFN initial guess
=0, enter fission guess (2 *)
=1, enter flux guess (3 *)
=2, use fluxes from previous case

35) IPRT cross section print option
=0, print cross sections
=1, do not print cross sections

36) IXTR
P_l mode;
=0, calculate Legendre coefficients
=1, read Legendre coefficients from card-image input on I/O unit 5
DDX mode;
=0, calculate angular transfer probabilities
=1, read angular transfer probabilities from I/O unit 62
=−1, read angular transfer probabilities and quadrature constants from I/O unit 62

/16 * / Floating point data

1) EV first eigenvalue guess for search

2) EVM eigenvalue modifier for search
The second eigenvalue guess = EV ± EVM where the plus sign is taken if the system is supercritical for the first guess.

3) EPS general convergence criterion
This criterion is applied to tests on the integral inner iteration convergence, lambda (λ) and fission density.

4) BF buckling factor, normally 1.420892

5) DY cylinder or plane height for buckling correction

6) DZ plane depth for buckling correction

7) DFM1 transverse dimension for void streaming correction

8) XNF source normalization factor
If XNF=0.0, no normalization is performed.

9) PV 0.0, k_0 or p_0 according to IPVT = 0, 1 or 2

10) RYF λ_2 relaxation factor, normally set 0.5

11) XLAL criterion for pointwise flux convergence
Not used if XLAL=0.0.
12) XLAH upper limit for $|\lambda-1.0|$ used in linear search, normally set 0.05
13) EQL eigenvalue change epsilon for search calculations
When the difference between two successive $\lambda <$ EQL, a new eigenvalue is calculated.
If $|1-\lambda| <$ EQL, the linear search is used to complete the search.
14) XNPM new parameter oscillation damper for linear search, normally set 0.75

T Terminator

* Array Data

<Data Block 2> Cross Sections

/13$/ P_l; Nuclide identification numbers from data set on I/O unit 8 (MTP≠0)
(MTP entries)
DDX; I/O unit of DDX library from which cross sections for each nuclide are read
(MTP≠0)
(MTP entries)
/14*/ Cross sections (MCR≠0 and IANISN≦1)
(IHM * IGM * NCR entries)

Note that no data of Data Block 2 are necessary in DDX mode if MTP=0.

T Terminaror

<Data Block 3> Fixed Source

/17*/ Distributed volume source (IQM>0)
IENRGY = 0;
((Q(i,g), i=1, IM), g=1, IGM) (IM * IGM entries)
IENRGY = 1;
Enter 17* for each group, and each array is followed by
"T". (IM entries for each group)
/18*/ Shell source (IPM>0)
MM = ISN+1 (IGE=1, 3) or ISN * (ISN+4)/4 (IGE=2)
IENRGY = 0;
((Q(m,i,g), m=1, MM), i=1, IPM), g=1, IGM)
(MM * IPM * IGM entries)
IENRGY = 1;
Like as for 17* (MM * IPM entries for each group)

T Terminator

<Data Block 4> Flux or Fission Guess (IFN<2)

/2*/ Fission density (IFN=0) (IM entries)

/3 */ Flux guess (IFN=1) (IM * IGM entries)
((F(i,g), i=1, IM), g=1, IGM)

T Terminator

<Data Block 5> Remainder of Data

/1 */ Fission spectrum (IGM entries)
/4 */ Radii by interval boundary (IM+1 entries)
/5 */ Velocities (IGM entries)
/6 */ Angular quadrature weights (MM entries)
/7 */ Angular quadrature cosines (MM entries)
/8$/ Zone numbers by interval (IM entries)
/9$/ Material numbers by zone (IZM entries)
/10$/ P_i; mixture numbers in mixing table (MS entries)
DDX; number of nuclides by mixture (MT entries)
A user can omit this input if IANISN=3.
/11$/ P_i; component numbers in mixing table (MS entries)
DDX; nuclide ID numbers for all mixtures (MTP entries)
/12 */ P_i; number densities in mixing table (MS entries)
DDX; number densities (MTP entries)
/19$/ P_i; order of scattering by zone (ISCT>0) (IZM entries)
DDX; few angle number for each angle (IPUN=1) (ISCT entries)
In DDX mode, 19$ data is used in cross section collappsing.
See the description for 27$ data.
/20 */ Radius modifiers by zone (IEVT=4) (IZM entries)
Each spatial mesh width ΔR_i is modified by using the eigenvalue EV and the radial modifier of the zone RM_z as follows:
$\Delta R_i^n = \Delta R_i^o(1.0+\mathrm{EV}\times RM_z)$.
/21 */ Density factors by interval (IDFM=1) (IM entries)
/22$/ Material numbers for activities (ID3>0) (ID3 entries)
/23$/ Table position for activation cross section (ID3>0) (ID3 entries)
/24$/ Diffusion calculation markers (IDAT2=1) (IGM entries)
=0, S_n transport theory
=1, S_2 calculation
=2, homogeneous flux
/25 */ Right boundary albedo by group (IBR=3) (IGM entries)
/26 */ Left boundary albedo by group (IBL=3) (IGM entries)
/27$/ Few group parameters (IFG=1)
1) ICON type of collapsed cross section
=0, no effect
=1, microscopic cross section desired
=2, macroscopic cross section desired
(minus implies cell weighting over all zones)
=3, macroscopic cross section desired
(cell-weighting for arbitrary zones)

2) IHTF position of total cross section in weighted cross section table
(automatically set in DDX mode)

3) IHSF position of self scattering cross section in weighted cross section table
(automatically set in DDX mode)

4) IHMF table length of weighted cross section
(automatically set in DDX mode)

5) IPUN option

P_l mode; output

=0, no effect

=1, write weighted cross sections on I/O unit 7 (card-image output)

=2, obtain a weighted cross section file on I/O unit 11

DDX mode; angle collapsing

=0, no effect

=1, angle collapsing (19$)

In DDX mode, weighted cross sections are always written on the I/O unit 11.

/28$/ Few group number for each multi-group (IFG=1) (IGM entries)

/29$/ Cell numbers for each zone, which become the numbers for cell weighted cross sections
(IFG=1, ICON=3) (IZM entries)

/34 * / P_l constants (IXTR=1) (JT * MM entries)

T Terminator

4.3 Job Control Instruction

4.3.1 Job Control Statements

A sample of job control statements for a FACOM-M-series computer of JAERI is shown in **Fig. 4.1**. The overlay structure of ANISN-DD is also shown in this figure as input data for the linkage editor. An executive load module of ANISN- DD has been prepared in JAERI with a member name ANISNDD in the file J3803. ANISNDD.LOAD. The size of common for ANISN-DD in this module is 30 k words, and a user should replace the main routine by user's one having an appropriate size of common as described in Section 4.3.3.

4.3.2 I/O File Requirement

Files of I/O required by ANISN-DD are summarized in **Table 4.1**. Format of DDX library, and a details of contents and their formats for each output file in DDX mode are as follows:

(1) Double-Differential Form Cross Section Library

m = 1, Element

1) MAXI, IDUMMY, IDUMMY, MATNO, (TITLE(i), i=1, 12)

2) (MAXSD(i), i=1, MAXI)

3) $(\sigma_{pn}^{g'},\sigma_f^{g'},\sigma_c^{g'},\nu\sigma_f^{g'},\sigma_t^{g'},g'=1,\text{MAXI})$

g' = 1, MAXI

4) $((I(k;g'\rightarrow g),k=1,\text{MAXMU}),\ g=g',\ g'+\text{MAXSD}(g')-1)$

Table 4.1 ANISN–DD file requirement

I/O unit	Remarks	I/O* DDX mode	I/O* P_l mode
1	Scratch file for cross section	A I/O	A I/O
2	Scratch file for cross section	A I/O	A I/O
3	Scratch file for flux etc.	A I/O	A I/O
4	P_l cross section library	X	A I
8	Scratch file for flux etc.	A I/O	A I/O
9	Necessary for NXOUT = 1 in P_l mode	X	A I/O
11	Collapsed cross section	B O	B O
14	Restart file (NRESAT = 1)	B I	B I
15	Restart file (NRESAT = 1)	B O	B O
16	Output for shell source	B O	B O
	(IIANLL = 2)		
20	Scratch for boundary total flux	B I/O	B I/O
	(IIBOUD = 1)		
24	Group-independent macro-DDX	A I/O	X
25	Source input file (IINPT = 1)	B I	B I
30	Output file for plotting etc.	B O	B O
	(NPLOT = 1)		
40	Collapsed cross section for DOT	X	B O
	or TWOTRAN (NXSOUT = 1, NPU = 2, 3)		
50	Scratch file for DDX mixing	B I/O	X
	DCB = (RECFM = F, DSORG = DA)		
	(IANISN = 2, 4)		
51	Scratch file for DDX mixing	B I/O	X
	(IANISN = 2, 4)		
52	Scratch file for DDX mixing	B I/O	X
	(IANISN = 2, 4)		
55	Scratch file for data input	A I/O	A I/O
60	Scratch file for DDX * ATP	B I/O	X
61	Scratch file for summary edit	A I/O	X
62	Angular transfer probability	B I	X
	(IXTR = 1, −1)		
MTT(i)	Input DDX libraries	B I	X
	(IANISN = 2, 4)		
90	Check write (dummy file is allowed)	A O	A O
5	Card-image input for ANISN–DD	A I	A I
6	Output of final result	A O	A O

*A : always necessary file.
B : conditionally necessary file.
X : unnecessary file.
I : read-only file.
O : write-only file.

```
//JCLG JOB
// EXEC JCLG
//SYSIN DD DATA,DLM='++'
// JUSER XXXXXXXX,MORI,0431.110
  T.6  C.3  W.4  I.5
  OPTP PASSWORD=XXXXXX,MSGCLASS=R
//*********************************************
//*  J3803.DDX.CNTL(GOANISN2)
//*  ANISN-DD ( BY DDX )
//*********************************************
//    EXEC FORT77,A='SOURCE'
       COMMON /BULKBU/ D(1),LIM1,DUMY(600000)
       COMMON /PMMBUF/ P(1),LIMP,DUMMY2(2000)
             LIM1   =  600000
             LIMP   =  2000
       CALL ERRSET(257,300,-1,1,1,257)
       CALL ANISN
       STOP
       END
//FORT77.SYSPRINT DD DUMMY
//    EXEC LKED77,A='OVLY'
//OLDLM  DD DSN=J3803.ANISNDD.LOAD,DISP=SHR,UNIT=D0430
//SYSIN  DD *
    ENTRY MAIN
    INCLUDE OLDLM(ANISNDD)
    OVERLAY ANSO1
    INSERT PLSNT,FIDO,TP,ADJNT,S804,S805,S814,WOT8,S966,FFREAD
    OVERLAY ANSO1
    INSERT GUTS,S807,S810,S821,S824,S833,DT,CELL,S851
    OVERLAY ANSO1
    INSERT FINPR,FINPR1,PUNSH,DTFPUN,FLTFX,NWSUB1,NWSUB2,ACTPRT
    INSERT WOTYT
    OVERLAY ANSO4
    INSERT BT,SUMARY,FACTOR,NWSUB3,NWSUB4
    OVERLAY ANSO4
    INSERT FEWG,WATE,CONVT,CRATE
    OVERLAY ANSO4
    INSERT DDFEWG,FMICRO,FMACRO
    NAME TEMPNAME(R)
// EXEC ANY
// EXEC GO,OBSIZE=137
//*----------- FT1,FT2 : CROSS SECTION STORAGE ----------------------
//FT01F001 DD UNIT=WK10,SPACE=(TRK,(200,10)),DCB=(BLKSIZE=19069)
//FT02F001 DD UNIT=WK10,SPACE=(TRK,(200,10)),DCB=(BLKSIZE=19069)
//*----------- FT3,FT8 : FLUX & ANGULAR FLUX STORAGE ----------------
//FT03F001 DD UNIT=WK10,SPACE=(TRK,(200,10)),DCB=(BLKSIZE=19069)
//FT08F001 DD UNIT=WK10,SPACE=(TRK,(200,10)),DCB=(BLKSIZE=19069)
//*----------- FT9 : GROUP INDEPENDENT X-SEC. FOR DOT,TWOTRAN -------
//FT09F001 DD UNIT=WK10,SPACE=(TRK,(50,10)),DCB=(BLKSIZE=19069)
//*----------- FT11 : COLLAPSED X-SEC. FOR DOT,TWOTRAN --------------
//FT11F001 DD DSN=J3803.FEWGXS.DATA,UNIT=D0430,SPACE=(TRK,(5,1)),
//         DISP=(NEW,CATLG,DELETE),DCB=(RECFM=VBS,LRECL=X,BLKSIZE=19069)
//*----------- FT20 : BOUNDARY TOTAL FLUX STRAGE (IIBOUD=1) ---------
//FT20F001 DD UNIT=WK10,SPACE=(TRK,(50,10)),DCB=(BLKSIZE=19069)
//*----------- FT24 : GROUP INDEPENDENT X-SEC. (DDX TYPE) -----------
//FT24F001 DD UNIT=WK10,SPACE=(TRK,(20,20)),DISP=(NEW,PASS),
//         DCB=(RECFM=VBS,LRECL=X,BLKSIZE=19069)
//*----------- FT25 : INPUT SOURCE ----------------------------------
//FT25F001 DD DUMMY
//*----------- FT50 : WORK FILE FOR MIXING (DDX MODE) ---------------
//*                    ( NEEDED WHEN IANISN = 2 )
//*----------- FT51 : MIXED OR WEIGHTED BUT NOT GROUP INDEPENDENT X-SEC
//*                    ( NEEDED WHEN IANISN = 2 OR IFG = 1 )
//*----------- FT52 : TEMPORARY STORAGE OF DDX LIBRARY --------------
//*                    ( NEEDED WHEN IANISN = 2 )
//FT50F001 DD UNIT=WK10,SPACE=(TRK,(300,10)),DCB=(RECFM=F,DSORG=DA)
//FT51F001 DD UNIT=WK10,SPACE=(TRK,(100,10)),
//         DCB=(RECFM=VBS,LRECL=X,BLKSIZE=19069)
//FT52F001 DD UNIT=WK10,SPACE=(TRK,(100,10)),
//         DCB=(RECFM=VBS,LRECL=X,BLKSIZE=19069)
//*----------- FT55 : TEMPORARY STORAGE OF INPUT DATA ---------------
//FT55F001 DD UNIT=WK10,SPACE=(TRK,(2,1)),
//         DCB=(RECFM=VBS,LRECL=X,BLKSIZE=19069)
//*----------- FT60 : STORAGE FOR ANGULAR TRANSFER FUNCTION ---------
//*----------- FT61 : ANGULAR DEPENDENT SOURCE (FOR SUMMARY) --------
//*----------- FT62 : ANGULAR TRANSPORT FUNCTION (PMM) --------------
//FT60F001 DD UNIT=WK10,SPACE=(TRK,(500,100)),
//            DCB=(LRECL=X,BLKSIZE=19069)
//FT61F001 DD UNIT=WK10,SPACE=(TRK,(100,50)),DCB=(BLKSIZE=19069)
//FT62F001 DD UNIT=WK10,SPACE=(TRK,(100,50)),DCB=(BLKSIZE=19069)
//*----------- ARBITRARY FILE NO. : INPUT DDX-LIBRARY ---------------
//FT71F001 DD DSN=J3803.DDXLIB3.DATA,DISP=SHR,LABEL=(,,,IN)  (DDXLIB3)
//*----------- FT04 : PL CROSS SECTION INPUT ------------------------
//*T04F001 DD DSN=J9067.ENDGIX.DATA,DISP=SHR,LABEL=(,,,IN)   (B-4)
//*T04F001 DD DSN=J9067.JENGIX.DATA,DISP=SHR,LABEL=(,,,IN)   (J-3)
//*----------- FT90 : CHECK WRITE -----------------------------------
//FT90F001 DD DUMMY
//*T90F001 DD SYSOUT=*,          ( CHECK WRITE )
//*  DCB=(RECFM=FB,LRECL=137,BLKSIZE=1370)
//*----------- FT30 : OUTPUT OF PLOT DATA ---------------------------
//FT30F001 DD DSN=J3803.PLTANISN.DATA(SAMPLE),DISP=OLD
//SYSIN DD DSN=J3803.FNS.DATA(BENCH2),DISP=SHR,LABEL=(,,,IN)
++
//
```

Fig. 4.1 Job control statements for ANISN–DD.

(2) Processed Cross Section (I/O Unit 24)

1) MAXMU, (DUMMY, i=1, 5)
2) (XMU(i), i=1, MAXMU+1)
3) MT, MBSUM, IHM, IGMNEU, NDDXE, (DUMMY, i=1, 3)
4) (MTT(i), i=1, MBSUM) : data in 13$
5) (MB(i), i=1, MT) : data in 10$
6) (MC(i), i=1, MBSUM) : data in 11$
7) (XMD(i), i=1, MBSUM) : data in 12*
8) g = 1, IGMNEU
   (DUMMY, i=1, ITH−3), $\Sigma_a^m(g)$, $\nu\Sigma_f^m(g)$, $\Sigma_t^m(g)$,
   (($\Sigma_s^m(k, g\text{-}g'+1\rightarrow g)$, k=1, MAXMU), g'=1, IHMM), m=1, MT)

Note that IHMM=(IHM−IHT)/MAXMU and MBSUM=MTP (data in 15$). The cross section library of this type is called as "group-independent form library".

(3) Collapsed DDX Library (I/O Unit 11 if IFG=1)

Microscopic cross section (if ICON=1)

For each nuclide in each zone,

1) IGMF, IZ, IDUM, IDUM, MATN, (T(i), i=1, 12)
   IGMF : number of collapsed groups
   IZ : zone number
   IDUM : dummy data
   MATN: nuclide ID number
   T : problem title (48 characters)
2) (MAXSD(i), i=1, IGMF) : number of slowing down groups
3) 1-D cross section data σ_x
4) energy-angle probability distribution I

Macroscopic cross section (if ICON=2, 3)

i) group-independent form (if NXSOUT=0)

1) MAXMU, (DUMMY, i=1, 5)
2) (XMU(i), i=1, MAXMU+1)
3) IZM, IZM, IHMF, (DUMMY, i=1, 5)
4) DUMMY, i=1, IZM
5) DUMMY, i=1, IZM
6) DUMMY, i=1, IZM
7) DUMMY, i=1, IZM
8) group-independent data

Note that this file has the same structure as the I/O unit 24.

ii) DDX type (if NXSOUT=1)

For each zone, the following data are written.

1) IGMF, ICON, IDUMMY, IZ, (T(i), i=1, 12)
2) (IGMF, i=1, IGMF) : the same as MAXSD(i)
3) ($\tilde{\Sigma}_{pr,G}$,0.0,$\tilde{\Sigma}_{a,G}$,$\nu\tilde{\Sigma}_{f,G}$,$\tilde{\Sigma}_{t,G}$, G=1,IGMF)
4) energy-angle probability distribution $\tilde{I}$

Note that this file has the same structure as the double-differential form cross section library.

(4) Conventional P_l Cross Section Library

Group-independent form library (if ID2=1)

IANISN = 0 ;
- i = 1, IGM
  - 1) ((CRX(j, i, m), j=1, IHM), m=1, MTP)

IANISN = 1 ;
- i = 1, IGM
  - m = 1, MTP
    - 1) (CRX(j, m, i), j=1, IHM)

Material-organized library (if ID2=0)

IANISN = 0 ;
- m = 1, MTP
  - 1) IGM, IHM, IC, MATNO, (TITLE(i), i=1, 12)
  - 2) ((CRX(j, i, m), j=1, IHM), i=1, IGM)

IANISN = 1 ;
- m = 1, MTP
  - 1) IGM, IHM, IC, MATNO, (TITLE(i), i=1, 12)
  - i = 1, IGM
    - 2) (CRX(j, i, m), j=1, IHM)

(5) Output File for Plotting (I/O Unit 30 if NPLOT=1)

1) (T(i), i=1, 12) : problem title (48 characters)
2) IGM, IGMNEU, IGMGAM, IM, IZM, IIBOUD, IISPTM, IIANLL
3) ($E_n(i)$, i=1, IGMNEU+1) (if IGMNEU>0)
4) ($E_\gamma(i)$, i=1, IGMGAM+1) (if IGMGAM>0)
5) (R(i), i=1, IM+1) : spatial boundary
6) (M(i), i=1, IM) : zone number
7) ((XN(i, j), i=1, IM+1), j=1, IGMNEU) (if IGMNEU>0)
   : neutron total flux processed according to IIBOUD and IISPTM
8) ((XN(i, j), i=1, IM+1), j=1, IGMGAM) (if IGMGAM>0)
   : γ-ray total flux processed according to IIBOUD and IISPTM
9) $NELM_n$: number of reaction rates calculated for neutron
- n = 1, $NELM_n$
  - 10) (CM(i), i=1, 18) : title for reaction
  - 11) (RR(i), i=1, IP) : reaction rate,
    IP=IM or IM+1, depending on IIBOUD.
12) $NELM_\gamma$: number of reaction rates calculated for γ-ray
- n = 1, $NELM_\gamma$
  - 13) (CM(i), i=1, 18) : title for reaction
  - 14) (RR(i), i=1, IP) : reaction rate

1, IGM (if ID1=1 or 3)

15) ((XND(i, m), i=1, IM+1), m=1, MM) :
angular flux per unit solid angle and group. If IIANLL=3, these values are those at the midpoint of each spatial mesh.

(6) Angular Transfer Probability (I/O Unit 62 if | IXTR | =1)
See the description for the MONTA code in Section 7.2.

(7) Important Scratch Files

I/O unit 52 for processing DDX

In the first stage of mixing process fot the i-th media, DDX data of constituent elements of this media are copied from input DDX libraries to this scratch file. Contents are as follows:

- m = 1, Element (=MB(i))
  - g' = 1, IGM
    1) $((I(k; g' \rightarrow g), k=1, \mathrm{MAXMU}), g=g', g'+\mathrm{MAXSD}(g')-1)$

I/O unit 50 for processing DDX

This is a direct access file with record length of 4 * MAXMU * IGM. IGM records are required in an adjoint calculation. In a forward one, on the other hand, that depends on memory storage size available for the processing. IGM records are sufficient if all DDX data can be processed at a time. If it is impossible, IGM source groups are divided into several clusters of groups which are processed at a time, and each cluster requires N records, where N is the number of groups into which neutrons in this cluster slow down.

I/O unit 51 for processing DDX

- m = 1, Media
  1) IHM(m)
  - g = 1, IGM
    2) (DUMMY, i=1, ITH−3), $\Sigma_a^m(g), \nu\Sigma_f^m(g), \Sigma_t^m(g)$,
    $((\Sigma_s^m(k, g-g'+1 \rightarrow g), k=1, \mathrm{MAXMU}), g'=1, \mathrm{IHMM}), m=1, \mathrm{MT})$
  3) MEND (=9999)

Note that IHMM=(IHM(m)−IHT)/MAXMU and that IHM in the processed cross section library described in (1) is the maximum one of IHM(m).

I/O unit 60 for scattering kernel matrix

IDAT1 < 3 ;

- g = 1, IGM
  1) $((((X(m' \rightarrow m, g' \rightarrow g, j), m'=1, \mathrm{MM}), m=1, \mathrm{MM}), j=1, \mathrm{MT}), g'=\mathrm{MIG}, g)$

IDAT1 = 3 ;

- g = 1, IGM
  - g'= MIG, g
    1) $(((X(m' \rightarrow m, g' \rightarrow g, j), m'=1, \mathrm{MM}), m=1, \mathrm{MM}), j=1, \mathrm{MT})$

X and MIG are defined by

$$X(m' \rightarrow m, g' \rightarrow g, j) = w_{m'} \cdot \Sigma^j(g' \rightarrow g, m' \rightarrow m),$$

and

$$\mathrm{MIG} = \mathrm{MAX}\left[g - \frac{\mathrm{IHM}-\mathrm{IHT}}{\mathrm{MAXMU}} + 1, 1\right].$$

4.3.3 Memory Requirement

The memory storage requirement by ANISN-DD is the order of 400,000 + 4× (size of common BULKBU and PMMBUF in words). These common sizes depend on the problem solved and some

parameters such as IDAT1. Note that IDAT1 is automatically changed by the code according to the common size allowed for the problem (common BULKBU) and that ANISN-DD terminates by printing the message about the common size required for the present problem if the size is insufficient. The ANISN-DD code also stops by printing a similar message, when the size of common PMMBUF is insufficient for the calculation of angular transfer probability. The size of the common PMMBUF must be greater than *MAX*, where *MAX*=MAXMU÷ISN+4 for IGE=1 or 3 and *MAX*=MAXMU+3 for IGE=2. The ANISN-DD code adopts the flexible-dimensioning technique. A user must specify the size of both commons as follows:

```
C ——— MAIN ROUTINE OF ANISN-DD
      COMMON/BULKBU/D(1), LIM1, DUMY(xxxxxx)
      COMMON/PMMBUF/P(1), LIMP, DUMMY2(yyyy)
      LIM1 = xxxxxx
      LIMP = yyyy
      CALL ERRSET (257, 300, -1, 1, 1, 257)
      CALL ANISN
      STOP
      END
```

4.4 Sample Problem and Input Data

The geometrical arrangement of the sample problem and the sample input data for ANISN-DD are shown in **Figs. 4.2** and **4.3**, respectively. This problem is one of the JAERI-U.S. fusion neutronics calculation benchmarks[23]. The cross sections of the thermal group (125th group) are given by cards. The specification of this problem is as follows:

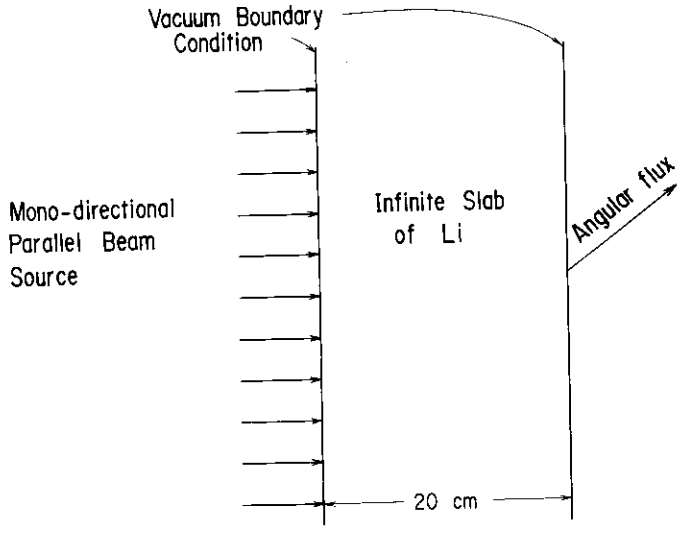

Fig. 4.2 Schematic diagram of ANISN-DD sample problem.

```
LIST
    4    0    0    0                                                    / A
    0    2    1 -125  125    0    0    0    0    0    1    0   20     / B
  126                                                                   / C
 1.6487E+7
 1.62310E+07 1.59800E+07 1.57320E+07 1.54880E+07 1.52480E+07 1.50120E+07
 1.47790E+07 1.45500E+07 1.43240E+07 1.41020E+07 1.38830E+07 1.36680E+07
 1.34560E+07 1.32480E+07 1.30420E+07 1.28400E+07 1.26410E+07 1.24450E+07
 1.22520E+07 1.20620E+07 1.18750E+07 1.16910E+07 1.15100E+07 1.13310E+07
 1.11560E+07 1.09830E+07 1.08120E+07 1.06450E+07 1.04800E+07 1.03170E+07
 1.01570E+07 9.99990E+06 9.39400E+06 8.82490E+06 8.29020E+06 7.78790E+06
 7.31610E+06 6.87280E+06 6.45640E+06 6.06520E+06 5.69780E+06 5.35250E+06
 5.02820E+06 4.72360E+06 4.43740E+06 4.16860E+06 3.91600E+06 3.67870E+06
 3.45590E+06 3.24650E+06 3.04980E+06 2.86500E+06 2.69140E+06 2.52840E+06
 2.37520E+06 2.23130E+06 2.09610E+06 1.96910E+06 1.84980E+06 1.73770E+06
 1.53350E+06 1.35330E+06 1.19430E+06 1.05400E+06 9.30130E+05 8.20840E+05
 7.24380E+05 6.39270E+05 5.64150E+05 4.97860E+05 4.39360E+05 3.87740E+05
 3.42170E+05 3.01970E+05 2.66490E+05 2.35170E+05 2.07540E+05 1.83150E+05
 1.61630E+05 1.42640E+05 1.25880E+05 1.11090E+05 9.80350E+04 8.65150E+04
 7.63490E+04 6.73780E+04 5.94610E+04 5.24740E+04 4.63080E+04 4.08670E+04
 3.60650E+04 3.18270E+04 2.80870E+04 2.47870E+04 2.18740E+04 1.93040E+04
 1.50340E+04 1.17090E+04 9.11860E+03 7.10160E+03 5.53070E+03 4.30730E+03
 3.35460E+03 2.61250E+03 2.03460E+03 1.58460E+03 1.23410E+03 9.61100E+02
 5.82930E+02 3.53570E+02 2.14450E+02 1.30070E+02 7.88910E+01 4.78500E+01
 2.90230E+01 1.76030E+01 1.06770E+01 6.47580E+00 3.92780E+00 2.38230E+00
 1.44490E+00 8.76400E-01 5.31560E-01 3.22410E-01 1.0001E-05          / D
    1                                                                  / E
   22                                                                  / F
  1.0  0.9  0.8  0.7  0.6  0.5  0.4  0.3  0.2  0.1  0.0
 -0.1 -0.2 -0.3 -0.4 -0.5 -0.6 -0.7 -0.8 -0.9 -1.0                     / M
  306  0.73493  0.0  940.368   0.0  941.103
  307  0.97000  0.0    0.0454  0.0    1.0154
 -100    / X
   US-JAERI BENCHMARK PROBLEM 2 (LI)
15**
       1    0   20   16    1          0    0    1   21    0
     125    3    4    0    1          0    2    1    1    0
       0    1    1   40    1          0    0    0   10    0
       0    0    0    1    1          0
16**
     0.0       0.0       1.0E-4    1.420892   0.0
     0.0       0.0       1.0       0.0        0.5
     1.0E-3    0.0       0.0       0.0  T
13**
     F   71  T
18**
    16R  0.0  0.009629  3Q17
    16R  0.0  0.1323    3Q17
    16R  0.0  0.06996   3Q17
    16R  0.0  0.007289  3Q17
    16R  0.0  0.001358  3Q17
    16R  0.0  0.0005460 3Q17
    16R  0.0  0.0003398 3Q17
    16R  0.0  0.0003089 3Q17
    16R  0.0  0.001107  16R      0.0  0.0011358 16R      0.0  0.0010484
    16R  0.0  0.00098789 16R     0.0  0.0010282 16R      0.0  0.0011466
    16R  0.0  0.0012462 16R      0.0  0.0013172 16R      0.0  0.0015086
    16R  0.0  0.0016357 16R      0.0  0.0017890 16R      0.0  0.0019299
    16R  0.0  0.0020846 16R      0.0  0.0021684 16R      0.0  0.0021959
    16R  0.0  0.0023012 16R      0.0  0.0025051 16R      0.0  0.0046303
    16R  0.0  0.0076168 16R      0.0  0.0049592 16R      0.0  0.0034095
    16R  0.0  0.0028088 16R      0.0  0.0028308 16R      0.0  0.0028955
    16R  0.0  0.0029859 16R      0.0  0.0029866 16R      0.0  0.0030687
    16R  0.0  0.0030561 16R      0.0  0.0059949 16R      0.0  0.0058960
    16R  0.0  0.0058291 16R      0.0  0.0056769 16R      0.0  0.0051135
    16R  0.0  0.0045217 16R      0.0  0.0039068 16R      0.0  0.0033709
    16R  0.0  0.0025389 16R      0.0  0.0016556
      F   0.0     T
 3**
      F   1.0  T
 1**
      F   1.0
 4**
      20I 0.0  21.0
 5**          F       1.0
 6**
    0.0         0.0244936  0.0413296  0.0392569  0.0400796  0.0643754
    0.0442097   0.1090850  0.1371702  0.1371702  0.1090850  0.0442097
    0.0643754   0.0400796  0.0392569  0.0413296  0.0244936
 7**
    -1.0        -0.9805009 -0.9092855 -0.8319966 -0.7467506 -0.6504264
    -0.5370966 -0.3922893 -0.1389568 0.1389568  0.3922893  0.5370966
    0.6504264   0.7467506  0.8319966  0.9092855  0.9805009
 8**       F 1
 9**         1
10**
           2
11**
     306  307
12**
     3.6980-3  4.2650-2
21**  0.0     F 1.0
   T
STOP
```

Fig. 4.3 Sample input for ANISN-DD.

(1) Geometry : infinite slab of 20 cm thick natural lithium

(2) Material composition : natural lithium consisting of

^{6}Li : 3.698×10^{21},

^{7}Li : 4.265×10^{22}.

(3) Source :

An external mono-directional fusion source[23] is incident perpendicularly on the left side of the slab. Source intensity is normalized to unity.

(4) Spatial mesh specification :

Void : 1 interval (a density factor is used.)

Li : 20 intervals

The intervals are equally spaced.

(5) Boundary condition :

The vacuum boundary condition is assumed on each side of the infinite slab. The incident beam is presented by the shell source option.

(6) Angular quadrature : S_{16}

5. DOT-DD : Two-Dimensional S_n Transport Code

5.1 New Features of DOT-DD

A two-dimensional S_n code DOT-DD and its auxiliary code UNCL-DD, which can use the DDX library as well as the conventional multi-group library with the P_l expansion, have been developed on the basis of the DOT 3.5 and GRTUNCL codes[9], respectively. The UNCL-DD code calculates a first collision source in R-Z geometry, which reduces the ray effect effectively in DOT-DD calculation for a problem containing a spatially and energetically isolated external source. The newly developed DOT-DD code has the following functions:

(1) forward transport calculation in two-dimensional X-Y, R-Z and R-Θ geometry,

(2) adjoint transport calculation,

(3) to solve a fixed source problem with one of an external volume source, a shell source and a first collision source calculated by the UNCL-DD code,

(4) to solve a criticality problem.

These two codes are vectorized to reduce computation time.

5.1.1 Cross Section

The DOT-DD code can use both the DDX and the conventional multi-group cross section library with the Legendre expansion method for scattering anisotropy. The cross section processing by UNCL-DD is quite similar to that by DOT-DD described in this section.

(1) DDX Library

When the DDX library is used, input data and cross section processing in DOT-DD are quite similar to those in ANISN-DD. Several subroutines are commonly used in both codes. In DOT-DD like ANISN-DD, a user can use processed macroscopic cross sections and bypass the cross section mixing process by setting $|A02| = 3$. If the cross section mixing process is selected ($|A02| = 2$ or 4), a user must specify the input parameters MTP and MT of 61$ array, an array of MT length, MB(j) of 10$ array in Data Block 10, and three arrays of MTP length, MC(i), MXD(i) and MTT(i) of 11$, 12* arrays in Data Block 10 and 13$ array in Data Block 4. Since the meaning of these variables and arrays is the same as that in ANISN-DD, see Section 4.1.1. The format of the processed group-independent form library is also the same as that used in ANISN-DD. Note that the cross sections of thermal group in the DDX library can be replaced with those read from the I/O unit 65 if necessary.

(2) P_l Library

When the cross section library with the P_l expansion is used (A02=0 or 1), the cross section treatment is similar to that of DOT 3.5 except for the meaning of an input parameter IGIXS which specifies the type of input cross section library. The DOT-DD code can use the material-organized library[17] and two types of group-independent ones. If IGIXS=0, MTP sets of cross sections are read from the material-organized library on the I/O unit NLIB with the format shown as IANISN=1 in Section 4.3.2. If IGIXS≠0, MTP sets of cross sections are read from the group-independent library on the I/O unit |IGIXS|. The sign of IGIXS specifies the format of the group-independent library; a negative IGIXS value means the library of type IANISN=1, and positive one corresponds to that of IANISN=0. By the mixing process of cross section, MT sets of cross sections are prepared on the I/O

unit NCR1 in the group-independent form with the format of IANISN=0. Note that the parameter values IDAT1=2 and 3 in UNCL-DD correspond to IGIXS>0 and <0 in DOT-DD, respectively, and that the I/O unit numbers are different in both codes.

5.1.2 Solution Algorithm and Angular Transfer Probability

The solution algorithm is similar to that in DOT 3.5[9] except for the calculation of scattering source with the DDX.

When the DDX is used, the scattering source term is calculated by Eq.(2-28) not using P_l moments of flux but using angular fluxes. The angular transfer probabilities $P(k,m',m)$ defined by Eq.(2-29) are calculated externally, and DOT-DD reads them from the I/O unit 61. Then the probabilities $\Sigma(g'\to g,m'\to m)$ are calculated by Eq.(2-30). When the input parameter A03 is specified between zero and 10,000, these probabilities are multiplied by the quadrature weight $w_{m'}$ and stored on the I/O unit 62. If A03>10,000, they are calculated every outer iteration to prevent overflow of work-disk. In this case, the data of $P(k,m',m)\cdot w_{m'}$ and DDX are written on the I/O units 62 and 63, respectively. The parameter A03 is reset to be A03-10,000. By setting A03<0, DOT-DD reads $w_{m'}\cdot\Sigma(g'\to g,m'\to m)$ from the I/O unit 62. The angular transfer probabilities for S_8 and S_{16} calculations have been prepared by using the MONTA code which is described in Section 7.2, and the details are given in Appendix 3.

5.1.3 First Collision Source

The subroutine to calculate a first collision source in DOT 3.5 does not work in DOT-DD. However, UNCL-DD, which calculates the first collision source and the uncollided flux at the midpoint of each spatial mesh in R-Z geometry for a DOT-DD calculation, has been developed on the basis of the GRTUNCL code[9].The UNCL-DD code can be also used with both DDX and P_l (libraries. The calculation procedure with the latter library is the same as that in GRTUNCL.)

When the DDX is used, on the other hand, the first collision source is calculated for each quadrature direction, not for the P_l moments, based on a similar algorithm to that used in DOT-DD. This is written for the m-th direction as

$$Q^{fc}_{g,m}=\sum_{g}\phi^{unc}_{g'}\cdot\sum_{k}\frac{\Sigma^{l}_{S}(k;g'\to g)}{2\pi\Delta\mu k}\times\frac{4\pi}{\Delta\Omega_m}\int_{\Delta\Omega m}d\Omega\delta_{\mu^*,k}, \tag{5-1}$$

where

$$\delta_{\mu^*,k}=\begin{cases}1 & \text{for } \mu_{k+1}\leqq\mu^*=\Omega\cdot\Omega_{in}\leqq\mu_k,\\ 0 & \text{otherwise,}\end{cases}$$

Ω_{in} and $\phi^{unc}_{g'}$ are an incident direction at the midpoint of the current spatial mesh and an uncollided flux at this point, respectively. The total collision source:

$$Q^{fc}_{g}=\sum_{m}w_mQ^{fc}_{g,m}, \tag{5-2}$$

the difference:

$$A_{g,m}=Q^{fc}_{g,m}-Q^{fc}_{g}. \tag{5-3}$$

and the uncollided flux $\phi^{unc}_{g'}$ are written on an output file. If a fission source is included, an isotropic one is added to Q^{fc}_{g}. In DOT-DD, the first collision source in the m-th direction is obtained by

$$Q^{fc}_{g,m}=A_{g'm}+Q^{fc}_{g}. \tag{5-4}$$

Equation (5-1) is calculated in UNCL-DD by

$$Q^{fc}_{g,m}=\sum_{g}\phi^{unc}_{g'}\cdot\sum_{k}\Sigma^{l}_{S}(k;g'\to g)P(k,m), \tag{5-5}$$

by using angular transfer probabilities defined by

$$P(k,m) = \frac{1}{2\pi \Delta\mu k} \frac{4\pi}{\Delta\Omega_m} \int_{\Delta\Omega m} d\Omega \delta_{\mu^*,k}.$$

$$= \frac{2}{\Delta\mu_k w_m} p(k,m), \tag{5-6}$$

where

$$p(k,m) = \frac{1}{4\pi} \int_{\Delta\Omega m} d\Omega \delta_{\mu^*,k} \tag{5-7}$$

Note that $P(k,m)$ and $p(k,m)$ satisfy the following relations.

$$\sum_{k} \frac{\Delta\mu_k}{2} P(k,m) = 1,$$

$$\sum_{m} w_m P(k,m) = 1, \tag{5-8}$$

and

$$\sum_{k} p(k,m) = w_m,$$

$$\sum_{m} p(k,m) = \frac{\Delta\mu_k}{2}. \tag{5-9}$$

In the calculation of angular transfer probability, the numerical integration or the Monte Carlo calculation is usually necessary because of the double-integration in Eq.(2-29). In UNCL-DD, however, an analytical method is applied since this code assumes that an incident direction is fixed to the mono-direction Ω_m, that is, integration over outgoing direction alone is required, as seen from Eqs.(5-1) and (5-6). The procedure to calculate $p(k,m)$ is described below.

(1) Calculation of $p(k,m)$

When we consider a unit sphere, any direction vector $\Omega = (\mu,\eta,\xi)$ has one-to-one correspondence to a point on this sphere. Accordingly, let Ω denote both a direction vector and a point on the unit sphere in this section. We define two types of regions or subsets on this sphere, which are schematically shown in **Fig. 5.1**, by

$W_m = \{\Omega \mid \Omega \in m\text{-th element of an } S_n \text{ quadrature set}\}$, and

$D_k = \{\Omega \mid \mu_{k+1} \leqq \Omega \cdot \Omega_{in} \leqq \mu_k\}$,

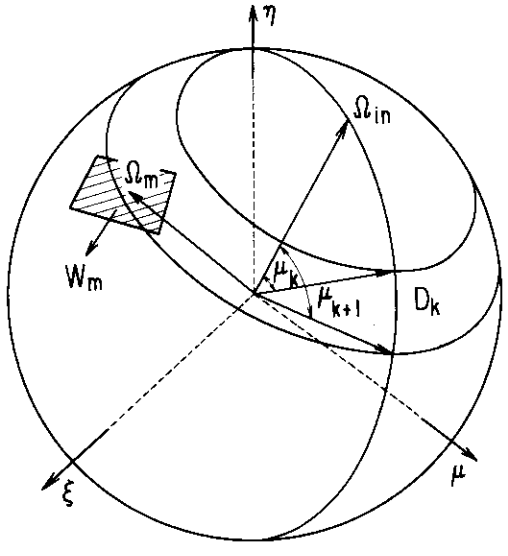

Fig. 5.1 Example of regions W_m and D_k on a unit sphere.

where μ_k and μ_{k+1} are boundaries of the k-th DDX angle bin ($\mu_1=1$). Then, Eq. (5-7) is written, by using the notations for the set algebra, as

$$p(k,m)=P(\mu_{k+1}\leqq\Omega\cdot\Omega_{in}\leqq\mu_k\cap\Omega\in W_m)=S(D_k\cap W_m)=S(D_k\cap W_m)/4\pi, \quad (5\text{-}10)$$

where $S(W)$ = area of a region W on the unit sphere.
Equation (5-10) can be rewritten as

$$\begin{aligned} p(k,m)&=[S(\{D_1\cup D_2\cup\ldots\cup D_k\}\cap W_m)-S(\{D_1\cup D_2\cup\ldots\cup D_{k-1}\}\cap W_m)]/4\pi \\ &=[S(C_k\cap W_m)-S(C_{k-1}\cap W_m)]/4\pi, \end{aligned} \quad (5\text{-}11)$$

where

$$C_k=D_1\cup D_2\ldots\cup D_k=\{\Omega\mid\mu_{k+1}\leqq\Omega\cdot\Omega_{in}\leqq1.0\}\ . \quad (5\text{-}12)$$

The UNCL-DD code obtains $p(k,m)$ based on Eq.(5.11) by calculating $S(C_k\cap W_m)$ by the method described below.

(2) Calculation of $S(C_k\cap W_m)$

At first, we can use the following obvious relations:

$$S(C_k\cap W_m)=\begin{cases} S(W_m) & \text{if } W_m\subset C_k. \\ S(C_k) & \text{if } C_k\subset W_m. \\ 0 & \text{if } C_k\cap W_m=\phi. \end{cases} \quad (5\text{-}13)$$

In the other cases, the boundary line of C_k ($\Omega\cdot\Omega_{in}=\mu_{k-1}$) traverses the region W_m, as shown in **Fig. 5.2.** In this case, $S(C_k\cap W_m)$ can be calculated by the following method.

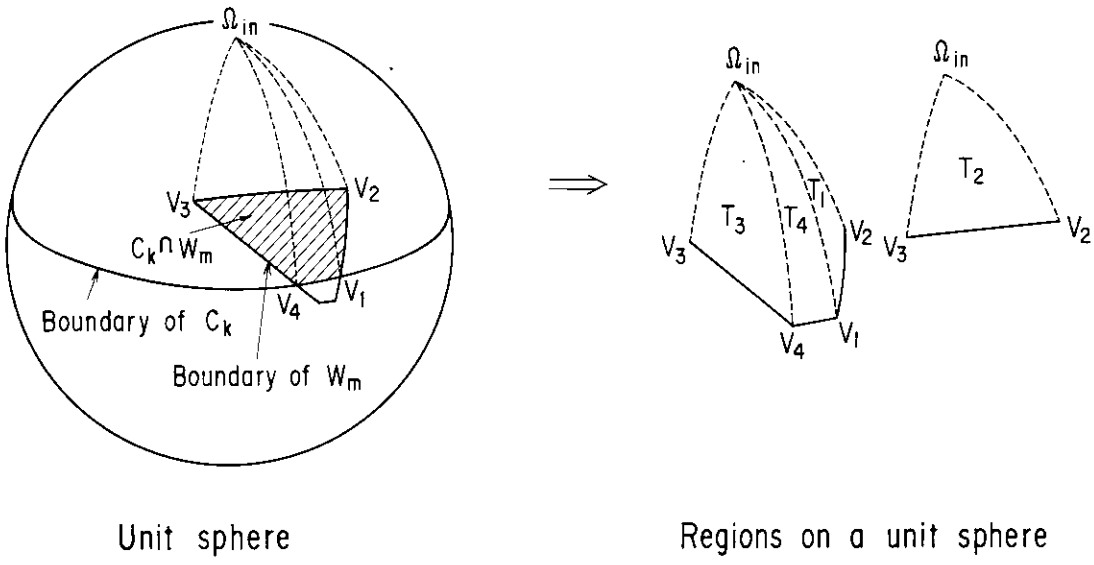

Fig. 5.2 Diagram for illustrating the calculation algorithm of $S(C_k\cap W_m)$.

1) Obtain the crossing points of the C_k and W_m boundary lines (v_1 and v_4 in **Fig. 5.2**).
2) Let v_l ($l=1, 2\ldots N$) be vertexes of the region $C_k\cap W_m$. N is the number of vertexes and the ordering of vertexes is taken in a counter-clockwise manner looking from the outside of the unit sphere.
3) Let T_l ($l=1, 2\ldots N$) denote triangular regions whose boundaries are two great circles (a great circle is a circle on the surface of sphere, with the center of the sphere as its center) determined by Ω_{in} and v_l and by Ω_{in} and v_{l+1} (broken lines in the figure), and a boundary line of $C_k\cap W_m$ between v_l and v_{l+1} (solid line in the figure). Note that "$l+1$" is taken as "1" when $l=N$.
4) Calculate $S(C_k\cap W_m)$ by the following formula:

$$S(C_k \cap W_m) = \sum_{l=1}^{N} \varepsilon_l S(T_l), \tag{5-14}$$

where ε_l is either $+1$ or -1 depending on the order of three vertexes of the triangle T_l looking from the outside of the sphere:

$$\varepsilon_l = \begin{cases} +1 & \text{if } v_l \to v_{l+1} \to \Omega_{in} \text{ is counter-clockwise.} \\ -1 & \text{if } v_l \to v_{l+1} \to \Omega_{in} \text{ is clockwise.} \end{cases} \tag{5-15}$$

(3) Calculation of $S(T_l)$

The area of the triangular region T_l, $S(T_l)$, is calculated by the following three methods according to the type of its side line $v_l \to v_{l-1}$. Note that the other sides of T_l are parts of great circles.

1) Line $v_l \to v_{l+1}$ is a part of a great circle, that is, all sides of T_l are parts of great circles. In this case, we can use the formula of area for a spherical triangle:

$$S(T_l) = \angle[v_l \Omega_{in} v_{l-1}] + \angle[\Omega_{in} v_{l-1} v_l] + \angle[v_{l+1} v_l \Omega_{in}] - \pi, \tag{5-16}$$

where a notation $\angle[\alpha\beta\gamma]$ indicates an angle on a unit sphere made by lines $\alpha \to \beta$ and $\gamma \to \beta$ (in radian). If we consider α, β and γ as vectors from the center of the unit sphere, $\angle[\alpha\beta\gamma]$ is calculated by

$$\cos(\angle[\alpha\beta\gamma]) = \frac{\alpha \cdot \gamma - (\alpha \cdot \beta)(\gamma \cdot \beta)}{\sqrt{[1-(\alpha \cdot \beta)^2][1-(\gamma \cdot \beta)^2]}}. \tag{5-17}$$

This formula is derived from the fact that this angle is equal to that between two projected vectors of α and γ on a plane vertical to β.

2) Line $v_l \to v_{l+1}$ is a part of the boundary of C_k. In this case, T_l is not a spherical triangle but a part of C_k bounded by two great circles passing Ω_{in}. Accordingly, the area is calculated by the following formula:

$$\begin{aligned} S(T_l) &= S(C_k) \cdot (\angle[v_l \Omega_{in} v_{l+1}] / 2\pi) \\ &= 2\pi(1-\mu_k) \cdot (\angle[v_l \Omega_{in} v_{l-1}] / 2\pi) = (1-\mu_k) \cdot \angle[v_l \Omega_{in} v_{l-1}] \end{aligned} \tag{5-18}$$

3) Any position vector corresponding to a point on line $v_l \to v_{l+1}$ has a constant cosine against a specified direction vector Γ other than Ω_{in} (see **Fig. 5.3**). Note that this case equals the case 2) mentioned above when $\Gamma = \Omega_{in}$. In this case, we define the following three regions:

P' : has three vertexes v_l, v_{l-1} and Ω_{in} like T_l, but a boundary line between v_l and v_{l+1} is a part of a great circle.

Q : has three vertexes v_l, v_{l+1} and Γ, and both lines $\Gamma \to v_l$ and $\Gamma \to v_{l+1}$ are parts of great circles and a boundary between v_l and v_{l-1} is shared with T_l.

Q' : has three vertexes v_l, v_{l+1} and Γ like Q, but a boundary line between v_l and v_{l+1} is a part of a great circle.

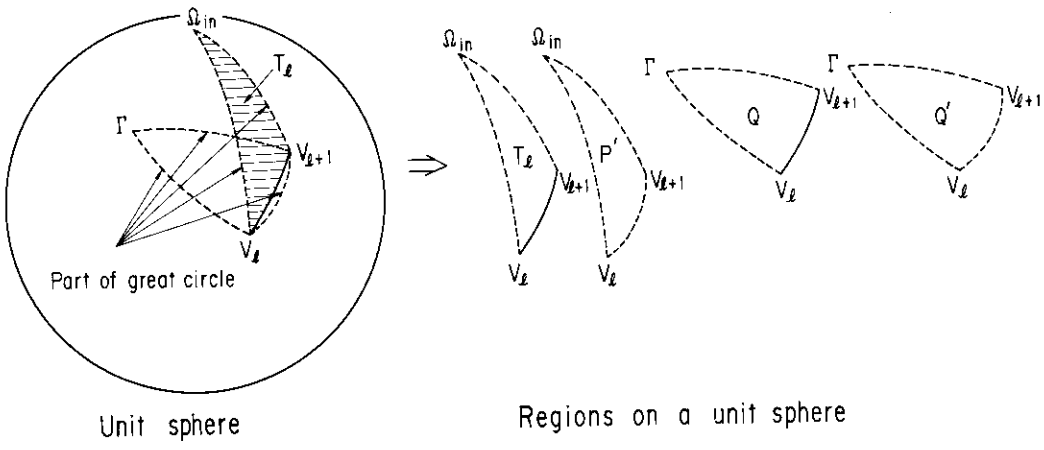

Fig. 5.3 Diagram for illustrating the calculation algorithm of $S(T_l)$.

The areas, $S(P')$ and $S(Q')$, and $S(Q)$ are calculated by the same methods as those for the cases 1) and 2), respectively. Then, $S(T_l)$ is obtained by

$$S(T_l)=S(P')+\kappa \cdot (S(Q)-S(Q')), \tag{5-19}$$

where κ is either $+1$ or -1 depending on the location of Γ and Ω_{in} on the surface of unit sphere which is divided into two parts by the great circle passing v_l and v_{l+1}:

$$\kappa=\begin{cases}+1 & \text{if } \Omega_{in} \text{ and } \Gamma \text{ belong to the same part.}\\ -1 & \text{if } \Omega_{in} \text{ and } \Gamma \text{ belong to the different parts.}\end{cases} \tag{5-20}$$

(4) Region Boundary of W_m -

In order to obtain P or p by the above procedure, it is necessary to define explicitly the shape of region W_m or its boundary, though no definite region boundary is given in the quadrature set. The UNCL -DD code assumes that the unit sphere are divided as shown in **Fig. 5.4**, which is called as "igloo" type. In this case, the boundary lines are determined from the quadrature directions and their weights. As an option, a user can select another "honeycomb" type division which is shown in **Fig. 5.5.** In this case, a boundary line consists of points at equal distance from relevant quadrature directions. As a result, $S(W_m)$ with the "honeycomb" type boundaries is automatically determined by the code. Note that the calculated $S(W_m)/4\pi$ is slightly different from the weight given by the quadrature set. We recommend to use the "igloo" type, especially in the case of low order S_n approximation.

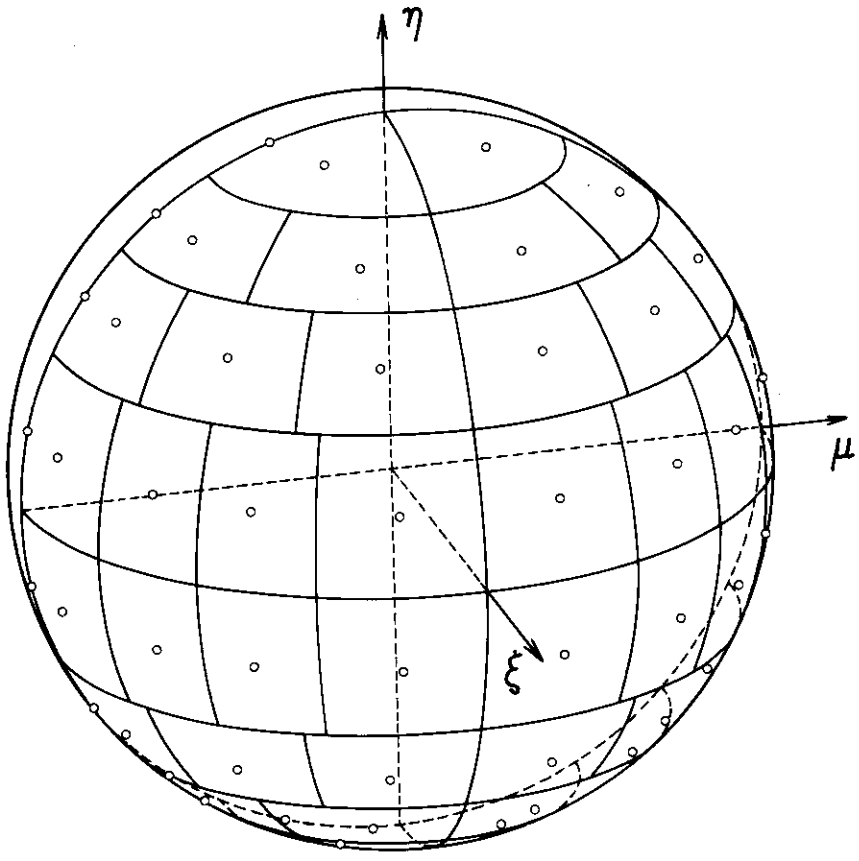

Fig. 5.4 Sub-regions on a unit sphere defined to calculate angular transfer probabilities ("Igloo" type).

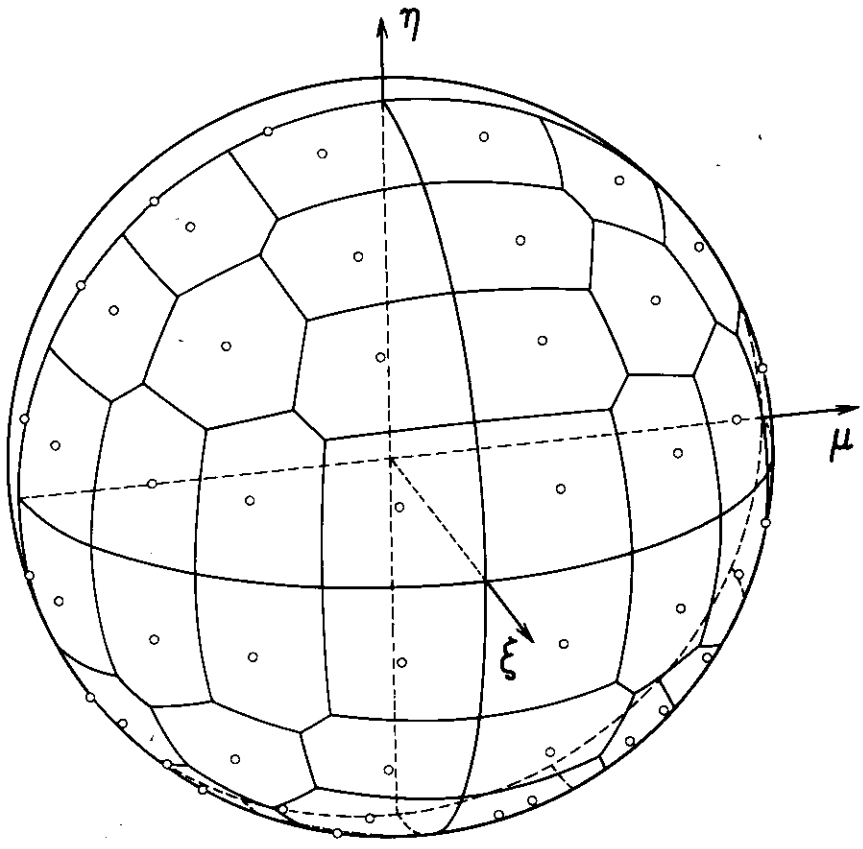

Fig. 5.5 Sub-regions on a unit sphere defined to calculate angular transfer probabilities ("Honeycomb" type).

5.1.4 Speed-Up of Calculation

If the DDX option is selected, DOT-DD consumes more CPU time than the case with the P_l cross sections in the scattering source calculation. The amount of this calculation is approximately proportional to

MM * MM * NSD * (IMJM − MT * MAXMU) for DDX, and

n * (2 * IGM * MM + NSD) * IMJM for P_l,

where

MM =number of S_n quadrature directions,
NSD =number of total slowing downs,
IGM =number of energy groups,
MAXMU =number of DDX angle bins,
MT =number of materials,
n =number of P_l moments = $(l-1)(l+2)/2$.

This quantity for DDX is generally larger by orders than that for P_l cross sections. The difference becomes larger with increasing S_n order (MM) since the calculation amount is proportional to MM^2 in the former case. Note that NSD and 2 * IGM * MM are nearly of the same order and that IMJM is larger than MT * MAXMU in a typical problem.

Accordingly, several subroutines treating the scattering source calculation are vectorized in order to reduce CPU time. The vectorized subroutines are OUTER, OUTERD, INNER, GRIND, PMMM and PMMM2. The inner iteration is not vectorized in the present code since the convergence of inner iteration is supposed to be faster than that with the P_l cross sections owing to non-negative scattering probability. As a result of the vectorization, speed-up of the order of 14 is achieved. Some subroutines of UNCL-DD

are also vectorized, which realizes the speed-up ratio by a factor of 11. A detail of the speed-up is described in Section 5.4.3. We recommend that a user run DOT-DD and UNCL-DD on a vector computer.

In addition to the vectorization, it is recommended that DOT-DD be run by utilizing the fast input/output capability such as FACOM fast I/O device for large and frequently used scratch files, i.e. those on the I/O units NCR1, NFLUX1, NSCRAT and 62.

5.1.5 Restart Function of DOT-DD

A two-dimensional S_n transport calculation generally requires a lot of CPU time, and therefore a function of restart is available in the original DOT 3.5 code. If the consumed CPU time exceeds the time limit, DOT 3.5 obtains tentative fluxes of every group by one or two inner iterations and prepares a complete restart file. In its restart calculation, the results of aborted run are used as an initial flux guess, and the fluxes of already converged groups are recalculated. This is necessary and useful for eigenvalue problems or fixed source problems with upscattering and/or fission since lower energy fluxes would influence higher energy ones through upscattering or fission. For a typical fusion neutronics calculation which is a fixed source problem and usually includes no fission source, i.e. the one-outer-iteration problem, it is, however, unnecessary to recalculate the fluxes already converged. Furthermore, the scattering source calculation by using the DDX is more complicated and time-consuming compared with that using the P_l cross sections. Accordingly, the outer iteration and restart procedure in DOT-DD are slightly modified from those in DOT 3.5.

The DOT-DD code, when the DDX is used, compares consumed CPU time with the time limit given by a user, and terminates the calculation if the consumed time reaches the time limit. Then the restart file is prepared from the converged fluxes above the group for which inner iterations converge and the guess fluxes below this group. In a restart run, the data in the restart file from the aborted run is read in as an initial flux guess in the same way as in the DOT 3.5 calculation, but the flux calculation (scattering source and inner iteration calculations) can be skipped for the first IS2 groups by setting IS2$\neq$0 in 61$ array, which specifies a converged group in the previous run. In this case, the code creates a new angular flux file (NAFT) and a restart file (NFLSV) for these groups by copying input files (NAFTIN and NFLUX1), if any. Note that this restart procedure can be used for the one-outer-iteration problem, and that if the problem is not the case, the restart should be performed in the same way as that of DOT 3.5 (set IS2=0). In the P_l mode run of DOT-DD, the restart procedure is similar to that of DOT 3.5.

5.2 Input Instruction

5.2.1 DOT-DD

The DOT-DD code reads input data from the I/O unit 5 with the FIDO format and cross sections of thermal group from the I/O unit 65 with the FORTRAN77 free format if necessary. The code adopts the default value shown in the text if zero is entered for that parameter.

(1) Card-Image Input from FT05F001 with FIDO Format

<Data Block −1>

Problem title (A72)

* Control Data Section

<Data Block 0>

/61$/ Integer data

1) A02 cross section type and execution mode
   = 0, forward calculation with Legendre expansion cross section
   = 1, adjoint calculation with Legendre expansion cross section
   = +2, mixing of forward DDX type cross section only
   = −2, mixing of adjoint DDX type cross section only
   = +3, forward calculation with DDX type cross section already mixed
   = −3, adjoint calculation with DDX type cross section already mixed
   = +4, both of +2 and +3
   = −4, both of −2 and −3
2) A03 P_l; maximum order of Legendre expansion of scattering
   DDX; number of angle bins of DDX
   If A03 > 10,000, A03 is set A03−10,000, and the products of angular transfer probabilities and cross sections (scattering kernel matrices) are calculated in every outer iteration to prevent work-disk overflow. If A03 < 0, the scattering kernel matrices are read from the I/O unit 62.
3) IZM number of material zones
4) IM number of "radial" spatial intervals in X or R direction
5) JM number of "axial" spatial intervals in Y, Z or Θ direction
6) IGM number of energy groups
   In DDX mode, if IGM is negative, the number of groups is | IGM | and cross sections for the | IGM | −th group are read from the I/O unit 65.
7) IHT position of σ_t in cross section table (normally set 3 in DDX mode)
8) IHS P_l ; position of $\sigma_{g,g}$ in cross section table
   DDX; position of beginning of $\sigma_{g,g}$ (normally set 4 in DDX mode)
9) ITL cross section table length
   (automatically set in DDX mode)
10) M01 mixing table length (no effect in DDX mode)
11) MCR number of cross section sets to be read from card-image input on I/O unit 5 (set 0 in DDX mode)
12) MTP P_l; number of cross section sets from file
   DDX; sum of the numbers of nuclides used in each materials
13) MT P_l; total number of cross section sets
   DDX; number of mixtures to be prepared by mixing process (| A02 | =2, 4), or number of mixtures in a macroscopic cross section library (| A02 | =3)
14) IP5 storage mode
   = 0, fluxes and moments or angular fluxes for all groups stored internally if possible
   = 1, fluxes and moments or angular fluxes for all groups stored externally during iteration
15) A04 number of angles in quadrature set
   Note that A04 = $n(n+4)/2$, where n is the order of S_n approximation.
16) IGE geometry type
   = 0, XY geometry (rectangular)
   = 1, RZ geometry (cylindrical)
   = 2, RΘ geometry (circular)
17) B01 left boundary condition
   = 0, vacuum (no incoming flux)
   = 1, reflected (mirror symmetry)
   = 2, periodic (repeating)

= 4, left boundary source input from card-image input on I/O unit 5 (18 *)
= 6, left boundary source input from file on I/O unit NBSO

18) B02 right boundary condition
= 0, 1, 2, 4, 6 same as for B01
= 3, white (isotropic incoming flux, total incoming equal to total outgoing)
= 5, albedo boundary condition (same as 3 except incoming flux, a fixed fraction of outgoing)

19) B04 bottom boundary condition
= 0–6, same as for B02

20) B03 top boundary condition
= 0–6, same as for B02

21) D05 outer iteration limit

22) S04 initial limit of inner iteration per group (effective in seach calculation)

23) G07 final limit of inner iteration per group
If G07 < 0, enter group-wise values in 28$ array.

24) MODE flux calculation model
= 0, mixed linear-step mode
The step model is used when a linear extrapolation yields negative flux.
= 1, linear model only
= 2, step model only
= 3, weighted difference model only
= 4, mixed linear-weighted difference mode
The weighted difference model is used when a linear extrapolation yields negative flux.

25) I04 problem type
= 0, fixed, distributed-volume source
= 1, k-multiplication factor
= 2, α-time absorption
= 3, c-concentration search (not available in DDX mode)
= 4, δ-zone thickness search
= 5, fixed boundary source, exterior or interior
= 6, analytic first collision source on I/O unit NPSO
= −6, analytic first collision source generated by DOT-DD internally, and written on I/O unit NPSO (not available in DDX mode)

26) IP1 acceleration technique
= 0, space-independent scaling
= 1, over relaxation
= 2, space-dependent scaling (WWESOL)

27) S02 type of parametric eigenvalue search (used only if I04=2, 3, 4)
= 0, search for k_{eff}=1.0 and α=0.0
= 1, search for specified k_{eff}=S03 and α=0.0
= 2, search for specified α=S03 and k_{eff}=1.0
The parameter S03 is given in 63 * array.

28) IZ number of radial zones for zone thickness search (used only if I04=4)

29) JZ number of axial zones for zone thickness search (used only if I04=4)

30) IZC zone convergence
= 0, no effect
= N, number of zones specified in 32$ array for convergence test

31) IB4 scattering order (no effect in DDX mode)
= 0, no effect
= 1, order of P_l expansion by group entered in 31$ array
32) ISC theory selector
= 0, no effect
= 1, type of flux solution by group in 29$ array
33) IZ3 first collision flux input
= 0, no effect
= N, length of source angular distribution table (33*, 34*)(used if I04=−6)
34) M07 flux guess input
= 0, A(G)
Enter a single 3* array containing IGM values. Input flux is uniform in space, and is energy dependent.
= 1, N(I,J,G)
Enter IGM 3* arrays, each containing IM*JM values. Input flux is space and energy dependent.
= 2, A(G)*N(I,J)
Enter two 3* arrays: IGM values in first and IM*JM values in second. Input flux is separable in space and energy.
= 3, A(G)*B(I)*C(J)
Enter three 3* arrays: IGM values in first, IM values in second, and JM values in third. Input flux is separable in all variables.
= 4, B(I,G)*B(J,G)
Enter two 3* arrays for each group: IM values in first and JM values in second. Input flux is separable in spatial variables only.
= 5, restart fluxes from I/O unit NFLUX1
Do not enter 3* array data block.
35) M06 method of input for distributed-volume source
= 0, 1, 2, 3, 4, same as for M07 except source array is designated by 17*
= 5, source on I/O unit NBSO, organized as S(I,J,G) as in M07=1
36) IZ1 radial interior boundary source input
= 0, no effect
= N, source for radial boundary (1<N≦IM) on I/O unit 5 (15*)
= −N, source on I/O unit NBSO
37) IZ2 axial interior boundary source input
= 0, N, −N, same as IZ1, for axial boundary (1<N≦JM)
38) IB5 radial interior boundary angular flux output
= 0, no effect
= N, write angular fluxes for angles with positive μ's at radial boundary N on I/O unit NBFT
= −N, write angular fluxes for angles with negative μ's at radial boundary N
39) IB6 axial interior boundary angular flux output
= 0, no effect
= N, write angular fluxes for angles with positive η's at axial boundary N on I/O unit NBFT
= −N, write angular fluxes for angles with negative η's at axial boundary N
40) IZ4 final total scattering source output

= 0, no effect
= N, write final total scattering source on I/O unit N

41) IB2 cross section and scalar flux print
= 0, print cross section and scalar flux
= 1, bypass cross section print
= 2, bypass scalar flux print
= 3, both 1 and 2

42) M05 number of activity edits desired (not usable in DDX mode)

43) IB1 zone balance tables
= 0, no effect
= N, number of zones specified in 30$ array for which zone balance tables are desired

44) IP3 output of fission density on card-image file
= 0, no effect
= 1, write fission density on I/O unit 7 (IM * JM array)

45) IAFT angular flux output
= 0, no effect
$= \pm 1$, write angular flux output on I/O unit NAFT
$= \pm 2$, print angula flux
$= \pm 3$, both 1 and 2
If IAFT $<$ 0, flags of angular flux output for each mesh must be given in 9$ array in Data Block 2.6. If IAFT $>$ 0, enter JBRL and JBRU in 62$ array. In this case, angular fluxes at the center of axial meshes from JBRL to JBRU are printed out and/or written on the file.

46) IP4 angular flux output control
= 0, no effect
= 1, output angular flux without doing extra outer iteration
This option can be used in one-outer-iteration problems. If IAFT = 0, IP4 is set to be zero in the code.

47) IS2 flux calculation bypassing (effective only in DDX mode)
The code bypasses the flux calculation from group 1 to group IS2, and creates a restart file (NFLSV) and an angular flux file (NAFT), if any, by copying flux guess file (NFLUX1). This option must be used with M07 = 5, IFLUX0 $>$ 0 and IP4 = 1.

48) IS3 reaction rate distribution for radial direction
= 0, no effect
= N, calculate reaction rate for N axial meshes
Enter response function from card-image input. This option is not usable in the present code.

49) IZ5 minimum iteration count of space point rescaling (WWESOL)
(default 8)

50) IZ6 maximum iteration count of space point rescaling (WWESOL)
(default 100)

51) IMG inner iteration count before space point rescaling

52) IP2 space point rescaling after every IP2 inner iteration

53) IB3 damping constant in space point rescaling

54) ITI scalar flux print
= 0, ordinary print
= 1, flux per unit lethargy
= 2, both 0 and 1

If ITI>0, enter energy boundaries as 1 * data in Data Block 11 and these data are written on an angular flux file, if any.

55) IFLUX flux guess preparation control (ignored if IFLUX=0)
(IFLUX=(IFLUX0+100*IFLUX1)*IFLUXS)

IFLUXS
= 1, no effect
= −1, print flux guess as written on I/O unit NFLUX1

IFLUX0
= 0, no effect
= NN, prepare flux guess on I/O unit NFLUX1 according to IFLUX1 (NN must be > 0 when IFLUX1>0)

IFLUX1
= 0, copy a flux guess from I/O unit NN onto I/O unit NFLUX1 such that:
(1) If | I04 | =6, the code subtracts uncollided flux, which must be supplied on I/O unit NPSO, from the flux guess.
(2) If IGMI≠0, the code copies only IGMI groups from unit NN to NFLUX1, filling remainder of NFLUX1 with "0". This option is useful if a previous problem aborts.
= 1, as for IFLUX1=0, but subtraction of uncollided flux is bypassed.
= 2, flux guess from unit NN is converted from IGMI groups, IA03I order of Legendre expansion (l of P_l), and IA04I directions in angular quadrature to IGM groups, A03 order, and A04 directions. (only in P_l mode)
= 3, two-dimensional flux guess is synthesized from two one-dimensional guesses entered from card-image input on I/O unit 5.

56) IGMI number of groups of input flux guess
If IFLUX1=0 or 1, groups IGMI+1 through IGM, if any, are filled with "0". This is useful in restarting an aborted problem. (default IGM)

57) IA03I order of Legendre expansion of input flux guess
(required only if IFLUX1=2, otherwise enter "0")

58) IA04I number of directions in angular quadrature of input flux guess
(required only if IFLUX1=2, otherwise enter "0")

59) ISRCE source preparation control
= 0, no effect
= N, copy source from I/O unit N
(1) If I04=5, the source is placed on the I/O unit NBSO to be used as either an external or internal fixed boundary source.
(2) If I04=6, a first collision source is placed on the I/O unit NPSO.

60) IGIXS cross section preparation control (no effect in DDX mode)
= 0, no effect
= N, copy group-independent cross sections from I/O unit | N | to NCR1
If N<0, the format of input cross section library is that given as IANISN=1 in Section 4.3. If N>0, IANISN=0.

61) IPRT first collision source print
= 0, no effect
= 1, print uncollided flux, μ's and η's
= 2, print uncollided flux, μ's and η's and first collision source

/62$/ Integer data (default value in ( ))

1) NCR1 I/O unit number of first scratch file (2)
A group-independent cross section input file, if any, goes here.

2) NFLUX1 I/O unit number of third scratch file (3)
A flux input file, if any, goes here.
3) NSCRAT I/O unit number of second scratch file (4)
4) NBSO I/O unit number of boundary source or distributed-volume source input file (14)
5) NPSO I/O unit number of first collision source input file (15)
6) NFLSV I/O unit of scalar flux and flux moments (P_l) or angular flux (DDX) output file (9)
This file is used as a restart file.
7) NAFT I/O unit number of angular flux output file (10)
If NAFT>100, DOT-DD defines NAFTIN=NAFT/100 and NAFT=NAFT-100 * NAFTIN, and creates a new angular flux file NAFT by copying angular flux of group 1 to IS2 from NAFTIN. This option (NAFT>100) must be used with IS2>0.
8) NBFT I/O unit number of interior boundary angular flux output file (11)
9) NGAM I/O unit number of activity output file (12)
10) NZBT I/O unit number of scratch file for zone balance table data (13)
11) NLIB P_l: I/O unit number of input cross section file (8)
DDX: I/O unit number of mixed DDX library (8)
12) NBUF no effect
13) JBRL (effective if IAFT>0)
= 0, no effect
= N, lower axial interval number to output angular flux
14) JBRU (effective if IAFT>0)
= 0, no effect
= N, upper axial interval number to output angular flux

/63 * / Floating point data
1) S01 source normalization factor (ignored if S01=0.0)
If S01<0.0, print out of distributed source is bypassed.
2) EPS general convergence criterion
This criterion is applied to tests on the integral inner-iteration convergence, lambda (λ) and the fission density.
3) G06 criterion for pointwise flux convergence
This criterion is not used if G06=0.0. If G06≠0.0, the integral inner iteration flux test is not used.
4) G05 CPU execution time limit in minutes
This parameter is not used if G05=0.0.
5) S03 parametric eigenvalue for search
This parameter is used only if I04=2, 3, 4 and S02>0.
6) EV first eigenvalue guess for search
This parameter is used only if I04=2, 3, 4.
7) EVM eigenvalue modifier for search
This parameter is used only if I04=2, 3, 4. The second eigenvalue guess = EV±EVM where the plus sign is taken if the system is supercritical for the first guess.
8) LAL criterion for search convergence
This parameter is used only if I04=2, 3, 4. After $|\lambda-1|$ >LAL, the linear search is used to complete the problem. Recommended value = 0.01.
9) EPSA criterion for new parameters
This parameter is used only if I04=2, 3, 4. When the difference between two successive λ becomes less than EPSA, a new eigenvalue is calculated. At the first

modification, the criterion is taken to be 3 * EPSA.

10) LAH upper limit on $|\lambda-1.0|$ used in linear search
This parameter is used only if I04=2, 3, 4. Recommended value = 0.05.

11) POD parameter oscillation damper for linear search
This parameter is used only if I04=2, 3, 4. $EV_{new} = EV_{old} + POD * EQ * (1-\lambda)$, where EQ is a measure of slope. Recommended value = 0.75.

12) SH position of point source on z-axis
The input parameter SH and the following three ones (HSA, SF and ZEXC) are used only if I04=-6.

13) HSA cosine of point source cone angle

14) SF point source magnitude
If SF<0, normalization of $f(\eta)$ given in 34* array is bypassed. If SF=0.0, no normalization is carried out in the code.

15) ZEXC exclusion radius

16) XDUM1 no effect

17) XDUM2 no effect

18) SPE convergence criterion for space point rescaling (default 0.0001)

T Terminator

* Array Data

<Data Block 1>

/7*/ Quadrature direction cosines μ and η
The μ's precede the η's. (2 * A04 entries)

T Terminator

<Data Block 2>

/6*/ Quadrature weights (A04 entries)

T Terminator

<Data Block 2.5> (|ITH| >1, in DDX mode)

/8*/ Angle mesh boundaries of DDX from 1 to -1 (A03+1 entries)

T Terminator

<Data Block 2.6> (IAFT<0)

/9$/ Angular flux output flags for each mesh (IM * JM entries)
A flag for each spatial mesh consists of five digits and non zero digits require the angular flux output at the mesh midpoint or boundaries corresponding to the digits:

digit 1 (10^4) : left boundary

digit 2 (10^3) : right boundary
digit 3 (10^2) : bottom boundary
digit 4 (10^1) : top boundary
digit 5 (10^0) : midpoint

T Terminator

<Data Block 3> (IFLUX1>1)

	if IFLUX1=2	* if IFLUX1=3
		*
/64$/	Old group number for each new group (IGM entries) (Default : old group = new group)	* Old group number for each new group (IGM entries) (Default : old group = new group)
		*
		*
/65*/	New total flux by group, arbitrary units (IGM entries) (Enter only if 66* is also entered.)	* Radial flux by interval, then by group, followed by axial flux (IGM*(IM+JM) entries) (Default : flux=0.0)
/66*/	Old total flux by group, arbitrary units (IGMI entries) (Default : old flux = new flux)	* Old total flux by group, arbitrary units (IGMI entries) (Default : old flux is taken from first spatial interval of radial flux.)
		*

T Terminator

<Data Block 4>

/13$/ P_i; Nuclide ID numbers for cross-sections from I/O unit NLIB (MTP entries)
DDX; I/O unit of DDX library for each nuclides (MTP entries)
/14*/ Cross section (MCR≠0) (ITL*IGM*MCR entries)

T Terminator

<Data block 5> (I04=0 and M06=0, 1, 2, 3, 4)

/17*/ Fixed distributed-volume source
When more than one 17* array is required, each must be followed by a "T".

T Terminator

<Data Block 6> (I04=5 and B01=4 or B02=4 or B03=4 or B04=4)

/18*/ Fixed exterior boundary source
Enter IGM 18* arrays, each of which consists of the following data:
1) ((C1(m,j), m=1, MMRT), j=1, JM) (if B01=4)
C1 : left boundary source
MMRT: number of directions having $\mu > 0.0$
2) ((C2(m,j), m=1, MMLT), j=1, JM) (if B02=4)

C2 : right boundary source
MMLT: number of directions having $\mu < 0.0$

3) ((C3(m,j), m=1, MMDN), j=1, JM) (if B03=4)
C3 : top boundary source
MMDN: number of directions having $\eta < 0.0$

4) ((C4(m,j), m=1, MMUP), j=1, JM) (if B04=4)
C4 : bottom boundary source
MMUP: number of directions having $\eta > 0.0$

The ordering of m is the same as specified by the quadrature direction set. Note that each array must be followed by a "T".

T Terminaor

<Data Block 7> (IZ1>0 or IZ2>0)

/15*/ Fixed interior boundary source
Enter IGM 15* arrays, each of which must be followed by a "T".
The number of entries in each array is
MM*JM entries (if IZ1>0),
or
MM*IM entries (if IZ2>0).

T Terminator

<Data Block 8> (| ITH | <2 and IB4=1)

/31$/ Order of scattering by group (≦A03) (IGM entries)

T Terminator

<Data Block 9> (M07=0, 1, 2, 3, 4)

/3*/ Initial flux
When more than one 3* array is required, each must be followed by a "T".

T Terminator

<Data Block 10>

/1*/ Fission spectrum (IGM entries)
/2*/ Axial (Y,Z,Θ) interval boundaries (JM+1 entries)
/4*/ Radial (X,R,R) interval boundaries (IM+1 entries)
/5*/ Velocities (I04≠−6) or source (I04=−6) by group (IGM entries)
/8$/ Zone numbers by interval, starting at lower left corner of mesh, sweeping from left to right, then from bottom to top (IM*JM entries)
/9$/ Material numbers by zone (IZM entries)
/10$/ P_i; mixture numbers in mixing table (M01 entries)
DDX; number of nuclides by mixture (MT entries)

/11$/ P_i; component numbers in mixing table (M01 entries)
DDX; nuclide ID numbers for all mixtures (MTP entries)
/12$/ P_i; number densities in mixing table (M01 entries)
DDX; number densities (MTP entries)
/19$/ Material numbers for activity print (M05 entries)
/20$/ Cross section table position for activity print (M05 entries)
/21$/ Radial search zone numbers (I04=4) (IM entries)
/22*/ Radial zone modifiers (I04=4) (IZ entries)
See the description of 20* array for ANISN-DD.
/23$/ Axial search zone numbers (I04=4) (JM entries)
/24*/ Axial zone modifiers (I04=4) (JZ entries)
See the description of 20* array for ANISN-DD.
/25*/ Right boundary albdeo (B02=5) (JM*IGM entries)
/26*/ Top boundary albedo (B03=5) (IM*IGM entries)
/27*/ Bottom boundary albdeo (B04=5) (IM*IGM entries)
/28$/ Inner iteration maximum by group (G07<0) (IGM entries)
/29$/ Number of quadrature angles by group (ISC=1) (IGM entries)
Enter "0" for diffusion theory; otherwise A04.
/30$/ Zone numbers for zone balance tables (IB1 entries)
/32$/ Zone numbers for zones of convergence (IZC entries)
/33*/ Direction cosines, η's, for source input to uncollided flux calculation (I04=-6) (IZ3 entries)
/34*/ Source magnitude, f(η), for uncollided flux calculation (I04=-6) (IZ3 entries)

T Terminator

<Data Block 11> (ITI>0)

/1*/ Energy boundaries (IGM+1 entries)

T Terminator

(2) Card-Image Input from FT65F001

If IGM of 61$ is negative, cross sections of the | IGM | -th group are read from the I/O unit 65 with the FORTRAN77 free format.

Enter the following thermal group cross sections for nuclides needed:

nuclide ID, $\sigma_{production}$, $\sigma_{fission}$, $\sigma_{capture}$, $\nu\sigma_{fission}$, σ_{total}

Data input is terminated by an arbitrary negative integer and /. As for nuclides for which no data is given, thermal cross sections are set to be 0.0.

5.2.2 UNCL-DD

Input data for UNCL-DD are read from the I/O units 5 and 65. Those from the I/O unit 5 are read with the FIDO format,and those from the I/O unit 65 with the FORTRAN77 free format.

(1) Card-Image Input from FT05F001 with FIDO Format

<Data Block 0>

Problem title (A72)

* Control Data Section

<Data Block 1>

/1$/ Integer data

1) ITH
- = 0, forward calculation with Legendre expansion cross section
- = 1, adjoint calculation with Legendre expansion cross section (unusabale)
- = +2, mixing of forward DDX type cross section only
- = −2, mixing of adjoint DDX type cross section only
- = +3, forward calculation with DDX type cross section already mixed
- = −3, adjoint calculation with DDX type cross section already mixed
- = +4, both of +2 and +3
- = −4, both of −2 and −3

2) ISCT P_i; maximum order of Legendre expansion of scattering
DDX; number of angle bins of DDX
Sign of ISCT indicates the way of angle division in the calculation of angular transfer probabilities.
ISCT>0 : "igloo" type
ISCT<0 : "honeycomb" type

3) IZM number of material zones

4) IM number of radial spatial intervals in X or R direction

5) JM number of axial spatial intervals in Y, Z or Θ direction

6) IGM number of energy groups
In DDX mode, if IGM is negative, the number of groups is | IGM | and cross sections of the | IGM | −th group are read from the I/O unit 65.

7) IHT position of σ_t in cross section table (normally set 3 in DDX mode)

8) IHS P_i; position of $\sigma_{g,g}$ in cross section table DDX; position of beginning of $\sigma_{g,g}$ (normally set 4 in DDX mode)

9) IHM cross section table length (automatically set in DDX mode)

10) MS mixing table length (no effect in DDX mode)

11) MCR number of cross section sets to be read from card-image inp on I/O unit 5 (set 0 in DDX mode)

12) MTP P_i; number of cross section sets from file
DDX; sum of the numbers of nuclides used in each materials

13) MT P_i; total number of cross section sets
DDX; number of mixtures to be prepared by mixing process (| ITH | =2, 4) or number of mixtures in a macroscopic cross section library (| ITH | =3)

14) IDT1 storage mode and format of P_i library (set 0 in DDX mode)
- = 0, cross sections are stored internally if possible and input P_i library is material-organized one.
- = 1, cross sections are stored externally during calculation and input P_i library is material -organized one.
- = 2, cross sections are stored externally during calculation and input group-independent cross sections are IANISN=0 type ones.
- = 3, cross sections are stored externally during calculation and input group-independent cross sections are IANISN=1 type ones.

15) NOA quadrature angle point for ring source (RRT>0.0)

Set 1 for a point source (RRT=0.0)

16) LBL track length (byte) of direct access device used for direct access work-file (FT90 for uncollided flux, FT91 for first collision source)

17) NBL maximum record length (byte) of direct access work-file (FT90 and FT91)
Actual record size is determined automatically in the code.
<recommended values for JAERI system>

unit name	LBL	NBL
TSSWK	47470	23460
WK10	19060	19060

<memory size needed at least>
FT90: IGM * IM * JM * 4 (byte)
FT91: IGM * IM * JM * 4 * noma (byte)
(noma = MM+1 for DDX, (ISCT+1) * (ISCT+2)/2 for P_i)

18) NERC no effect

19) IPRTC print option for cross sections
= 0, print cross sections
= 1, bypass cross section print out

20) MM P_i; no effect
DDX; number of angles in angular quadrature set (A04 of DOT)

21) NPSO I/O unit number of first collision source and uncollided flux output

22) IPRTF print uncollided flux from group 1 to group IPRTF

23) IPRTS print first collision source from group 1 to group IPRTS

24) IZ3 angle number specifying angular distribution of source
Set 0 for an isotropic source.

25) IGMS2 group number of gamma-ray

26) IMS2 radial mesh number of gamma-ray distribution calculation

27) JMS2 axial mesh number of gamma-ray distribution calculation

/2*/ Source parameters

1) XNF normalization or multiplication constant:

	* XNF<0	* XNF=0	* XNF>0
IZ3=0	* multiply source from 3* by | XNF |	* no effect	* normalize source from 3* to | XNF
IZ3>0	* multiply source from 3* by | XNF |	* enter angular distribution from 14* by group	* normalize sources from 3* to | XNF |

2) ZPT z-coordinate of source

3) RPT distance of source from z-axis

T Terminator

<Data Block 2> (| ITH | >1)

/6 * / Quadrature weights (MM entries)

T Terminator

/7 * / Quadrature μ's and η's (2 * MM entries)

T Terminator

/8 * / Angle mesh boundaries of DDX from +1 to −1 (ISCT+1 entries)

T Terminator

<Data Block 3> (MTP>0 or MCR>0)

/13$/ P_i; Nuclide identification numbers from data set on I/O unit 4 (MTP≠0) (MTP entries)
DDX; I/O unit of DDX library from which cross sections for each nuclide are read (MTP≠0) (MTP entries)

/14 * / cross sections (MCR≠0 and IANISN≦1)
(IHM * IGM * MCR entries)

T Terminator

<Data Block 4>

/1 * / fission spectrum (IGM entries)
/2 * / Axial (Y, Z, Θ) interval boundaries (JM+1 + JMS2+1 entries)
/3 * / Source strength by group (IGM entries)
/4 * / Radial (X, R, R) interval boundaries (IM+1 + IMS2+1 entries)
/6 * / Angular quadrature weights of ring source (RPT>0.0)
If PRT=0.0, enter "1.0". (NOA entries)
/7 * / Angular quadrature angles of ring source (RPT>0.0)
Enter values from −1.0 to 1.0 (transferred to θ between 0 and π). If RPT=0.0, enter "1.0". (NOA entries)
/8$/ Zone numbers by interval, starting at lower left corner of mesh, sweeping from left to right, then from bottom to top. (IM * JM entries)
/9$/ Material numbers by zone (IZM entries)
/10$/ P_i; mixture numbers in mixing table (M01 entries)
DDX; number of nuclides by mixture (MT entries)
/11$/ P_i; component numbers in mixing table (M01 entries)
DDX; nuclide ID numbers for all mixtures
(MTP entries)
/12 * / P_i; number densities in mixing table (M01 entries)
DDX; nuclide densities (MTP entries)

T Terminator

<Data Block 5> (IZ3>0)

/13 * / Axial cosines of angle for which source strength are given (IZ3 entries)
Note that in the adjoint mode, no inversion of input data for angles is performed in the code.

/14 * / Source strength for cosines given by 13 *
(IZ3 or IZ3*IGM (if XNF=0.0 and IZ3>0) entries)

T Terminator

(2) Card-Image Input from FT54F001

If IGM of 1$ is negative, cross sections of the | IGM | -th group must be given on the I/O unit 65. The UNCL-DD code read them with the FORTRAN77 free format. Enter the following thermal group cross sections for nuclides needed:

nuclide ID, $\sigma_{production}$, $\sigma_{fission}$, $\sigma_{capture}$, $\nu\sigma_{fission}$, σ_{total}

Data input is terminated by an arbitrary negative integer and /. As for nuclides for which no data is given, thermal cross sections are set to be 0.0.

5.3 Job Control Instruction

5.3.1 Job Control Statements

A sample of job control statements for successive execution of UNCL-DD and DOT-DD on the FACOM VP-100 vector computer of JAERI is shown in **Fig. 5.6.** Executive load modules of these two codes have been prepared in JAERI with member names UNCL10VP and DOT10VP in the file J3803. DOTDD.LOAD. The size of common in both codes in this module is 100 k words, and a user should replace the main routine by user's one having an appropriate size of common as describedin Section 5.3.3.

5.3.2 I/O File Requirements

Files of I/O required by DOT-DD and UNCL-DD are summarized in **Tables 5.1** and **5.2.** In DOT-DD calculation, the "permanent scratch" files, NCR1, NSCRAT and NFLUX1 are always required, and must always be unique files. The other files are conditionally required. The conditions are shown in parentheses in second column of **Table 5.1.** If any of NBS0, NPS0, NFLSV, NAFT, NBFT and NZBT are not required, they can be set equal to any of the three permanent scratch files. The NGAM file must be unique. If activity output is not necessary, assign NGAM to a dummy file. Details of contents and their formats for output and scratch files are described below. All fluxes given in output files are group -fluxes and angular fluxes are those per unit weight.

(1) Files for Cross Sections

Files used with DDX library are the same as those in ANISN-DD calculation described in Section 4.3.2. As for the P_l library, see Section 5.1.1.

(2) Angular Flux File (I/O Unit NAFT)

1) (ID(i), i=1, 90), (SH(i), i=1, 3), KAF, KAFCC, KAFTB, KAFLR

ID(i) : parameters in common
Title=ID(1) to ID(18),
MM=ID(22), IGE=ID(23), IZM=ID(24), IM=ID(25),
JM=ID(26), IGM=ID(45), ITI=ID(67), IS3=ID(66)

KAF : number of angular flux outputs = KAFCC+KAFTB+KAFLR

KAFCC : number of angular flux outputs at the mesh center

KAFTB : number of angular flux outputs at the axial boundary

KAFLR : number of angular flux outputs at the radial boundary

```
//JCLG   JOB
// EXEC JCLG
//SYSIN DD DATA,DLM='++'
// JUSER XXXXXXXX,MORI,0431.01
 T.7  C.5 I.5 W.4
 OPTP MSGCLASS=X PASSWORD=XX CLASS=4
//***************  J3803.DDX.CNTL(DDUNCDOT)  **********************
//*
//* <><><><><><><><><><><><><><><><><><><><><><><><><><><><><><><><><><>
//* <> UNCL-DD : CALCULATE FIRST COLLISION SOURCE & UNCOLLIDED FLUX <>
//* <><><><><><><><><><><><><><><><><><><><><><><><><><><><><><><><><><>
//*
// EXEC FORT77
C
C   MAIN ROUTINE
C
      PARAMETER ( MEMORY = 1000000 )
      COMMON /BULKBU/  D(MEMORY)
      D(1)  =  MEMORY
      CALL DTLIST
      CALL CONTRL
      STOP
      END
// EXEC LKED
//OLDLM DD DSN=J3803.DOTDD.LOAD,DISP=SHR
   ENTRY MAIN
   INCLUDE OLDLM(UNCL10VP)
   NAME TEMPNAME(R)
//*****************************************************************
//UNCL    EXEC GO
//FT06F001      DD SYSOUT=*
//FT01F001      DD UNIT=WK10,SPACE=(TRK,(500,100),RLSE)
//FT02F001      DD UNIT=WK10,SPACE=(TRK,(500,100),RLSE)
//* ----- PROCESSED DDX ------------------------------------------
//FT04F001 DD DSN=&&WK04,DISP=(,PASS),
//    DCB=(RECFM=VBS,LRECL=X,BLKSIZE=19069),SPACE=(TRK,(100,10)),
//    UNIT=WK10
//**** OUTPUT FILE (UNCOLLIDED FLUX AND FIRST COLLISN SOURCE) ****
//FT15F001 DD DSN=&&WK15,DISP=(,PASS),
//    DCB=(RECFM=VBS,LRECL=X,BLKSIZE=19069),SPACE=(TRK,(100,10)),
//    UNIT=WK10
//*****************************************************************
//FT90F001 DD DSN=&&BUF1,DISP=(,DELETE),UNIT=TSSWK,
//  DCB=RECFM=F,SPACE=(TRK,(20,0))
//FT91F001 DD DSN=&&BUF2,DISP=(,DELETE),UNIT=TSSWK,
//  DCB=RECFM=F,SPACE=(TRK,(300,0))
//*****************************************************************
//*
//* ----- NDI'S = INPUT DDX LIBRARIES (SPECIFIED IN 13¥) -------------
//FT71F001 DD DSN=J3803.DDXLIB3.DATA,DISP=SHR,LABEL=(,,,IN)
//*
//* ----- DIRECT ACCESS FILE FOR MIXING < NDO > ----------------------
//FT50F001  DD UNIT=TSSWK,SPACE=(TRK,100),DCB=RECFM=F,DISP=(,DELETE)
//* ----- WORK FILE FOR MIXING < NDOA > ------------------------------
//FT51F001  DD UNIT=WK10,SPACE=(TRK,(100,50),RLSE),DCB=BLKSIZE=19069
//* ----- WORK FILE FOR MIXING < NDM > -------------------------------
//FT52F001  DD UNIT=WK10,SPACE=(TRK,(100,50),RLSE),DCB=BLKSIZE=19069
//*
//SYSIN DD DSN=J3803.DOTDD.DATA(UNCLDDTF),DISP=SHR
//*
//* <><><><><><><><><><><><><><><><><><><><><><><><><><><><><><><><><><>
//* <>          DOT-DD : TWO-DIMENSIONAL SN TRANSPORT CODE          <>
//* <><><><><><><><><><><><><><><><><><><><><><><><><><><><><><><><><><>
//*
// EXEC FORT77
C
C   SET CORE SIZE OF DOT-DD
C
      SUBROUTINE ALOCAT(LOC,SUB)
      PARAMETER( LIMIT =  1000000 )
      COMMON /DCOMMN/ D(LIMIT)
    1 IF(LOC.GT.0) GO TO 10
      LOC  =  LIMIT
      GO TO 999
   10 CONTINUE
      CALL SUB(D,LOC)
  999 RETURN
      END
/*
```

Fig. 5.6 Job control statements for successive execution of UNCL–DD and DOT–DD.

```
// EXEC LKED
//OLDLM DD DSN=J3803.DOTDD.LOAD,DISP=SHR
//SYSIN    DD *
  ENTRY    MAIN
  INCLUDE OLDLM(DOT10VP)
  NAME     TEMPNAME(R)
//*
//DOT  EXEC GO,A='HIO=(2,3,4,62)',OBSIZE=137
//FT06F001  DD SYSOUT=*
//*
//* ----- SCARATCH FILE ------------------------------------------------
//FT02F001  DD UNIT=WK10,SPACE=(CYL,50,,CONTIG)              < NCR1   >
//*
//* ----- SCRATCH FILE -------------------------------------------------
//FT03F001  DD UNIT=WK10,SPACE=(CYL,50,,CONTIG)              < NFLUX1 >
//*
//* ----- SCARTCH FILE -------------------------------------------------
//FT04F001  DD UNIT=WK10,SPACE=(CYL,50,,CONTIG)              < NSCRAT >
//*
//FT07F001  DD UNIT=WK10,SPACE=(TRK,(150,50),RLSE),
//          DCB=(RECFM=VBS,BLKSIZE=19069)
//*
//* ----- PROCESSED DDX ------------------------------------------------
//FT08F001  DD DSN=&&WK04,DISP=SHR                           < NLIB   >
//*
//* ----- RESART OUTPUT ------------------------------------------------
//FT09F001  DD DUMMY                                         < NFLSV  >
//*
//* ----- RESTART INPUT ------------------------------------------------
//FT20F001  DD DUMMY                                         < IFLUX0 >
//*
//* -------------------------------------------------------------------
//FT11F001  DD UNIT=WK10,SPACE=(TRK,(90,10),RLSE),           < NBFT   >
//          DCB=(RECFM=VBS,BLKSIZE=19069,LRECL=X)
//FT12F001  DD UNIT=WK10,SPACE=(TRK,(30,10),RLSE)            < NGAM   >
//*
//* ----- WORK FILE FOR ZONE BALANCE TABLE -----------------------------
//FT13F001  DD UNIT=WK10,SPACE=(TRK,(30,10),RLSE)            < NZBT   >
//*
//* ----- BOUNDARY SOURCE ----------------------------------------------
//FT14F001  DD UNIT=WK10,SPACE=(TRK,(30,10),RLSE)            < NBSO   >
//*
//* ----- XPMM = X-SEC * SCATTERING KERNEL MATRIX (NP) -----------------
//FT62F001  DD UNIT=WK10,SPACE=(CYL,50,,CONTIG)              < NP     >
//FT63F001  DD UNIT=WK10,SPACE=(TRK,(50,10))                 < NPP    >
//*
//* ----- FIRST COLLISION SOURCE & UNCOLLIDED FLUX ---------------------
//FT15F001  DD DSN=&&WK15,DISP=SHR                           < NPSO   >
//*
//*
//* ----- ANGULAR TRANSFER PROBABILITY < NDP > -------------------------
//*T61F001  DD DSN=J3803.IGL0048.DATA,DISP=SHR,LABEL=(,,,IN)   (S-48)
//FT61F001  DD DSN=J3803.IGL00160.DATA,DISP=SHR,LABEL=(,,,IN)  (S-160)
//*
//* ----- ANGULAR FLUX OUTPUT FILE < FT41 > ----------------------------
//FT10F001 DD DSN=J3803.PLTDOT.TDS.DATA(TOFDD),DISP=SHR      < NAFT   >
//*
//* ----- SCALAR FLUX OUTPUT FILE (------------------------------------
//FT41F001 DD DUMMY
//*
//SYSIN DD DSN=J3803.DOTDD.DATA(DOTDDTF),DISP=SHR
++
//
```

Fig. 5.6 (Continued)

Table 5.1 DOT-DD file requirement

I/O unit	Remarks	I/O* DDX mode	I/O* P_l mode
NCR1	Scratch for cross section (P_l) and distributed source (P_l and DDX)	A I/O	A I/O
NFLUX1	Scratch for flux from previous outer iteration	A I/O	A I/O
NSCRAT	Scratch for flux from present outer iteration	A I/O	A I/O
NBS0	Boundary source file (I04 = 5 or I04 = 0 and M06 = 5)	B I/O	B I/O
NPS0	First collision source file (|I04| = 6)	B I/O	B I/O
NFLSV	Restart file for next run	B O	B O
NAFT	Angular flux file (|IAFT| = 1 or 3)	B O	B O
NAFTIN	Angular flux file from aborted run (Input value of NAFT > 100)	B I	B I
NBFT	Interior boundary angular flux (IB5 > 0 or IB6 > 0)	B O	B O
NGAM	Pointwise activities If M05 ≠ 0, dummy file is allowed	A O	A O
NZBT	Scratch for zone balance calculation (IB1 ≠ 0)	B I/O	B I/O
NLIB	Group-independent macro-DDX in DDX Material-organized library in P_l (MTP > 0 and IGIXS = 0 in P_l)	A I/O	B I
IFLUX0	Initial flux guess from previous run (IFLUX0 ≠ 0)	B I	B I
ISRCE	First collision or boundary source (ISRCE ≠ 0)	B I	B I
|IGIXS|	Group independent P_l library (IGIXS ≠ 0)	X	B I
MTT(i)	DDX library input file (|A02| = 2 or 4)	B I	X
41	Scalar flux file	A O	A O
50	Scratch file for DDX mixing DCB = (RECFM = F, DSORG = DA) (|A02| = 2 or 4)	A I/O	X
51	Scratch file for DDX mixing (|A02| = 2 or 4)	B I/O	X
52	Scratch file for DDX mixing (|A02| = 2 or 4)	B I/O	X
61	Angular transfer probability	A I	X
62	Scratch file for DDX * ATP	A I/O	X
63	Scratch file for source	A I/O	X
65	Card-image input for thermal group (IGM < 0)	B I	X
5	Card-image input for ANISN-DD	A I	A I
6	Output of final result	A O	A O

*A : always necessary file.
B : conditionally necessary file.
X : unnecessary file.
I : read-only file.
O : write-only file.

Table 5.2 UNCL-DD file requirement

I/O unit	Remarks	I/O* DDX mode	I/O* P_l mode
1	Scratch file for cross section (IDAT1 = 1 or 3 in P_l) (IDAT1 > 0 in DDX)	B I/O	B I/O
2	Macroscopic P_l cross sections (IDAT1 ≠ 0 in P_l)	X	B I/O
4	Group independent macroscopic DDX P_l library input file	A I/O	A I
15	Output of first collision source	A O	A O
MTT(i)	DDX library input file (|ITH| = 2 or 4)	B I	X
50	Scratch file for DDX mixing DCB = (RECFM = F, DSORG = DA) (|ITH| = 2 or 4)	B I/O	X
51	Scratch file for DDX mixing (|ITH| = 2 or 4)	B I/O	X
52	Scratch file for DDX mixing (|ITH| = 2 or 4)	B I/O	X
90	Scratch file for uncollided flux DCB = (RECFM = F, DSORG = DA)	A I/O	A I/O
91	Scratch file for first collision source DCB = (RECFM = F, DSORG = DA)	A I/O	A I/O
65	Card-image input for thermal group (IGM < 0)	B I	X
5	Card-image input for ANISN-DD	A I	A I
6	Output of final result	A O	A O

*A : always necessary file.
B : conditionally necessary file.
X : unnecessary file.
I : read-only file.
O : write-only file.

2) (M2(i), i=1, IZM) : material I.D. in zone i

3) ((M0(i,j), i=1, IM), j=1, JM), ((MC(i,j), i=1, IM), j=1, JM),
((MA(i,j), i=1, IM), j=1, JM+1), ((MR(i,j), i=1, IM+1), j=1, JM)

M0(i,j) : zone number of spatial mesh (i,j)

MC(i,j) : indicator of angular flux output at the mesh center
(0/N = no/ written as the N-th angular flux)

MA(i,j) : similar to MC, but for axial boundary

MR(i,j) : similar to MC, but for radial boundary

4) (K7(i), i=1, IGM) : fission spectrum

5) ($w(m)$, m=1, MM), ($\mu(m)$, m=1, MM), $\eta(m)$, m=1, MM),
(R(i), i=1, IM+1), (Z(j), j=1, JM+1)

$w(m)$, $\mu(m)$, $\eta(m)$: angular quadrature set

R(i) : radial boundaries (X or R)

Z(i) : axial boundaries (Y or Z or Θ)

6) (ENERGY(i), i=1, IGM+1) (if ITI > 0) : energy boundaries

7) (M6(m), m=1, MM) : symmetric direction number

g=1, IGM
  k=1, KAF
    8) (AFLUX(*m*,*N*), *m*=1, MM) : *N*-th angular flux
  9) ((V0(*i*,*j*), *i*=1, IM), *j*=1, JM) : mesh volume (result of search)
  10) (R1(*i*), *i*=1, IM+1) : radial boundaries (result of search)
  11) (Z1(*j*), *j*=1, JM+1) : axial boundaries (result of search)
g=1, IGM
  12) ((XN(*i*,*j*), *i*=1, IM), *j*=1, JM) : scaler flux including uncollided flux

(3) Scalar Flux File (I/O Unit 41)

1) (ID(*i*), *i*=1, 18) : problem title
2) (ID(*i*), *i*=19, 90) : parameters in common
3) (R1(*i*), *i*=1, IM+1), (Z1(*j*), *j*=1, JM+1),
((M0(*i*,*j*), *i*=1, IM), *j*=1, JM), ((M2(*i*), *i*=1, IZM),
(ENERGY(*i*), *i*=1, IGM+1) : see the descriptions in (1)

g=1, IGM
  4) ((XN(*i*,*j*), *i*=1, IM), *j*=1, JM) : scalar flux including uncollided flux
n=1, NRESP (if IS3>0)
  5) (DETTL(*i*), *i*=1, 18), (RFUNC(*i*), *i*=1, IGM)
  DETTL : title for reaction
  RFUNC : response
  6) ((F2(*i*,*j*), *i*=1, IM), *j*=1, JM) : reaction rate

(4) Boundary Source File (I/O Unit NBS0)

Exterior boundary source (I04=5)

g=1, IGM
  1) ((C1(*m*,*j*), *m*=1, MMRT), *j*=1, JM) (if B01=4 or 6)
  C1 : left boundary source
  MMRT: number of directions having $\mu > 0.0$
  2) ((C2(*m*,*j*), *m*=1, MMLT), *j*=1, JM) (if B02=4 or 6)
  C2 : right boundary source
  MMLT: number of directions having $\mu < 0.0$
  3) ((C3(*m*,*j*), *m*=1, MMDN), *j*=1, JM) (if B03=4 or 6)
  C3 : top boundary source
  MMDN: number of directions having $\eta < 0.0$
  4) ((C4(*m*,*j*), *m*=1, MMUP), *j*=1, JM) (if B04=4 or 6)
  C4 : bottom boundary source
  MMUP: number of directions having $\eta > 0.0$

The ordering of *m* is the same as specified by the quadrature direction set.

Interior boundary source (I04=5)

g=1, IGM
  1) ((C5(*m*,*j*), *m*=1, MM), *j*=1, IJM)
  C1 : interior boundary source
  IJM : =JM if IZ1≠0, =IM if IZ2≠0

Distributed-volume source (I04=0 and M06=5)

In this case, DOT-DD reads the distributed-volume source on the I/O unit NBS0 with the following

format:

g=1, IGM
1) ((C6(i,j), i=1, IM), j=1, JM)
C6 : distributed-volume source

(5) First Collision Source File (I/O Unit NPS0)

g=1, IGM
1) $Q_g^c(i,j)$, i=1, IM), j=1, JM), (((A$_{g,m}$(i,j), i=1, IM), j=1, JM), m=1, NOMA)
Q_g^c : total collided source
$A_{g,m}$: see Section 5.1.3 as for DDX; P_l moments of first collision source
(NOMA=MM in DDX and $=l(l+3)/2$ in P_l mode)

g=1, IGM
2) (($\phi_g^{unc}(i,j)$, i=1, IM), j=1, JM) : uncollided flux

(6) Restart Data File (I/O Unit NFLSV)

g=1, IGM
1) ((XN(i,j), i=1, IM), j=1, JM),
(((J3(i,j,m), i=1, IM), j=1, JM), m=1, NOMA),
((B2(m,j)),m=1, MM), j=1, JM), ((B4(m,j), m=1, MM), i=1, IM)
XN : scalar flux
J3 : angular flux at mesh center in DDX mode (NOMA=MM)
flux moment in P_l mode (NOMA=$l(l+3)/2$)
B2 : angular flux at external radial boundaries
B4 : angular flux at external axial boundaries

(7) Interior boundary Angular Flux File (I/O Unit NBFT)

g=1, IGM
1) ((AIF(m,j), m=1, MM1), j=1, JM) (if IB5≠0)
AIF : angular flux at the | IB5 | -th radial boundary
MM1 : MMRT if IB5>0; = MMLT if IB5<0 (see (4))
2) ((AJF(m,j), m=1, MM2), i=1, IM) (if IB6≠0)
AJF : angular flux at the | IB6 | -th axial boundary
MM2 : = MMUP if IB6>0; = MMDN if IB6<0 (see (4))

(8) Pointwise Activity File (I/O Unit NGAM)

m=1, | M05
1) ((ACT(i,j), i=1, IM), j=1, JM) : pointwise activity

(9) Angular Transfer Probability (I/O Unit 61)

The angular transfer probabilities for S_8 and S_{16} calculations have been prepared, and the detail is given in Section 7.2 and Appendix 3.

(10) Important Scratch Files

NCR1

DDX mode;

g=1, IGM
1) ((Q0(i,j), i=1, IM), j=1, JM)
Q0 : distributed source including first collision one

P_l mode;

g=1, IGM
  1) ((C0(i,k), i=1, ITL), k=1, MT), ((Q0(i,j), i=1, IM), j=1, JM)
     C0 : P_l cross sections
     Q0 : distribted source including first collision one

NFLUX1 and NSCRAT

DDX mode; the same as NFLSV

P_l mode;

This file is the same as NFLSV if IP5=1 and IB4=0. If IB4≠0, NOMA is replaced with that of each group since P_l order of scattering is variable with group. If IP5=0, then

g=1, IGM
  1) ((B2(m,j)), m=1, MM), j=1, JM), ((B4(m,i), m=1, MM), i=1, IM)
     B2 : angular flux at external radial boundaries
     B4 : angular flux at external axial boundaries

Note that the I/O unit numbers of three scratch files (NCR1, NFLUX1 and NSCRAT) are interchanged each other during calculations. Accordingly, these files require the same size as the maximum one.

I/O unit 62 for scattering kernel matericeS

A03 < 10,000 and IFOT = 0;

g = 1, IGM
  1) ((($X(m'\to m,g'\to g,j),m'$=1, MMVP), m=1, MM), j=1, MT), g'=MIG, g)

A03 < 10,000 and IFOT = 1;

g = 1, IGM
  g'= MIG, g
    1) (($X(m'\to m,g'\to g,j),m'$=1, MMVP), m=1, MM), j=1, MT)

The parameter MMVP is a minimum integer such that MMVP = 4n+2 and MMVP>MM, where n is an integer. The array X and the parameter MIG are defined by

$$X(m'\to m,g'\to g,j) = w_{m'} \cdot \Sigma^j(g'\to g,m'\to m),$$

and

$$\mathrm{MIG}=\mathrm{MAX}\left[\, g-\frac{\mathrm{IHM}-\mathrm{IHT}}{\mathrm{MAXMU}}+1,\ 1\,\right].$$

A03 > 10,000 and NANJA ≧ MM;

1) (($Y(k,m',m)$, m'=1, MMVP), m=1, MM), k=1, MAXMU)

A03 > 10,000 and NANJA < MM;

l = 1, MM, NANJA
  1) (($Y(k,m',m)$, m'=1, MMVP), m=1, M(l)), k=1, MAXMU)

Y and M(l) are defined by

$$Y(k,m',m)=w_{m'} \cdot P(k,m',m),$$

and

$$\mathrm{M}(l)=l\times\mathrm{NANJA}.$$

Note that the parameters IFOT and NANJA are determined by the code according to the common size available for the scattering source calculation.

I/O unit 63 for scattering source calculation (A03 > 10,000)

g = 1, IGM
  1) (($\Sigma_s^m(k,g-g'+1\to g)$,$k$=1, MAXMU), g'=1, IHMM), m=1, MT)

5.3.3 Memory Requirements

The memory storage requirement in bytes by DOT-DD is the order of 800,000 +4× (size of common DCOMMN in words). That by UNCL-DD is about 700,000 + 4× (size of common BLKBU in words). The necessary common size depends on the problem solved and storage mode. The storage mode is automatically changed by the codes according to the common size allowed for the problem. If the common size is insufficient, these two codes terminate by printing the messasge about the common size required for the present problem. Both DOT-DD and UNCL-DD adopt the flexible-dimensioning technique. A user must specify the size of both commons by changing parameters LIMIT and MEMORY in the following subroutines:

```
C------ ALOCAT DETERMINES THE SIZE OF COMMON DCOMMN IN DOT-DD
C
      SUBROUTINE ALOCAT (LOC, SUB)
      PARAMETER (LIMIT = 1000000)
      COMMON /DCOMMN/ D(LIMIT)
    1 IF(LOC.GT.0) GO TO 10
      LOC = LIMIT
      GO TO 999
   10 CONTINUE
      CALL SUB(D, LOC)
  999 RETURN
      END

C------ MAIN ROUTINE OF UNCL-DD
C
      PARAMETER (MEMORY = 1000000)
      COMMON /BULKBU/ D(MEMORY)
      D(1) = MEMORY
      CALL DTLIST
      CALL CONTRL
      STOP
      END
```

5.4 Sample Problem

In this section, two sample problems for DOT-DD and UNCL-DD are presented :one uses S_{16} approximation; the other S_8. The CPU time, I/O and memory requirements by these problems with the DDX library are compared with those with the conventional P_l library. The speed-up ratio by using the vector computer is also shown.

5.4.1 Specification of Sample Problem

(1) Problem 1

The angle-dependent leakage spectrum from the 5 cm thick Li_2O slab measured at the FNS facility[24] is analyzed by UNCL-DD and DOT-DD. The configuration of system is shown in **Fig. 5.7.** The specification of this problem is as follows:

(1) Geometry : cylinder with 31.4 cm radius and 5.06 cm thickness in air
($0 \leq r \leq 31.4$ cm, and $20 \leq z \leq 25.06$ cm)

(2) Material composition : see **Table 5.3**

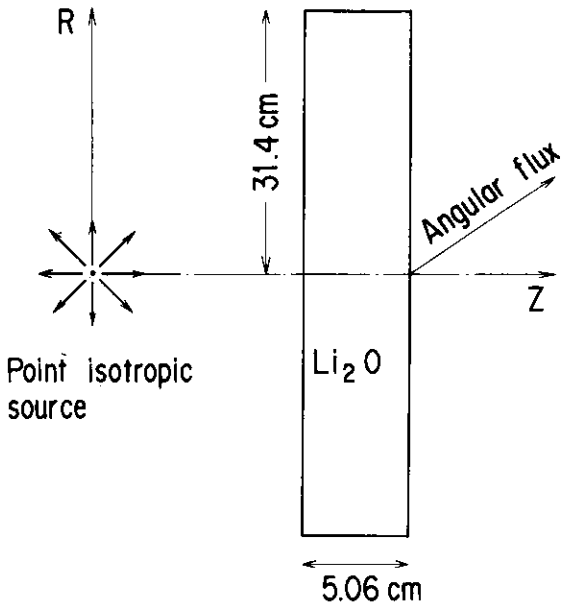

Fig. 5.7 Calculation model of angle-dependent leakage spectra from Li_2O slab (DOT-DD sample problem 1).

Table 5.3 Material composition for sample problems[a]

Isotope	Problem 1		Problem 2	
	Air	Li_2O	Air	Li_2O
Li-6		4.2729-3		4.150-3
Li-7		5.3422-2		5.190-2
O-16	4.9210-5[b]	2.8848-2	4.921-5	2.800-2
Cr		2.9922-4		3.470-4
Mn		0.0		1.750-5
Fe		1.1024-3		1.260-3
Ni		1.3086-4		1.530-4

[a] Units in 10^{24} atoms/cm^3
[b] Read as 4.9210×10^{-5}

(3) Source : first collision source by UNCL-DD
Isotoropic point 14 MeV source is located at the origin.
Source intensity is normalized to 1.17, which has been experimentally determined.

(4) Spatial mesh specification :
Radial : 16 intervals
Axial : 7 intervals
Five axial intervals are equally spaced in the Li_2O region.
Two axial intervals are taken in an air region.

(5) Boundary condition :
Reflective boundary condition at the radial center, and vacuum boundary condition at the outer boundary of the system.

(6) Angular quadrature : S^{16}

(7) Angular transfer probability : "Igloo" type

(8) Calculated energy range : above 400 keV (71 groups)

(2) Problem 2

Problem 2 is an analysis of the distribution of neutron flux in a Li_2O cylinder of 30 cm in radius and 60 cm in thickness. This problem was adopted as a benchmark problem in JAERI-U.S. collaborative program, and the results by two-dimensional S_n and Monte Carlo calculations were compared between two countries[23]. The configuration of system is shown in **Fig. 5.8.** The specification of this problem is as follows:

(1) Geometry : cylinder with 30 cm radium and 60 cm thickness in air
($0 \leqq r \leqq 30$ cm, and $20 \leqq z \leqq 80$ cm)

(2) Material composition : see **Table 5.3**

(3) Source : first collision source by UNCL-DD
Isotropic point 14 MeV source is located at the origin.
Source intensity is normalized to unity.

(4) Spatial mesh specification :
Radial : 16 intervals
Axial : 34 intervals
The innermost and outermost radial intervals and first, third, fourth and last axial ones in the Li_2O zone have width of 1 cm, and the other intervals are 2 cm wide in this zone. Two axial intervals are taken in an air region.

(5) Boundary condition :
Reflective boundary condition is adopted at the radial center, and vacuum boundary condition at the outer boundary of the system.

(6) Angular quadrature : S_8

(7) Angular transfer probability : "Igloo" type

(8) Calculated energy range : from thermal energy to about 16 MeV (125 groups)

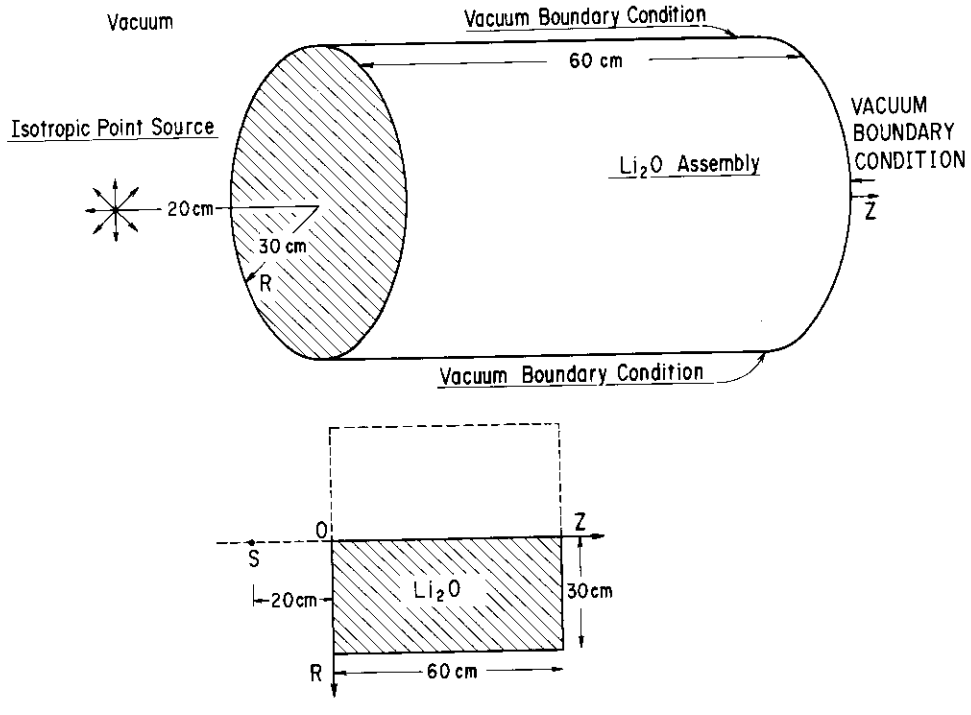

Fig. 5.8 Schematic diagram for DOT-DD sample problem 2.

5.4.2 Sample Input

Sample inputs of Problem 1 for UNCL-DD and DOT-DD are shown in **Figs. 5.9** and **5.10**, respectively. Those of Problem 2 are similar to these data, which are not presented here.

```
              TSS UTILITY COMMAND  V10L20   LIST  DATE 88.06.03  TIME 11

                  DATA SET NAME : J3803.DOTDD.DATA(UNCLDDTF)

 UNCL-DD, LI2O SLAB TOF 5.06CM  (21X7)
1**   4   20    2   21    7      71     3    4    0    0
      0    7    2    0    1   47400 23460    0    1  160
     15    0    0    0   F0
2**  1.170E+00  0.0  0.0        T
6**
  0.0       2R0.13586-1               0.0       4R0.97681-2
  0.0         0.64738-2   0.50390-2   0.64738-2 1N3
  0.0         0.64634-2 2R0.71124-2   0.64634-2 1N4
  0.0         0.64634-2   0.14381-2   0.36342-2   0.14381-2   0.64634-2
            1N5
  0.0         0.64738-2   0.71124-2   0.36342-2 1N3          1Q6
  0.0         0.97681-2   0.50390-2   0.71124-2   0.14381-2   0.71124-2
              0.50390-2   0.97681-2 1N7
  0.0         0.13586-1   0.97681-2 2R0.64738-2 1N4          1Q8
1Q80
 T
 7**
  -0.2108197 -0.1490710  M1
  -0.4216365 -0.3944050 -0.1490710  M2
  -0.5577738 -0.5374840 -0.3944050 -0.1490710  M3
  -0.6666666 -0.6497860 -0.5374840 -0.3944050 -0.1490710  M4
  -0.7601172 -0.7453560 -0.6497860 -0.5374840 -0.3944050 -0.1490710 M5
  -0.8432740 -0.8299930 -0.7453560 -0.6497860 -0.5374840 -0.3944050
  -0.1490710  M6
  -0.9189367 -0.9067650 -0.8299930 -0.7453560 -0.6497860 -0.5374840
  -0.3944050 -0.1490710  M7
  -0.9888265 -0.9775250 -0.9067650 -0.8299930 -0.7453560 -0.6497860
  -0.5374840 -0.3944050 -0.1490710  M8    Q80
   3R -0.977525  5R -0.906765  7R -0.829993  9R -0.745356 11R -0.649786
  13R -0.537484 15R -0.394405 17R -0.149071  3R +0.977525  5R +0.906765
   7R +0.829993  9R +0.745356 11R +0.649786 13R +0.537484 15R +0.394405
  17R +0.149071  T
 8**   9I 1.0  9I 0.0  -1.0   T
13**   F  71  T
 1**   F0.0
 3** 4.1870-03  3.0442-02  5.6720-02   1.5066-01   2.0433-01   2.4421-01
     1.4910-01  1.0157-01  2.7734-02   1.8224-02   1.3982-02   7.6375-03
     5.1968-03  3.3103-03  2.0963-03   1.7692-03   1.3273-03   1.0954-03
     9.7219-04  7.4823-04  6.9592-04   6.5358-04   4.3625-04   3.9180-04
     3.2845-04  4.4962-04  4.6194-04   3.4234-04   3.1346-04   2.9034-04
     3.3582-04  3.2534-04  1.4579-03   1.2805-03   1.1031-03   1.0030-03
     1.1811-03  1.3286-03  1.4246-03   1.5303-03   1.7902-03   2.0530-03
     2.0148-03  2.1403-03  2.3476-03   2.4229-03   2.3660-03   2.3298-03
     2.6527-03  2.8466-03  3.0132-03   3.0277-03   2.7030-03   2.7509-03
     2.8563-03  2.8835-03  2.9604-03   3.0646-03   2.8341-03   3.1908-03
     5.7571-03  5.7500-03  5.4543-03   5.2738-03   4.4992-03   3.6129-03
     2.8341-03  1.9704-03  1.1736-03   6.1921-04   1.3073-04
 2**  0.0   18.0  4I 20.0  25.06
 4**  9I0.0  9I 10.0  30.0   31.40
 6**   1.0
 7**   1.0
 8**   21R1    1Q21     21R2    4Q21
 9**     1   2
10**     1   6
11**    816
        306   307   816  2400  2600  2800
12**   4.92100E-5
       4.27290E-3 5.34220E-2 2.88477E-2 2.99223E-4 1.10240E-3
       1.30864E-4
     T
     T
```

Fig. 5.9 Sample input for UNCL-DD.

```
 DOT-DD: LI20 SLAB 5.06CM.  DDXLIB3, (21X7)
'  ==== INITIAL RUN
61¥¥   3 10020   2   21    7       71    3    4    0    0
       0    7    2    0  160       1    1    0    0    0
       1   30   30    4    6       2    0    0    0    0
       0    0    0    0    0       0    0    0    0    0
       3    0    0    0   -1       1    0    0    0    0
       2    1    1    1    0       0    0    0    0    0
       0
62¥¥   6Z 10 3Z 8 F0
'  ==== RESTART
' 61¥¥  3 10020   2   21    7       71    3    4    0    0
'      0    7    2    0  160       1    1    0    0    0
'      1   10   10    4    6       2    0    0    0    0
'      0    0    0    5    0       0    0    0    0    0
'      3    0    0    0   -1       1   39    0    0    0
'      2    1    1    1 -120      40    0    0    0    0
'      0
' 62¥¥   6Z 2110 3Z 8 F0
63**   0.0    1.000E-03   0.0    98.0     0.0     0.0
       0.0    0.0         0.0    0.0      0.0     1.00E-03
       0.0    0.000       0.0    0.0      0.0     0.0   T
 6**
   0.0       2R0.13586-1              0.0       4R0.97681-2
   0.0         0.64738-2   0.50390-2   0.64738-2 1N3
   0.0         0.64634-2 2R0.71124-2   0.64634-2 1N4
   0.0         0.64634-2   0.14381-2   0.36342-2   0.14381-2   0.64634-2
             1N5
   0.0         0.64738-2   0.71124-2   0.36342-2 1N3         1Q6
   0.0         0.97681-2   0.50390-2   0.71124-2   0.14381-2   0.71124-2
               0.50390-2   0.97681-2 1N7
   0.0         0.13586-1   0.97681-2 2R0.64738-2 1N4         1Q8
 1Q80
  T
 7**
    -.2108197 -.1490710  M1
    -.4216365 -.3944050 -.1490710  M2
    -.5577738 -.5374840 -.3944050 -.1490710  M3
    -.6666666 -.6497860 -.5374840 -.3944050 -.1490710  M4
    -.7601172 -.7453560 -.6497860 -.5374840 -.3944050 -.1490710  M5
    -.8432740 -.8299930 -.7453560 -.6497860 -.5374840 -.3944050
    -.1490710  M6
    -.9189367 -.9067650 -.8299930 -.7453560 -.6497860 -.5374840
    -.3944050 -.1490710  M7
    -.9888265 -.9775250 -.9067650 -.8299930 -.7453560 -.6497860
    -.5374840 -.3944050 -.1490710   M8          Q80
    3R -.977525  5R -.906765  7R -.829993  9R -.745356 11R -.649786
   13R -.537484 15R -.394405 17R -.149071  3R +.977525  5R +.906765
    7R +.829993  9R +.745356 11R +.649786 13R +.537484 15R +.394405
   17R +.149071
   T
 8**  9I 1.0  9I 0.0 -1.0 T
'  ===== NEW OPTION FOR ANGULAR FLUX OUTPUT
'  (LEFT)*10000 + (RIGHT)*1000 + (BOTTOM)*100 + (TOP)*10 + (CENTER)
 9¥¥  21R0  21R0  21R101  21R0  21R0  21R0  21R11  T
'
13¥¥   F  71 T
'  ==== 3*  ONLY INITIAL RUN
 3**   F 1.0E-5 T
 1**   F0.0
 2**    0.0  18.0 4I 20.0  25.06
 4**   9I 0.0  9I10.0 30.0 31.40
 5**   F1.0
 8¥¥   21R1   1Q21
       21R2   4Q21
 9¥¥   1    2
10¥¥   1    6
11¥¥    816
        306   307   816  2400  2600  2800
12**   4.92100-5
       4.27290-3 5.34220-2 2.88477-2 2.99223-4 1.10240-3 1.30864-4
  T
 1** 1.64870E+7 1.62310E+7 1.59800E+7 1.57320E+7 1.54880E+7 1.52480E+7
     1.50120E+7 1.47790E+7 1.45500E+7 1.43240E+7 1.41020E+7 1.38830E+7
     1.36680E+7 1.34560E+7 1.32480E+7 1.30420E+7 1.28400E+7 1.26410E+7
     1.24450E+7 1.22520E+7 1.20620E+7 1.18750E+7 1.16910E+7 1.15100E+7
     1.13310E+7 1.11560E+7 1.09830E+7 1.08120E+7 1.06450E+7 1.04800E+7
     1.03170E+7 1.01570E+7 9.99990E+6 9.39400E+6 8.82490E+6 8.29020E+6
     7.78790E+6 7.31610E+6 6.87280E+6 6.45640E+6 6.06520E+6 5.69780E+6
     5.35250E+6 5.02820E+6 4.72360E+6 4.43740E+6 4.16860E+6 3.91600E+6
     3.67870E+6 3.45590E+6 3.24650E+6 3.04980E+6 2.86500E+6 2.69140E+6
     2.52840E+6 2.37520E+6 2.23130E+6 2.09610E+6 1.96910E+6 1.84980E+6
     1.73770E+6 1.53350E+6 1.35330E+6 1.19430E+6 1.05400E+6 9.30130E+5
     8.20840E+5 7.24380E+5 6.39270E+5 5.64150E+5 4.97860E+5 4.39360E+5
     3.87740E+5 3.42170E+5 3.01970E+5 2.66490E+5 2.35170E+5 2.07540E+5
     1.83150E+5 1.61630E+5 1.42640E+5 1.25880E+5 1.11090E+5 9.80350E+4
     8.65150E+4 7.63490E+4 6.73780E+4 5.94610E+4 5.24740E+4 4.63080E+4
     4.08670E+4 3.60650E+4 3.18270E+4 2.80870E+4 2.47870E+4 2.18740E+4
     1.93040E+4 1.50340E+4 1.17090E+4 9.11860E+3 7.10160E+3 5.53070E+3
     4.30730E+3 3.35460E+3 2.61250E+3 2.03460E+3 1.58460E+3 1.23410E+3
     9.61100E+2 5.82930E+2 3.53570E+2 2.14450E+2 1.30070E+2 7.88910E+1
     4.78500E+1 2.90230E+1 1.76030E+1 1.06770E+1 6.47580E+0 3.92780E+0
     2.38230E+0 1.44490E+0 8.76400E-1 5.31560E-1 3.22410E-1 1.00000E-5
    T
    T
++
//
```

Fig. 5.10 Sample input for DOT–DD.

5.4.3 Comparison of Computer Resources Required

The computer resources required in the DDX and P_5 calculations are compared in **Table 5.4.** Both DDX and P_5 libraries have the same energy structure. The number of DDX angle bins are 20.

Table 5.4 Computer resources required by sample problems[a]

(1) Problem 1 (S_{16}, 71 groups)

		DDX library		P_5 library	
		Vector	Scalar	Vector	Scalar
UNCL-DD	CPU (min.)	0.56	5.99	0.11	0.11
	VU (min.)	0.31	0.0	0.02	0.0
	I/O	5000	5000	2700	2700
	Memory (Mbyte)	3.78	3.70	1.63	1.60
DOT-DD	CPU (min.)	4.16	58.16	3.09	3.72
	OUTER[b]	2.49	51.52	0.10	0.11
	INNER[b]	0.30	5.18	0.06	0.09
	GRIND[b]	1.05	1.12	2.83	3.40
	VU (min.)	2.65	0.0	0.01	0.0
	I/O	4500	4500	1100	1100
	Memory (Mbyte)	3.59	3.49	1.84	1.74

(2) Problem 2 (S_8, 125 groups)

		DDX library		P_5 library	
		Vector	Scalar	Vector	Scalar
UNCL-DD	CPU (min.)	2.13	20.68	0.86	0.86
	VU (min.)	1.55	0.0	0.0	0.0
	I/O	13500	13500	9700	9700
	Memory (Mbyte)	4.28	4.20	3.86	3.83
DOT-DD	CPU (min.)	5.94	49.88	7.33	8.58
	OUTER[b]	2.06	42.75	0.98	1.07
	INNER[b]	0.31	3.91	0.26	0.33
	GRIND[b]	2.30	2.43	5.41	6.52
	VU (min.)	2.13	0.0	0.08	0.0
	I/O	11000	11000	10500	10500
	Memory (Mbyte)	1.58	1.48	1.08	0.98

[a] FACOM VP-100 computer is used.
[b] Subroutine names.

6. MORSE-DD : Three-Dimensional Monte Carlo Code

6.1 New Features of MORSE-DD

The first version of MORSE-DD has been developed on the basis of widely used MORSE-CG and released in 1984[3]. After the verification test by extensive benchmark calculations, this version has been successfully used in experimental analyses such as JAERI-U.S. collaborative program on fusion blanket neutronics experiments[25),26),27)].

After the release, a number of functions have been added up to the present. The main improvements are as follows:

(1) A torus geometry is added to the combinatorial geometry (CG) package.

(2) Three variance reduction techniques are added.

(3) Source generation routine is available for the D-T neutron from the titanium-tritide target bombarded by an accelerated deuteron beam.

(4) A modified version with supergrouping ability, which is named as MORSE-DSG, is developed in order to reduced the required memory for the DDX data.

(5) All input data except those defining unit bodies and zones in the geometry description are read with the FORTRAN77 free format.

The MORSE-DD code with the DDX cannot be applied to adjoint problems since this code does not rearrange the DDX data for adjoint calculation. In this section, new functions of MORSE-DD are described in detail.

6.1.1 Cross Section

The MORSE-DD code can use both the DDX and the conventional P_l cross sections. The cross sections are read from a binary cross section file like the original MORSE-CG code. The format of DDX library is described in Section 4.3.2. That of P_l library is also shown there as those of IANISN=0 and ID2=0 (material-organized library).

The processing and sampling processes by using the P_l cross sections are the same as those in the original code. The methods for the DDX are described in this section. The macroscopic cross sections are calculated by mixing the microscopic cross sections with use of atomic number densities. The macroscopic DDX is calculated by

$$\Sigma_s(k;\ g'\to g)=\sum_i N\sigma^i_{pr,g'}I_i(k;\ g'\to g), \tag{6-1}$$

and the energy-angle distribution is given by

$$\bar{I}(k;\ g'\to g)=\frac{\Sigma_s(k;g'\to g)}{\Sigma_{pr,g'}}, \tag{6-2}$$

where $\Sigma_{pr,g'}$ is a macroscopic production cross section defined by

$$\Sigma_{pr,g'}=\sum_i N\sigma^i_{pr,g'}. \tag{6-3}$$

The energy group and scattering angle of emitted neutrons are determined from this energy-angle distribution $\bar{I}$ by using the stratified sampling method. The scattering matrix is obtained by

$$\Sigma_s(g'\to g)=\sum_k \Sigma_s(k;\ g'\to g). \tag{6-4}$$

We define a cross section of scattering by which neutron energy remains above the energy cut off of cross section data by

$$\Sigma^*_{s,g'} = \sum_{g=g'}^{INGP} \Sigma_s(g' \to g), \tag{6-5}$$

where INGP is the last group number of cross section data used in the present calculation, which is not always the same as that of DDX library. Then the energy distribution is presented by

$$P_E(g' \to g) = \Sigma_s(g' \to g)/\Sigma^*_{s,g'}. \tag{6-6}$$

The angular distribution corresponding to this $(g' \to g)$ scattering is obtained by

$$P_A(k \mid g' \to g) = \frac{\Sigma_s(k; g' \to g)}{\Sigma_s(g' \to g)}. \tag{6-7}$$

Since the energy and angular distributions of Eqs.(6-6) and (6-7) are given in the form of table, the method to determine a flight direction after a collision is slightly modified. In the original MORSE-CG code or the present code with the P_i cross sections, the flight direction is determined among the discrete directions which are obtained by using a generalized Gaussian quadrature. However, such procedure is not necessary if we use the present probability table. At first, the secondary energy is determined by sampling from the probability table for energy distribution by using a random number, and then the scattering angle is determined by sampling from a cumulative probability table for angular distribution by using a random number in the range of $0 < R < 1$. The cumulative probability is given by

$$P(\mu \mid g' \to g) = \int_{-1}^{\mu} P_A(k \mid g' \to g), \tag{6-8}$$

$$P(-1 \mid g' \to g) = 0, \qquad P(1 \quad g' \to g) = 1.$$

This probability is presented by piece-wise linear functions. Hence, the cosine of scattering angle μ can be continuously obtained. That is, a value of μ is uniquely determined corresponding to a random number. Accordingly, no ray effect[2] appears, and also the negative flux or the negative weight problem is eliminated since the probability $P_A(k \mid g' \to g)$ is non-negative in the range of $-1 \leqq \mu \leqq 1$.

6.1.2 Geometry

As the geometry module, MORSE-DD adopts the combinatorial geometry package (CG) which is described in detail in Reference 17. The combinatorial geometry describes a complex three-dimensional configuration by considering unions, differences and intersections of simple bodies. The geometry package of the original MORSE-CG code includes nine simple bodies: (1) rectangular parallelpiped (RPP), (2) BOX (an RPP randomly oriented in space), (3) sphere (SPH), (4) right circular cylinder (RCC), (5) right elliptical cylinder (REC), (6) truncated right angle cone, (7) ellipsoid (ELL), (8) right angle wedge (WED or RAW) and (9) arbitrary convex polyhedron of 4, 5 or 6 sides (ARB).

The original geometry package, however, cannot treat a torus geometry which usually appears in fusion reactor analyses. In MORSE-DD, a new body of elliptical torus (ELT) is added to the package. The ELT is specified by **V**, the center of the hole, **N**, a unit vector defining the axis of revolutionl, RM, the distance to the center of the ellipse from the hole center, R1, R2, the semi- axes of the ellipse, and τ the angle in degree unit between the direction of R2 and the major radius direction, as shown in **Fig. 6.1**.

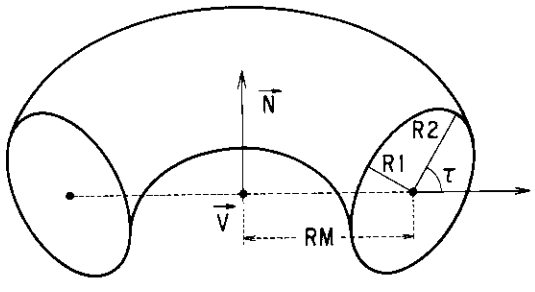

Fig. 6.1 Unit body of elliptical torus, ELT.

6.1.3 External Source

The source routines should be supplied by a user in the MORSE code. The basic information to specify is geometry of source cell, angular distribution and energy spectrum. The types of sources installed in the present code are described below. Source particles can be generated from a combination of ten types of sources at a time. Note that this external source is used as an initial fission guess in eigenvalue (k_{eff}) problems. In this case, isotropic emission should be selected, and no source biasing is allowed.

(1) Geometry of Source Cell and Density Distribution of Source Particle

The coordinates of source particle are denoted by X_s, Y_s and Z_s, and random numbers are by R_1, R_2 and R_3 which are in the range of $0<R_i<1$. The coordinates (X_s, Y_s, Z_s) can be rotated by an arbitrary angle around the origin. Note that the rotation of the coordinates is commonly used in that of flight direction of source particle. A description of the rotation is given in Part (4) of this section. The available source geometry is described below.

1) Point

$$X_s=\mathrm{X0},\quad Y_s=\mathrm{Y0},\quad Z_s=\mathrm{Z0}. \tag{6-9}$$

2) Rectangular Parallelpiped with Uniform Distribution

Each side should be parallel to coordinate axes. The averaged particle density is constant in $\mathrm{XL}\leqq\chi\leqq\mathrm{XR}$, $\mathrm{YL}\leqq y\leqq\mathrm{YR}$, $\mathrm{ZL}\leqq z\leqq\mathrm{ZR}$.

$$\begin{aligned} X_s&=R_1\cdot(\mathrm{XR}-\mathrm{XL})+\mathrm{XL},\\ Y_s&=R_2\cdot(\mathrm{YR}-\mathrm{YL})+\mathrm{YL},\\ Z_s&=R_3\cdot(\mathrm{ZR}-\mathrm{ZL})+\mathrm{ZL}. \end{aligned} \tag{6-10}$$

3) Rectangular Parallelpiped with Cosine Distribution

The averaged particle density is the cosine distribution along x, y and z axes.

$$\begin{aligned} X_s&=\frac{1}{\pi}\cdot(\mathrm{XR}-\mathrm{XL})\cdot\left\{\sin^{-1}(2R_1-1)+\frac{\pi}{2}\right\}+\mathrm{XL},\\ Y_s&=\frac{1}{\pi}\cdot(\mathrm{YR}-\mathrm{YL})\cdot\left\{\sin^{-1}(2R_2-1)+\frac{\pi}{2}\right\}+\mathrm{YL},\\ Z_s&=\frac{1}{\pi}\cdot(\mathrm{ZR}-\mathrm{ZL})\cdot\left\{\sin^{-1}(2R_3-1)+\frac{\pi}{2}\right\}+\mathrm{ZL}. \end{aligned} \tag{6-11}$$

4) Cylinder with Uniform Distribution

The averaged particle density is constant in $0\leqq r\leqq\mathrm{XR}$, $\mathrm{ZL}\leqq z\leqq\mathrm{ZR}$. The axis of cylinder should be parallel to z-axis.

$$\begin{aligned} X_s&=\mathrm{XR}\cdot\sqrt{R_1}\cdot\cos\theta+\mathrm{X0},\\ Y_s&=\mathrm{XR}\cdot\sqrt{R_1}\cdot\cos\theta+\mathrm{Y0},\\ Z_s&=(\mathrm{ZR}-\mathrm{ZL})\cdot R_3+\mathrm{ZL}, \end{aligned} \tag{6-12}$$

where $\theta=2\pi\cdot R_2$.

5) Cylinder with Cosine Distribution along z-axis

The averaged particle density is constant in (x,y) plane and cosine distribution along z-axis.

$$\begin{aligned} X_s&=\mathrm{XR}\cdot\sqrt{R_1}\cdot\cos\theta+\mathrm{X0},\\ Y_s&=\mathrm{XR}\cdot\sqrt{R_1}\cdot\cos\theta+\mathrm{Y0},\\ Z_s&=\frac{1}{\pi}\cdot(\mathrm{ZR}-\mathrm{ZL})\cdot\left\{\sin^{-1}(2R_3-1)+\frac{\pi}{2}\right\}+\mathrm{ZL}, \end{aligned} \tag{6-13}$$

where $\theta=2\pi\cdot R_2$.

6) Sphere and Spherical Shell with Uniform Distribution

The averaged particle density is uniform in $0\leqq r\leqq\mathrm{XR}$ (sphere) or $\mathrm{XL}\leqq r\leqq\mathrm{XR}$ (spherical shell).

Sphere

$$\begin{aligned} X_s &= \mathrm{XR}\cdot R_1^{1/3}\cdot R_2+\mathrm{X0}, \\ Y_s &= \mathrm{XR}\cdot R_1^{1/3}\cdot\sqrt{1-R_2^2}\cdot\cos\left[(2R_3-1)\pi\right]+\mathrm{Y0}, \\ Z_s &= \mathrm{XR}\cdot R_1^{1/3}\cdot\sqrt{1-R_2^2}\cdot\sin\left[(2R_3-1)\pi\right]+\mathrm{Z0}, \end{aligned} \tag{6-14}$$

Spherical shell

$$\begin{aligned} X_s &= \left\{(\mathrm{XR}^3-\mathrm{XL}^3)R_1+\mathrm{XL}^3\right\}^{1/3}\cdot R_2+\mathrm{X0}, \\ Y_s &= \left\{(\mathrm{XR}^3-\mathrm{XL}^3)R_1+\mathrm{XL}^3\right\}^{1/3}\cdot\sqrt{1-R_2^2}\cdot\cos\left\{(2R_3-1)\pi\right\}+\mathrm{Y0}, \\ Z_s &= \left\{(\mathrm{XR}^3-\mathrm{XL}^3)R_1+\mathrm{XL}^3\right\}^{1/3}\cdot\sqrt{1-R_2^2}\cdot\sin\left\{(2R_3-1)\pi\right\}+\mathrm{Y0}. \end{aligned} \tag{6-15}$$

7) Circular Plane with Uniform Distribution

The averaged particle density is uniform on a plane of $0\leqq r\leqq \mathrm{XL}$. The plane should be perpendicular to z-axis.

$$\begin{aligned} X_s &= \mathrm{XL}\cdot\sqrt{R_1}\cdot\cos\theta+\mathrm{X0}, \\ Y_s &= \mathrm{XL}\cdot\sqrt{R_1}\cdot\cos\theta+\mathrm{Y0}, \\ Z_s &= \mathrm{Z0}, \end{aligned} \tag{6-16}$$

where $\theta=2\pi\cdot R_2$.

8) Cylindrical Shell with Uniform Distribution

The averaged particle density is uniform in $\mathrm{XL}\leqq r\leqq \mathrm{XR}$, $\mathrm{ZL}\leqq z\leqq \mathrm{ZR}$. The axis of cylinder should be parallel to z-axis.

$$\begin{aligned} X_s &= \left\{(\mathrm{XR}^2-\mathrm{XL}^2)R_1+\mathrm{XL}^2\right\}^{1/2}\cdot\cos\theta+\mathrm{X0}, \\ Y_s &= \left\{(\mathrm{XR}^2-\mathrm{XL}^2)R_1+\mathrm{XL}^2\right\}^{1/2}\cdot\sin\theta+\mathrm{Y0}, \\ Z_s &= (\mathrm{ZR}-\mathrm{ZL})\cdot R_2+\mathrm{ZL}, \end{aligned} \tag{6-17}$$

where $\theta=2\pi\cdot R_3$.

(2) Angular Distribution of Source Particle

A user can choose an angular distribution of source particles among the following options. The direction cosines to x-, y-, z- coordinate axes, U_s, V_s and W_s are determined by using random numbers. The direction (U_s, V_s, W_s) can be rotated by an arbitrary angle in MORSE-DD. This function of rotation removes the restriction that z-axis is always polar direction.

1) Mono-directional Distribution

$$\begin{aligned} U_s &= \mathrm{UINP}, \\ V_s &= \mathrm{VINP}, \\ W_s &= \mathrm{WINP}. \end{aligned} \tag{6-18}$$

2) Isotropic Distribution

$$\begin{aligned} U_s &= 2\cdot R_1-1, \\ V_s &= \sqrt{1-U_s^2}\cdot\cos\theta, \\ W_s &= \sqrt{1-U_s^2}\cdot\sin\theta, \end{aligned} \tag{6-19}$$

where $\theta=2\pi\cdot R_2$.

3) Cosine Distribution against z Direction

$$\begin{aligned} W_s &= \sqrt{R_1} \qquad \text{for NEMIS}=3, \\ W_s &= -\sqrt{R_1} \qquad \text{for NEMIS}=-3, \\ U_s &= \sqrt{1-W_s^2}\cdot\cos\theta, \\ V_s &= \sqrt{1-W_s^2}\cdot\sin\theta, \end{aligned} \tag{6-20}$$

where $\theta=2\pi\cdot R_2$.

4) Arbitrary Distribution

The probability distributions in polar and azimuthal angle bins, ANGDIS(I,J) and FAIDIS(J), should be given by a user in input data as a function of angle (J) and energy (I). After determining the energy group I1, the interval of polar angle, J1, is sampled from the cumulative probability function as

$$\sum_{J=1}^{J1}\text{ANGDIS}(I1,J) > R_1. \tag{6-21}$$

By using the random number R_1, W_s is determined by

$$W_s = \frac{Ppc - R_1}{\text{ANGDIS}(I1,J1)} \cdot \{\text{DEG}(J1) - \text{DEG}(J1+1)\} + \text{DEG}(J1+1), \tag{6-22}$$

where

$$Ppc = \sum_{J=1}^{J1}\text{ANGDIS}(I1,J), \tag{6-23}$$

and DEG(J) is cosine of a polar angular boundary. Similarly, the interval of azimuthal angle is sampled, and U_s and V_s are determined as follows:

$$Pac = \sum_{K=1}^{K1}\text{FAIDIS}(K), \tag{6-24}$$

$$\varphi = 2\pi \cdot \left[\frac{Pac - R_2}{\text{FAIDIS}(K1)} \cdot \{\text{FAI}(K1) - \text{FAI}(K1+1)\} + \text{FAI}(K1+1)\right], \tag{6-25}$$

$$U_s = \sqrt{1-W_s^2}\cdot\cos\varphi,$$

$$V_s = \sqrt{1-W_s^2}\cdot\sin\varphi, \tag{6-26}$$

where FA1(K) is an azimuthal angular boundary in degree.

5) Cosine Distribution against Radial Direction

At first, the flight direction cosines U_s', V_s' and W_s' are determined from the cosine distribution against z-axis, and rotated by an angle which corresponds to the rotation of z-axis to a direction from the origin of source cell to a point where source particle generated. The rotation is presented by

$$(U_s, V_s, W_s) = \Pi \cdot (U_s', V_s', W_s'), \tag{6-27}$$

where Π is the matrix to rotate the direction.

(3) Energy Distribution of Source Particles

1) Arbitrary Stepwise Distribution

The probability distribution should be given by a user for energy bins, which is ready by the subroutine SORIN.

2) Watt's Fission Spectrum

$$f(E) \sim e^{-E/a}\sinh\sqrt{bE}, \tag{6-28}$$

where a and b are 0.965×10^6 eV and 2.289×10^{-6} eV^{-1}, respectively.[10]

3) Arbitrary Distribution

The probability distribution should be given by a user for discrete energy points. The source energy is determined by linearly interpolating in log-log or linear-linear scale between the input energy points.

4) Mono-Energy Distribution

The Source particle has a constant energy.

5) *D-T* Neutrons Generated by Accelerated Deuteron Beam

In fusion neutronics experiments, a neutron source is usually generated by the (d,t) reactions caused by an accelerated deutron (d^+) beam. MORSE-DD can generate this type of source neutrons by taking account of the kinematrics of a two-body reaction and the energy loss of deuterons in a target.

Bombarding deuterons are slowed down in the target, and during this process neutron generation reactions are possible at various energy of deuterons. Neutron energy emitted depends on that of deuteron though such an energy dependence is small since an emitted neutron energy is about 14 MeV which is very high compared with about 300 keV of deuteron's one. Nevertheless, such energy dependence is taken into account on the basis of Reference 18 where the reaction probability is given depending on deuteron

energy. By using this probability, a deuteron energy causing the (d,t) reaction, E_1 is determined in the range of $0<E_1<325$ keV.

Angular distribution of emitted neutrons is almost isotropic in the center of mass (c.m.) system, but an anisotropic effect is considered by using the experimental formula given by Benveniste et al.[19] as follows:

$$\frac{\sigma(\theta_n)}{\sigma(0)}=0.998+0.0213\cos\theta_n-0.0190\cos^2\theta_n, \tag{6-29}$$

which is given for incident deuterons at E=350 keV. An emission angle in the c.m. system θ_n is sampled from this formula.

After determination of E_1 and θ_n, an emission angle φ_n in the laboratory system is obtained by the following rotation:

$$\sin\varphi_n=\pm\frac{\sin\theta_n}{\sqrt{1+2\gamma\cos\theta_n+\gamma^2}}, \tag{6-30}$$

(minus sign is taken if $\theta_n<-\gamma$)

or

$$\cos\varphi_n=\frac{\gamma+\cos\theta_n}{\sqrt{1+2\gamma\cos\theta_n+\gamma^2}}, \tag{6-31}$$

where

$$\frac{1}{\gamma^2}=\frac{m_a(m_1+m_2)}{m_nm_1}\left(\frac{m_2}{m_1+m_2}+\frac{Q}{E_1}\right), \tag{6-32}$$

m_1= mass of incident deuteron,

m_2= mass of target triton,

m_n= mass of neutron,

m_a= mass of alpha particle,

E_1= incident energy of deuteton causing the reaction, and

Q= 17.6 MeV(total released kinetic energy).

Then, the emitted neutron energy in the laboratory system E_n is determined by the following formula considering an effect of the relativistic theory.

$$E_n(E_1,\varphi_n)=W_n-m_n, \tag{6-33}$$

where

$$W_n=\frac{1}{2a}\left\{-b\pm\sqrt{4ac}\right\}, \tag{6-34}$$

$$a=(W_1+m_2)^2-(W_1^2-m_1^2)\cos^2\varphi_n,$$

$$b=-(m_1^2+m_2^2+m_n^2-m_a^2+2m_2W_1)(W_1+m_2),$$

$$c=(m_1^2+m_2^2+m_n^2-m_a^2+2m_2W_1)^2/4+m_n^2(W_1^2-m_1^2)\cos^2\varphi_n,$$

and

$$W_1=m_1+E_1=\text{(total energy of deuteron.)}$$

A user should note the following points:

(i) The energy and flight direction of emitted neutron are determined by the reaction kinematics as mentioned above. Accordingly, input data for the present source are quite different from those for the other types. No data inputis required for energy and angular distributions. A specification of the input parameter NSORCE=9 is all that is required for this option. See the input instructions for external sources.

(ii) Neutrons are generated on a circular plane of radius XR and center (X0,Y0,Z0), which is perpendicular to the deuteron beam. We assume a chopped Gaussian distribution with a peak at the center.

Let R_1 and R_2 be random numbers between $0\leq R_i\leq 1$. Then

$$X_s = X0 + XR \cdot \cos\theta \cdot r,$$
$$Y_s = Y0 + YR \cdot \sin\theta \cdot r, \qquad (6\text{-}35)$$
$$Z_s = Z0,$$

where

$$\theta = 2\pi R_2 \text{ and } r = \sqrt{-\ln\{1-(1-(1-e^{-1})R_1\}},$$

which corresponds to the sampling from a probability density

$$P(r) = \frac{\exp(-r^2)}{\int_0^1 r\exp(-r^2)} \qquad (0 \leqq r \leqq 1) \qquad (6\text{-}36)$$

(iii) The deuteron beam is assumed to be parallel to z-axis in the positive direction.

(iv) The point estimator is not available since direct contributions from the source cannot be evaluated in the present procedure used in this estimator. For a user who needs a flux at a point, the following calculation is recommended: Set NSORCE=9 and NEMIS=4, and give an energy-dependent angular distribution of D-T neutrons (see the input instruction for external sources). By doing so, MORSE-DD generates source neutrons by the present method, and evaluatels the direct contributions by using the given angular distribution. The angular distribution can be obtained by a MORSE-DD calculation in a void by using the track length estimators.

This source routine has been originally programed by Seki et al.[20] and the modified routine is installed into MORSE-DD.

(4) Rotation of Flight Direction and Spatial Coordinates

We consider two coordinate systems shown in **Fig. 6.2**. One is a fixed coordinate system (X,Y,Z) where geometry of the present problem is defined and the random walk is carried out. The other is one which is determined by rotating the former system by angles, φ, θ and ϕ. The rotation of coordinate system is presented by the following relation between the coordinates in both systems:

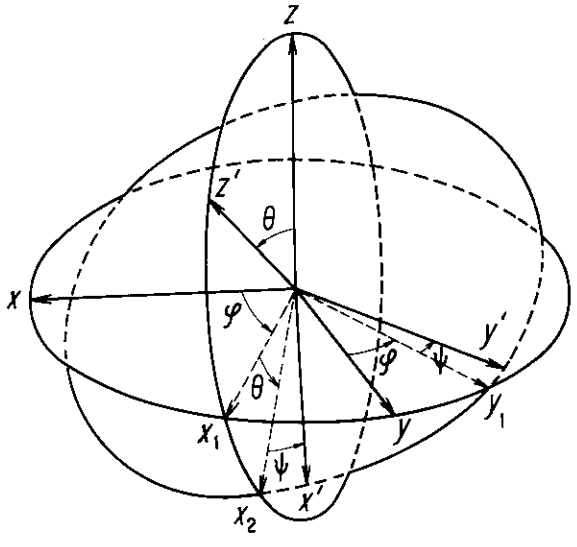

Fig. 6.2 Rotation of flight direction and spatial coordinates.

$$\begin{bmatrix} X' \\ Y' \\ Z' \end{bmatrix} = \mathbf{R}_z(\phi)\mathbf{R}_y(\theta)\mathbf{R}_z(\varphi)\begin{bmatrix} X \\ Y \\ Z \end{bmatrix}, \qquad (6\text{-}37)$$

where $\mathbf{R}_z(\phi)$, $\mathbf{R}_y(\theta)$ and $\mathbf{R}_z(\varphi)$ are rotation matrices defined by

$$\mathbf{R}_z(\varphi)=\begin{bmatrix}\cos\varphi & \sin\varphi & 0\\ -\sin\varphi & \cos\varphi & 0\\ 0 & 0 & 1\end{bmatrix}, \tag{6-38}$$

$$\mathbf{R}_y(\theta)=\begin{bmatrix}\cos\theta & 0 & -\sin\theta\\ 0 & 1 & 0\\ \sin\theta & 0 & \cos\theta\end{bmatrix}, \tag{6-39}$$

$$\mathbf{R}_z(\phi)=\begin{bmatrix}\cos\phi & \sin\phi & 0\\ -\sin\phi & \cos\phi & 0\\ 0 & 0 & 1\end{bmatrix}, \tag{6-40}$$

That is, the present rotation is performed in three steps. At first, the X- and Y-coordinate axes are rotated by the angle φ around Z-axis. The second step is the rotation of the X_1- and Z-axes around the rotated Y_1-axis by the angle θ, and the last one is performed around the rotated Z'-axis by the angle ϕ for the X_2- and Y_1-axes.

When this option is selected, spatial coordinatels or flight directions of source particles are, at first, determined probabilistically in the (X',Y',Z') coordinate system by using source cell geometry data and angular distributions given by a user. Then the coordinates are transformed to those in the (X,Y,Z) coordinate system by the following formula:

$$\begin{aligned}\begin{bmatrix}X\\ Y\\ Z\end{bmatrix} &= \left[\mathbf{R}_z(\phi)\mathbf{R}_y(\theta)\mathbf{R}_z(\varphi)\right]^{-1}\begin{bmatrix}X'\\ Y'\\ Z'\end{bmatrix}\\ &=\mathbf{R}_z(-\varphi)\mathbf{R}_y(-\theta)\mathbf{R}_z(-\phi)\begin{bmatrix}X'\\ Y'\\ Z'\end{bmatrix}\\ &=\begin{bmatrix}\cos\theta\cos\varphi\cos\phi-\sin\varphi\sin\phi & -\cos\theta\cos\varphi\sin\phi-\sin\varphi\cos\phi & \sin\theta\cos\varphi\\ \cos\theta\sin\varphi\cos\phi+\cos\varphi\sin\phi & -\cos\theta\sin\varphi\sin\phi+\cos\varphi\cos\phi & \sin\theta\sin\varphi\\ -\sin\theta\cos\phi & \sin\theta\sin\phi & \cos\theta\end{bmatrix}\begin{bmatrix}X'\\ Y'\\ Z'\end{bmatrix}\end{aligned} \tag{6-41}$$

In this equation, (X,Y,Z) corresponds to the spatial coordinates (X_s,Y_s,Z_s) or the flight direction (U_s,V_s,W_s), which are defined above in this section. Note that the flight direction is transformed by the rotation of the spatial coordinates in the MORSE-DD code.

6.1.4 Variance Reduction Techniques

The original MORSE code has several types of importance sampling techniques for variance reduction. Almost all of them, i.e., the Russian roulette and splitting at each collision, the exponential transform and the energy biasing at each collision are optionally available in MORSE-DD. In addition to these techniques, three techniques have been implemented in the present code.

(1) Splitting with Russian Roulette Based on the Importance of Phase Space Cell

The Russion roulette and splitting based on the importance of each phase space cell can be performed on particles which cross over the phase space cell boundaries as a result of streaming or a collision. This technique is perhaps the simplest and most reliable of all the variance reduction techniques used in the general codes. Basically, when particles pass from a cell of lower importance to one of higher importance, they are increased in number to provide better statistics, but if they head in the opposite direction, they are killed in an unbiased manner to avoid wasting time on them. This procedure can be applied at the geometry region surfaces and/or collisions by a user's choice. We called the former procedure as the geometry splitting with Russian roulette and the latter as the energy one.

Each phase space cell, which is defined by the geometry region and the energy group, is assigned an importance I_i by a user. The assigned importances can have any value: they are not limited to integers. Let

I_b and I_a be importances of the cells to which a present particle with a weight W belongs before and after a crossing of the cell boundary. If the importance ratio I_a/I_b is greater than unity, that is, if the particle enters the cell of higher importance, the particle is split into a number of identical particles of lower weight. The number of resulting particles, n, is determined probabilistically to preserve the expected number of splits. Denoting n_1 to be the largest integer which is less than or equal to I_a/I_b, $p=I_a/I_b-n_1$ is defined. Then $n=n_1+1$ is selected with probability p, and $n=n_1$ with probability $1-p$. The same weight $W\times I_b/I_a$, which is the expected weight, is assigned to each particle in order to minimize dispersion of weights. On the other hand, if the particle enters the cell of lower importance ($I_a/I_b<1$), the Russian roulette game is played with surviving probability of I_a/I_b. If the particle survives, its weight is increased by a factor of I_b/I_a. Note that in the present procedure weight is not preserved at each splitting or Russian roulette except for the case of splitting with an integer importance ratio, but that the expected value is unbiased.

The present splitting with Russian roulette is a very reliable variance reduction technique when the randolm walk is carried out in the analog manner where there are no weight biasing in the source and no weight reduction or increment corresponding to absorbing or multiplying reactions. This is because the weights of all particles are the same in a phase space cell no matter which geometrical path or collision the particles have taken to get to the cell. In MORSE-DD, however, a particle weight is changed at each collision owing to the non-absorption probability. Furthermore, this code allows the weight biasing in the source. Accordingly, the present technique alone cannot suppress dispersion of weights in a cell, especially in a system containing highly absorbing materials. In such a case, a user should apply this technique together with the other ones which reduce the dispersion of weights like a weight window or a weight kill with Russian roulette described below.

(2) Weight Window

The weight window technique is a type of phase space splitting and Russian roulette. A weight window consists of an upper bound W_u and a lower one W_l for a partile weight. When a particle with a weight W enters a new phase space cell owing to streaming or a collision, the weight W is compared with the weight window (upper and lower bounds). The weight is put into the window or the particle is killed by splitting with Russian roulette when it is out of the window. The recipe is as follows. If W is less than W_l, then Russian roulette game is played on this particle with surviving probability W/W_{av}, where W_{av} is an average weight such as $W_l<W_{av}<W_u$. If the particle survives, it has a weight W_{av}. On the other hand, if W is greater than W_u, the particle is split so that the resulting particles have their weights within the window. The number of splits, n, is determined probabilistically. By using $p=W/W_{av}-n_1$, where n_1 is the largest integer less than or equal to W/W_{av}, $n=n_1+1$ is selected with probability p, and $n=n_1$ with probability $1-p$. Then the same weight W_{av} is assigned to each particle.

This technique is applied at geometry region surfaces and/or collisions by a user's choice. Note that a user should assign the average weight W_{av} and the lower bound W_l for each phase space cell. By using these parameters, the code determines the upper bound W_u by

$$W_u=W_{av}\times\ \{(\frac{W_{av}}{W_l}-1)\times 0.5+1\} \tag{6-42}$$

(3) Forced Collision

Sometimes, one desires to cause collisions in a relatively small geometry region which are important to the problem. In such a case, it is necessary to force particles to have collisions in these regions. Furthermore, since contributions to flux at a point come only from collisions except for the direct contributions from the source, forced collisions will be useful in some problems. On the contrary, if collision probability is biased and decreased, more particles than those in a normal sampling case can pass through the region without collisions, which is a preferable situation in solving the deep penetration problem.

Each phase space cell is assigned a forced collision probability P by a user. The probability P should be in the range of $0<P<1$. If a particle with a weight W enters a geometry region of which forced collision probability is P, the particle is forced either to collide within the region with probability P or to pass through the region without a collision with probability $1-P$. The weight of the colliding particle is changed to $W\times(1-e^{-\Sigma_t l})/P$, where l is a distance which the particle must travel before exiting the region. A collision point of this particle is determined from the probability given by

$$f(x)=\frac{\Sigma_t e^{-\Sigma_t x}}{1-e^{-\Sigma_t l}}, \quad 0\leqq x\leqq l. \tag{6-43}$$

That is, the distance traveled before the collision, χ, is calculated by using a random number R as

$$x=-\frac{1}{\Sigma_t}\ln\ \{(1-R(1-e^{-\Sigma_t l})\}\ . \tag{6-44}$$

The particle passing through the region with no collision has a weight $W\times e^{-\Sigma_t l}/(1-P)$, and is moved to the boundary exiting the region in question.

Note that the forced collision usually disperses particle weights since l strongly depends on the direction of path. Furthermore, this technique generates particles with a small weight in small regions. A user should pay attention to these points if he uses the Russian roulette and/or weight cut off techniques together with the forced collision.

6.1.5 Tallies

The MORSE-DD code provides five standard tallies. These basic tallies can be easily modified by a user. All tallies are normalized to be one starting particle. They are a function of energy. Time or angle dependent quantities can be obtained by point and surface crossing estimators. The tally data are edited on a user file, and a user can process them into interesting quantities such as reaction rates by using auxiliary codes.

(1) Flux at a Point

The flux alkt a detector point consists of the contribution to a detector directly from a source and that from collisions, which is written as follows:

$$\Psi(r_d,\Omega)=\int dr'S(r',\Omega)\frac{1}{|r'-r_d|}\exp(-\beta(r',r_d))+$$
$$+\int dr'\int d\Omega'\,\Sigma_s P(\Omega'\to\Omega)\delta\left(\Omega,\frac{r'-r_d}{|r'-r_d|}\right)\Psi(r',\Omega')$$
$$\times\frac{1}{|r'-r_d|^2}\exp(-\beta(r',r_d)), \tag{6-45}$$

where

$$\beta(r',r_d)=\int_0^{|r'-r_d|}\Sigma_t\left(r-R\frac{(r'-r_d)}{|r-r_d|}\right)dR. \tag{6-46}$$

The MORSE-DD code calculates the flux on the basis of the following formula,

$$\bar{\Psi}(r_d,\Omega)=\sum_i W_i P_i\frac{1}{|r_i-r_d|^2}\exp(-\beta(r_i,r_d))$$
$$+\sum_j W_j\frac{\Sigma_s(r_j)}{\Sigma_t(r_j)}P(\mu)\frac{1}{|r_j-r_d|^2}\exp(-\beta(r_j,r_d)), \tag{6-47}$$

where

W_i = particle weight born at the source,
W_j = particle weight before a collision,
P_i = probability of particle being born in the direction of detector within unit solid angle,

$P(\mu)$ = probability that a scattering angle will be μ.

The first term is called as an uncollided flux and the second one as a last flight or next event estimator. As seen from the above expression, this scheme has a $1/R^2$ singularity (R is distance between collision and detector points) for a detector in a scattering medium which makes the theoretical variance of the estimator infinite. The probability P_i is determined from the angular distribution of sourcle particle defined in the sourcle routines. The probability $P(\mu)$ is calculated by using the scattering probability matrix of Eq.(6-2) as follows:

$$P_{g'\to g}(\mu)=\frac{1}{2\pi}\frac{\bar{I}(k;g'\to g)}{\Delta\mu_k}, \tag{6-48}$$

where k shows the angle bin such as $\mu_{k+1}\leqq\mu<\mu_k$, and

$g'\to g'$: energy transfer from group g' to g,,

$\Delta\mu_k$: width of k-th angle bin.

It is recommended that the point estimator should be used in regions of little scattering (e.g. air) or in voids because a large-weighted particle interacting arbitrarily close to the detector can severely perturb both the estimator result and its variance due to the $1/R^2$ singularity. To cope with this difficulty, MORSE-DD can apply the bounded sphere approximation[21] in the neighbouring region of the detector.

In the bounded sphere approximation, we assume that the scattering is isotropic and uniform within a spherical region surrounding the detector point. By doing so, the $1/R^2$ singularity can be removed by scoring $\exp(-\Sigma_t r)/4\pi c^2$ instead of $\exp(-\Sigma_t r)/4\pi r^2$ for the collision within this sphere. In the code, c is given by the formula,

$$c^2=a^2\left\{\frac{2}{\lambda^2}+\left(1+\frac{2}{\lambda}\right)/(1-\exp\lambda)\right\}, \tag{6-49}$$

where

a= radius of sphere,

$\lambda=\Sigma_t a$

For a typical problem, the values of a is on the order of $0.1\sim0.5$ in mean free path unit.

When a point estimator is used, the computation time rapidly increases with increasing number of detectors. To reduce the computation time, the code can use the probabilistic sampling of collision event outside an imaginary sphere of a specified radius R_{min}[22]. When a real collision occurs outside the sphere, this event is scored with the probability $(R_{min}/R)^2$. For the scored event, the score is increased by a factor of $(R/R_{min})^2$. This technique is effective for a large system.

(2) Flux and Current across a Surface

The current between angles μ_1 and μ_2 through a surface S is given by

$$J(\mu_1\leqq\mu\leqq\mu_2)=\int_S ds\int_{\mu_1}^{\mu_2}d\mu\int_0^{2\pi}d\varphi\Psi(r,\mu,\varphi)\mu, \tag{6-50}$$

where

μ= cosine of polar angle between normal direction of surface and particle flight direction,

φ= azimuthal angle.

The flux between angles μ_1 and μ_2 integrated over S is given by

$$\Psi(S,\mu_1\leqq\mu\leqq\mu_2)=\int_S ds\int_{\mu_1}^{\mu_2}d\mu\int_0^{2\pi}d\varphi\ \{\mu\Psi(r,\mu,\varphi)\}\ \frac{1}{\mu}, \tag{6-51}$$

The flux in the i-th cosine bin is obtained by scoring the particle crossing S as

$$\bar{\Psi}_i=\sum_{\mu_i\leqq\mu_j<\mu_{i-1}}W_j/|\mu_j|/S. \tag{6-52}$$

It is well known that this surfacle crossing estimator for flux has the $1/\mu$ singularity; the grazing angles in this procedure result in an infinite variance. In order to overcome this problem, we assume a constant angular flux in the range of $|\mu|\leqq\varepsilon$[9], which is also assumed in the original MORSE code. Under this

assumption, the flux within this range is estimated by scoring $2/\varepsilon$ instead of $1/|\mu|$. This procedure insures a finite variance. Note that ε is fixed to be 0.01 in MORSE–DD.

The current tally is given by

$$\bar{J}_i = \sum_{\mu_i \leqq \mu_i < \mu_{i+1}} W_j/S, \tag{6–53}$$

Note that the present current tally is not the net current of nuclear reactor theory, but equal to the particles crossing S.

(3) Track Length Estimator

The flux is calculated by summing the track length traveling in a specified region as follows:

$$\bar{\Psi} = \sum_i W_i \cdot l_i/V, \tag{6–54}$$

where

l_i= track length of particle i in the specified region,

W_i= weight of particle i,

V= volume of the region.

The track length estimator is very reliable for both the detector count and its variance.

Note that the detector region is the same as the geometry region which is defined by input data for geometry description.

(4) Collision Estimator

The collision estimator scores W/Σ_t at each collision event that occurs within a specified region of volume V. That is, the flux is calculated by

$$\bar{\Psi} = \sum_i W_i \cdot \frac{1}{\Sigma_{ti}} /V. \tag{6–55}$$

The collision estimator tends to suffer from a bad statistics in optically thin regions since few collisions occur there. This statistical problem is usually improved by using the track length estimator. The surface crossing, track length and collision estimators tend to suffer from increasing statistical errors as the volume of the detector region becomes arbitrarily small. The next event (point detector) estimator is a candidate for such problems. A user should be careful in choosing effective estimators for his problem.

6.1.6 Super–Group Treatment of Random Walk Process

The MORSE–DD code requires a large amount of memory to store lots of DDX data when a complicated problem with many materials is to be solved. It is useful to save memory for wide applications to practical problems. The modified version of MORSE–DD has been developed to be executed with a moderate memory size by adding supergrouping ability, i.e., by partitioning fine energy groups into as many as 20 energy bands. This version is named as MORSE–DSG.

The MORSE–DSG code, at first, determines the energy band structure from the DDX data size and memory available for the storage of the DDX data so that each band contains about equal amounts of data. Then this code produces the corresponding data subsets and writes them on three direct access files for the succeeding random walk process. The data subsets consist of (1) permanently stored cross sections of which scattering matrices and angular distribution data are banded (see Section 6.3.3), (2) sampling parameter data for variance reduction (7×MGPREG) and (3) splitting, Russian roulette and scattering counters (8×MGPREG+8×NMTG×MXREG). Required storage sizes in MORSE–DD are shown in the parentheses. In the random walk process, the data subsets of each energy band are read from the direct access files and neutrons within the current energy band in the neutron bank are pursued until they leak out from the system or are slowed down into lower energy bands. The slowed–down neutrons are put back

into the neutron bank. This neutron bank data treatment is slightly changed for efficient usage of the bank. The random walk is carried out once from the highest energy band down to the lowest one in a batch. Accordingly, MORSE-DSG cannot be applied to a fixed source problem with fission reactions which generate neutrons with higher energy than the current energy band.

Three modes of run can be selected in MORSE-DSG depending on the computer restrictions such as I/O and CPU time restrictions. These are

(1) preparation of the super-group DDX data subsets,

(2) random walk and edit,

(3) continuous run of (1) and (2).

Note that the energy splitting with Russian roulette based on importance is not available in MORSE-DSG.

An auxiliary code ZRECNO is prepared for a user to get information about the banded data subsets and the required block size of three direct access files. It is recommended that ZRECNO be executed before a MORSE-DSG run. How to use ZRECNO is given in Section 6.5.2.

6.2 Input Instructions

6.2.1 MORSE-DD

(1) Random Walk Input Instructions

The input read by the subroutine INPUT1 is as follows:

CARD A (20A4)

Title card.

NOTE: Any character other than a blank or alphanumeric in column one will terminate the job.

CARD B (*)

1) NSTRT number of particles per batch
2) NMOST maximum number of particles allowed in the banks
   The parameter NMOST may equal NSTRT if no splitting, no fission and no secondary generation are in the problem.
3) NITS number of batches
4) NQUIT number of sets of NITS batches to be run without calling subroutine INPUT
5) NGPQTN number of neutron groups being analyzed
6) NGPQTG number of gamma-ray groups being analyzed
   When the DDX is used, NGPQTG should be equal to 0.
7) NMGP number of primary particle groups of cross section data to be stored
   The parameter NMGP should be the same as NGP (or the same as NGG when NGP =0) on CARD XB read by the subroutine XSEC.
8) NMTG total number of groups of cross section data to be stored
   The parameter NMTG should be the same as NGP+NGG on CARD XB read by the subroutine XSEC.
9) NCOLTP option for a collision file
   = 0, no effect
   > 0, the collision file is written by the user routine BANKR.
   In the present code, BANKR writes no collision data.

(*) means FORTRAN77 free-formatted input.

10) IADJM adjoint problem indicator
= 0, forward calculation
> 0, adjoint calculation (not available in DDX mode)
11) AXTIM maximum clock time in minutes allowed for the problem
For example, 4.5 entered here allows 4 and 1/2 minutes.
12) MEDIA number of cross section media
The parameter MEDIA should agree with NMED on CARD XB read by the subroutine XSEC.
13) MEDALB albedo scattering
= 0, no albedo information to be read in
< 0, albedo only problem
No cross sectionns are to be read.
> 0, coupled albedo and transport problem
Albedo scattering medium is absolute value of MEDALB.

NOTE: The present code contains the default version of subroutine ALBDO which performs the specular reflections. By using this, a reflection boundary condition can be expressed in the combinatorial geometry presentation. If arbitrary albedo scattering is necessary, a user must modified the subroutines ALBDO and ALBIN. Albedo data must be read by the latter subroutine which performs nothing in the present code.

CARD C (*)

1) ISOUR source option
If ISOUR>0, source particles are emitted in energy group ISOUR. If ISOUR<0 or if ISOUR=0 and NGPFS≠0, SORIN is called for input of CARDS E1 and E2.
2) NGPFS number of energy groups for source spectrum
The source spectrum is defined in the first NGPFS groups. If ISOUR<0, NGPFS must be greater than 1.
3) ISBIAS source energy biasing
= 0, no effect
> 0, use source energy biasing
The input data for CARDS E2 are required.
4) NOTUSD an unused variable
5) WTSTRT weight assigned to each source particle
6) EBOTN lower energy limit of lowest neutron group (eV)
(group NGP)
7) EBOTG lower energy limit of lowest gamma–ray group (eV)
(group NMTG)
8) TCUT age in sec for time kill
Particles are retired at TCUT. If TCUT=0, no time kill is performed.
9) VELTH velocity of group NMGP when NGPQTM>0; i.e., thermal neutron velocity (cm/sec)

CARD D (*)

1) XSTRT
2) YSTRT } coordinates for source particles
3) ZSTRT
4) AGSTRT starting age for source particles

5) UNIP
6) VINP
7) WINP
} source particle direction cosines
If all are zero, isotropic directions are chosen.

NOTE: Source data on CARDs C and D will be overridden by any changes in the subroutine SOINP. The subroutine SOINP is called from the subroutine SOURCE.

CARDS E1 (*) (Omit if ISOUR>0 or if ISOUR=NGPFS=0)
(FS(i), i=1, NGPFS) unnormalized fraction of source particles in each group

CARDS E2 (*) (Omit if ISOUR>0 or if ISOUR≦0 and ISBIAS=0)
(BFS(i), i=1, NGPFS) relative importance of a source in each group

CARDS F (*)
(ENER(i), i=1, NMTG) upper energy group boundaries (in eV)
Note that the lower energies of groups NMGP and MNTG were read on CARD C.

CARD G (*) (Omit if NCOLTP on CARD B ≦ 0)
1) NHISTR I/O unit number for the first collision file
2) NHISMX the highest I/O number for a collision file
3) (NBIND(J), J=1, 36) an index to indicate the collisions to be written on file
39) (NCOLLS(J), J=1, 13) an index to indicate the types of collisions to be put on file
NOTE; A user should modify the subroutine BANKR to create a collision file.

CARD H (Z12) on 32 bit machines (IBM, FACOM etc.); (O20) on 36 bit machines (CDC, NEC etc.)
RANDOM starting random number
In a restart run, this value is replaced by the value read fromthe restart file.

CARD I (*)
1) ISRK1 index indicating splitting with Russian roulette
= 0, no effect
> 0, splitting at collisions (similar to original code)
=-1, splitting with Russian roulette at zone boundaries based on cell importance
=-2, splitting with Russian roulette at zone boundaries based on weight window
2) ISRK2 index indicating splitting with Russian roulette at collisions
= 0, no effect
> 0, Russian roulette at collisions (similar to original code)
=-1, splitting with Russian roulette at collisions based on cell importance
=-2, splitting with Russian roulette at collisions based on weight window
3) NPAST index indicating exponential transform or forced collision
= 0, no effect
> 0, exponential transformation
The subroutine DIREC is required.
< 0, forced collision
4) NOLEAK index indicating non-leakage
= 0, no effect
> 0, non-leakage

5) IEBIAS index indicating energy biasing at collisions
   = 0, no effect
   > 0, energy biasing at collisions (not usable in the present code)
6) MXREG number of regions described by geometry input
   This value will be set 1 if MXREG ≦ 0.
7) MAXGP group number of the last group for variance reduction
   In the first MAXGP groups, the Russian roulette, splitting, exponential transform and forced collision are performed. For an adjoint problem, set MAXGP=NMTG (on CARD B).

The first two data on this line is corresponding to NSPLT and NKILL in the original MORSE-CG code.

CARD J (*) (Omit if | ISRK1 | + | ISRK2 | + | NPAST | = 0
1)~6) NPG1, NDG, NGP2, NRG1, NDRG, NRG2
   From energy group NGP1 to energy group NGP2, inclusive, in steps of NDG and from region NRG1 to NRG2, inclusive, in step of NDRG, the following weight standards and exponential transform or forced collision parameters are assigned. If NGP1=0, groups 1 to MAXGP will be used; if NRG1=0, regions 1 to MXREG will be used (both in steps of one). Usually NDG=1 and NDRG=1.
7) WTHIHI upper bound of weight or cell importance
   If ISRK1>0, splitting will occur for particles with a weight greater than WTHIHI. If ISRK1=-1 or ISRK2=-1, WTHIHI is importance assigned to these cell regions.
8) WTLOW1 lower bound of weight
   The Russian roulette is played on particles with a weight below WTLOW1 if required (ISRK1=-2, ISRK2>0 or ISRK2=-2).
9) WTAVE weight given to particles surviving Russian roulette or weight window
10) PATH path-length stretching or forced collision parameter
   If NPAST>0, path-length stretching will be performed by the exponential transform (usually 0 ≦ PATH<1). If NPAST<0, forced collision will occur in these regions with the probability PATH (usually 0 < PATH < 1).

The CARD J inputs can be repeated if necessary. The termination of these inputs must be indicated by a new line with a negative value of NGP1 and / (ex., -1 and /).

CARD K (*) (Omit if IEBIAS on CARD I ≦ 0)
((EPROB(IG, NERG), IG=1, NMTG), NREG=1, MXREG)
   values of relative energy importance of particles leaving a collision in region NREG
NOTE: Input for each region must start on a new line.

CARD L (*)
1) NSOUR generation of source particles
   ≧ 0, external fixed source
   > 0, fission source generated in a previous batch
2) MFISTP index for fission
   ≦ 0, no fission in the problem
   > 0, fission may occur

3) NKCALC number of the first batch to be included in the estimate of k_{eff}
If NKCALK $\leq$ 0, no estimate of k_{eff} is made.

4) NORMF option for the weight standards and fission weights
The weight standards and fission particle weights given by CARD J and CARD M are unchanged if NORMF $\leq$ 0; otherwise fission weights will be multipled, at the end of each batch, by the latest estimate of k_{eff} and the weight standards are multiplied by the ratio of fission weights produced in previous batch to the average starting weight for the previous batch. For time-dependent decaying systems, NORMF should be $>$ 0.

CARDS M (*) (Omit if MFISTP on CARD L $\leq$ 0)
(FWLO(I), I=1, MXREG) values of the weight to be assigned to fission neutrons generated in each region

CARDS N (*) (Omit if MFISTP on CARD L $\leq$ 0)
(FSE(IG,IMED), IG=1, NMTG), IMED=1, MEDIA)
fission spectrum of medium IMED
NOTE: Input for each medium must start on a new line.

CARDS O (*) (Omit if NGPQTN=0 or NGPQTG=0, i.e., enter for coupled neutron- gamma-ray problem)
((GWLO(IG,NREG), IG=1, NMGP or NMTG-NMGP), NREG=1, MXREG)
secondary particle generation probability in region NREG
The input data for NMGP groups are read for each region in a forward problem, and those for NMTG-NMGP groups for an adjoint problem.
NOTE: Input for each region must start on a new line.

(2) Combinatorial Geometry Module Input Instructions

The combinatorial geometry input data is read by the JOMIN subroutine, except for the region volumes VNOR(I), which are read by the GTVLIN subroutine whenvever IVOPT=3. For clarity of terminology, the terms "region" and "media" have essentially the same meaning as in the O5R Geometry Package[28], but are constructed in a different manner. The term "zone" is the same as the "region" as defined in the original combinatorial geometry package. The term "body" has the same meaning as in the original combinatorial geometry package.

CARD CGA (2I5, 10X, 10A6)
IVOPT option for region volumes
= 0, volumes are set equal to 1.
= 1, concentric sphere volumes are calculated.
= 2, slab volumes (1-dim.) are calculated.
= 3, volumes are read from card-image input on I/O unit 5.
IDBG option for debugging
= 0, no effect
> 0, debug print
The subroutine PR is called to print results of combinatorial geometry calculations during execution. Use only for debugging.
JTY alphanumeric title for geometry input (columns 21-80)

CARDS CGB (2X, A3, 1X, I4, 6D10.3)

One set of CARDS CGB is required for each body and for the END line (see **Table 6.1**). Leave columns 1–6 blank on all continuation lines.

ITYPE body type or END to terminate reading of body data (for example BOX, RPP, ARB, etc.)
NOTE: Leave blank for continuation lines.

IALP body number assigned by a user
NOTE: All input body numbers must form a sequence set beginning at 1. If left blank, numbers are assigned sequentially. Assign either all or none of the numbers. Leave blank for continuation lines.

FPD(I) real data required for the given body
Real data for each body are shown in **Table 6.1**.
NOTE: This data must be in cm.

Table 6.1 Body data required by each body type

Line columns	ITYPE	IALP	Real data defining						Number of lines needed
Body type	3-5	6-10	11-20	21-30	31-40	41-50	51-60	61-70	
BOX	BOX	IALP is assigned by the user or by the code if left blank.	Vx	Vy	Vz	H1z	H1y	H1z	1 of 2
			H2x	H2y	H2z	H3x	H3y	H3z	2 of 2
Right parallel-piped	RPP		Xmin	Xmax	Ymin	Ymax	Zmin	Zmax	1
Sphere	SPH		Vx	Vy	R	–	–	–	1
Right circular cylinder	RCC		Vx	Vy	Vz	Hx	Hy	Hz	1 of 2
			R	–	–	–	–	–	2 of 2
Right elliptic cylinder	REC		Vx	Vy	Vz	Hx	Hy	Hz	1 of 2
			R1x	R1y	R1z	R2x	R2y	R2z	2 of 2
Ellipsoid	ELL		Vx	Vy	Vz	V2x	V2y	V2z	1 of 2
			L	–	–	–	–	–	2 of 2
Truncated right cone	TRC		Vx	Vy	Vz	Hx	Hy	Hz	1 of 2
			L1	L2	–	–	–	–	2 of 2
Right angle wedge	WED or RAW		Vx	Vy	Vz	H1x	H1y	H1z	1 of 2
			H2x	H2y	H2z	H3x	H3y	H3z	2 of 2
Arbitrary polyhedron	ARB		V1x	V1y	V1z	V2x	V2y	V2z	1 of 5
			V3x	V3y	V3z	V4x	V4y	V4z	2 of 5
			V5x	V5y	V5z	V6x	V6y	V6z	3 of 5
			V7x	V7y	V7z	V8x	V8y	V8z	4 of 5
			Face descriptions (see note below)						5 of 5
Elliptical torus	ELT		Vx	Vy	Vz	Nx	Ny	Nz	1 of 2
			RM	R1	R2	T	–	–	2 of 2

NOTE : The fifth line of the ARB input contains a four-digit number for each of the six faces of an ARB body. The format is 6D10.3, beginning in column 11.

CARDS CGC (2X, A3, I5, 9(A2, I5))

"Input zone" specification data. One set of lines are required for each input zone with input zone numbers being assigned sequentially.

IALP IALP must be a nonblank for the first line of each set of lines defining an input zone. If IALP is blank, this line is treated as a continuation of the previous zone line. IALP = 'END' denotes the end of zone description.

NAZ total number of zones that can be entered upon leaving any of the bodies defined for this input zone (some zones may be counted more than once). Leave blank for continuation lines for a given zone. (If NAZ $\leq$ 0 on the first line of the zone data, then it is set to be 5). This is used to allocate blank common. Alternate IIBIAS(I) and JTY(I) for all bodies defining this input zone.

IIBIAS(I) specify the "OR" operator if required for the JTY(I) body.

JTY(I) body number with the (+) or (−) sign as required for the zone description.

NOTE: A pair of IIBIAS(I) and JTY(I) should be repeated on a line nine times at most.

CARDS CGD (*)

MRIZ(I) region number assigned to the I-th input zone
(I = 1 to the number of input zones)
Region numbers must be sequentially defined from 1.

CARDS CGE (*)

MMIZ(I) medium number filling the I-th input zone
(I = 1 to the number of input zones)
Medium numbers must be sequentially defined from 1.

NOTE: In addition to designating a cross section mixture number, the medium number can be used for three other purposes:

A. 0 < MMIZ(I) < 1000 → cross section mixture number
(MMIZ(I) ≠ MEDALB)

B. MMIZ(I) = 0 → external void
(used as the vacuum boundary)

C. MMIZ(I) = 1000 → internal void
(no collision in this zone)

D. MMIZ(I) = MEDALB → albedo scattelring medium
(reflection medium)

CARDS CGF (*) (Omit if IVOPT ≠ 3)

VNOR(I) volume of the I-th region
(I = 1 to MXREG, the number of regions)

(3) Cross Section Module Input Instructions

CARD XA (20A4)

Title for cross sections. This title is also written on a file in P_l mode, if a processed file is written; therefore, it is suggested that the tile be definitive.

CARD XB (*)

1) NGP number of primary groups of cross section data to be stored
The parameter NGP should be same as NMGP on CARD B.
2) NDS number of primary downscatters for NGP (usually NGP)
3) NGG number of secondary groups of cross sections data to be stored
4) NDSG number of secondary downscatters for NGG (usually NGG)
5) INGP total number of groups of cross section data to be stored

6) ITBL cross section table length
The parameter ITBL is the number of cross sections for each group, which is usually equal to the number of down scatters + the number of upscatters +3.

7) ISGG location of within-group scattering cross sections
The parameter ISGG is usually equal to the number of upscatters +4.

8) NMED number of media (cross section mixtures)
The parameter NMED should be same as MEDIA on CARD B.

9) NELEM number of elements
Cross sections for NELEM elements are to be read in.

10) NMIX number of mixing operations (elements times density operations) to be performed
The parameter NMIX must be ≥ 1.

11) NCOEF number of coefficients for each element, including P_0
Set 1 if the DDX is used.

12) NSCT P_l ; number of discrete angles (usually NCOEF/2)
DDX ; number of angle bins

13) ISTAT flag to store Legendre coefficients for point estimators (no effect in DDX mode)
= 0, no effect
> 0, store Legendre coefficients

14) IDDX cross section type
= 0, P_l expansion type cross section
= 1, DDX

CARD XC (*)

1) IRDSG switch to print input cross sections
= 0, no effect
= 1, print the cross sections as they are read

2) ISTR switch to print cross sections as they are stored
= 0, no effect
= 1, yes
Note that the code prints no cross section if ISTR<0 in DDX mode (IDDX=1).

3) IFMU switch to print intermediate results of μ's calculation
= 0, no effect
= 1, yes

4) IMOM switch to print moments of angular distribution
= 0, no effect
= 1, yes

5) IPRIN switch to print angles and probabilities
= 0, no effect
= 1, yes

6) IPUN switch to print results of bad Legendre coefficients
= 0, no effect
= 1, yes

7) IDTF format of P_l cross sections (no effect in DDX mode)
= 0, ANISN format[7]
= 1, DTF-IV format[29]

8) IXTAPE I/O unit number of an ANISN-type cross section file
In P_l mode (IDDX=0), this is an input file of cross section data. Set 0 if cross sections are entered from card-image input on the I/O unit 5. If IDDX=1, a DDX library is read from the I/O unit 99 and the processed ANISN-type cross sections are written on the I/O unit IXTAPE. If negative, the processed cross sections and the other necessary data from a previous run will be read. In this case (IXTAPE<0), no cross sections from card-image input and no mixing data may be entered when IDDX=0, while all cross section data (element ID and mixing data etc.) are required when IDDX=1. The absolute value of IXTAPE is the I/O unit number for the processed ANISN-type cross sections. The additional processed DDX library is read from the I/O unit 96.

9) JXTAPE I/O unit number of a processed cross section file to be written (no effect in DDX mode)
This processed file will contain the title data, the variables from common LOCSIG and the pertinent cross sections from blank common. The parameter JXTAPE is dummy input for DDX mode. In the case of DDX mode, I/O units of processed cross sections to be written are the units 96 and IXTAPE.

10) IO6RT I/O unit number of a point cross section file in O6R format[30]

11) IGOPT last group (MORSE multi-group structure) for which the O6R point cross sections are to be used
The parameter IGOPT must be $\leq$ NMGP.

CARD XC' (*) (Omit if IDDX $\neq$ 1)
Boundaries of angular interval (NSCT entries in descending order). The last data should be equal to -1.

CARD XD (*) (Omit if IXTAPE $\leq$ 0 and IDDX=0)
Element identifiers for cross sections in a file (NELEM entries). In DDX mode (IDDX=1), the code reads the cross sections of last group (the NMGP-th group) from the following CARD XE for elements specified by negative identifiers. If element identifiers are in the same order as elements on a file, the efficiency of the code is increased due to fewer file rewinds.

CARD XE (*) (Omit if all element identifiers on CARD XD > 0)
CARD XE data are repeated for all elements specified by negative identifiers (- sign and I.D. number).

1) MAT element identifier
2) SIGT0 total cross section of the NMGP-th group
3) SIGPR production cross section of the NMGP-th group
4) SIGC absorption cross section of the NMGP-th group
5) SIGF fission cross section of the NMGP-th group
6) SIGFE $\nu\sigma_f$ of the NMGP-th group

CARD XF (*) (Omit if IXTAPE<0 and IDDX=0)
NMIX (see CARD XB) lines are required.

1) KM medium number

2) KE element number occurring in medium KM
NOTE: A negative value of KE indicates last mixing operation for that medium. Failure to have a negative value causes the code not to generate angular probabilities for that medium (LEGEND and ANGLE are not called) in P_l mode.

3) RHO density of element KE in medium KM

CARD XG (Omit if IXTAPE $\neq$ 0)

Cross sections (for INGP groups with a table length ITBL for NELEM elements each with NCOEF coefficients).
If cross sections are given in free form, a line with " * " in column 2 and 3 must precede the actual data. The ANISN format[7] is assumed if IDTF$\leqq$0; otherwise, the DTF-IV format[29].

CARD XH (*) (Omit if IO6RT$\leqq$0)

NXPM number of point cross section sets per medium found on an O6R file[30]
= 1, total cross section only
= 2, total + scattering cross section
= 3, total, scattering, and ν * fission cross section.

(4) Analysis Module Input Instructions

The following data are read from card-image linput on the I/O unit 5 by the subroutine SCORIN.

CARD AA (20A4)

Title information which will be immediately output.

CARD BB (*)

1) ND number of detectors
Set 1 if ND$\leqq$0.

2) NNE number of primary particle (neutron) energy bins to be used
The parameter NNE must be $\leqq$ NE.

3) NE total number of energy bins
Set 0 if NE$\leqq$0.

4) NT number of time bins for each detector
The parameter NT may be nagative, in which case | NT | values of time bin boundaries are to be read and used for every detector. Set 0 if | NT | $\leqq$ 1.

5) NA number of angle bins
Set 0 if NA $\leqq$ 1.

6) NRESP number of energy-dependent response functions to be used
Set 1 if NRESPk $\leqq$ 0.

7) NEX number of extra arrays of size NMTG to be set aside
These extra arrays are useful, for example, as a place to store an array of group-to-group transfer probabilities for estimator routines.

8) NEXND number of extra arrays of size ND to be set aside
These extra arrays are useful, for example, as a place to store detector-dependent counters.

9) NTAPE indicator of restart file if NTAPE>0
The result of a previous run is read from the I/O unit NTAPE, and the data for a next run is written on the I/O unit NTAPE+1.

10) NNBAT dummy input (set 0)
11) NRUN2 indicator of restart calculation
= 0, first run
= 1, restart run
12) IOUTE unit of output flux
= 0, per unit lethargy
= 1, per unit energy
13) IEST indicator of flux estimator
= 0, point estimator
= 1, surface cross estimator (sphere with the center located at the origin)
= 2, surface cross estimator (circular plane perpendicular to z-axis)
= 3, track length estimator
= 4, collision estimator
= −1, arbitrary combination of above estimators

NOTE: For the estimators except for point one, the detector regions or detector surfaces should be defined by the geometry input.

14) INCF option to calculate uncollided flux
= 0, no effect
= 1, calculate uncollided flux
This option is effective only for the point estimator.
15) IOUTF brief output indicator consisting of a two-digit integer (IOUTF1 * 10 + IOUTF2).

IOUTF1 : indicator for the results of edit
= 3, only integrated response
= 2, response + energy dependent total flux
= 1, response + energy dependent total flux − angular flux
= 0, all

IOUTF2 : indicator for random walk information (groupwise)
= 4, no output
= 3, regionwise real collision, albedo collision, fission
= 2, 3 + splitting
= 1, 2 + Russian roulette
= 0, all

CARD BB1 (*) (Omit if IEST ≠ −1)
1) IE1 number of point estimators
2) IE2 number of surface cross estimators (sphere)
3) IE3 number of surface cross estimators (circular plane)
4) IE4 number of track length estimators
5) IE5 number of collision estimators

NOTE: IE4 and IE5 should be equal to the number of regions defined by the geometry data excluding outer void regions.

CARD CC (*)

One line of CARD CC data is required by each point or surface cross estimator. Accordingly, ND lines are required if IEST=0, 1, 2, and (IE1+IE2+IE3) lines if IEST = −1.

1)~5) X, Y, Z, RMAX, RMIN location of point or surface cross estimator

For the point estimator,

(X,Y,Z) : detector location.

RMAX : radius (cm) of sphere in which the bounded sphere approximation is applied.

RMIN : radius (cm) of sphere defining the region in which the probabilistic scoring of collision event is applied to reduce computation time.
When a real collision occurs outside an imaginary sphere with radius RMIN, this even is scored with the probability $(RMIN/R)^2$, where R is a distance between the detector and the collision point. Beware that RMIN is larger than RMAX.

NOTE: The same values of RMAX and RMIN, which are defined on the last line, are commonly used for all the point estimators.

For the surface cross estimator (sphere), the detector is the surface of sphere with radius R and with the center at the origin ($R^2=X^2+Y^2+Z^2$).

For the surface cross estimator (circular plane), the detector surface is the circular plane perpendicular to z-axis of radius X with the center at (0,0,Z). These detectors should be defined in increasing order of Z.

Note that RMAX and RMIN are dummy data for the surface cross estimator.

CARD DD (20A4)

Title or units for responses for all detectors.
This will be printed out in columns 54 through 133 of the title for calculated responses.

CARD EE (20A4)

Title or units for each response for all detectors.

CARD FF (*)

Response function values. NMTG values will be read in each set of CARD FF data. Input order is from energy group 1 to NMTG (order of decreasing energy).

NOTE: NRESP sets of CARD EE and FF data will be read in the following order: EE, FF1, ... FFN, EE, FF1, ... FFN, etc.

CARD GG (20A4) (Omit if NE≦1)

Units for energy-dependent fluence for all detectors.

CARDS HH (*) (Omit if NE≦1)

Energy group numbers defining lower limit of energy bins in order of increasing group number (NE entries).
The NNE-th entry must equal NGPQTN if NNE>0; the NE-th entry must be set to NMGP + NGPQTG for a combined problem, or else NGPQTG or NGPQTN.

CARD II (20A4) (Omit if | NT | ≦1)

Units for time-dependent responses for all detectors.

CARD JJ (20A4) (Omit if | NT | ≦1 or NE≦1)

Units for time-and energy-dependent fluence for all detectors.

CARD KK (*) (Omit if | NT | ≦1)

Upper limits of time bins for each detector in order of increasing time and detector number (NT

entries for each detector).
The values for each detector must start on a new line. | NT | values only are read if NT is negative. They are then used for every detector.

CARD LL (20A4) (Omit if NA≦1)
Units for angle- and energy-dependent fluence for all detectors.

CARD MM (*) (Omit if NA≦1)
Upper limits of angle bins (NA entries).
These data are actually cosine bins; the NA-th value must equal one.

Following the inputs for the analysis module, enter input data for user-written subroutines INSCOR, SOURCE and ENDRUN.

(5) External Source Module Input Instruction

The input for external source module is read by the subroutine SOINP called from the subroutine SOURCE. If ISOUR on CARD C is greater than zero, energy spectra given in this section are all meaningless, but spatial and angular distributions are effective.

CARD S1 (*)
IS number of source
If IS<0, intensities of | IS | sources are biased. If IS=0, an isotropic point source at (XSTRT, YSTRT, ZSTRT) given by CARD D is assumed. In this case, no further data are read by SOINP.

CARD S2 (*)
(S(I), I=1, IS) relative intensity of the i-th source

CARD S2B (*) (Omit if IS>0)
(SB(I), I=1, IS) relative biased intensity of the i-th source
Source particles are generated by intensities SB(I), and their weights are adjusted by multiplying factors S(I)/SB(I).

Repeat CARDs S3 ~ S15 for IS sources.

CARD S3 (*)
1) NSORCE geometry and spatial distribution of source
The parameter NSORCE is also used to specify the *D-T* neutron source. Parameters X0, Y0, Z0, XL, XR, YL, YR, ZL, ZR are entered by CARDs S4 and S5.
= 1, point source at (X0, Y0, Z0)
= 2, rectangular parallelpiped (RPP) source, distributed uniformly in the RRP (XL<x<XR, YL<y<YR, ZL<z<ZR)
= 3, rectangular parallelpiped (RPP) source, with cosine distribution
The distribution function in x-direction is expressed as follows:

$$P(\chi)=\frac{1}{2}\cos\{\pi(\frac{\chi-XL}{XR-XL}-\frac{1}{2})\} \quad (XL<\chi<XR)$$

Distribution functions for y-and z-directions are defined in the same manner.

= 4, cylindrical source, with uniform distribution
The cylinder axis is parallel to z-axis. The center of the bottom is located at (X0, Y 0, ZL). The radius is XR, and ZL $<$ z $<$ ZR.

= 5, cylindrical source, with uniform in radial direction but cosine distribution in axial direction
The geometrical parameters are same as those of option 4.

= 6, sphere or spherical shell source, with uniform distribution
The center of the sphere is located at (X0, Y0, Z0). Parameters XL and XR are inner and outer radius, respectively.

= 7, circular plane source, with uniform distribution
The plane is perpendicular to z-axis. The center of the circular plane is located at (X0, Y0, Z0), and the radius is XL.

= 8, cylindrical shell source, with uniform distribution
The center of the bottom is located at (Z0, Y0, ZL). Parameters XL and XR are inner and outer radius, respectively. The z-coordinate value is between ZL and ZR.

= 9, D-T neutron source by accelerated d^+ beam
Source neutrons are generated on the circular plane of radius XR and center (X0, Y0, Z0) perpendicular to z-axis. The radial distribution is the chopped Gaussian with the peak at the center. When this option is selected, energy and angular distributions are determined by the reaction kinematics. Accordingly, the other parameters, NEMIS, NSPEC, ETOP and EBOT become meaningless. Note that this sourcle option cannot be used with point estimators (see Section 6.1.3).

2) NEMIS angular distribution of source particles

= 1, mono-directional

= 2, isotropic

= 3, cosine distribution against z-direction
$>$ 0, positive direction only
$<$ 0, negative direction only
i.e.

$$\mathrm{P}(\cos\theta)=\begin{cases} 2\cos\theta & (0\leqq\theta\leqq\pi/2) \quad (\mathrm{NEMIS}=3), \\ -2\cos\theta & (\pi/2\leqq\theta\leqq\pi) \quad (\mathrm{NEMIS}=-3), \end{cases}$$

where θ is the polar angle to z-axis.

= 4, arbitrary emission

= 5, cosine distribution against radial direction
$>$ 0, outward only
$<$ 0, inward only
This option can be used with NSORCE=6.

3) NSPEC source energy spectrum (effective only if ISOUR$\leqq$0)

= 0, arbitrary spectrum defined by CARDs E1 and E2

= 1, Watt's fission spectrum

= 2, arbitrary energy-pointwise spectrum per unit energy given by CARDs S7 and S8
Interpolation between input energies is linear-linear.

= −2, arbitrary energy-pointwise spectrum per unit lethargy given by CARDs S7 and S8
Interpolation between input energies is log-log.

= 3, mono-energy (energy defined in CARDs S7 and S8)

4) ETOP lower limit of energy when NSPEC=1

5) EBOT upper limit of energy when NSPEC=1

6) JDIREC rotation of direction and spatial coordinates of source particles

= 1, no rotation

= 2, permutation of x, y and z coordinate values:
x→y, y→z, z→x

= 3, permutation of x, y and z coordinate values:
x→z, y→x, z→y

= 4, arbitrary rotation of direction
See CARD S15.

= 5, arbitrary rotation of direction and position
The rotation of a position vector is performed around the origin. See CARD S15.

CARD S4 (*)

1)~3) X0, Y0, Z0 geometrical input of source (I)
See the description of NSORCE in CARD S3 and Table 6.2.

CARD S5 (*)

1)~6) XL, XR, YL, YR, ZL, ZR geometrical input of source (II)
See the description of NSORCE in CARD S3 and **Table 6.2**.

Table 6.2 Geometry Input for Source

NSORCE	X0	Y0	Z0	XL	XR	YL	YR	ZL	ZR
1	X0	Y0	Z0	–	–	–	–	–	–
2	–	–	–	XL	XR	YL	YR	ZL	ZR
3	–	–	–	XL	XR	YL	YR	ZL	ZR
4	X0	Y0	–	–	XR	–	–	ZL	ZR
5	X0	Y0	–	–	XR	–	–	ZL	ZR
6	X0	Y0	Z0	XL	XR	–	–	–	–
7	X0	Y0	Z0	XL	–	–	–	–	–
8	X0	Y0	–	XL	XR	–	–	ZL	ZR
9	X0	Y0	Z0	–	XR	–	–	–	–

CARD S6 (*) (Enter if NEMIS=1)

1)~3) UINP, VINP, WINP direction cosine

CARD S7 (*) (Enter if | NSPEC | ≧2 and ISOUR≦0)

IMAX1 number of energy points defining the energy spectrum
The parameter IMAX1 should be ≧2 if | NSPEC | =2.

CARD S8 (*) (Enter if | NSPEC | ≧2 and ISOUR≦0)

1)~2) (E(I), FE(I)) source spectrum
Unit for FE(I) is per unit lethargy or per unit energy when NSPEC on CARD S3 is -2 or 2, respectively. When NSPEC=3 (mono-energy), E(IMAX1) is the energy of source particles, and FE(I) is meaningless.

Enter IMAX1 lines for S8.

CARD S9 (*) (Omit if NEMIS $\neq$ 4)

1) IMAX number of energy boundaries to define angular distribution (IMAX $\leq$ 101)
The angular distributions are defined for (IMAX−1) energy intervals.

2) JMAX number of polar angle meshes (| JMAX | $\leq$20)
If JMAX<0, distribution for polar angle is biased.
If | IS | =1, maximum JMAX allowed is 200.

3) KMAX number of azimuthal angle meshes (KMAX $\leq$ 20)

CARD S10 (*) (Enter if NEMIS=4)

(ENG(I), I=1, IMAX) upper energy boundary for the I-th angular distribution

CARD S11 (*) (Enter if NEMIS=4)

(DEG(I), I=1, | JMAX |) cosine bins of polar angles (angles to z-axis) to difine angular distribution
These data should be entered in decreasing order.

CARD S12 (*) (Enter if NEMIS=4)

(ANGDIS(I,J), J=1, | JMAX | −1) angular distribution for polar angle bins defined on CARD S11.
The polar angle of source particle generated within the I-th energy interval is determined from this probability. The probability is normalized such that

$$\sum_{j=1}^{JMAX-1} ANGDIS(I,j)=1.0 \quad \text{for each I.}$$

IMAX−1 sets of CARD S12 are required. See the description for CARD S12B.

CARD S12B (*) (Enter if NEMIS=4 and JMAX<0)

(ANGBS(I,J), J=1, JMAX | −1) biased probability for ANGDIS
Normalization is performed similarly to ANGDIS.

NOTE: If both CARD S12 and CARD S12B are necessary, enter IMAX−1 sets of pairs of CARD S12 and CARD S12B in the following order:

$$S12_1, S12B_1, S12_2, S12B_2, \cdots S12_{IMAX-1}, S12B_{IMAX-1}.$$

CARD S13 (*) (Enter if NEMIS=4 and KMAX>0)

(FAI(I), I=1, KMAX) azimuthal angle bins to define azimuthal probability (in degree unit)
These angles are measured in a counter-clockwise manner from x-axis, z-axis being the polar.

CARD S14 (*) (Enter if NEMIS=4 and KMAX>0)

(FAIDIS(I), I=1, KMAX-1) azimuthal distribution
The probabililty is normalized such that

$$\sum_{i=1}^{KMAX-1} FAIDIS(i)=1.0.$$

This probability is used for all energy groups.

CARD S15 (*)1 (Enter if JDIREC > 3)

θ,φ,ϕ rotation angles for flight direction and spatial coordinates (in degree unit)
Angles θ, φ and ϕ are shown in **Fig. 6.2**. The geometry of the present problem is described in the (X,Y,Z) coordinate system, and a flight direction of particle is also presented in this coordinate system. As a result of the rotation by the angles, θ, φ and ϕ, flight direction and spatial coordinates of source particle are sampled in the (X', Y', Z') coordinate system by using the angular distribution and the source cell geometry data given by CARDS S1 ~ S14. See Section 6.1.3(4) for a detailed description.

6.2.2 Additional Input for MORSE-DSG

The MORSE-DSGl code requires input data on CARD B' in addition to those for MORSE-DD. The CARD B' data are read just after CARD B.

CARD B' (*)

1) IDDX calculation mode
   = 1, preparation of banded macroscopic DDX data subsets
   = 2, Monte Carlo calculation using banded macroscopic DDX already prepared
   = 3, continuous run of 1 and 2

NOTE: Input for IDDX on CARD XB is meaningless in MORSE-DSG.

2) NSCT¥ number of DDX angle bins
   This parameterl should be the same as NSCT on CARD XB.

3) NELEM¥ number of elements
   This parameter should be the same as NELEM on CARD XB.

4) NMIX¥ number of mixing operations
   This parameter should be the same as NMIX on CARD XB.

5) NPXS size of permanent cross section storage in word

6.3 Job Control Instruction

6.3.1 Job Control Statements

A sample of job control statements for FACOM-M series computer of JAERI is shown in **Fig. 6.3** and **6.4** for MORSE-DD and MORSE-DSG, respectively. Executive load modules of MORSE-DD and MORSE-DSG have been prepared in JAERI with member names of DD and DSG in the file J3803.MORSEDD.LOAD, respectively. The size of blank common in these load modulels is 70 k words, and a user should repalce the main routine by user's one having an appropriate size of blank common. The main routine is as follows:

```
C* * * *   MAIN ROUTINE FOR MORSE-DD AND MORSE=DSG  * * * * * * * *
C* * * *   NC  : BLANK COMMON(xxxxx=70000 in the present load module)
C* * * *   VREG : REGION VOLUME(yyy=300 in the present load module)
C* * * *
          REAL * 8 VREG
          COMMON NC(xxxxx)
          COMMON /TLE2/ VREG(yyy)
          COMMON /APOLLO/ AGSTRT,DDF,DEADWT(26),ITOUT,ITIN
          DATA JUNK/Z48484848/
          NLFT = xxxxx
          DO 5 I=1, NLFT
```

```
      5 NC(I) = JUNK
        ITOUT = 6
        ITIN = 5
        CALL MORSE(NLFT)
        STOP
        END
```

```
//JCLG  JOB
// EXEC JCLG
//SYSIN DD DATA,DLM='++'
// JUSER XXXXXXXX,TA.MORI,0431.100
   T.7 C.5 W.3 I.5
 OPTP MSGCLASS=R,PASSWORD=XX
//*********************************************
//****  J3803.MORSECG.CNTL(BENCH3)  *************
//*********************************************
// EXEC FORT77,SO='J3803.MORSEUP',Q='.FORT',
//      A='ELM(MAIN90)'
// EXEC LKEDIT77,LM='J3803.MORSEDD',CNTL=NO
 INCLUDE OLDLM(DD)
 ENTRY MAIN
 NAME TEMPNAME
// EXEC ANY
// EXEC GO
//* --- DDX LIBRARY ------------------------------------------------
//FT99F001 DD DSN=J3803.DDXLIB3.DATA,DISP=SHR,LABEL=(,,,IN)
//*
//* --- SCRATCH FILE FOR DDX PROCESSING ----------------------------
//FT98F001 DD SPACE=(TRK,(100,40)),UNIT=WK10,DISP=(NEW,PASS),
//  DCB=(BLKSIZE=19068,LRECL=4766,RECFM=VBS,BUFNO=2)
//* --- PROCESSED DDX ----------------------------------------------
//FT96F001 DD SPACE=(TRK,(100,40)),UNIT=WK10,DISP=(NEW,PASS),
//  DCB=(BLKSIZE=19068,LRECL=4766,RECFM=VBS,BUFNO=2)
//*
//* ----- TALLY FILE -----------------------------------------------
//FT95F001 DD DSN=J3803.MORSE2.BNC3LIB3.DATA,DISP=(NEW,CATLG,CATLG),
//  DCB=BLKSIZE=23476,SPACE=(TRK,(2,1)),UNIT=D0430
//*
//* --- PROCESSED ENERGY TRANSFER MATRIX ( IXTAPE ) ----------------
//FT20F001 DD SPACE=(TRK,(30,30)),UNIT=WK10,DISP=(NEW,PASS),
//  DCB=(BLKSIZE=19068,LRECL=4766,RECFM=VBS,BUFNO=2)
//* --- PROCESSED PL LIBRARY ( JXTAPE ) ----------------------------
//FT21F001 DD SPACE=(TRK,(30,30)),UNIT=WK10,DISP=(NEW,PASS),
//  DCB=(BLKSIZE=19068,LRECL=4766,RECFM=VBS)
//*
//* --- SCRATCH FILE FOR CG GEOMETRY PACKAGE -----------------------
//FT16F001 DD SPACE=(TRK,(5,5)),UNIT=WK10,DISP=(NEW,PASS),
//  DCB=(BLKSIZE=19068,LRECL=4766,RECFM=VBS)
//*
//* ----- RESTART IN ( NTAPE ) -------------------------------------
//FT08F001 DD DSN=J3803.BENCH3.REST.DATA,DISP=SHR
//*
//* ----- RESTART OUT ( NTAPE + 1 ) --------------------------------
//FT09F001 DD DSN=J3803.BENCH3.REST.DATA,DISP=SHR
//*
//SYSIN DD DSN=J3803.MORSECG.DATA(BENCH3TR),DISP=SHR
++
//
```

Fig. 6.3 Job control statements for MORSE–DD.

```
//JCLG JOB
//JCLG EXEC JCLG
//SYSIN DD DATA,DLM='++'
// JUSER XXXXXXXX,TA.MORI,0431.01
   T.10 W.3 I.7 C.7 NGT
 OPTP PASSWORD=XX,MSGCLASS=R
//************     'J3803.DDX2.CNTL(DSG)'      **********************
// EXEC FORT77
C---------------- ISIZEZ = BLANK COMMON SIZE -----------
      PARAMETER ( ISIZEZ =1600000 )
C-------------------------------------------------------
      COMMON NC(ISIZEZ)
      COMMON /APOLLO/ AGSTRT,DDF,DEADWT(26),ITOUT,ITIN
      DATA JUNK/Z48484848/
      NLFT  = ISIZEZ
      DO 5 I=1,NLFT
      NC(I) = JUNK
    5 CONTINUE
      ITOUT = 6
      ITIN  = 5
      CALL MORSE(NLFT)
      STOP
      END
/*
//FORT77.SYSPRINT DD DUMMY
// EXEC LKEDIT77,LM='J3803.MORSEDD',CNTL=NO
 INCLUDE OLDLM(DSG)
 ENTRY MAIN
 NAME TEMPNAME(R)
// EXEC ANY
// EXEC GO
//* ------ FT65-FT68 : CHECK WRITE ---------------------------------
//FT65F001  DD DUMMY
//FT66F001  DD DUMMY
//FT67F001  DD DUMMY
//FT68F001  DD DUMMY
//*
//* ------ FT16 : SCRATCH  -----------------------------------------
//FT16F001 DD SPACE=(TRK,(50,30)),UNIT=WK10,DISP=(NEW,DELETE),
//    DCB=(BLKSIZE=19068,LRECL=4766,RECFM=VBS,BUFNO=2)
//*
//* ------ FT71 : WEIGHT AND PATH DATASET --------------------------
//FT70F001 DD DISP=(NEW,PASS),UNIT=WK10,
//    DCB=(RECFM=F,LRECL=16000,BLKSIZE=16000,DSORG=DA,BUFNO=1),
//    SPACE=(16000,(35))
//*
//* ------ FT72 : SCATTERING COUNTER DATASET -----------------------
//FT71F001 DD DISP=(NEW,PASS),UNIT=WK10,
//    DCB=(RECFM=F,LRECL=16000,BLKSIZE=16000,DSORG=DA,BUFNO=1),
//    SPACE=(16000,(76))
//*
//* ------ PROCESSED DDX ( IXTAPE ) --------------------------------
//FT20F001 DD SPACE=(TRK,(50,30)),
//    UNIT=WK10,DISP=(NEW,DELETE),
//    DCB=(BLKSIZE=19068,LRECL=4766,RECFM=VBS,BUFNO=2)
//*
//* ------ FT98 : SCRATCH FOR ELEMENT DATA -------------------------
//FT98F001 DD SPACE=(TRK,(500,100)),UNIT=WK10,DISP=(NEW,DELETE),
//    DCB=(BLKSIZE=19068,LRECL=4766,RECFM=VBS,BUFNO=2)
//*
//* ------ FT96 : BAND MACRO CROSS SECTION -------------------------
//FT96F001 DD DSN=J3803.XP2BES.DATA,DISP=SHR,
//    DCB=(RECFM=F,LRECL=16000,BLKSIZE=16000,DSORG=DA,BUFNO=1),
//    SPACE=(16000,(560)),UNIT=D0430
//*
//* ------ FT99 : DDX LIBRARY --------------------------------------
//FT99F001 DD DSN=J3803.DDXLIB3.DATA,DISP=SHR,LABEL=(,,,IN)
//*
//* ------ FT08,FT09 : RESTART IN/OUT DATASET (NTAPE,NATAPE+1) -----
//FT08F001 DD DSN=J3803.RESTA2.DATA,DISP=SHR
//FT09F001 DD DSN=J3803.RESTA2.DATA,DISP=SHR
//*
//* ------ FT95 : TALLY FILE ---------------------------------------
//FT95F001 DD DSN=J3803.PLOT.SAMPLE.DATA,DISP=(NEW,CATLG,CATLG),
//  UNIT=TSSWK2,SPACE=(TRK,(40,20))
//*
//* ------ MORSE INPUT CARD DATA -----------------------------------
//SYSIN DD DSN=J2350.FNS.DATA(P2BE5),DISP=SHR,LABEL=(,,,IN)
++
//
```

Fig. 6.4 Job control statements for MORSE-DSG.

6.3.2 I/O File Requirements

Files of I/O required by MORSE-DD and MORSE-DSG are summarized in **Tables 6.3** and **6.4**, respectively. Files on the I/O units 70, 71 and 96 for MORSE-DSG are direct access ones. The others are sequential ones. The record length of three direct access files is fixed to be 16000 bytes (4000 words). The format of DDX library and details of output files are described in this section. A P_l library which MORSE-DD can read is the material-organized one shown as IANISN=0 type in Section 4.3.2.

Table 6.3 MORSE-DD file requirement

I/O unit	Remarks	I/O*	
		DDX mode	P_l mode
99	DDX library	I	X
98	Scratch file for cross sections	I/O	X
96	Processed cross section in DDX mode	I/O	X
95	Output of tally data	O	O
16	Scratch file for CG geometry package	I/O	I/O
IXTAPE	P_l library	I/O	I
	Scratch file for cross section in DDX		
JXTAPE	Processed cross section in P_l mode	X	I/O
NTAPE	Restart data from the previous run	I	I
NTAPE+1	Restart dump for the following job	O	O
	This is overwritten every 10 batches		
6	Output of final results	O	O
5	Card-image input data for MORSE-DD	I	I

*X : unnecessary file.
I : read-only file.
O : write-only file.

Table 6.4 MORSE-DSG file requirement

I/O unit	Remarks	I/O* DDX mode
99	DDX library	I
98	Scratch file for cross sections	I/O
96	Processed cross section in DDX mode	I/O
	DCB=(RECFM=F, DSORG=DA)	
95	Output of tally data	O
71	Scratch file for banded counter data	I/O
	DCB=(RECFM=F, DSORG=DA)	
70	Scratch file for weight standard data	I/O
	DCB=(RECFM=F, DSORG=DA)	
16	Scratch file for CG geometry package	I/O
IXTAPE	Scratch file for cross section in DDX	I/O
NTAPE	Restart data from the previous run	I
NTAPE+1	Restart dump for the following job	O
	This is overwritten every 10 batches	
6	Output of final results	O
5	Card-image input data for MORSE-DD	I

* I and O mean read-only and write-only files, respectively.

(1) DDX-Library (I/O Unit 99)

A binary file is read by MORSE-DD and MORSE-DSG. The format is given in Section 3.6.3.

(2) Processed Cross Sections (I/O Unit 96)

MORSE-DD

$m=1$, Media

  $g=1$, Group

    1) $\Sigma_{pr,g}$, $\Sigma_{f,g}$, $\Sigma_{c,g}$, $\nu\Sigma_{f,g}$, $\Sigma_{t,g}$, $(\Sigma_s(g\rightarrow g'),g'=1,\mathrm{INGP})$

    2) $((P(k;\ g\rightarrow g'),k=1,\mathrm{NSCT}),g'=1,\mathrm{INGP})$,

    where $P(k;\ g\rightarrow g')=-\int_1^{\mu_-} I(\mu,g\rightarrow g')$.

MORSE-DSG

In MORSE-DSG, this file is a direct access one with a fixed record length. The file structure is as follows:

1) Control data

$m=1$, Media

2) Non-banded cross section data

  $n=1$, Band

  3) Cross section data subset of each band

The control data contain the following values.

MXBAND	: maximum number of band set to be 20
MXMEDA	: maximum number of media set to be 20
IEBAND (4,21)	: starting group, the numbers of groups and scattering matrix elements of one media for each band, and the number of groups above the band
ITBAND	: number of bands
IMXRBD	: band number containing the largest data
IMXRSZ	: data size of IMXRBD-th band = IEBAND(3,IMXRBD)
ITGRUP	: total number of energy group = NMGP
IMXGBD	: band number consisting of the largest energy groups
IMXGSZ	: number of groups in the IMXGBD-th band
ISIZE3	: common size for scattering matrix of one media
ISIZE4	: the largest size of scattering matrix of one media = NMGP × (NMGP+1)/2
NMTG¥	: = NMTG
NSCT¥	: = NSCT
MEDIA¥	: = MEDIA
NELEM¥	: = NELEM
NMIX¥	: = NMIX
NPXS	: common size allowed for permanent cross section
NPXS¥	: used size for permanent cross section storage
IMIND(20)	: starting record number for each media
IBIND(20)	: starting record number for each band in media data; starting record of band i and media j = IMIND(j) + IBIND(i) − 1
M(3 * NMIX)	: list of mixing table
INGS(NGP)	: index to $\Sigma_{g,g'}$ (primary)
INSG(NGG)	: index to $\Sigma_{g,g'}$ (secondary)
IDL(NELEM)	: list of element I.D. numbers

INNN(NGP) : number of down scatters for each primary group
IGGG(NGG) : number of down scatters for each secondary group
IBTTBL(20) : total data size in each band

The non-banded data for each medium consist of

$(\Sigma_{t,g}, g=1,\text{INGP}), (\Sigma_{s,g}, g=1,\text{INGP}), (\Sigma_{s,g}/\Sigma_{t,g}, g=1,\text{INGP})$, and $(\nu\Sigma_{f,g}/\Sigma_{t,g}, g=1,\text{INGP})$.

The banded data for band i consist of

$((\Sigma_s(g\rightarrow g'), g'=g, g+\text{NDS}(g)-1, g=\text{IH,IL})$, and

$(((P(k;\ g\rightarrow g')^*, k=1,\text{NSCT}), g'=g, g+\text{NDS}(g)-1), g=\text{IH,IL})$,

where NDS(g) is the number of slowing down from group g, and

IH = IEBAND(1,i),

IL = IEBAND(1,i) + IEBAND(2,i) − 1.

(3) Group Transfer Matrices (I/O Unit IXTAPE)

DDX mode

- l =1, Element
  - 1) MATNO, MATNO, K, MATNO, (TITLE(i), i=1,12)
  - 2) $((\sigma(i,j), i=1,\text{ITBL}), j=1,\text{INGP})$

The microscopic cross section $\sigma(i, j)$ is the same as P_0 component of P_l cross sections. In a DDX mode run, these matrices are calculated from the DDX data, and are used only to obtain the maximum slowing down group.

P_l mode

In this case, this file is an input file of cross sections.

- l =1, Element
  - n =1, NCOEF (P_l order + 1)
    - 1) MATNO, MATNO, K, MATNO, (TITLE(i), i=1,12)
    - 2) $((\sigma(i,j), i=1,\text{ITBL}), j=1,\text{NMTG})$

(4) Tallies (I/O Unit 95)

1) (E(g), g=1, NE+1) : energy boundaries

- k =1, Detector
  - 2) ((F(g),DF(g)), g=1,NE) : total flux and fractional standard deviation (1σ)
  - 3) (A(m), m=1,NA+1) (if NA>0) : boundaries of angle bins
- k =1, Detector
  - 4) (((FA(m,g),ΔFA(m,g), m=1,NA), g=1,NE) (if NA<0): angular flux and fractional standard deviation (1σ)
- k =1, Detector
  - 5) ((UF(g),ΔUF(g)), g=1,NE) (if INCF=1): uncollided total flux and fractional standard deviation (1σ)
- k =1, Detector
  - 6) (((UFA(m,g),ΔUFA(m,g), m=1,NA), g=1,NE) (if INCF=1 and NA<0): uncollided angular flux and fractional standard deviation (1σ)

(5) Restart Data File (I/O Unit NTAPE+1)

1) RANDOM : next random number
2) NBATS, NSTRT : number of batches already calculated and number of particles per batch
3) LL, LLL, (A(i), i=LL,LLL) : data in blank common which are tally arrays of the sums over all batches and the sums squared batch estimates (LL=LOCUD+1 and LLL=LMAX)

4) LL, LLL, (A(i), i=LL,LLL) (if MFISTP>0 and NSOUR<0) :
data in blank common which are fission bank arrays
(LL=NFISBN+1 and LLL=NFISBN+ 7*NMOST)

5) NITSK, ITCUT, FNK, FKSUM, VARK, FNKFW, FWFW, NFISH, FTOTL, FWATE, WATEF, WFSUM (if NFISTP>0) :
parameters of fission neutron generation and estimator of k_{eff}

6) LL, LLL, (A(i), i=LL,LLL) (if MFISTP>0 and NORMF>0) :
data in blank common which are weights assigned to fission neutrons
(LL=LOCFWL+1 and LLL=LOCFWL+ MXREG)

7) LL, LLL, (A(i), i=LL,LLL) (if MFISTP>0, NORMF>0 and NKCALC<0)
data in blank common which are current weight standard
(LL=LOCWTS+1 and LLL=LOCWTS+ 3*NGPREG)

The restart data file described here is generated by MORSE-DD. That for MORSE-DSG is similar, but it does not contain records 4) to 7) since a fission problem is not solved by MORSE-DSG.

6.3.3 Memory Requirements

The memory storage requirement in bytes by MORSE-DD and MORSE-DSG is the order of 780,000+4×(blank common size in words). The size of the blank common used in cross section processing is different between the P_l and the DDX modes. It is also different between MORSE-DD and MORSE-DSG.

The blank common size required for processing DDX in MORSE-DD is given by

$$\text{Memory}=3\times\text{NMIX}+2\times(\text{NGP}+\text{NGG})+\text{NELEM}$$
$$+\text{Maximum}\begin{cases}\text{INGP}\times(\text{NDS}+\text{NDSG})+\text{INGP}\times\text{INGP}+5\times\text{NGP}+\text{INGP}\times\text{INGP}\times(\text{NSCT}+1).\\ 2\times(\text{NSCT}\times\text{NGP}\times\text{NGP}+5\times\text{NGP}).\\ [6\times\text{NGP}+(\text{NSCT}+1)\times\text{NDSNGP}]\times\text{NMED}+\text{NGP}\times\text{NSCT}+\text{NGP}+5.\end{cases}$$

When the processed cross sections have been prepared on the I/O units 96 and IXTAPE, MORSE-DD requires only

$$\text{Memory}=3\times\text{NMIX}+2\times(\text{NGP}+\text{NGG})+\text{NELEM}$$
$$+\ [6\times\text{NGP}+(\text{NSCT}+1)\times\text{NDSNGP}]\ \times\text{NMED}$$

for the permanent cross section storage.

In MORSE-DSG, the blank common size for permanent cross section storage is determined so that it may be less than an input value NPXS. If IDDX≠2, however, a work area M_{work} is required for cross section processing with the following size:

$$M_{work}=\text{Maximum}\begin{cases}\text{INGP}\times(\text{NDS}+\text{NDSG})+\text{INGP}\times\text{INGP}+5\times\text{NGP}+\text{INGP}\times\text{INGP}\times(\text{NTCT}+1).\\ (\text{NSCT}\times\text{NGP}\times(\text{NGP}+\text{IMXGSZ})+10\times\text{NGP}+\text{NGP}\times\text{IMXGSZ}).\end{cases}$$

Accordingly, the blank common size required in this case is

$$\text{Memory}=\text{maximum}\begin{cases}\text{NPXS}.\\ 3\times\text{NMIX}+2\times(\text{NGP}+\text{NGG})+\text{NELEM}+M_{work}.\end{cases}$$

In addition to cross section storage, blank common areas for sampling parameters, splitting, Russian roulette and scattering counters are reduced from 7×MGPREG+8×(NGPREG+8×NMTG×MXREG in MORSE-DD to 12×NXREG×IMXGSZ in MORSE-DSG.

6.4 Sample Problem and Input Data

Input data for MORSE-DD to solve the sample problem 2 described in Section 5.4 are shown in **Fig. 6.5**. The brief description and parameters are as follows:

```
JAERI-US BENCHMARK PROBLEM 3  LI2O SLAB  (DDL/J3P1)
2000  4000 100 1 125    0 125 125 0 0  18.0  2 0   / B
   -1  70  0 , , 1.0  1.0E-5  0. 0. 2200.        / C
    0.  0.  0.  0.  0.  0.  0.                    / D
 9.6290-3 9.6290-3 9.6290-3 9.6290-3 1.3230-1 1.3230-1 1.3230-1
 1.3230-1 6.9960-2 6.9960-2 6.9960-2 6.9960-2 7.2890-3 7.2890-3
 7.2890-3 7.2890-3 1.3580-3 1.3580-3 1.3580-3 1.3580-3 5.4600-4
 5.4600-4 5.4600-4 5.4600-4 3.3980-4 3.3980-4 3.3980-4 3.3980-4
 3.0890-4 3.0890-4 3.0890-4 3.0890-4 1.1070-3 1.1358-3 1.0484-3
 9.8789-4 1.0282-3 1.1466-3 1.2462-3 1.3172-3 1.5086-3 1.6357-3
 1.7890-3 1.9299-3 2.0846-3 2.1684-3 2.1959-3 2.3012-3 2.5051-3
 4.6303-3 7.6168-3 4.9592-3 3.4095-3 2.8088-3 2.8308-3 2.8955-3
 2.9859-3 2.9866-3 3.0687-3 3.0561-3 5.9949-3 5.8960-3 5.8291-3
 5.6769-3 5.1135-3 4.5217-3 3.9068-3 3.3709-3 2.5389-3 1.6556-3 / E1
 1.649E+07 1.623E+07 1.598E+07 1.573E+07 1.549E+07 1.525E+07 1.501E+07
 1.478E+07 1.455E+07 1.432E+07 1.410E+07 1.388E+07 1.367E+07 1.346E+07
 1.325E+07 1.304E+07 1.284E+07 1.264E+07 1.245E+07 1.225E+07 1.206E+07
 1.188E+07 1.169E+07 1.151E+07 1.133E+07 1.116E+07 1.098E+07 1.081E+07
 1.065E+07 1.048E+07 1.032E+07 1.016E+07 1.000E+07 9.394E+06 8.825E+06
 8.290E+06 7.788E+06 7.316E+06 6.873E+06 6.456E+06 6.065E+06 5.698E+06
 5.353E+06 5.028E+06 4.724E+06 4.437E+06 4.169E+06 3.916E+06 3.679E+06
 3.456E+06 3.247E+06 3.050E+06 2.865E+06 2.691E+06 2.528E+06 2.375E+06
 2.231E+06 2.096E+06 1.969E+06 1.850E+06 1.738E+06 1.534E+06 1.353E+06
 1.194E+06 1.054E+06 9.301E+05 8.208E+05 7.244E+05 6.393E+05 5.642E+05
 4.979E+05 4.394E+05 3.877E+05 3.422E+05 3.020E+05 2.665E+05 2.352E+05
 2.075E+05 1.832E+05 1.616E+05 1.426E+05 1.259E+05 1.111E+05 9.804E+04
 8.652E+04 7.635E+04 6.738E+04 5.946E+04 5.247E+04 4.631E+04 4.087E+04
 3.607E+04 3.183E+04 2.809E+04 2.479E+04 2.187E+04 1.930E+04 1.503E+04
 1.171E+04 9.119E+03 7.102E+03 5.531E+03 4.307E+03 3.355E+03 2.613E+03
 2.035E+03 1.585E+03 1.234E+03 9.611E+02 5.829E+02 3.536E+02 2.144E+02
 1.301E+02 7.889E+01 4.785E+01 2.902E+01 1.760E+01 1.068E+01 6.476E+00
 3.928E+00 2.382E+00 1.445E+00 8.764E-01 5.316E-01 3.224E-01  / F
001234567123          /  H
 -1 1 0 0 0 16 125    /  I
  1  1  125  1  1 16       1.0      0.0     1.0  0.0 / J
  1  1  125  1  1  1        8.0    1.3-2   2.6-2  0.0 / J
  1  1  125  2  1  2        8.0    1.3-2   2.6-1  0.0 / J
  1  1  125  3  1  3       30.0    3.3-3   6.6-3  0.0 / J
  1  1  125  4  1  4       80.0    1.3-3   2.6-3  0.0 / J
  1  1  125  5  1  5      216.0    4.6-4   9.2-4  0.0 / J
  1  1  125  6  1  6      582.0    1.7-4   3.4-4  0.0 / J
  1  1  125  7  1  7     2563.0    3.8-5   7.6-5  0.0 / J
  1  1  125  8  1  8        0.5    2.0-1   4.0-1  0.0 / J
  1  1  125  9  1  9        0.4    2.5-1   5.0-1  0.0 / J
  1  1  125 10  1 10        1.5    6.6-2   1.2-1  0.0 / J
  1  1  125 11  1 11        4.0    2.5-2   5.0-2  0.0 / J
  1  1  125 12  1 12       11.0    9.0-3   1.8-2  0.0 / J
  1  1  125 13  1 13       29.0    3.4-3   6.8-3  0.0 / J
  1  1  125 14  1 14      128.0    7.8-4   1.5-5  0.0 / J
110  1  125  1  1  1        8.0    1.3-6   2.6-6  0.0 / J
110  1  125  2  1  2        8.0    1.3-6   2.6-6  0.0 / J
100  1  125  3  1  3       30.0    3.3-7   6.6-7  0.0 / J
100  1  125  4  1  4       80.0    1.3-7   2.6-7  0.0 / J
 90  1  125  5  1  5      216.0    4.6-8   9.2-8  0.0 / J
 90  1  125  6  1  6      582.0    1.7-8   3.4-8  0.0 / J
 90  1  125  7  1  7     2563.0    3.9-9   9.8-9  0.0 / J
110  1  125  8  1  8        0.5    2.0-5   4.0-5  0.0 / J
110  1  125  9  1  9        0.4    2.5-5   5.0-5  0.0 / J
100  1  125 10  1 10        1.5    6.6-6   1.3-5  0.0 / J
100  1  125 11  1 11        4.0    2.5-6   5.0-6  0.0 / J
 90  1  125 12  1 12       11.0    9.0-7   1.8-6  0.0 / J
 90  1  125 13  1 13       29.0    3.4-7   6.8-7  0.0 / J
 90  1  125 14  1 14      128.0    7.8-8   1.5-7  0.0 / J
 -1                                                / J
    0     0     0     0    /  L
    3     0          LI2O SLAB
  RCC     1       0.0          0.0      20.       0.00      0.0       60.
                   5.
  RCC     2       0.0          0.0      20.       0.00      0.0        4.
                  30.
  RCC     3       0.0          0.0      24.       0.00      0.0       11.
                  30.
  RCC     4       0.0          0.0      35.       0.00      0.0       10.
                  30.
  RCC     5       0.0          0.0      45.       0.00      0.0       10.
                  30.
  RCC     6       0.0          0.0      55.       0.00      0.0       10.
                  30.
  RCC     7       0.0          0.0      65.       0.00      0.0       10.
                  30.
  RCC     8       0.0          0.0      75.       0.00      0.0        5.
                  30.
  RCC     9       0.0          0.0      20.       0.00      0.0       60.
                  30.
  RCC    10       0.0          0.0     -10.       0.00      0.0      105.
                  40.
  END
```

Fig. 6.5 Sample input for MORSE–DD.

```
  1          +1      +2
  2          +1      +3
  3          +1      +4
  4          +1      +5
  5          +1      +6
  6          +1      +7
  7          +1      +8
  8          -1      +2
  9          -1      +3
 10          -1      +4
 11          -1      +5
 12          -1      +6
 13          -1      +7
 14          -1      +8
 15          -9     +10
 16         -10
 END
1 2 3 4 5 6 7 8 9 10 11 12 13 14 15 16  / CGD  REGION #
                                        / CGE  MATERIAL #
14*1  2  0                                                    392.7 10996. 30238. 27489.
314.16 863.94 785.4  785.4  785.4  785.4                      / CGF  VOLUME
27489. 27489. 27489. 13775.  1.0    1.0
     XSEC OF LI6,LI7,O16,SUS,JENDL/3PR1,DDX20
125 125 0 0 125     128 4 2 7 8     1 20 0 1                  / XB
 0  -1  0  0  0  0 0 20  0  0  0                              / XC
 0.9 0.8 0.7 0.6 0.5 0.4 0.3 0.2 0.1 0.0 -0.1 -0.2 -0.3 -0.4 -0.5
                                                            / XC' DDX COSINES
-0.6 -0.7 -0.8 -0.9 -1.0                                    / XD
-0306 -0307 -0816 -2600 -2800 -2400 -1197                   / XE  XSEC'S OF
 306   941.103   0.73493   940.368   0.0   0.0              / XE THE LAST GROUP
 307    1.0154    0.970     0.0454   0.0   0.0              / XE
 816   3.74979   3.7496    0.00019   0.0   0.0              / XE
2600     13.91     11.35      2.56   0.0   0.0              / XE
2800     10.68      7.77      2.91   0.0   0.0              / XE
2400      4.68      3.14      1.54   0.0   0.0              / XE
1197      2.90      2.54      0.36   0.0   0.0              / XE
   1   1 4.1500E-3   / XF
   1   2 5.1900E-2   / XF
   1   3 2.8000E-2   / XF
   1   4 1.2600E-3   / XF
   1   5 1.5300E-4   / XF
   1   6 3.4700E-4   / XF    MIXING OPERATIONS
   1  -7 1.7800E-5   / XF
   2  -3 4.9210E-5   / XF
  POINT ESTIMATOR
15 125 125 0 0   1 5 2 8 0   0 0 -1 , , , /  BB  ( NRUN2 IS 11'TH )
                                        /  BB1
  0  0  0 15  0
     INTEGRATED FLUX
     INTEGRATED FLUX
                                        /  FF  RESPONSE
125*1.0
 /LETHARGY
  1  2  3  4  5  6  7  8  9 10 11 12 13 14 15 16 17 18 19 20
 21 22 23 24 25 26 27 28 29 30 31 32 33 34 35 36 37 38 39 40
 41 42 43 44 45 46 47 48 49 50 51 52 53 54 55 56 57 58 59 60
 61 62 63 64 65 66 67 68 69 70 71 72 73 74 75 76 77 78 79 80
 81 82 83 84 85 86 87 88 89 90 91 92 93 94 95 96 97 98 99 100
101 102 103 104 105 106 107 108 109 110
111 112 113 114 115 116 117 118 119 120
121 122 123 124 125          / HH   LOWER ENERGY GROUPS OF ENERGY BINS
 1       / S1  ========== NEUTRON SOURCE
 1.0     / S2
 1 4 0  17000000. 1000. 1 / S3
 0.0 0.0 0.0    / S4   SOURCE POSITION
 6*0.000        / S5   DUMMY
 2  3  0        / S9   IMAX,JMAX,KMAX
 20000000. 10. / S10  ENERGY
 1.0 .5547 -1. / S11  ANGLE
 1.0    0.     / S12  DISTRIBUTION
```

Fig. 6.5 (Continued)

(1) Geometry : 16 regions (14 regions in Li_2O zone, one void (air) region and an outer void region)
Region boundaries in the Li_2O zone :
Axial boundaries : 20, 24, 35, 45, 55, 65, 75 and 80 cm
Radial boundaries : 0, 5 and 30 cm

(2) Tally : Energy-dependent fluxes and integrated fluxes by track length estimator (15 detectors)
Detector 1 to 7 : Li_2O zones with $r<5$ cm
Detector 8 to 14 : Li_2O zones with $5<r<30$ cm
Detector 15 : void (air) zone
The detector numbers are the same as the region numbers. No detector is specified in an outer void zone.

(3) Variance reduction technique :
The Russian roulette kill and splitting at spatial boundaries based on cell importance and the Russian roulette kill at collision are used. The same cell importance is assigned to all energy groups.

6.5 Auxiliary Codes and Supplementary Subrountines

6.5.1 Supplementary Subroutines

An auxiliary subroutine package MORSEUP is prepared for several different types of calculations by MORSE-DD and MORSE-DSG.

Module BDRYXC

Current through the sphere is estimated by the surface crossing estimator. Card-image input for DBRYXC is the same as that for spherical surface crossing estimator of flux in MORSE-DD.

Module BDRZC

The BDRZC module is the current estimator for the circular plane perpendicular to z-direction. Input is the same as for the flux estimator.

Module DIRECX

Path-length stretching is carried out on the x-component of path. Note that path-length stretching is performed on the radial component of path in the standard MORSE-DD code.

Module DIRECZ

Path-length stretching is carried out on the z-component of path.

6.5.2 ZRECNO

An auxiliary code for MORSE-DSG, ZRECNO, is prepared for a user to get information about the band structure in super-group and the required size of three direct access files. This code is executed in TSS mode. A user should prepare the following TSS command procedure.

```
PROC 0
X ALLOC DA( * ) F(FT05F001)
X ALLOC DA( * ) F(FT06F001)
CALL 'J3803.DDUTY.LOAD(ZRECNO)'
EXIT
```

The sample execution of ZRECNO is as follows:

```
.ZRECNO
MORSE-DD DDX LIBRARY BAND STRUCTURE CALCULATION
<<<< INPUT PARAMETER OF BAND STRUCTURE >>>
    LIMIT OF BAND=======>20 BAND
    LIMIT OF MEDIA=======>20 MEDIA
---->NUMBER OF NEUTRON ENERGY GROUP (NMTG) ?
02000 ?
125
---->NUMBER OF ANGLES (NSCT) ?
02300 ?
20
---->NUMBER OF MEDIA (MEDIA) ?
02500 ?
6
---->NUMBER OF ELEMENT (NELEM) ?
02700 ?
11
---->NUMBER OF MIXING (NMIX) ?
02900 ?
11
---->NUMBER OF REGION (NREG) ?
03100 ?
214
---->SIZE OF PERMANENT CROSS SETION (NPXS) <WORD> ?
03400 ?
280000
---->RECORD LENGTH OF BAND CROSS SECTION FILE (FT96) <WORD> ?
03700 ?
4000
---->RECORD LENGTH OF WEIGHT & PATH BAND FILE (FT70) <WORD> ?
03730 ?
4000
---->RECORD LENGTH OF COUNTER BAND FILE (FT71) <WORD> ?
03760 ?
4000
<<<< PRINT OUT OF RESULT >>>
        ---- BAND STRUCTURE ----
BAND NO.        FIRST E.G.        NUMBER E.G.
      1               1                18
      2              19                22
      3              41                31
      4              72                54
              ---- RECORD NUMBER (CROSS SECTION) ----
MEDIA NO.    MEDIA REC.NO    BAND NO.    BAND REC.NO
      1              2             1              1
      2             47             2             13
```

3	92	3	25
4	137	4	37
5	182		
6	227		

USING MAX NUMBER OF RECORD	RECORD LENGTH (WORD)	RECORD LENGTH (BYTE)	NUMBER OF BAND
271	4000	16000	4

—— RECORD NUMBER (WEIGHT & PASS, COUNTER) ——

BAND NO.	W & P REC.NO	BAND NO.	COUNTER REC.NO
1	1	1	1
2	8	2	17
3	17	3	36
4	29	4	63

	USING MAX NUMBER OF RECORD	RECORD LENGTH (WORD)	RECORD LENGTH (BYTE)	UNIT NO.
WEIGHT & PASS	50	4000	16000	70
COUNTER	110	4000	16000	71

From the above result, we can know that the 125 fine energy groups are banded into the 4 super–groups and that three direct access files on the I/O units 96, 70 and 71 require the sizes of 271, 50 and 110 records, respectively. Note that ZRECNO calculates the required data size of banded cross sections by assuming that a scattering matrix contains NMTG$\times$(NMTG+1)/2 word data. Accordingly, its result might be slightly larger than that required in an actual MORSE–DSG calculation since the size of a scattering matrix might be less than the above value.

7. Auxiliary Codes

7.1 REACT

The REACT code calculates the reaction rate by using the output from ANISN-DD (I/O unit 30), DOT-DD (I/O unit 41 or NAFT) MORSE-DD (I/O unit 95) and MORSE-DSG (I/O unit 95). The response cross sections with the same energy structure as the 125 group DDX library have been prepared in a PDS (PartitioinedData Set) file. The ID numbers of these cross sections are shown in **Table 7.1**.

The REACT code reads input data with the FORTRALN77 free format. The input is as follows:

Table 7.1 Identification of reaction cross sections in 125-group library for response calculation[a]

Reaction	ID name	Data library	MAT	MT
^{6}Li(n, α)T	LI6107	ENDF/B-IV	1271	107
	LIJ107	JENDL-3PR1	306	107
^{7}Li(n, n'α)T	LI7091	ENDF/B-IV	1272	91
	LIJ205	JENDL-3PR1	307	205
Li(n, x)T[b]	LIJN	JENDL-3PR1	Both above	
^{27}Al(n, α)^{24}Na	A17107	ENDF/B-IV	6193	107
	A17107B5	ENDF/B-V	6313	107
^{58}Ni(n, 2n)^{57}Ni	NI8016	ENDF/B-IV	6419	16
	NI8016B5	ENDF/B-V	6433	16
	NI2B	Measured value by Ikeda et al.[c]		
^{58}Ni(n, p)^{58}Co	NI8103	ENDF/B-IV	6419	103
	NI8103B5	ENDF/B-V	6433	103
	NI8B	Measured value by Ikeda et al.[c]		
^{197}Au(n, 2n)^{196}Au	AU7016	ENDF/B-IV	1283	16
	AU7016B5	ENDF/B-V	6379	16
^{197}Au(n, γ)	AU7102	ENDF/B-IV	1283	102
	AU7102B5	ENDF/B-V	6379	102
^{115}In(n, n')^{115m}In	IN5051B5	ENDF/B-V	6437	51
^{93}Nb(n, 2n)	NB2B	Measured value by Ikeda et al.[c]		
^{90}Zr(n, 2n)	ZR2B	Measured value by Ikeda et al.[c]		
^{235}U(n, f)	U25018	ENDF/B-IV	1261	18
^{238}U(n, f)	U28018	ENDF/B-IV	1262	18
^{238}U(n, γ)	U28102	ENDF/B-IV	1262	102
^{232}Th(n, f)	TH2018	ENDF/B-IV	1296	18
^{237}Np(n, f)	NP7018	ENDF/B-IV	1263	18
^{239}Pu(n, f)	PU9018	ENDF/B-IV	1264	18
^{239}Pu(n, γ)	PU9102	ENDF/B-IV	1264	102

[a] Weighting function : 1/E.
Cross section of the 125-th group is zero.
[b] Natural lithium (^{6}Li : 0.07406, ^{7}Li : 0.92594).
[c] Reference 32.

CARD A (*)

1) ND number of detectors used in MORSE calculation
(no effect for ANISN–DD and DOT–DD)

2) NE number of energy groups
If NE < 0, cross sections of the | NE | –th group are read from card–image input on the I/O unit 5.

3) NRES number of reactions to be calculated

4) IPOLT switch to plot the results
= 0, no effect
The calculated reaction rates are, however, stored in the memory to be plotted later.
= 1, plot reaction rate distributions calculated up to the present

5) IN I/O unit number of flux input file

6) IFLUX transport code used in flux calculation
=–3, DOT–DD (total flux file (I/O unit 41))
=–2, DOT–DD (angular flux file (I/O unit NAFT))
=–1, ANISN–DD
= 0, MORSE–DD or –DSG

7) ILETH unit of flux (no effect for ANISN–DD and DOT–DD)
= 0, per unit energy
= 1, per unit lethargy

8) IND number of sets of detectors (no effect for ANISN–DD and DOT–DD)

9) RNORM normalization factor

10) ICON option for groupwise edit
= 1, no effect
= 0, print groupwise reaction rates
=–1, print cumulative reaction rates

CARD B (*) (Enter if IFLUX=0 or IND>1)

(IMX(I), I=1, IND) the last detector number of each set
If IMX(I) is negative, the reaction rate calculated for the detectors (IMX(I–1)+1 ~ | IMX(I) |) are not plotted. For these detectors, interpolation cannot be perfo-rmed. Note that IMX(IND) must equal ND.

CARD C (A8)

Title for the input flux.

CARD D (*) (Enter if IFLUX=0)

(R(I), I=1, ND) x–coordinates for the detector I
The input values R(I) are used as x–coordinate of plotted figure. These values are also used in the interpolation. Note that R(I) must be assigned to all detectors though results for some detectors are not plotted.

CARD E (*) (Enter if IFLUX=–1)

1) NTYPE option for ANISN–DD flux
= 0, calculate reaction rate at each spatial mesh
> 0, calculate zone–integrated reaction rate in NTYPE zones

(*) means FORTRAN77 free–formatted input.

2) IR geometry in ANISN-DD calculation
= 1, slab
= 2, cylinder (not usable)
= 3, sphere

CARD E' (*) (Enter if NTYPE>0 and IFLUX=-1)
(IRR(I), I=1, NTYPE) boundaries of zones
The I-th zone consists of spatial meshes between IRR(I-1)+1 and IRR(I). The code sets IRR(0)=0.

CARD F (*) (Enter if IFLUX=-2 or -3)
1) NTYPE option for DOT-DD flux
= 0, calculate radial distributions at INDZ axial meshes if INDR=0 or axial distributions at INDR radial meshes if INDZ=0
= 1, calculate zone-integrated radial distributions
=-1, calculate zone-averaged radial distributions
= 2, calculate zone-integrated axial distributions
=-2, calculate zone-averaged axial distributions
2) INDR number of radial meshes or zones
3) INDZ number of axial meshes or zones
Either INDR or INDZ must be non-zero if NTYPE=0. Both of them must be non-zero if NTYPE ≠ 0.

CARD F' (*) (Enter if NTYPE=0 and IFLUX=-2 or -3)
Axial or radial mesh numbers at which reaction rates are calculated
(INDR or INDZ entriesl).

CARD F" (*) (Enter if | NTYPE | =1 or 2 and IFLUX=-2 or -3)
(ID(I), I=1, INDR) boundaries of radial zones
The I-th radial zone consists of radial meshes between ID(I-1)+1 and ID(I). The code sets ID(0)=0.

CARD F"' (*) (Enter if | NTYPE | =1 or 2 and IFLUX=-2 or -3)
(ID2(J), J=1, INDZ) boundaries of axial zones
The J-th axial zone consists of axial meshes between ID2(I-1)+1 and ID2(J). The code sets ID2(0)=0.

CARD G (A8)
ID name of response cross section in a PDS file.

CARD G' (*) (Enter if NE<0)
Cross section of the | NE | -th group.

NRES sets of CARDs G and G' should be repeated.

If IPLOT on CARD A is one, the REACT code reads the following input data, plots the results and obtains reaction rates at any positions by an interpolation. If IPLOT=0, REACT returns to CARD A. In this case, no input for CARD A terminates the job.

CARD H (A40)

Title for the figure.

CARD I (*)

1) XWIDTH length of x-axis in mm unit
2) YWIDTH length of y-axis in mm unit

A set of CARDs J to N is repeated for all the cases to be plotted. The number of repetition is the number of lines drawn in the present figure.

CARD J (*)

1) NEXP number of spatial points at which reaction rates are required
2) IUNIT option for C/E calculation
   = 0, no effect
   = 1, read experimental values on CARDs L and M and calculate C/E
   Error of C/E is statistical uncertainty in calculation.
   =−1, read experimental values and their errors on CARDs L, M and N and calculate C/E
   Error of C/E includes experimental ones.
3) NOPT Interpolation method
   = 1, linear-log
   = 2, linear-linear

If NOPT<0, Akima's interpolation method[31] is used.

CARD K (*)

(RR(I), I=1, NEXP) x-ordinates of points at which reaction rates are required

CARD L (A8) (Enter if IUNIT=1 or −1)

Title for experimental values.

CARD M (*) (Enter if IUNIT=1 or −1)

(REX(I), I=1, NEXP) dxperimental value at the I-th position

CARD N (*) (Enter if IUNIT=−1)

(EEX(I), I =1,NEXP) error of experimental value on CARD M

Return to CARD A. If no further data are entered, the job is terminated.

A sample of input and JCL is shown in **Fig. 7.1**. The REACT code with these input data calculates reaction rates of $^{6}Li(n,\alpha)T$ and $^{7}Li(n,n'\alpha)T$ by using the fluxes from MORSE-DD and DOT-DD calculations for the problem 2 described in Sections 5.4 and 6.4, and plots the results in one figure.

```
//JCLG JOB
//JCLG EXEC JCLG
//SYSIN DD DATA,DLM='++'
// JUSER   31823803,MORI.TAKAMAS,0431.100,FIBJOB
   T.3 W.0 C.3 I.4 GRP
  OPTP PASSWORD=  ,MSGCLASS=R,CLASS=0
//********  'J3803.DDX.CNTL(RRDOTB3)'  **********
//*      REACT : CALCULATON OF REACTION RATE      *
//*                                               *
//*************************************************
//  EXEC LMGO,LM=J3803.DDUTY,PNM=REACTVP
// EXPAND GRNLP,SYSOUT=M
//* ---- RESPONSE LIBRARY ------------------------------------------
//RESPONSE  DD DSN=J3803.PROFDDX2.PDS124G.DATA,DISP=SHR
//*
//* ---- TALLY FILE FROM MORSE-DD (FT95F001) ----------------------
//FT11F001 DD DISP=SHR,LABEL=(,,,IN),DSN=J3803.MORSE2.BNC3LIB3.DATA
//*
//* ---- ANGULAR FLUX FILE FROM DOT-DD (NAFT) ---------------------
//FT12F001 DD DSN=J3803.PLTDOT.TDS.DATA(B3DD),DISP=SHR,LABEL=(,,,IN)
//FT13F001 DD DSN=J3803.PLTDOT.TDS.DATA(PLB3),DISP=SHR,LABEL=(,,,IN)
//*
//SYSIN DD *
   15 -125    2    0   11          0    1    3  0.2226      1
    7    14   -1
MORSE-DD
   22.  29.5  40.  50.  60.  70.  77.5
   22.  29.5  40.  50.  60.  70.  77.5
   0.0
LIJ107
689.
LIJ205
0.0
    0 -125    2    0   12         -2    0    0  1.000000    1
DOT(DDL)
   -2  2  8
    3 16
    2  5 11 16 21 26 31 34
LIJ107
689.
LIJ205
0.0
    0 -125    2    1   13         -2    0    0  1.000000    1
DOT(P5)
   -2  2  8
    3 16
    2  5 11 16 21 26 31 34
LIJ107
689.
LIJ205
0.0
REACTION RATE IN LI2O CYLINDER
150. 200.
0 0 0
0 0 0
0 0 0
0 0 0
0 0 0
0 0 0
0 0 0
0 0 0
0 0 0
0 0 0
0 0 0
0 0 0
++
//
```

Fig. 7.1 Sample JCL and input data for REACT.

7.2 MONTA

The MONTA code calculatels the angular transfer probability $P(k, m', m)$ defined by Eq.(2–29) by using the Monte Carlo method. The results of MONTA are used in ANISN–DD (cylindrical geometry) and DOT–DD. In this code, two–dimensional quadrature directions are determined from one –dimensional ones (user's input values) by assuming the level symmetric condition. Accordingly, input quadrature directions XM(i) must satisfy the following level symmetric condition:

$$(XM(i))^2-(XM(i-1))^2=\text{constant}. \qquad (7\text{–}1)$$

Ordering of calculated quadrature directions is as follows: η levels are taken in ascending order for negative η values and then in descending order for positive η. In each η level, μ is taken in ascending order from negative to positive. An example of the ordering is shown for the S_6 quadrature in **Fig. 7.2**. As for the boundaries between the quadrature directions, a user can choose either the "igloo" type boundaries or the "honeycomb" type ones. These two types of boundaries are shown in **Figs. 5.1** and **5.2**. The Monte Carlo results for $P(k,m',m)$ are normalized iteratively to satisfy both of Eqs.(2–30) and (2–32) within a specified error criterion.

The MONTA code reads input data with the FORTRAN77 free format except for CARDs A, C and E. CARD E is read with the FIDO format. The input is as follows:

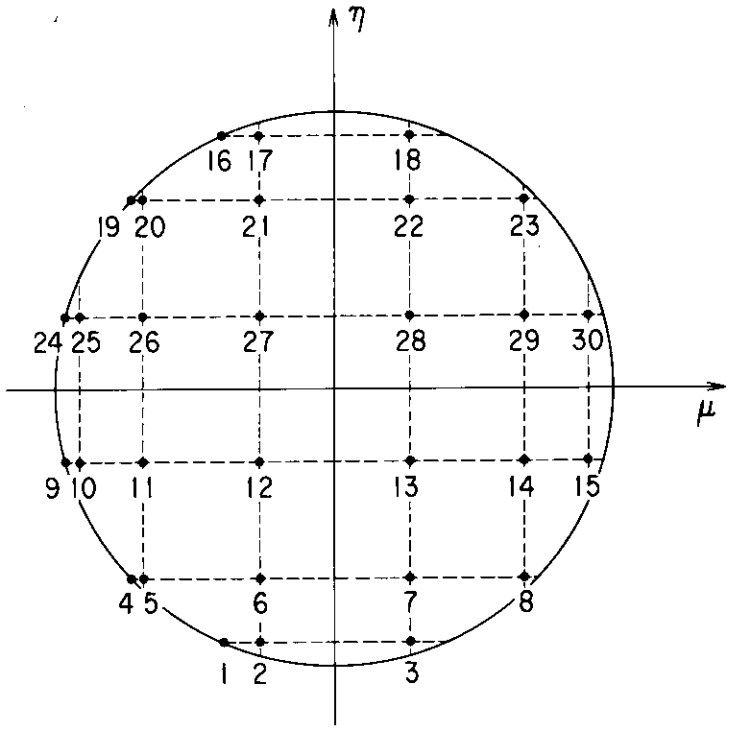

Fig. 7.2 Ordering of quadrature directions in S_6 approximation.

CARD A (A72)

Title.

CARD B (*)

1) IRST

= 0, initial run

= 1, restart run

2) N order of quadrature set
The number of directions determined by MONTA, NS, is $|N| * (|N|+4)/2$. Positive N means "igloo" type is used as boundaries between directions, and negative one means "honeycomb" type.
3) MU number of DDX angle bins
4) NR number of sets of two points on a hemisphere randomly taken for the integration of Eq.(2-29)
5) NORM maximum number of interations for normalization (normally set 100)
6) EPSN normalization error criterion (normally set 0.0000001)
7) ISYM symmetry correction
= 0, no effect
= 1, take into account the symmetry in the quadrature set
8) MST, IMST, MLT print option
Calculated angular transfer probability is printed out from the MST-th outgoing angle to the MLT-th one by every IMST angles.

CARD C (Z12)
Starting random number.

CARD D (*)
(XM(i), i=1, N+1) one-dimensional angular quadrature cosines given in ascending order
NOTE: Eq.(7-1) must be satisfied.

CARD E (FIDO format) (Enter if N>0)
(WSN(i), i=1, NS) Angular quadrature weight
These array data are read with the FIDO format (array number 1). For example,
1 * * 0.0 2R 0.25 Q3 T

CARD F (*)
(XXMU(i), i=1, MU+1) angle bin boundaries of DDX from 1 to -1

A sample of input and JCL is shown in **Fig. 7.3**. Since MONTA is programed in order to utilize a vector computer, it is recommended that a user run this code on a vector computer. The I/O file requirement is summarized in **Table 7.2**. The output file on the I/O unit 10 consists of the following five records.

1) MU, NS, NN, (T(i), i=1, 18), N, RND :
MU : number of DDX angle bins
NS : number of quadrature directions in two-dimension
NN : number of sets of two points on a hemisphere randomly taken to calculate Eq.(2-29)
T : title (72 characters)
N : order of quadrature set
RND: initial random number
2) (XXMU(i), i=1, MU+1) : angle bin boundaries of DDX
3) $(w_m, m=1,NS), (\mu_m, m=1,NS), \eta_m, m=1,NS)$ calculated quadrature weights and directions
4) $(((P(k,m',m), k=1,MU), m,=1,NS)$:
angular transfer probabilities for DOT-DD
5) $(((P'(k,m',m), k=1,MU), m'=1,NS/2), m=1,NS/2)$:
angular transfer probabilities for ANISN-DD (cylinder)

```
//JCLG JOB
//JCLG EXEC JCLG
//SYSIN DD DATA,DLM='++'
// JUSER XXXXXXXX,SASAKI,0431.01
   T.7 W.2 I.4 C.4
 OPTP PASSWORD=XX,CLASS=1
//*************************************************************
//*  J3803.SASAKI.CNTL(MONTAGO)                               *
//*  CALCULATION OF ANGULAR TRANSFER PROBABILITY FOR DOT-DD    *
//*************************************************************
//*
// EXEC FORT77
      SUBROUTINE SIZE(L)
      PARAMETER (LIMIT=700000)
      COMMON A(LIMIT)
      L = LIMIT
      RETURN
      END
//*************************************************************************
// EXEC LKED
//OLDLM DD DSN=J3803.DDUTY.LOAD,DISP=SHR
  ENTRY MAIN
  INCLUDE OLDLM(MONTAVP)
  NAME TEMPNAME(R)
// EXEC GO
//*---------- FT07 : BCD OUTPUT FILE OF QUADRATURE SET ---------------
//FT07F001 DD SYSOUT=*
//*---------- FT10 : BINARY OUTPUT FILE ------------------------------
//FT10F001 DD DSN=J9021.IGL00160.DATA,  (S160)
//  UNIT=D0430,DISP=(,CATLG,DELETE),SPACE=(TRK,(50,10),RLSE)
//*---------- FT11 : RESTART DATA FILE  ------------------------------
//FT11F001 DD UNIT=WK10,SPACE=(TRK,(30,30))
//*T11F001 DD DSN=J9021.IGLOORR.DATA,   (S160)
//* UNIT=D0430,DISP=(,CATLG,DELETE),SPACE=(TRK,(90,50),RLSE)
//* DISP=SHR
//*- - - - - - - - - - - - - - - - - - - - - - - - - - - - - -
//SYSIN DD *  (S160)
 *** S16 --> S160  (1985/10/7)
0 16 20  5000000 50 0.0000001 1 1 20 160     /  B
57893BF89AB9
-1.0       -0.9775250 -0.9067650 -0.8299930
-0.7453560 -0.6497860 -0.5374840 -0.3944050
-0.1490710  0.1490710  0.3944050  0.5374840
 0.6497860  0.7453560  0.8299930  0.9067650
 0.9775250                                  /  D
 1**
    .0 .13586-1  N1
    .0 .97681-2  .97681-2  N2
    .0 .64738-2  .50390-2  .64738-2  N3
    .0 .64634-2  .71124-2  .71124-2  .64634-2  N4
    .0 .64634-2  .14381-2  .36342-2  .14381-2  .64634-2  N5
    .0 .64738-2  .71124-2  .36342-2  .36342-2  .71124-2  .64738-2 N6
    .0 .97681-2  .50390-2  .71124-2  .14381-2  .71124-2  .50390-2
       .97681-2  N7
    .0 .13586-1  .97681-2  .64738-2  .64634-2  .64634-2  .64738-2
       .97681-2  .13586-1  N8    Q80
 T
 1.0 0.9 0.8 0.7 0.6 0.5 0.4 0.3 0.2 0.1 0.0 -0.1
 -0.2 -0.3 -0.4 -0.5 -0.6 -0.7 -0.8 -0.9 -1.0  /  F
/*
++
//
```

Fig. 7.3 Sample JCL and input data for MONTA.

Table 7.2 MONTA file requirement

I/O unit	Contents
7	BCD output of two-dimensional quadrature constants
10	Binary output of angular transfer probability
11	Restart file
5	Card-image input data
6	Output of results

8. Comparison of Sample Problem Results Using DDX and P_l Cross Sections

Results of the sample problems described in Chapters 4, 5 and 6 are presented and compared with those by the conventional P_l method. The first figure in this chapter (**Fig. 8.1**) shows the results of ANISN-DD sample problem. The angular flux spectra on each side of a 20 cm thick infinite lithium slab have been calculated by using three DDX libraries (DDL/J3P1, DDL/F6 and DDL/I) and one conventional P_5 library (JENGIX[33]). All the libraries are based on JENDL-3PR1. The difference between these three DDX libraries comes from the treatment of energy-angle distributions of neutrons emitted from the reactions such as the continuum inelastic scattering of which the reaction kinematics is not known. In DDL/J3P1 which is a standard DDX library presented in Chapter 2, those energy-angle distributions have been calculated from angular and energy distributions given in Files 4 and 5 of JENDL /3PR1, respectively. Those in DDL/F6 are based on double-differential data given in File 6. An isotropic distribution in the laboratory system is assumed in DDL/I. The latter two libraries were produced tentatively for comparison. The JENGIX P_5 library has been produced by using the MAXS-N system [28] with the same assumption that those reactions are isotropic in the laboratory system.

In the energy range corresponding to the elastic peak of 15 MeV source neutrons (around 9 MeV and around 14 MeV in the backward and forward directions, respectively), a significant difference is observed in the backward direction ($\mu=-0.75$) between the DDX and JENGIX results, though difference is hardly seen in the forward direction ($\mu=0.75$). The outgoing neutron energies from the elastic scattering by constituent nuclides are summarized in **Table 8.1**. In the case of JENGIX ($\mu=-0.75$), several ghost peaks and negative fluxes appear above the elastic peak, which are ascribed to the approximation used in the P_5 expansion method. On the other hand, the calculations with the DDX libraries predict sufficiently well the elastic peaks in both directions. Below 10 MeV where secondary neutrons from the continuum inelastic scattering contribute, the JENGIX and DDL/I results show good agreement in both directions, and also the agreement is good between the DDL/J3P1 and DDL/F6 results. This fact means the divergence of results observed in this energy range is mainly caused by the different treatment of angular distributions of continuum inelastic scattering.

Similar observation can be obtained in the DOT-DD sample problem 1 (angle dependent leakage neutron energy spectrum from a 5 cm thick Li_2O cylinder), as is seen in **Fig. 8.2**. In this case, a ghost peak and a negative flux appear in the JENGIX result even for a forward direction ($\mu=0.39$).

Figure 8.3 shows comparison of calculated tritium production rates by $^6Li(n,\alpha)T$ and $^7Li(n,n'\alpha)T$ reactions (T_6 and T_7) in the DOT-DD sample problem 2 (Li_2O cylinder system of 60 cm thickness and 60 cm diameter). The codes used are DOT-DD (DDL/J3P1 and JENGIX) and MORSE-DD (DDL/J3P1). The results of MORSE-DD and DOT-DD calculations using the same DDX library agree with each other within statistical uncertainties in the former results. Between the DDX and P_5 results by DOT-DD, no large difference is seen in this figure. From detailed comparison in **Table 8.2**, however, the discrepancies of 3.3 % are found in the deep region for both reactions. For volume-integrated tritium production rates (TPRs), 2.0, 0.5 and 0.8 % differences for T_6, T_7 and total TPR, respectively, are also found between the results by using both libraries. This 2 % difference for T_6 is not so small as to be negligible, though such a difference is hardly observed for T_7 since T_7 is dominated by the uncollided flux component from the source neutrons in the present problem. Moreover, a significant difference is observed in the leakage neutron spectra from the present system, as seen in **Fig. 8.4**. This difference, especially in the reflected component of flux, will cause a serious disagreement in the analysis of the closed system such as the Phase II experiment of the JAERI-U.S. collaborative program on fusion blanket neutronics [26),27)], where the back scattering is important.

From the present comparison, superiority of the DDX is obvious, especially in the analysis of differential quantities such as neutron energy spectra which are frequently used to examine the adequacy of nuclear data used. Accordingly, we can recommend to use the DDX instead of the conventional P_l cross sections in analyses where an accurate treatment of scattering anisotropy is necessary.

Table 8.1 Outgoing neutron energy from elastic scattering with an incident energy 15 MeV*

Nuclide	Scattering angle cosine, μ		
	−0.75	0.39	0.75
Lithium-6	8.32	12.2	13.8
Lithium-7	9.06	12.6	14.0
Oxygen-16	12.04	13.9	14.5

* Calculated values (in MeV) by the kinematics:

$$E=\frac{E'}{(A+1)^2}(A^2-1+\mu^2+2\mu\sqrt{A^2-1+\mu^2}).$$

Table 8.2 Comparison of calculated tritium production rates (DOT–DD sample problem 2)

Region (cm)	$^6Li(n,\alpha)T$			$^7Li(n,n'\alpha)T$			Natural lithium[a]		
	DOT–DD (DDX)	DOT–DD (P_3)	MORSE–DD (DDX)	DOT–DD (DDX)	DOT–DD (P_3)	MORSE–DD (DDX)	DOT–DD (DDX)	DOT–DD (P_3)	MORSE–DD (DDX)
20-24	3.137-1[b]	1.002[c]	1.021[c]	2.980-1[b]	0.996[c]	1.017[c]	2.992-1[b]	0.996[c]	1.017[c]
24-35	1.139-0	0.988	0.983	4.297-1	0.993	0.996	4.823-1	0.992	0.993
35-45	8.648-1	0.977	0.991	1.414-1	0.992	0.999	1.950-1	0.987	0.996
45-55	5.805-1	0.971	0.995	5.432-2	0.995	1.004	9.329-2	0.984	1.000
55-65	3.425-1	0.969	0.990	2.076-2	1.006	1.002	4.459-2	0.985	0.995
65-75	1.713-1	0.967	0.992	7.829-3	1.020	1.004	1.994-2	0.986	0.996
75-80	3.518-2	0.967	0.999	1.732-3	1.032	1.005	4.209-3	0.992	1.001
Total (20-80)	3.447-0	0.980	0.992	9.534-1	0.995	1.004	1.138-0	0.992	1.001

(Statistical uncertainty in the MORSE–DD result is about 1% (1σ).)

[a] Natural lithium; ^6Li:^7Li = 0.07406 : 0.92594.

[b] (Tritium/atom. sec. source) × (volume).
Read as 3.137×10^{-1}.

[c] Ratio to the values by DOT–DD with the DDX library.

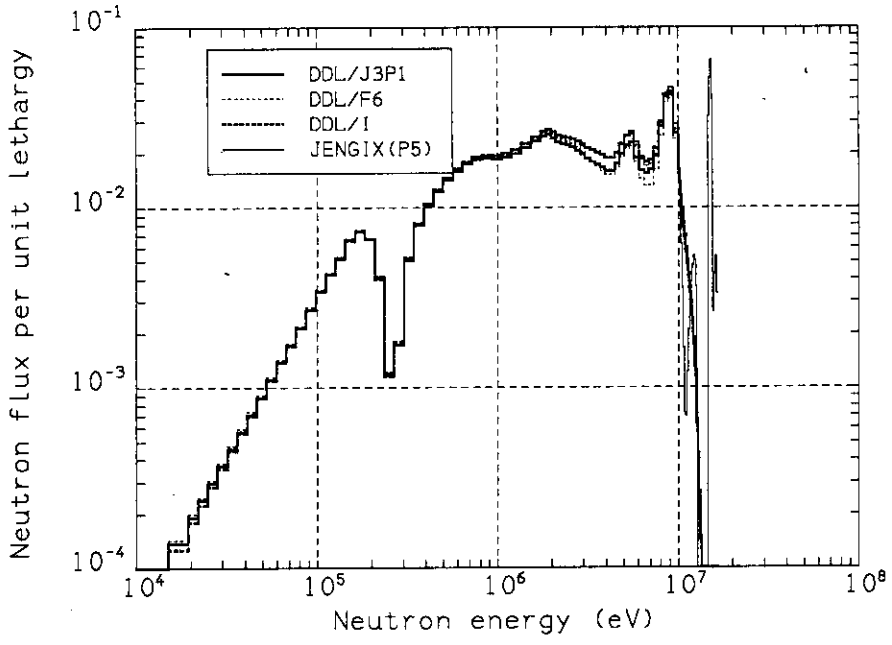

(A) Angular Flux from Lithium Slab in Reflected Direction (μ=-0.75)

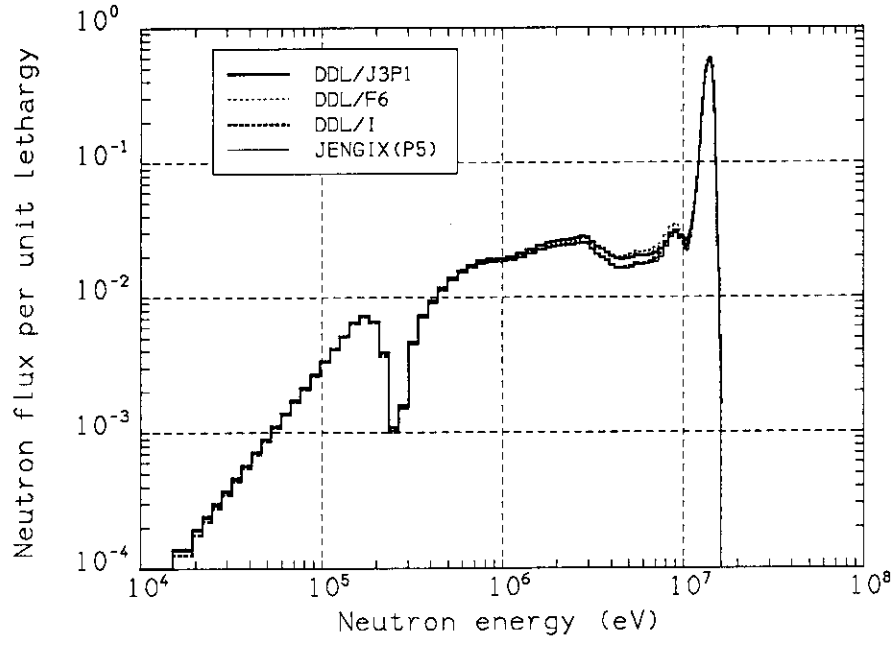

(B) Angular Flux from Lithium Slab in Forward Direction (μ=0.75)

Fig. 8.1 Leakage neutron spectra from a 20 cm thick lithium slab calculated by ANISN–DD (ANISN–DD sample problem).

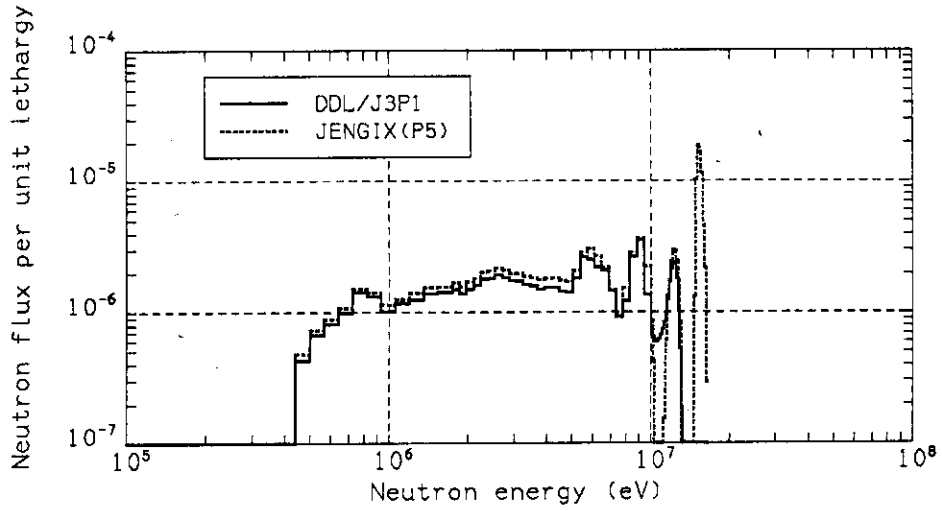

(A) Leakage Flux Spectrum (μ=-0.75)

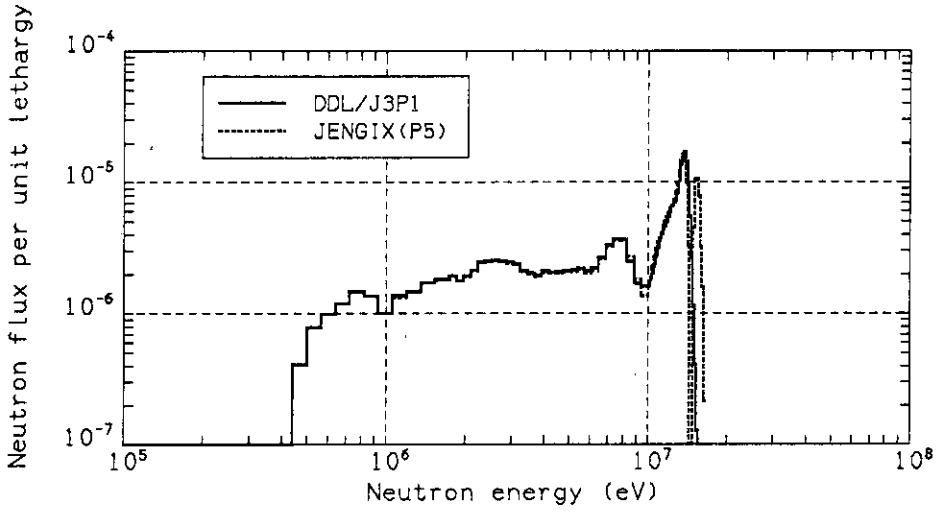

(B) Leakage Flux Spectrum (μ= 0.39)

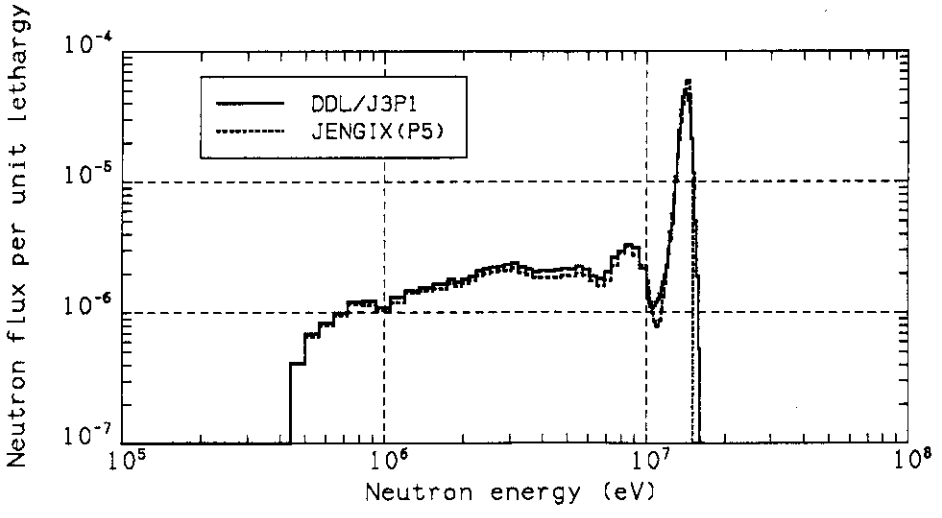

(C) Leakage Flux Spectrum (μ= 0.75)

Fig. 8.2 Leakage neutron spectra from a Li_2O cylinder of 31.4 cm radius and 5.06 cm thickness calculated by DOT–DD (DOT–DD sample problem 1).

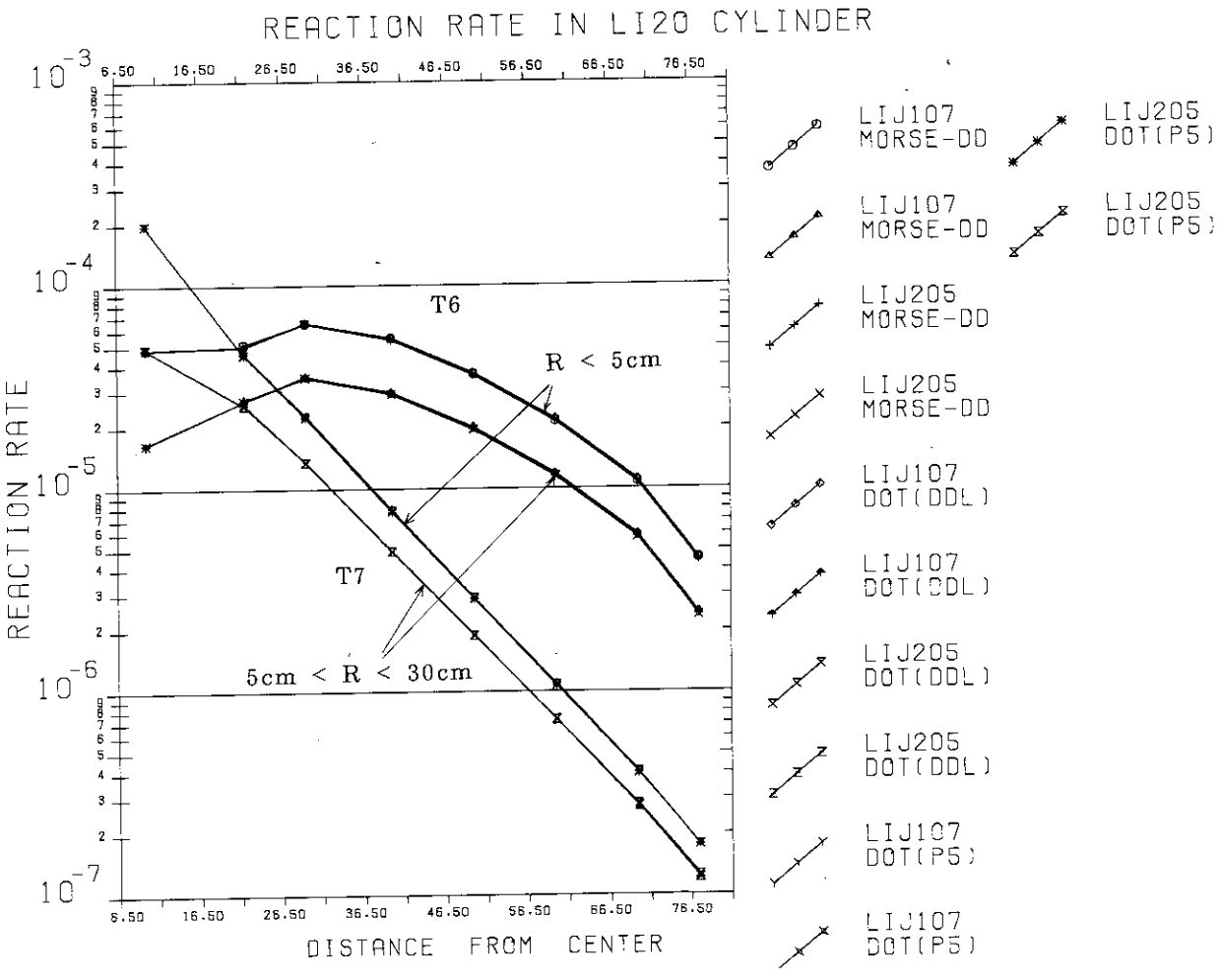

Fig. 8.3 Tritium production rates calculated by DOT–DD (DOT–DD sample problem 2).

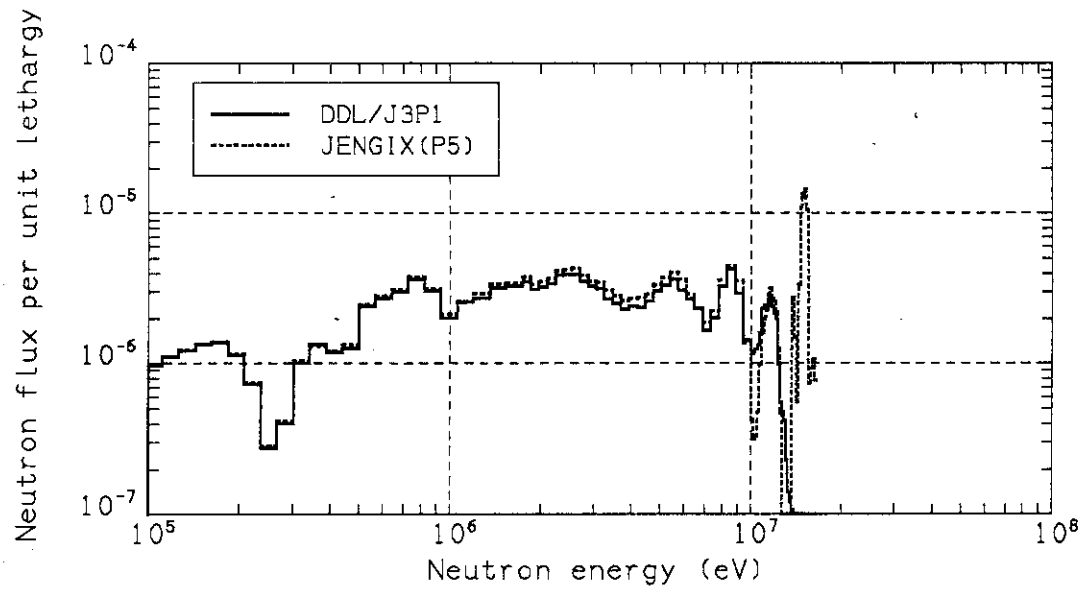

(A) Leakage Flux Spectrum (μ=-0.79)

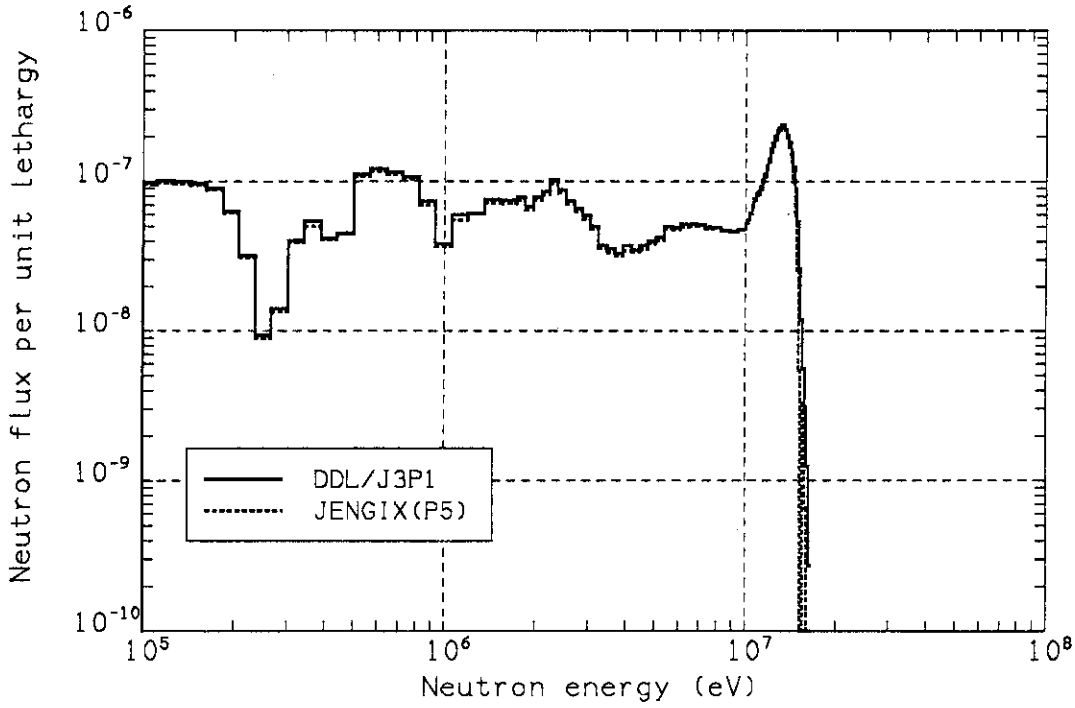

(B) Leakage Flux Spectrum (μ= 0.79)

Fig. 8.4 Leakage neutron spectra from a Li_2O cylinder of 30 cm radium and 60 cm thickness calculated by DOT−DD (DOT−DD sample problem 2).

9. Summary

A group of computer codes have been developed to realize the accurate transport calculation by using the multi-group double-differential form cross sections. By using this type of cross sections instead of the conventional P_l expansion type ones, the energy-angle correlated reaction kinematics can be correctly taken into account in the multi-group transport calculation. As a result, transport phenomena in materials with highly anisotropic scattering can be solved more accurately compared with the conventional method. The superiority of the present method to the conventional one has been shown by comparison of the sample problem results.

The present codes have been developed mainly for the application in the fusion neutronics field. These have been successfully used in the analyses of fusion neutronics experiments carried out at the FNS facility of JAERI [23),25),26),27)]. These codes and calculation algorithms employed are also applicable to other fields where anisotropy of scattering plays an important role. For example, a transport calculation of spallation neutrons is one of such fields. It would be difficult to obtain a reliable result by using the conventional P_l method since spallation neutrons have a very high energy component for which the scattering anisotropy is very strong.

Acknowledgment

The authors would like to acknowledge Dr. Y. Ishiguro of JAERI for his helpful suggestions and encouragement through the course of this study.

9. Summary

A group of computer codes have been developed to realize the accurate transport calculation by using the multi-group double-differential form cross sections. By using this type of cross sections instead of the conventional P_l expansion type ones, the energy-angle correlated reaction kinematics can be correctly taken into account in the multi-group transport calculation. As a result, transport phenomena in materials with highly anisotropic scattering can be solved more accurately compared with the conventional method. The superiority of the present method to the conventional one has been shown by comparison of the sample problem results.

The present codes have been developed mainly for the application in the fusion neutronics field. These have been successfully used in the analyses of fusion neutronics experiments carried out at the FNS facility of JAERI [23),25),26),27)]. These codes and calculation algorithms employed are also applicable to other fields where anisotropy of scattering plays an important role. For example, a transport calculation of spallation neutrons is one of such fields. It would be difficult to obtain a reliable result by using the conventional P_l method since spallation neutrons have a very high energy component for which the scattering anisotropy is very strong.

Acknowledgment

The authors would like to acknowledge Dr. Y. Ishiguro of JAERI for his helpful suggestions and encouragement through the course of this study.

References

1) Takahashi A., Rusch D.: "Fast Rigorous Numerical Method for the Solution of the Anisotropic Neutron Transport Problem and the NITRAN system for Fusion Neutronics Application," KfK 2832/1,2 (1979).
2) Brockmann H.: Nucl. Sic. Eng. 77, 377 (1981).
3) Nakagawa M., Mori T.: "MORSE-DD: A Monte Carlo Code Using Multi-Group Double-Differential Form Cross Sections," JAERI-M 84-126 (1984).
4) Mori T., Nakagawa M., Ishiguro Y.: "PROF-DD: A Code System for Generation of Multi-Group Double -Differential Form Cross Section Library," JAERI-M 86-124 (1986).
5) Mori T., Sasaki M., Nakagawa M.: "ANISN-DD: One-Dimensional Sn Transport Code Using Multi-Group Double-Differential Form Cross Sections," JAERI-M 87-123 (1987).
6) Nakagawa M., Mori T., Ishiguro Y.: "Benchmark Test of MORSE-DD Code Using Multi-Group Double -Differential Form Cross Sections," JAERI-M 85-009 (1985) 〔in Japanese〕.
7) Engle W.W. Jr.: "A User Manual for ANISN, A One Dimensional Discrete Ordinates Transport Code with Anisotropic Scattering," K-1693 (1967).
8) Koyama K., et al.: "ANISN-JR: A One-Dimensional Discrete Ordinates Code for Neutron and Gamma-ray Transport Calculations," JAERI-M 6954 (1977).
9) Rhodes W.A., Mynatt F.R.: "The DOT-III Two Dimensional Discrete Ordinates Transport Code," ORNL /TM-4280 (1973).
10) Emmett M.B.: "The MORSE Monte Carlo Radiation Transport Code System," ORNL-4972 (1975).
11) Sasaki M., Sato W., Nakagawa M., Mori T.: "A Users' Guide of a Plotting Program PLTJOINT," JAERI -M 88-036 (1988).
12) Drake M.K.(ed.): "Data Formats and Procedures for ENDF Neutron Cross Section Library", BNL 50274 (T-601), ENDF 102, Vol.1, (1970).
13) Shibata K.: ^{6}Li in JAERI-M 84-198, ^{7}Li in JAERI-M 84-204, ^{12}C in JAERI-M 84-221 (1984). Kikuchi Y.: unpublished for *Fe, Cr* and *Ni.*
14) Nakagawa T.: "Program RESENDD (Version 84-07): A Program for Reconstruction of Resonance Cross Sections from Evaluated Nuclear Data in the ENDF/B Format," JAERI-M 84-192 (1984).
15) Hasegawa A.: private communication (1984).
16) Cullen D.E.: "Program LINEAR (Version 79-1), Linearize Data in the Evaluated Nuclear Data File / Version B (ENDF/B) Format," "Program SIGMA1 (Version 79-1), Doppler Broaded Cross Section in the Evaluated Nuclear Data File / Version B (ENDF/B) Format," "Program RECENT (Version 79-1), Reconstruction of Energy-Dependent Neutron Cross Sections from Resonance Parameters in the ENDF/ B Format," UCRL-50400, Vol.17, Part A-C (1979).
17) Koyama K., et al.: "RADHEAT-V3, A Code System for Generating Coupled Neutron and Gamma-ray Group Constants and Analyzing Radiation Transport," JAERI-M 7155 (1977).
18) Benveniste J., Zenger J.: "Information on the Neutrons Produced in the $^{3}H(d,n)^{4}He$ Reaction," UCRL-4266 (1954).
19) Benveniste J., et al.: Nucl. Instrum. Methods, 7, 306 (1960).
20) Seki Y.: J. Nucl. Sci. Technol., 20 686, (1983).
21) Fraley S.K., et al.: Nucl. Sci. Eng., 70, 14 (1981).
22) Iida H., Seki Y. : ibid, 74, 210 (1980).
23) Nakagawa M., Mori T., et al.: "U.S./JAERI Fusion Neutronics Calculational Benchmarks for Nuclear Data and Codes Intercomparison," JAERI-M 85-201 (1985).
24) Oyama Y., Maekawa H.: "Measurements of Angle-Dependent Neutron Spectra from Lithium-Oxide Slab Assembly by the Time-of-Flight Method," JAERI-M 83-195 (1983).
25) Youseff M.Z., Nakagawa M., et al.: Fusion Technol., 10, 549 (1986).
26) Nakagawa M., et al.: "Analysis of Neutronics Parameters Measured in Phase II Experiments of the JAERI

-U.S. Collaborative Program, Part 1," Proc. Int. Symposium on Fusion Nuclear Technology, Tokyo, 1988 in print.

27) Youseff M.Z., et al.: "Analysis for Phase II Experiments of the JAERI/U.S. Collaborative Program on Fusion Blanket Neutronics, Part 2," ibid.

28) Irving D.C., et al.: "O5R: A General Purpose Monte Carlo Neutron Transport Code," ORNL-3622 (1965).

29) Lathrop K.D.: "DTF-IV, A Fortran Program for Solving the Multigroup Transport Equation with Anisotropic Scattering," LA-3373 (1965).

30) Thompson C.L., et al.: "O6R-ACTIFK, Monte Carlo Neutron Transport Code," ORNL CF 69-8-36 (1969).

31) Inoue S., et al. (edited): "Manual for JSSL (JAERI Scientific Subroutine Library," 3rd Edition, JAERI-M 82-095 (1982) [in Japanese] .

32) Ikeda Y., et al.: "Activation Cross Section Measurements for Fusion Reactor Structural Materials at Neutron Energy from 13.3 to 15.0 MeV Using FNS Facility," JAERI 1312 (1988).

33) Kosako K., et al.: "Neutron Cross Section Libraries for Analysis of Fusion Neutronics Experiments," JAERI -M 88-076 (1988) [in Japanese] .

34) Hasegawa A.: to be published (1988).

Appendix 1. FIDO Format(＊)

The transferral of input data to input forms or punched cards for a code requiring significant amounts of input is always a time consuming, distasteful and error-prone process. The original (fixed-form) FIDO formats were designed to reduce these difficulties. Lots of convenient options for array operation were prepared for a user to enter large amounts of data. A description of each option is given below. The usefulness of one of such options, the **F** option, which fills an array, is obvious, but it is somewhat harder to see the practical uses for some of the more obscure ones like **N**, **M** and **Q**. However, frequent use will turn up situations where these options are invaluable. For example, the S_n cosines are negated and reflected about $\mu=0.$, a fact of which suggests the use of the **M** option. Despite the usefulness of the options, there are justifiable complaints with the input formats; for example, where convenient options are not applicable, data can be hard to write because of the manner in which the data fields are spread on the card. This is especially true of integer arrays, where the data are right adjusted in 12-column fields. The fixed-form FIDO input forms help to some extent, but the actual key-punching is still troublesome.

This input format has been greatly improved by Ward Engle of ORNL who has designed and implemented an all-FORTRAN free-form FIDO input scheme which has data items separated by blank (as others do), but still allows all of the important convenient features of the earlier formats. The restrictions on the use of this input are essentially that a user writes the data in a form that he can interpret within the context of the FIDO option. Data can be easily written and key-punched, since there is no worry about which type character falls in which column or how many blanks are left between entries.

The free-form input can be interspersed with the fixed form input. To select free-form, an array is identified as either a **$$** or a ＊＊ array for interger and real arrays, respectively.

In the following, the fixed-form FIDO format is explained first with a description of the options. Then, restrictions and examples of the free-form FIDO input are given.

Type 1 Format (Fixed Form)

Each card is divided into six 12-digit data fields which are divided into 3 subfields. The first subfield is a 2-digit integer: and second subfield contains either a blank or one of the following characters: **$**, ＊, **R, I, T, S, F, A, C, E, Q, L, N, M, O, U, V, Z,** ＋ and －, which define the type of array operation. The third subfield contains either an integer or a real number. The contents of the first two subfields will define the operation to be performed on the third field.

The character (') in column 1 of a card will cause the contents of the card to be listed as comments, while the data is read in. Column 2 should contain the proper carriage control character; e.g., blank, 0, 1, 2, etc. This card is ignored as a data card. This option is also available with the free-form FIDO format.

Input Restrictions

The following restrictions must be observed when using the FIDO input format:

(1) Blank data fields are ignored.

(2) If the interpolation option (I) is used, the next data field may not be either blank or an **A** entry.

(3) The third subfield of a data field containing a **$** or a ＊ may contain an integer N. The next data entry is assumed to be the (N＋1)-th member of the array. Normally the third subfield is blank and ignored.

＊ All of the descriptions are cited from Reference 8.

The word "card" in this appendix corresponds to "line" in a card-image file on the I/O unit 5.

(4) All data arrays must be filled with the correct number of entries. A data array is ended by either starting a new data array or by ending a data block.

(5) Integer data in the third subfield must be right adjusted. Real data may be written with or without an exponent. If the decimal is omitted, it is assumed to be immediately to the left of the exponent field. If there is no exponent, the decimal point is assumed to be to the extreme right of the nine-column subfield.

Array Operation

$ indicates the beginning of an integer array. The first subfield identifies the array.

* indicates the beginning of a real array. The first subfield identifies the array.

R indicates that the entry in the third subfield is to be repeated by the number of times specified in the first subfield.

I indicates linear interpolation between the entry in the third subfield and the third subfield of the next data field. The number of points to be placed with an equal space is specified by the entry in the first subfield.

T indicates termination of a particular data block. A data block can contain any number of arrays. Data on a card after a **T** will be ignored.

S indicates skip. The first subfield defines the number of entries to be skipped. The third subfield can contain the first entry following the skips (i.e., 15S 1 enters a 1 in the 16th location of the present array). A blank third subfield would be ignored.

F is used to fill the remainder of an array with the data in the third subfield.

A is used to address a particular location in an array. This location is specified in the third subfield, while the first subfield is blank. The next non-blank data entry is entered in this location of the present array.

C is used to obtain a count of number of data read into an array up to the point where **C** is placed. An integer ZZ in front of the **C** will be used as an identification in producing a message as follows: " XX ENTRIES READ IN THE YY ARRAY at ZZC. " .

E may be used to end specifying data for an array. This option is particularly useful when it is desired to replace only some data in a particular array. The data in question are replaced, and the use of an **E** prevents having to count and skip to the end of the array.

L is similar to **I** except that a logarithmic interpolation is performed between the entry data. This option is particularly useful for defining energy structures equally spaced in lethargy unit.

Q is used to repeat a sequence of numbers. The length of the sequence is defined in the third subfield. The number of times to repeat the sequence is given in the first subfield.

N is used to repeat a sequence of numbers in reversed order. The length of the sequence is defined in the third subfield. The number of times to repeat the sequence is given in the first subfield.

M is used to negate and repeat an inverted sequence. The length of the sequence is defined in the third subfield. The number of times to repeat the sequence is given in the first subfield.

O is used to turn on (or off) the card image edit of input data. As with the **C** option, an integer in front of the **O** identifies the particular entry. The default (starting) condition is not to edit the data.

U is used to replace the input format for an array. The array number is given in the first subfield. The format, written in normal FORTRAN, is specified on the card immediately after the card containing a **U**. The parentheses normally capsulating a format should be included.

V specifies that the array identified in the first subfield will be read according to the last variable format read in.

Z is used to specify a string of zeros; e.g. 49Z would place forty-nine zeros into an array.

+ or − indicates exponentiation. The data in the third subfield is multiplies by $10^{\pm N}$, where N is an integer in the first subfield. This option allows one to specify a number up to nine significant digits.

Blank fields are ignored. One can use any or all fields on a card. For example, a set of blank cards sandwiched anywhere in a data array would be completely ignored.

Type 2 Format (Free Form)

The free-form FIDO input can be interspersed with the fixed form input. To select free-form, an array is identified as either a **$$** or a * * array for integer and real arrays, respectively.

In the free-form FIDO input, data items are separated by blank, and all of the important convenient features of the earlier formats are still allowed. By using this input format, a user can easily write and keypunch data, since it is unnecessary to worry about which type character falls in which column or how many blanks are left between entries.

Input Restrictions

The restrictions on the use of this input are essentially that a user writes the data in a form that he can interpret within the context of the FIDO option. They are summarized as follows:

(1) Any third subfield (data entry) must be followed by one or more blanks. This is an obvious restriction, otherwise data interpretation would be impossible.

(2) Only column 1-72 are used.

(3) Numbers with exponents must not have imbedded blank; e.g. use 1.0E+4, but not 1.0 E+4 or 1.0E +4.

(4) The old + and − options (second subfield) are not optional.

(5) No more than 9 digits in a number can be entered. The exponent is not counted; e.g. 9234+09 or 923400000+1 will work, but 9234000000 will not work. Nine-digit accuracy is clearly beyond the significance available for single precision IBM 360 floating point operations.

(6) A blank must not appear between items which fall in the first and second subfields with the old format, e.g., 24R, but not 24 R. Note that the 99 restriction on the number of repeats, interpolations, etc., has been eliminated.

(7) The **Z**-entry must be entered as 738Z, but not as Z738. The old format allowed either.

(8) The **Q**, **M** and **N** entries must be specified as Q4, but not as 4Q. The old format allowed either. An entry like 3Q4 accomplishes the same as Q4 Q4 Q4. This is now true for either format.

Example of Free-Form FIDO input

Some examples of the new format are given below:

```
1$$ 25R1 0 4 3Q3 2$$ 3R42 E T
```

The first 25 entries of the 1$ array are 1's followed by 0 and 4, and then the sequence 1 0 4 is repeated three times. The 2$ array has three 42's and then data input to the array ends. The T terminates a data block.

```
42 * * 0.0 0.1666667 0.3333333 N2
43 * * −1.0 −0.8819171 0.3333333 M2
```

This example puts 0.0, 0.1666667, 0.3333333, 0.3333333, 0.1666667 in the 42 * array and −1.0, −0.8819171, −0.3333333, 0.3333333, 0.8819171 in the 43 * array.

Appendix 2. LINEAR, RECENT and SIGMA1 Codes

The LINEAR, RECENT and SIGMA1 codes can be used in the PROF-DD system in place of the RESENDD code. The I/O file requirements and input instructions of these codes,are given in **Tables A 2.1 ~ A2.6**. A sample of input and JCL for a successive execution of these three codes is given in **Fig. A.2.1**.

Table A2.1 LINEAR file requirement

Logical unit	Contents	I/O
5	Card-image input data	I
6	Output report	O
10	Original ENDF/B data	I
11	Final ENDF/B data	O
12	Scratch	I/O

Table A2.2 RECENT file requirement

Logical unit	Contents	I/O
5	Card-image input data	I
6	Output report	O
10	Original ENDF/B data with linearized file 3	I
11	Final ENDF/B data	O
12-14	Scratch	I/O

Table A2.3 SIGMA1 file requirement

Logical unit	Contents	I/O
5	Card-image input data	I
6	Output report	O
10	Original ENDF/B data with linearized file 3	I
11	Final ENDF/B data	O
12	Scratch	I/O

Table A2.4 Input instruction for LINEAR

Card	Cols.	Description
1	1-11	Selection criteria (0 = MAT, 1 = ZA)
	12-22	This option is no longer used. The previous meaning of this option was . . . . . Minimum energy spacing selector = 0 – 6 Digit minimum energy spacing calculations. Standard 6 digit E11.4 output. = 1 – 8 Digit minimum energy spacing calculations. Standard 6 digit E11.4 output. = 2 – 8 Digit minimum energy spacing calculations. Variable 8 digit F format output. Experience has demonstrated that failure to set this option to 2 can result in significant errors in the final data. Therefore internally this option is always set to 2.
	23-33	Minimum cross section of interest (barns) (If 1.0E-10 or less is input the program will use 1.0E-10.) Energy intervals will not be sub-divided if the absolute value of the cross section within the interval is less than this value. An exception to this rule is near thresholds energy intervals will be sub-divided until convergence regardless of the magnitude of the cross section.
	34-44	Backward thinning option = 0 – Perform backward thinning. = 1 – No backward thinning (Keep all original data points and add more where required for linearizing).
2-N	1-11	Lower MAT or ZA limit
	12-22	Upper MAT or ZA limit Up to 100 MAT or ZA ranges may be specified, one range per card. The list of ranges is terminated by a blank card. If the upper limit of any request is less than the lower limit, the upper limit will be set equal to the lower limit. If the first request card is blank it will terminate the request list and all data will be retrieved.
VARY	1-11	Energy for error law
	12-22	Allowable fractional error for error law The acceptable linearizing error may be specified to be either energy independent (defined by a single error), or energy dependent (defined by up to 20 energy, error pairs). For the energy dependent case linear interpolation will be used to define the error at energies between those at which it is tabulated. In all cases the error law is terminated by a blank card. If only one energy-error pair is given, the law will be considered to be energy independent. If more than one pair is given it will be considered to be energy dependent (Note, energy independent form will run faster than the equivalent energy dependent form). For an energy dependent error law all energies must be ascending energy order. For convergence of the linearizing algorithm all errors must be positive. If an allowable error is not positive it will be set equal to the standard option (currently 0.001, corresponding to 0.1 per-cent). If the first error card is blank it will terminate the error law and the error will be treated as energy independent, equal to the standard option (currently 0.1 per-cent).

Table A2.5 Input instruction for RECENT

Card	Cols.	Format	Description
1	1-11	I11	Retrieval criteria (0 = MAT, 1 = ZA)
	12-22	E11.4	File 2 minimum absolute cross section (If 1.0E-10 or less in input the program will use 1.0E-10.)
	23-33		This option is no longer used. The former definition of this option was . .
		I11	Minimum energy spacing flag = 0 – 6 Digit minimum energy spacing. Standard 6 digit E11.4 output. = 1 – 8 Digit minimum energy spacing. Standard 6 digit E11.4 output. = 2 – 8 Digit minimum energy spacing. Variable 8 digit F format output. From experience it has been found that failure to set this option to 2 can result in large errors in the final data. Therefore internally this option is set to 2.
	34-44	I11	Operating mode. = 0 – Output mode. = 1 – Edit mode
	45-55	I11	Distant resonance treatment. = 0 – Exact. = 1 – Linear ratio over subinterval. = 2 – Linear ratio over interval.
	56-66	I11	Monitor mode selector = 0 – Normal operation. = 1 – Monitor progress of reconstruction of file 2 data. Each time a page of data points is written to the scratch file print out the total number of points on scratch and the lower and upper energy limits of the page (This option may be used in order to monitor the execution speed of long running jobs).
2-N	1-11	I11	Minimum MAT or ZA
	12-22	I11	Maximum MAT or ZA Up to 100 MAT or ZA ranges may be specified, one range per card. The list is terminated by a blank card. If the upper limit of any request is less than the lower limit the upper limit will be set equal to the lower limit. If the first request card is blank it will terminate the request list and cause all data to be retrived. List of requests.
VARY	1-11	E11.4	Energy for file 2 error law
	12-22	E11.4	Error for file 2 error law
VARY	1-11	E11.4	Energy for file 2 + 3 error law
	12-22	E11.4	Error for file 2 + 3 error law

The file 2 or file 2 + 3 error law may be energy independent (defined by a single error) or energy dependent (defined by up to 20 energy, error pairs), For the energy dependent case linear interpolation will be used to define the error at energies between those at which it is tabulated. In all cases each error law is terminated by a blank card. If only one energy, error pair is given for one law the law will be considered to be energy independent. If more than one pair is given it be considered to be energy dependent (Note, energy independent form will run faster than the equivalent energy dependent form). For an energy dependent error law all energies must be in ascending energy order. For convergence of the file 2 reconstruction algorithm all file 2 error law errors must be positive. If a file 2 error is not positive it will be set equal to the standard option (currently 0.001, corresponding to 0.1 per-cent). If a file 3 error is not positive it will be set equal to zero, indicating no thinning of the combined file 2 + 3 contributions. If the first card of either error law is blank it will terminate that error law and the error will be treated as energy independent, equal to the standard option (currently, 0.1 per-cent for file 2 and 0.0 for file 2 + 3).

Table A2.6 Input instruction for SIGMA1

Card	Cols.	Description
1	1-11	Selection criteria (0 = MAT, 1 = ZA)
	12-22	No longer used as an input option. The former meaning of thie parameter was . . . . . Minimum energy spacing selector = 0 − 6 Digit minimum energy spacing calculations. Standard 6 digit E11.4 output. = 1 − 8 Digit minimum energy spacing calculations. Standard 6 digit E11.4 output. = 2 − 8 Digit minimum energy spacing calculations. Variable 8 digit F format output. Experience has demonstrated that failure to use 2 for this option can result in significant errors in the final data. Therefore internally this option is always set to 2.
	23-33	Kelvin temperature
2-N	1-11	Lower MAT or ZA limit
	12-22	Upper MAT or ZA limit Up to 100 MAT or ZA ranges may be specified, one range per card. The list of ranges is terminated by a blank card. If the upper limit is less than the lower limit the upper limit will be set equal to the lower limit. If the first request card is blank it will terminate the list of requests and cause all data to be retrieved.
VARY	1-11	Energy for error law
	12-22	Error for error law The acceptable linearizing error can be given as an energy dependent function specified by up to 20 (energy, error) pairs and linear interpolation tabulate points. Energies must be in ascending order. The error law is terminated by a blank card. If the first error law card is blank it will terminate the error law and the error will be treated as energy independent, equal to zero, which indicates that the broadened data should not be thinned.

```
//JCLG  JOB
// EXEC JCLG
//SYSIN DD DATA,DLM='++'
// JUSER  XXXXXXXX,T.MORI,0431.110
   T.6 C.1 W.0 P.0 I.4
 OPTP  MSGCLASS=R,PASSWORD=XX
//******    'J3803.VIMLIB.CNTL(LRS)'    ***********
//  EXEC ANY
//*      ****************************************
//*      *          L I N E A R                 *
//*      ****************************************
//LINEAR   EXEC LMGO,LM='J2585.J9053.RECENT',PNM=LINEAR
//* ---- ENDF/B FORMATTED LIBRARY ----------------------------------
//FT10F001 DD LABEL=(,,,IN),DISP=SHR,DSN=J1615.JNDL3T20.DATA(T25055)
//*
//* ---- SELECTED MATERIAL LIBRARY ---------------------------------
//FT11F001 DD DSN=&&LINE,DISP=(NEW,PASS),
//          UNIT=TSSWK,SPACE=(CYL,(2,1),RLSE)
//*
//FT12F001 DD UNIT=WK10,SPACE=(CYL,(2,1)),DISP=(,DELETE)
//SYSIN DD * < LINEAR >
          0          2   1.000E-8          0
       3251          1

        0.0   0.001

/*
//*      ****************************************
//*      *          R E C E N T                 *
//*      ****************************************
//RECENT   EXEC LMGO,LM='J2585.J9053.RECENT',PNM=RECENT
//* ---- OUTPUT FROM LINEAR ----------------------------------------
//FT10F001 DD DSN=&&LINE,DISP=(OLD,DELETE),UNIT=
//*
//* ---- POINTWISE CROSS SECTION LIBRARY ---------------------------
//FT11F001 DD DSN=&&RCNT,DISP=(NEW,PASS),
//          UNIT=TSSWK,SPACE=(CYL,(2,1),RLSE),
//          DCB=(RECFM=FB,LRECL=80,BLKSIZE=6240)
//*
//FT12F001 DD UNIT=WK10,SPACE=(CYL,(5,1)),DISP=(,DELETE)
//FT13F001 DD UNIT=WK10,SPACE=(CYL,(7,3)),DISP=(,DELETE)
//FT14F001 DD UNIT=VIO,SPACE=(TRK,30),DCB=DSORG=PS
//SYSIN DD *   < RECENT >
          0   1.000E-8          0          0          0          0
          1       9999

        0.0   0.001

        0.0   0.001

/*
//*      ****************************************
//*      *          S I G M A 1                 *
//*      ****************************************
//SIGMA1   EXEC LMGO,LM='J2585.J9053.RECENT',PNM=SIGMA1
//* ---- OUTPUT FROM RECENT ----------------------------------------
//FT10F001 DD DSN=&&RCNT,DISP=(OLD,DELETE),UNIT=
//* ---- OUTPUT OF SIGMA1 (DOPPLER BROADENED CROSS SECTION ---------
//FT11F001 DD DSN=J3803.MN55J3T.DATA,DISP=(NEW,CATLG),
//          UNIT=TSSWK,SPACE=(CYL,(2,1),RLSE),
//          DCB=(RECFM=FB,LRECL=80,BLKSIZE=6240)
//*
//FT12F001 DD UNIT=WK10,SPACE=(CYL,(5,1)),DISP=(,DELETE)
//SYSIN DD *   < SIGMA1 >
          0          2     300.00
          1       9999

        0.0   0.001

/*
++
//
```

Fig. A2.1 Sample JCL and input data for LINEAR, RECENT and SIGMA1.

Appendix 3. Angular Transfer Probability for S_n Calculation

The angular transfer probabilities for S_8 and S_{16} calculations by DOT-DD and ANISN-DD (infinite cylinder system) have been prepared for users by using the MONTA code. They are stored on a magnetic disks with the file name shown in **Table A3.1**. The quadrature directions and weights are summarized in **Tables A3.2** and **A3.3**.

Table A3.1 File name of angular transfer probabilities

	Igloo type	Honeycomb type
S_8	J3803.IGLOO48.DATA	J3803.MONTA48.DATA
S_{16}	J3803.IGLOO160.DATA	J3803.MONTA160.DATA

Table A3.2 Quadrature set of S_8

Angle	Weight		ETA	MU
	Igloo	Honeycomb		
1	0.0	0.0	−0.9511862E+00	−0.3086055E+00
2	0.3024679E−01	0.2770480E−01	−0.9511862E+00	−0.2182171E+00
3	0.3024679E−01	0.2770480E−01	−0.9511862E+00	0.2182171E+00
4	0.0	0.0	−0.7867928E+00	−0.6172110E+00
5	0.2268510E−01	0.2372390E−01	−0.7867928E+00	−0.5773481E+00
6	0.2268510E−01	0.2366050E−01	−0.7867928E+00	−0.2182171E+00
7	0.2268510E−01	0.2366050E−01	−0.7867928E+00	0.2182171E+00
8	0.2268510E−01	0.2372390E−01	−0.7867928E+00	0.5773481E+00
9	0.0	0.0	−0.5773481E+00	−0.8164935E+00
10	0.2268510E−01	0.2367070E−01	−0.5773481E+00	−0.7867928E+00
11	0.2314805E−01	0.2471490E−01	−0.5773481E+00	−0.5773481E+00
12	0.2268510E−01	0.2372460E−01	−0.5773481E+00	−0.2182171E+00
13	0.2268510E−01	0.2372460E−01	−0.5773481E+00	0.2182171E+00
14	0.2314805E−01	0.2471490E−01	−0.5773481E+00	0.5773481E+00
15	0.2268510E−01	0.2367070E−01	−0.5773481E+00	0.7867928E+00
16	0.0	0.0	−0.2182171E+00	−0.9758964E+00
17	0.3024679E−01	0.2773450E−01	−0.2182171E+00	−0.9511862E+00
18	0.2268510E−01	0.2364290E−01	−0.2182171E+00	−0.7867928E+00
19	0.2268510E−01	0.2369060E−01	−0.2182171E+00	−0.5773481E+00
20	0.3024679E−01	0.2773240E−01	−0.2182171E+00	−0.2182171E+00
21	0.3024679E−01	0.2773240E−01	−0.2182171E+00	0.2182171E+00
22	0.2268510E−01	0.2369060E−01	−0.2182171E+00	0.5773481E+00
23	0.2268510E−01	0.2364290E−01	−0.2182171E+00	0.7867928E+00
24	0.3024679E−01	0.2773450E−01	−0.2182171E+00	0.9511862E+00
25	0.0	0.0	0.9511862E+00	−0.3086055E+00
26	0.3024679E−01	0.2770480E−01	0.9511862E+00	−0.2182171E+00
27	0.3024679E−01	0.2770480E−01	0.9511862E+00	0.2182171E+00
28	0.0	0.0	0.7867928E+00	−0.6172110E+00
29	0.2268510E−01	0.2372390E−01	0.7867928E+00	−0.5773481E+00
30	0.2268510E−01	0.2471490E−01	0.7867928E+00	−0.2182171E+00
31	0.2268510E−01	0.2471490E−01	0.7857928E+00	0.2182171E+00
32	0.2268510E−01	0.2372390E−01	0.7867928E+00	0.5773481E+00
33	0.0	0.0	0.5773481E+00	−0.8164935E+00
34	0.2268510E−01	0.2367070E−01	0.5773481E+00	−0.7867928E+00
35	0.2314805E−01	0.2471490E−01	0.5773481E+00	−0.5773481E+00
36	0.2268510E−01	0.2372460E−01	0.5773481E+00	−0.2182171E+00
37	0.2268510E−01	0.2372460E−01	0.5773481E+00	0.2182171E+00
38	0.2314805E−01	0.2471490E−01	0.5773481E+00	0.5773481E+00
39	0.2268510E−01	0.2367070E−01	0.5773481E+00	0.7867928E+00
40	0.0	0.0	0.2182171E+00	−0.9758964E+00
41	0.3024679E−01	0.2773450E−01	0.2182171E+00	−0.9511862E+00
42	0.2268510E−01	0.2364290E−01	0.2182171E+00	−0.7867928E+00
43	0.2268510E−01	0.2369060E−01	0.2182171E+00	−0.5773481E+00
44	0.3024679E−01	0.2773240E−01	0.2182171E+00	−0.2182171E+00
45	0.3024679E−01	0.2773240E−01	0.2182171E+00	0.2182171E+00
46	0.2268510E−01	0.2369060E−01	0.2182171E+00	0.5773481E+00
47	0.2268510E−01	0.2364290E−01	0.2182171E+00	0.7867928E+00
48	0.3024679E−01	0.2773450E−01	0.2182171E+00	0.9511862E+00

Table A3.3 Quadrature set of S_{16}

Angle	Weight		ETA	MU
	Igloo	Honeycomb		
1	0.0	0.0	−0.9775217E+00	−0.2108189E+00
2	0.1358595E−01	0.1222050E−01	−0.9775217E+00	−0.1490704E+00
3	0.1358595E−01	0.1222050E−01	−0.9775217E+00	0.1490704E+00
4	0.0	0.0	−0.9067620E+00	−0.4216349E+00
5	0.9768061E−02	0.9313200E−02	−0.9067620E+00	−0.3944035E+00
6	0.9768061E−02	0.9328300E−02	−0.9067620E+00	−0.1490704E+00
7	0.9768061E−02	0.9328300E−02	−0.9067620E+00	0.1490704E+00
8	0.9768061E−02	0.9313200E−02	−0.9067620E+00	0.3944035E+00
9	0.0	0.0	−0.8299902E+00	−0.5577717E+00
10	0.6473772E−02	0.6713300E−02	−0.8299902E+00	−0.5374820E+00
11	0.5038980E−02	0.7197000E−02	−0.8299902E+00	−0.3944035E+00
12	0.6473772E−02	0.6719500E−02	−0.8299902E+00	−0.1490704E+00
13	0.6473772E−02	0.6719500E−02	−0.8299902E+00	0.1490704E+00
14	0.5038980E−02	0.7197000E−02	−0.8299902E+00	0.3944035E+00
15	0.6473772E−02	0.6713300E−02	−0.8299902E+00	0.5374820E+00
16	0.0	0.0	−0.7453535E+00	−0.6666641E+00
17	0.6463375E−02	0.6101200E−02	−0.7453535E+00	−0.6497836E+00
18	0.7112373E−02	0.5299400E−02	−0.7453535E+00	−0.5374820E+00
19	0.7112373E−02	0.5290000E−02	−0.7453535E+00	−0.3944035E+00
20	0.6463375E−02	0.6118000E−02	−0.7453535E+00	−0.1490704E+00
21	0.6463375E−02	0.6118000E−02	−0.7453535E+00	0.1490704E+00
22	0.7112373E−02	0.5290000E−02	−0.7453535E+00	0.3944035E+00
23	0.7112373E−02	0.5299400E−02	−0.7453535E+00	0.5374820E+00
24	0.6463375E−02	0.6101299E−02	−0.7453535E+00	0.6497836E+00
25	0.0	0.0	−0.6497838E+00	−0.7601143E+00
26	0.6463375E−02	0.6107300E−02	−0.6497838E+00	−0.7453532E+00
27	0.1438095E−02	0.4974900E−02	−0.6497838E+00	−0.6497836E+00
28	0.3634186E−02	0.4028800E−02	−0.6497838E+00	−0.5374820E+00
29	0.1438095E−02	0.4976200E−02	−0.6497838E+00	−0.3944035E+00
30	0.6463375E−02	0.6120800E−02	−0.6497838E+00	−0.1490704E+00
31	0.6463375E−02	0.6120800E−02	−0.6497837E+00	0.1490704E+00
32	0.1438095E−02	0.4976200E−02	−0.6497838E+00	0.3944035E+00
33	0.3634186E−02	0.4028800E−02	−0.6497837E+00	0.5374820E+00
34	0.1438095E−02	0.4974900E−02	−0.6497838E+00	0.6497836E+00
35	0.6463375E−02	0.6107300E−02	−0.6497838E+00	0.7453532E+00
36	0.0	0.0	−0.5374822E+00	−0.8432708E+00
37	0.6473772E−02	0.6728600E−02	−0.5374822E+00	−0.8299899E+00
38	0.7112373E−02	0.5298300E−02	−0.5374822E+00	−0.7453532E+00
39	0.3634186E−02	0.4027400E−02	−0.5374822E+00	−0.6497836E+00
40	0.3634186E−02	0.4028200E−02	−0.5374822E+00	−0.5374820E+00
41	0.7112373E−02	0.5311800E−02	−0.5374822E+00	−0.3944035E+00
42	0.6473772E−02	0.6720300E−02	−0.5374822E+00	−0.1490704E+00
43	0.6473772E−02	0.6720300E−02	−0.5374822E+00	0.1490704E+00
44	0.7112373E−02	0.5311800E−02	−0.5374822E+00	0.3944035E+00
45	0.3634186E−02	0.4028200E−02	−0.5374822E+00	0.5374820E+00
46	0.3634186E−02	0.4027400E−02	−0.5374822E+00	0.6497836E+00
47	0.7112373E−02	0.5298300E−02	−0.5374822E+00	0.7453532E+00
48	0.6473772E−02	0.6728600E−02	−0.5374822E+00	0.8299899E+00
49	0.0	0.0	−0.3944037E+00	−0.9189332E+00
50	0.9768061E−02	0.9318200E−02	−0.3944037E+00	−0.9067616E+00
51	0.5038980E−02	0.7180300E−02	−0.3944037E+00	−0.8299899E+00
52	0.7112373E−02	0.5292100E−02	−0.3944037E+00	−0.7453532E+00
53	0.1438095E−02	0.4969300E−02	−0.3944037E+00	−0.6497836E+00
54	0.7112373E−02	0.5292200E−02	−0.3944037E+00	−0.5374820E+00
55	0.5038980E−02	0.7191800E−02	−0.3944037E+00	−0.3944035E+00

Table A3.3 (Continued)

Angle	Weight Igloo	Weight Honeycomb	ETA	MU
56	0.9768061E−02	0.9334800E−02	−0.3944037E+00	−0.1490704E+00
57	0.9768061E−02	0.9334800E−02	−0.3944037E+00	0.1490704E+00
58	0.5038980E−02	0.7191800E−02	−0.3944037E+00	0.3944035E+00
59	0.7112373E−02	0.5292200E−02	−0.3944037E+00	0.5374820E+00
60	0.1438095E−02	0.4969300E−02	−0.3944037E+00	0.6497836E+00
61	0.7112373E−02	0.5292100E−02	−0.3944037E+00	0.7453532E+00
62	0.5038980E−02	0.7180300E−02	−0.3944037E+00	0.8299899E+00
63	0.9768061E−02	0.9318200E−02	−0.3944037E+00	0.9067616E+00
64	0.0	0.0	−0.1490705E+00	−0.9888228E+00
65	0.1358595E−01	0.1222820E−01	−0.1490705E+00	−0.9775213E+00
66	0.9768061E−02	0.9334900E−02	−0.1490705E+00	−0.9067616E+00
67	0.6473772E−02	0.6717300E−02	−0.1490705E+00	−0.8299899E+00
68	0.6473772E−02	0.6109500E−02	−0.1490705E+00	−0.7453532E+00
69	0.6473772E−02	0.6111900E−02	−0.1490705E+00	−0.6497836E+00
70	0.6473772E−02	0.6728400E−02	−0.1490705E+00	−0.5374820E+00
71	0.9768061E−02	0.9325000E−02	−0.1490705E+00	−0.3944035E+00
72	0.1358595E−01	0.1224310E−01	−0.1490705E+00	−0.1490704E+00
73	0.1358595E−01	0.1224310E−01	−0.1490705E+00	0.1490704E+00
74	0.9768061E−02	0.9325000E−02	−0.1490705E+00	0.3944035E+00
75	0.6473772E−02	0.6728400E−02	−0.1490705E+00	0.5374820E+00
76	0.6473772E−02	0.6111900E−02	−0.1490705E+00	0.6497836E+00
77	0.6473772E−02	0.6109500E−02	−0.1490705E+00	0.7453532E+00
78	0.6473772E−02	0.6717300E−02	−0.1490705E+00	0.8299899E+00
79	0.9768061E−02	0.9334900E−02	−0.1490705E+00	0.9067616E+00
80	0.1358595E−01	0.1222820E−01	−0.1490705E+00	0.9775213E+00
81	0.0	0.0	0.9775217E+00	−0.2108189E+00
82	0.1358595E−01	0.1222050E−01	0.9775217E+00	−0.1490704E+00
83	0.1358595E−01	0.1222050E−01	0.9775217E+00	0.1490704E+00
84	0.0	0.0	0.9067620E+00	−0.4216349E+00
85	0.9768061E−02	0.9313200E−02	0.9067620E+00	−0.3944035E+00
86	0.9768061E−02	0.9328300E−02	0.9067620E+00	−0.1490704E+00
87	0.9768061E−02	0.9328300E−02	0.9067620E+00	0.1490704E+00
88	0.9768061E−02	0.9313200E−02	0.9067620E+00	0.3944035E+00
89	0.0	0.0	0.8299902E+00	−0.5577717E+00
90	0.6473772E−02	0.6713300E−02	0.8299902E+00	−0.5374820E+00
91	0.5038980E−02	0.7197000E−02	0.8299902E+00	−0.3944035E+00
92	0.6473772E−02	0.6719500E−02	0.8299902E+00	−0.1490704E+00
93	0.6473772E−02	0.6719500E−02	0.8299902E+00	0.1490704E+00
94	0.5038980E−02	0.7197000E−02	0.8299902E+00	0.3944035E+00
95	0.6473772E−02	0.6713300E−02	0.8299902E+00	0.5374820E+00
96	0.0	0.0	0.7453535E+00	−0.6666641E+00
97	0.6463375E−02	0.6101200E−02	0.7453535E+00	−0.6497836E+00
98	0.7112373E−02	0.5299400E−02	0.7453535E+00	−0.5374820E+00
99	0.7112373E−02	0.5290000E−02	0.7453535E+00	−0.3944035E+00
100	0.6463375E−02	0.6118000E−02	0.7453535E+00	−0.1490704E+00
101	0.6463376E−02	0.6118000E−02	0.7453535E+00	0.1490704E+00
102	0.7112373E−02	0.5290000E−02	0.7453535E+00	0.3944035E+00
103	0.7112373E−02	0.5299400E−02	0.7453535E+00	0.5374820E+00
104	0.6463375E−02	0.6101200E−02	0.7453535E+00	0.6497836E+00
105	0.0	0.0	0.6497838E+00	−0.7601143E+00
106	0.6463375E−02	0.6107300E−02	0.6497838E+00	−0.7453532E+00
107	0.1438095E−02	0.4974900E−02	0.6497838E+00	−0.6497836E+00
108	0.3634186E−02	0.4028800E−02	0.6497838E+00	−0.5374820E+00
109	0.1438095E−02	0.4976200E−02	0.6497838E+00	−0.3944035E+00
110	0.6463375E−02	0.6120800E−02	0.6497838E+00	−0.1490704E+00

Table A3.3 (Continued)

Angle	Weight Igloo	Honeycomb	ETA	MU
111	0.6463375E−02	0.6120800E−02	0.6497838E+00	0.1490704E+00
112	0.1438095E−02	0.4976200E−02	0.6497838E+00	0.3944035E+00
113	0.3634186E−02	0.4028800E−02	0.6497838E+00	0.5374820E+00
114	0.1438095E−02	0.4974900E−02	0.6497838E+00	0.6497836E+00
115	0.6463375E−02	0.6107300E−02	0.6497838E+00	0.7453532E+00
116	0.0	0.0	0.5374822E+00	−0.8432708E+00
117	0.6473772E−02	0.6728600E−02	0.5374822E+00	−0.8299899E+00
118	0.7112373E−02	0.5298300E−02	0.5374822E+00	−0.7453532E+00
119	0.3634186E−02	0.4027400E−02	0.5374822E+00	−0.6497836E+00
120	0.3634186E−02	0.4028200E−02	0.5374822E+00	−0.5374820E+00
121	0.7112373E−02	0.5311800E−02	0.5374822E+00	−0.3944035E+00
122	0.6473772E−02	0.6720300E−02	0.5374822E+00	−0.1490704E+00
123	0.6473772E−02	0.6720300E−02	0.5374822E+00	0.1490704E+00
124	0.7112373E−02	0.5311800E−02	0.5374822E+00	0.3944035E+00
125	0.3634186E−02	0.4028200E−02	0.5374822E+00	0.5374820E+00
126	0.3634186E−02	0.4027400E−02	0.5374822E+00	0.6497836E+00
127	0.7112373E−02	0.5298300E−02	0.5374822E+00	0.7453532E+00
128	0.6473772E−02	0.6728600E−02	0.5374822E+00	0.8299899E+00
129	0.0	0.0	0.3944037E+00	−0.9189332E+00
130	0.9768061E−02	0.9318200E−02	0.3944037E+00	−0.9067616E+00
131	0.5038980E−02	0.7180300E−02	0.3944037E+00	−0.8299899E+00
132	0.7112373E−02	0.5292100E−02	0.3944037E+00	−0.7453532E+00
133	0.1438095E−02	0.4969300E−02	0.3944037E+00	−0.6497836E+00
134	0.7112373E−02	0.5292200E−02	0.3944037E+00	−0.5374820E+00
135	0.5038980E−02	0.7191800E−02	0.3944037E+00	−0.3944035E+00
136	0.9768061E−02	0.9334800E−02	0.3944037E+00	−0.1490704E+00
137	0.9768061E−02	0.9334800E−02	0.3944037E+00	0.1490704E+00
138	0.5038980E−02	0.7191800E−02	0.3944037E+00	0.3944035E+00
139	0.7112373E−02	0.5292200E−02	0.3944037E+00	0.5374820E+00
140	0.1438095E−02	0.4969300E−02	0.3944037E+00	0.6497836E+00
141	0.7112373E−02	0.5292100E−02	0.3944037E+00	0.7453532E+00
142	0.5038980E−02	0.7180300E−02	0.3944037E+00	0.8299899E+00
143	0.9768061E−02	0.9318200E−02	0.3944037E+00	0.9067616E+00
144	0.0	0.0	0.1490705E+00	−0.9888228E+00
145	0.1358595E−01	0.1222820E−01	0.1490705E+00	−0.9775213E+00
146	0.9768061E−02	0.9334900E−02	0.1490705E+00	−0.9067616E+00
147	0.6473772E−02	0.6717300E−02	0.1490705E+00	−0.8299899E+00
148	0.6473772E−02	0.6109500E−02	0.1490705E+00	−0.7453532E+00
149	0.6473772E−02	0.6111900E−02	0.1490705E+00	−0.6497836E+00
150	0.6473772E−02	0.6728400E−02	0.1490705E+00	−0.5374820E+00
151	0.9768061E−02	0.9325000E−02	0.1490705E+00	−0.3944035E+00
152	0.1358595E−01	0.1224310E−01	0.1490705E+00	−0.1490704E+00
153	0.1358595E−01	0.1224310E−01	0.1490705E+00	0.1490704E+00
154	0.9768061E−02	0.9325000E−02	0.1490705E+00	0.3944035E+00
155	0.6473772E−02	0.6728400E−02	0.1490705E+00	0.5374820E+00
156	0.6473772E−02	0.6111900E−02	0.1490705E+00	0.6497836E+00
157	0.6473772E−02	0.6109500E−02	0.1490705E+00	0.7453532E+00
158	0.6473772E−02	0.6717300E−02	0.1490705E+00	0.8299899E+00
159	0.9768061E−02	0.9334900E−02	0.1490705E+00	0.9067616E+00
160	0.1358595E−01	0.1222820E−01	0.1490705E+00	0.9775213E+00